Queen Mary
University of London

Clonal expansion in the human upper gastrointestinal tract

Tania Ventayol-García

PhD Thesis

Supervisors

Prof Andrew Silver, Professor of Cancer Genetics

Prof Sir Nicholas Wright, Professor of Pathology and Tumour Biology

Abstract

The high incidence of gastrointestinal cancers in the general population and the presence of premalignant dysplastic precursor lesions in the gastrointestinal tract make the gastrointestinal tract an ideal environment to study cancer clonality and clonal expansion.

Background:
Intestinal metaplastic (IM) glands in the human stomach are clonal, contain multiple stem cells and spread by fission. This mechanism of gland fission causes field cancerisation. We hypothesised that gastric adenocarcinoma (GA) progresses through a series of genetic events arising from a founder mutation. A process analogous to niche succession may also take place in the normal oesophagus. We hypothesise that oesophageal squamous cell cancer occurs by a process of field cancerisation of the oesophagus. *RHBDF2* has been identified as the gene responsible for tylosis with oesophageal carcinoma (TOC). We hypothesise that *RHBDF2* germline gain of function mutations might be lost during tumour progression in TOC and this might affect iRhom2 localisation in the cell.

Methods and results:
A cohort of 23 patients with dysplasia and a cohort of 51 GA patients were screened for genes accounting for 75% of all somatic mutations previously reported in GA. Only 13% of dysplastic patients and 31.4% of GA patients had mutations. Three dysplastic patients and six GA patients were analysed by microdissection. Small gastric cancer foci in a cohort of hereditary diffuse gastric cancer (HDGC) patients (n=5) were also screened by laser-capture microdissection (LCM) for mutations in *TP53*. A cohort of 30 patients was screened for common mutations in OSCC and for *RHBDF2* mutations. 36.36% of the patients presented mutations. Three patients with mutations were randomly selected and areas of oesophageal squamous cell dysplasia and OSCC were analysed by LCM. Three TOC patients were also analysed by LCM and immunohistochemistry was performed for iRhom2 and ADAM17.

Conclusions:
The usual mutational events established for GA development during the metaplasia-dysplasia-carcinoma sequence (MCS) do not fit the results from either of our two LCM mutation studies in the human stomach. Dysplasia was shown to be clonal and GA demonstrates genetic heterogeneity through clonal evolution. Field cancerisation could not be detected in HDGC using *TP53* as a clonal marker. The low incidence of OSCC patients with mutations implies that other genes may be involved in the premalignant pathway leading to OSCC. Oesophageal squamous cell dysplasia and OSCC demonstrate clonal expansion through tumour progression. *RHBDF2* mutations do not occur in sporadic OSCC but germline *RHBDF2* mutations can be lost during tumour progression in TOC patients with LOH in 17q. Overall, the somatic mutation theory of carcinogenesis seems to hold true for both the progression to GA and OSCC, as both carcinomas seem to evolve from a single mutated stem cell and acquire genetic heterogeneity as the tumours evolve.

Publications

- Tania Ventayol-Garcia, Manuel Rodriguez-Justo, Lisa Pritchard, Joanne Chin-Aleong, Nicholas Wright, Andrew Silver & Stuart McDonald. Gastric adenocarcinoma is monoclonal in origin and demonstrates genetic heterogeneity through clonal evolution. (Writing in progress)

- Tania Ventayol-Garcia, Joanne Chin-Aleong, Manuel Rodriguez-Justo, Stuart McDonald, Nicholas Wright & Andrew Silver. Oesophageal squamous cell cancer and oesophageal squamous cell dysplasia are monoclonal in origin. (Writing in progress)

- Tania Ventayol-Garcia, Manuel Rodriguez-Justo, Joanne Chin-Aleong, Marco Novelli, Stuart McDonald, Andrew Silver & Nicholas Wright. Clonal expansion in oesophageal squamous cell carcinoma. William Harvey Day, October 2012.

- Tania Ventayol-Garcia. The clonal origins of gastric adenocarcinoma. Digestive Diseases Disorders Federation Joint Meeting, Liverpool, June 2012.

- Tania Ventayol-Garcia, Manuel Rodriguez-Justo, Lisa Pritchard, Trevor Graham, Marco Novelli, Nicholas Wright & Stuart McDonald. The clonal origins of gastric adenocarcinoma. Digestive Disease Week, San Diego, May 2012.

- Tania Ventayol-Garcia, Manuel Rodriguez-Justo, Trevor Graham, Marco Novelli, Nicholas Wright & Stuart McDonald. The clonal origins of gastric adenocarcinoma. William Harvey Day, London, October 2011.

- Gutierrez-Gonzalez, L., Graham, T. A., Rodriguez-Justo, M., Leedham, S. J., Novelli, M. R., Gay, L. J., Ventayol-Garcia, T., Green, A., Mitchell, I., Stoker, D. L., Preston, S. L., Bamba, S., Yamada, E., Kishi, Y., Harrison, R., Jankowski, J. A., Wright, N. A., and McDonald, S. A. (2011) The clonal origins of dysplasia from intestinal metaplasia in the human stomach, *Gastroenterology 140*, 1251-1260 e1251-1256.

- Tania Ventayol-Garcia, Trevor A Graham, Rosemary Jeffery, Janusz A Z Jankowski & Stuart A C McDonald. Genetic heterogeneity in Barrett's Oesophagus promotes biological changes that bestow a selective advantage. British Society of Gastroenterology, Liverpool, June 2010.

Acknowledgements

I would like to give special thanks to my primary supervisor Professor Andrew Silver for taking on a new student at such an advanced PhD stage and dedicating so much time to my projects. I would also like to thank my supervisor Professor Sir Nicholas Wright for giving me the opportunity to work in his laboratory and Professor David Kelsell and Dr Stuart McDonald for letting me work on their projects.

Special thanks to the people who have collaborated with me, Lisa Pritchard and especially Dr Lydia Gutierrez-Gonzalez for all her work in the project on the clonal origins of dysplasia from intestinal metaplasia. To Dr Manuel Rodriguez-Justo and Dr Joanne Chin-Aleong, thank you for all your time and effort, without your assistance on tissue collection none of this work would have been possible. I would like to thank the BICMS core pathology facility for all the immunohistochemistry work and serial tissue cutting performed. I would also like to thank Dr J. Risk, Dr A.Ellis and Dr J.K Field at the Department of Molecular & Clinical Cancer Medicine, Institute of Translational Medicine, for letting me use the data from their DNA extraction and pyrosequencing work carried out on two patients with tylosis. Finally, I would like to thank all the people from the different laboratories who have always been so helpful and kind, especially Sarah Etheridge, Dr Diana Blaydon, Dr Noor Jawad, Dr Biancastella Cereser, Dr Sebastian Zeki and Dr Shahabuddin Khan.

I would like to dedicate this thesis to my family, Los Garcia, without whose love and support none of this would have been possible. Firstly to my mum, Eva, for always being my Superwoman and teaching me to face every challenge with my chin-up; to my grandparents, Conchi & Paquito, for always taking care of me and loving me like a

daughter; and to my brothers, Alex and Pol, for making me smile even when I'm too far away for their hugs. To my Auntie Lolilla, for our fits of uncontrollable laughter and endless tears over the phone; to my Uncle Enriquinyo, for his strength, love and role as the MacGyver of the family; to my cousins Victorino and Arantxi, for always letting me spoil them and being my little brother and sister; and to my Uncle David, for our bread and sugar snacks and funny special bond. Finally, I would like to dedicate my thesis to my godmother and Auntie, Nuri, for always believing in me, for always making things better, for always having time to listen, for loving me, for taking care of me, for being the best person I will ever meet and for giving me the strength to finish this PhD in hopes that, wherever she is, I won't let her down.

Lastly, thank you to my friends, especially to my girls and most of the time soul mates: Babsy, Daniela, Kylie, Yvette and Nuria, for making me fall on the floor with laughter and holding my hand during the worst times; and to Dario, for bringing me back to life.

Querría dedicarle mi tesis a mi familia, Los García, ya que sin su amor y apoyo nunca hubiese sido posible. A mi madre, Eva, por ser siempre mi Superwoman y enseñarme a enfrentarme a cualquier problema con la cabeza bien alta; a mis abuelos, Conchi y Paquito, por cuidarme siempre y quererme como a una hija; y a mis hermanos, Alex y Pol, por siempre hacerme sonreír incluso cuando estoy demasiado lejos para sus besos y abrazos. A mi tía Lolilla, por nuestras risas contagiosas e incontables lágrimas al teléfono; a mi tío Enriquinyo, por su fuerza, amor y función como MacGyver de la familia; a mis primos Arantxi y Victorino, por dejarme mimarles y ser mis hermanos pequeños; y a mi tío David, por nuestras meriendas de pan con azúcar

y nuestro cariño especial. Finalmente, querría dedicarle mi tesis a mi madrina y tía, Nuri, por siempre creer en mí, por siempre hacer que todo fuese mejor, por siempre tener tiempo para escucharme, por quererme, por cuidarme, por ser la mejor persona que nunca haya conocido y por darme fuerza para acabar este doctorado con la esperanza de que, esté donde esté, no la decepcionaré.

Clonal expansion in the human upper gastrointestinal tract

Abstract……p1

Publications……...p2

Acknowledgements……...p4

Contents……p7

List of tables……....p11

List of figures……..p15

Abbreviations……..p21

1. Introduction……..……..p23

1. 1 Gastrointestinal stem cells……....p23

1. 2 Intestinal stem cells…….…..p26

1.2.1 Slowly cycling intestinal stem cells..…….…...p28

1.2.2 Fast dividing intestinal stem cells……..…….……..p29

1.2.3 Clonal analysis of the intestinal epithelium..…….……...p31

1. 3 Gastric stem cells…….……..p36

1.3.1 Gastric progenitor and stem cell markers…..…….…….....……p38

1.3.2 Clonal analysis of the gastric epithelium…….....…….p40

1. 4 Oesophageal stem cells…….…….p41

1.4.1 Oesophageal progenitor and stem cell markers……p42

1. 5 Stem cells in cancer in the gastrointestinal tract……....p44

1.5.1 Cancer stem cell markers in the gastrointestinal tract...……...…p46

1.5.2 Models of neoplastic development……...p47

1. 6 The adenoma-carcinoma sequence…….…….p49

1. 7 Genes involved in gastrointestinal cancers……..…p50

1.7.1 The *Wnt* signalling pathway……..…...p50

1.7.1.1. Adenomatous Polyposis Coli……..……p52

1.7.1.2. β-catenin……..p53

1.7.2 The *TP53* signalling pathway……..….p54

1.7.2.1. TP53 in cancer……..….p54

1.7.3 The *CDKN2A* signalling pathway……..……..p57

1. 8 Cancers of the small intestine, colon and rectum…….…..p57

1. 9 Gastric cancer…….……...p58

1.9.1 *CDH1* mutations in hereditary diffuse gastric cancer……...…p59

1.9.2 The gastric adenocarcinoma premalignant pathway…….p61

1.9.3 Intestinal metaplasia in the human stomach…….....p63

1.9.4 Dysplasia and gastric adenocarcinoma…….p64

1.9.5 Genetic instability in gastric adenocarcinoma…….....p66

1. 10 Oesophageal cancer…….…..p69

1.10.1 Barrett's oesophagus…….....p69

1.10.2 Genetic instability in Barrett's oesophagus and oesophageal adenocarcinoma……..…..p72

1.10.3 Oesophageal squamous cell carcinoma……..…..p73

1.10.4 Genetic instability in oesophageal squamous cell carcinoma……...p74

1.10.5 Tylosis with oesophageal cancer……..p75

1. 11 Hypothesis and aims……..….p78

2. Materials and Methods…….p82

2.1. Patients…….……..p82

2.1.1. Patients from Chapter 3.2.1……..…….……p82

2.1.2. Patients from Chapter 3.2.2……..…….……p82

2.1.3. Patients from Chapter 3.2.3……..……..……p83

2.1.4. Patients from Chapter 4 and Chapter 5……..……...……..p83

2.2 Tissue macrodissection……..…p84

2.3 Laser-capture microdissection…….……p84

2.4 Genomic PCR sequencing…….……...p85

2.5 Microsatellite loss of heterozygosity analysis…….……p87

2.6 DNA preparation and pyrosequencing…….…..p87

2.7 Histological staining and immunohistochemistry….…….……p88

2.7.1 Haematoxylin and Eosin staining……..……...p88

2.7.2 AB-PAS staining……..……p89

2.7.3 E-cadherin staining……..……p89

2.7.4 RHBDF2 staining……..……...p90

2.7.5 ADAM17 staining……..……..p90

3. Clonal expansion in the human stomach……p91

3.1. Introduction…….……..p91

3.1.1. Hypothesis and Aims……..……....p95

3.2 Results…….……...p95

3.2.1 The clonal origins of dysplasia from intestinal metaplasia……..p95

3.2.2 Clonal expansion in gastric adenocarcinoma…….p107

3.2.3 Clonal expansion in hereditary diffuse gastric cancer……....p135

3.3. Discussion…….……p149

4. Clonal expansion in oesophageal squamous cell cancer……..p155

4.1 Introduction…….…….……...…p155

4.1.1 Hypothesis and Aims……..……...p157

4.2 Results…….…….p158

4.3 Discussion…….……p180

5. Clonal expansion in tylosis with oesophageal cancer……...p183

5. 1 Introduction…….……p183

5.1.1 Hypothesis and Aims…….……...p186

5. 2 Results…….…….p186

5. 3 Discussion…….……p202

6. Discussion…….p205

6.1 Summary of findings……...…p205

6.2 Polyclonality, monoclonality and intratumour heterogeneity…….……p209

6.3 Limitations of the work presented in this thesis……...p211

6.4 Future directions…….p213

6.5 Final conclusions…….p215

7. Appendix……..p217

8. References……p243

List of Tables

Table 1.1. The most commonly mutated genes in gastric adenocarcinoma development.

Table 3.1. Only three patients had lesions with mutations in both metaplasia and dysplasia.

Table 3.2. Most metaplastic glands are wild type and all dysplastic glands are mutated.

Table 3.3. Association of the identified mutation with histology shows wild type intestinal metaplastic glands adjacent to large areas of mutated dysplastic glands in a strip of gastric epithelium from patient 1, block 6 strip 1.

Table 3.4. Association of the identified mutation with histology shows wild type intestinal metaplastic glands adjacent to large areas of mutated dysplastic glands in a second strip of gastric epithelium from patient 1, block 8 strip 3.

Table 3.5. Association of the identified mutation with histology suggests the clonal origins of dysplasia from intestinal metaplasia in a third strip of gastric epithelium from patient 1, block 9 strip 2.

Table 3.6. Association of the identified mutation with histology suggests that large areas of dysplasia are clonal in sequential strips of gastric epithelium from patient 2, block A20-1 strips 4, 6 and 7.

Table 3.7. Summary of mutations in genes selected from the COSMIC database for gastric adenocarcinoma.

Table 3.8. Summary of mutations identified in a cohort of gastric adenocarcinoma.

Table 3.9. Randomly selected patients for laser-capture microdissection.

Table 3.10. Association of identified mutations with histology and loss of heterozygosity shows clonal evolution in gastric adenocarcinoma in patient 8.

Table 3.11. Association of identified mutations with histology and loss of heterozygosity shows clonal evolution in a sequential specimen of gastric adenocarcinoma in patient 8.

Table 3.12. Association of identified mutations with histology and loss of heterozygosity shows that *TP53* mutations were not found in high grade dysplasia or intestinal metaplasia in patient 33.

Table 3.13. Summary of patients carrying E-cadherin mutations from families A and B.

Table 3.14. E-cadherin protein can be found expressed at a low level in the membrane of signet ring cells in some hereditary diffuse gastric cancer areas.

Table 4.1. Summary of mutations in genes selected from the COSMIC database for oesophageal squamous cell carcinoma.

Table 4.2. Randomly selected patients for laser-capture microdissection.

Table 4.3. Association of the identified mutations with histology shows *TP53* and *NFR2* mutations were found in all areas of oesophageal squamous cell carcinoma but not in dysplasia or hyperplasia in patient 4.

Table 4.4. Association of the identified mutation with histology shows *TP53* mutations were found in all areas of oesophageal squamous cell carcinoma but not in hyperplasia in patient 26.

Table 4.5. Association of the identified mutation with histology shows TP53 mutations were found in all areas of oesophageal squamous cell carcinoma but not in hyperplasia in patient 26.

Table 4.6. Association of the identified mutation with histology shows *TP53* mutations were found in all areas of oesophageal squamous cell carcinoma in patient 26.

Table 4.7. Association of the identified mutation with histology shows *TP53* mutations

were found in all dysplastic areas, in focal areas of oesophageal squamous cell carcinoma and in infiltrated oesophageal ducts in patient 28.

Table 4.8. Association of the identified mutation with histology shows *TP53* mutations were found in all dysplastic areas and in infiltrated oesophageal ducts in patient 28.

Table 4.9. Association of the identified mutation with histology shows *TP53* mutations were found in all dysplastic areas and in focal areas of oesophageal squamous cell carcinoma in patient 28.

Table 5.1. Summary of mutations in inactive rhomboid protein *RHBDF2* in specimens from sporadic and tylosis associated oesophageal squamous cell carcinoma patients.

Table 5.2. Oesophageal carcinoma from tylotic patients analysed by laser-capture microdissection.

Table 5.3. Association of the germline mutation with histology shows that the *RHBDF2* mutation was absent from areas of oesophageal squamous cell carcinoma from patient 2 indicating loss of heterozygosity of the mutated allele.

Table 5.4. Association of the germline mutation with histology shows that the *RHBDF2* mutation was present in all areas of oesophageal squamous cell carcinoma from patient 33 indicating there is no loss of heterozygosity of the mutated allele.

Table 5.5. Association of the germline mutation with histology shows that the *RHBDF2* mutation was absent from oesophageal squamous cell carcinoma, dysplasia or muscle epithelium obtained from patient 34 indicating loss of heterozygosity of the mutated allele.

Table 7.1. Primers and reaction conditions for Genomic PCR sequencing.

Table 7.2. Primers and reaction conditions for Microsatellite Loss of Heterozygosity Analysis.

Table 7.3. Summary of clinicopathological features in screened samples.

Table 7.4. Association of identified mutations and histology shows *TP53* mutations in gastric adenocarcinoma but not in benign areas in patient 27.

Table 7.5. Association of identified mutations and histology shows *TP53* mutations in gastric adenocarcinoma but not in intestinal metaplastic areas in patient 27.

Table 7.6. Summary of clinical features in screened samples.

List of Figures

Figure 1.1. The structure of the human small and large intestinal crypt.

Figure 1.2. The structure of the human stomach and the gastric corpus and pyloric glands.

Figure 1.3. The basic structure of human oesophageal epithelium.

Figure 1.4. The adenoma-carcinoma sequence leading to colorectal carcinomas.

Figure 1.5. Schematic illustration of interaction between E-cadherin and actin cytoskeleton.

Figure 1.6. The currently accepted metaplasia-dysplasia-carcinoma pathway in the development of Gastric Adenocarcinoma.

Figure 1.7. Clonal evolution models for Barrett's oesophagus from Leedham and colleagues (*155*).

Figure 1.8. RHBDF2 structure and working model of RHBDF2 and ADAM17 interaction in tylosis with oesophageal cancer.

Figure 3.1. Wild type intestinal metaplastic glands are found adjacent to large areas of mutated dysplastic glands in a strip of gastric epithelium from patient 1.

Figure 3.2. Wild type intestinal metaplastic glands are found adjacent to large areas of mutated dysplastic glands in a second strip of gastric epithelium from patient 1.

Figure 3.3. The clonal origins of dysplasia from intestinal metaplasia in a third strip of gastric epithelium from patient 1.

Figure 3.4. Analysis of sequential strips of gastric epithelium from patient 2 suggests that large areas of dysplasia are clonal.

Figure 3.5. Mutation frequencies are comparable to reports for gastric adenocarcinoma held in the COSMIC database.

Figure 3.6. Intestinal metaplastic glands are wild type but show loss of heterozygosity for microsatellites at 17p in patient 8.

Figure 3.7. Association of identified mutations with histology and loss of heterozygosity shows intestinal metaplastic glands are wild type but show loss of heterozygosity for microsatellites at 17p in patient 8.

Figure 3.8. Clonal ordering of mutations in gastric adenocarcinoma shows clonal evolution in patient 8.

Figure 3.9. Clonal ordering of mutations in a sequential specimen of gastric adenocarcinoma shows again clonal evolution in patient 8.

Figure 3.10. *TP53* mutations could be found in gastric adenocarcinoma but not in intestinal metaplastic glands in patient 10.

Figure 3.11. Association of the identified mutation with histology and loss of heterozygosity shows *TP53* mutations could be found in gastric adenocarcinoma but not in intestinal metaplastic glands in patient 10.

Figure 3.12. Wild type and mutated clones demonstrate a clonal relationship in patient 22.

Figure 3.13. Association of identified mutations with histology and loss of heterozygosity shows that wild type and mutated clones demonstrate a clonal relationship in patient 22.

Figure 3.14. *TP53* mutations found in gastric adenocarcinoma but not in intestinal metaplastic glands in patient 33.

Figure 3.15. Association of identified mutations with histology and loss of heterozygosity shows that *TP53* mutations were found in gastric adenocarcinoma but not in intestinal metaplastic glands in patient 33.

Figure 3.16. *TP53* mutations were not found in high grade dysplasia or intestinal

metaplasia in patient 33.

Figure 3.17. *TP53* mutations were found in high grade dysplasia and in gastric adenocarcinoma but not in intestinal metaplasia in patient 51.

Figure 3.18. Association of identified mutations with histology and loss of heterozygosity shows that *TP53* mutations were found in high grade dysplasia and in gastric adenocarcinoma but not in intestinal metaplasia in patient 51.

Figure 3.19. Phylogenetic trees provide evidence for a monoclonal origin for gastric adenocarcinoma.

Figure 3.20. Field cancerisation was not observed when using *TP53* mutations as a clonal marker in HDGC tissue from patient A3.

Figure 3.21. Screening for *TP53* exons 5 to 8 mutations and E-cadherin immunohistochemistry in HDGC tissue from patient A3.

Figure 3.22. Field cancerisation was not observed when using *TP53* mutations as a clonal marker in HDGC tissue from patient A4.

Figure 3.23. Screening for *TP53* exons 5 to 8 mutations and E-cadherin immunohistochemistry in HDGC tissue from patient A4.

Figure 3.24. Field cancerisation was not observed when using *TP53* mutations as a clonal marker in HDGC tissue from patient B1.

Figure 3.25. Screening for *TP53* exons 5 to 8 mutations and E-cadherin immunohistochemistry in HDGC tissue from patient B1.

Figure 3.26. Field cancerisation was not observed when using *TP53* mutations as a clonal marker in HDGC tissue patient B4.

Figure 3.27. Screening for *TP53* exons 5 to 8 mutations and E-cadherin immunohistochemistry in HDGC tissue from patient B4.

Figure 3.28. Field cancerisation was not observed when using *TP53* mutations as a

clonal marker in HDGC tissue from patient B5.

Figure 3.29. Screening for *TP53* exons 5 to 8 mutations and E-cadherin immunohistochemistry in HDGC tissue from patient B5.

Figure 3.30. Comparison between the phenotypic and genotypic events.

Figure 4.1. Mutation frequencies are comparable to reports for oesophageal squamous cell carcinoma held in the COSMIC database.

Figure 4.2. *TP53* and *NRF2* mutations were found in all areas of oesophageal squamous cell carcinoma but not in dysplasia or hyperplasia in patient 4.

Figure 4.3. *TP53* mutations were found in all areas of oesophageal squamous cell carcinoma but not in hyperplasia in patient 26.

Figure 4.4. *TP53* mutations were found in all areas of oesophageal squamous cell carcinoma but not in hyperplasia in patient 26.

Figure 4.5. *TP53* mutations were found in all areas of oesophageal squamous cell carcinoma in patient 26.

Figure 4.6. *TP53* mutations were found in all dysplastic areas, in focal areas of invasive oesophageal squamous cell carcinoma and in infiltrated oesophageal ducts in patient 28.

Figure 4.7. *TP53* mutations were found in all dysplastic areas and in infiltrated oesophageal ducts in patient 28.

Figure 4.8. *TP53* mutations were found in all dysplastic areas and in focal areas of invasive oesophageal squamous cell carcinoma in patient 28.

Figure 4.9. Phylogenetic trees provide evidence for a monoclonal origin for oesophageal squamous cell carcinoma.

Figure 5.1. The *RHBDF2* germline mutation was absent from areas of oesophageal squamous cell carcinoma from patient 2 indicating loss of heterozygosity of the

mutated allele.

Figure 5.2. The *RHBDF2* germline mutation was absent from areas of oesophageal squamous cell carcinoma from patient 2 indicating loss of heterozygosity of the mutated allele.

Figure 5.3. The *RHBDF2* germline mutation was present in all areas of oesophageal squamous cell carcinoma from patient 33 indicating there is no loss of heterozygosity of the mutated allele.

Figure 5.4. The *RHBDF2* germline mutation was absent from oesophageal squamous cell carcinoma, dysplasia or muscle epithelium obtained from patient 34 indicating loss of heterozygosity of the mutated allele.

Figure 5.5. Single-nucleotide polymorphism analysis reveals genetic instability in patient 34 but not in patient 33.

Figure 5.6. Oesophageal squamous cell dysplasia and carcinoma show cytoplasmic RHBDF2 and ADAM17 expression.

Figure 7.1. Loss of heterozygosity of microsatellite marker D17S1832 was observed in patient 8.

Figure 7.2. Loss of heterozygosity of microsatellite marker D17S1881 was observed in patient 8.

Figure 7.3. Loss of heterozygosity of microsatellite marker D17S1506E was observed in patient 8.

Figure 7.4. Loss of heterozygosity of microsatellite marker D17S1678 was observed in patient 8.

Figure 7.5. Loss of heterozygosity of microsatellite marker D17S1176 was observed in patient 8.

Figure 7.6. Loss of heterozygosity of microsatellite marker D17S1881 was observed in

patient 10.

Figure 7.7. Loss of heterozygosity of microsatellite marker D17S250 was observed in patient 10.

Figure 7.8. Loss of heterozygosity of microsatellite marker D17S1881 was observed in patient 22.

Figure 7.9. Loss of heterozygosity of microsatellite marker D17S1506E was observed in patient 22.

Figure 7.10. Loss of heterozygosity of microsatellite marker D17S1176 was observed in patient 22.

Figure 7.11. Loss of heterozygosity of microsatellite marker D17S250 was observed in patient 22.

Figure 7.12. Loss of heterozygosity of microsatellite marker D17S1678 was observed in patient 33.

Figure 7.13. Loss of heterozygosity of microsatellite marker D17S1176 was observed in patient 33.

Figure 7.14. Loss of heterozygosity of microsatellite marker D17S1832 was observed in patient 51.

Figure 7.15. Loss of heterozygosity of microsatellite marker D17S1506E was observed in patient 51.

Figure 7.16. *TP53* mutations found in gastric adenocarcinoma but not in benign areas in patient 27.

Figure 7.17. *TP53* mutations found in gastric adenocarcinoma but not in intestinal metaplastic glands in patient 27.

Figure 7.18. Phylogenetic tree provides evidence for a monoclonal origin for gastric adenocarcinoma in patient 27.

List of commonly used abbreviations

AFAP – Attenuated familial adenomatous polyposis

AML – Acute myeloid leukaemia

APC – Adenomatous Polyposis Coli

ARID1A – AT-rich interactive domain-containing protein 1A

BO – Barrett's oesophagus

CBC – Crypt base columnar cell

CDKN2A – Cyclin-dependent kinase inhibitor 2A or $p16^{INK4}$

CDH1 – E-cadherin

COSMIC – Catalogue of Somatic Mutations in Cancer

CSC – Cancer stem cell

CTNNB1 – β-catenin

CRC – Colorectal cancer

EGFR – Epidermal growth factor receptor

EMT – Epithelial-mesenchymal transition

FAP – Familial adenomatous polyposis

FAT4 – FAT tumor suppressor homolog 4

FISH – Fluorescent *in situ* hybridisation

GA – Gastric adenocarcinoma

HDGC – Hereditary diffuse gastric cancer

HGD – High grade dysplasia

IBD – Inflammatory bowel disease

ISC – Intestinal stem cell

LCM – Laser-capture microdissection

K-RAS – Kirsten-RAS

LEF – Lymphoid enhancer factor

LGD – Low grade dysplasia

LOH – Loss of heterozygosity

MCR – Mutation cluster region

MCS – Metaplasia-dysplasia-carcinoma sequence

MET – Mesenchymal-epithelial transition

MSI – Microsatellite instability

mtDNA – Mitochondrial DNA

NRF2 – nuclear factor erythroid-related factor 2

OA – Oesophageal adenocarcinoma

OSCC – Oesophageal squamous cell cancer

PCR – Polymerase chain reaction

PIK3CA – Phosphatidylinositol 3-kinase

PTEN – Phosphatase and tensin homolog

Rb – retinoblastoma protein

RHBDF2 – Inactive Rhomboid Protease, also known as *iRhom2*

ROS – Reactive oxygen species

TA – Transit amplifying cell

TCF – T-cell factor

TOC – Tylosis with oesophageal cancer

TP53 – Tumour protein 53

TSG – Tumour suppressor gene

UC – Ulcerative colitis

WT – Wild type

1. Introduction

1.1. Gastrointestinal stem cells

The gastrointestinal epithelial mucosa requires constant cellular regeneration due to its rate of cellular turnover. This continuous replacement maintains tissue homeostasis, and is dependent on the function of gastrointestinal tissue stem cells. Stem cells are undifferentiated, unspecialised cells whose potential ranges depending on their tissue-specificity. All stem cells have the ability to self-renew, maintaining their numbers by symmetrical or asymmetrical division producing two daughter stem cells or one stem cell and a more rapidly replicating transit-amplifying (TA) cell or progenitor cell (*1*), respectively. Such progenitor cells have limited proliferation potential and eventually give rise to reproductively sterile terminally differentiated cells (*2*). In the intestine, TA cells are thought to divide in the crypt proliferative zone where their progeny ultimately differentiate into the mature intestinal epithelial cell types (*3*).

Gastrointestinal stem cells are a subset of tissue-restricted adult stem cells and are generally considered multipotent and able to differentiate into a limited number of cell types. Although it is difficult to identify these adult stem cells morphologically, they are characterised by residing within a stem cell 'niche', a specialised stem cell compartment or anatomical location that provides an optimal micro-environment for stem cell function in tissue generation, maintenance and repair (*4*). Within the intestine, such compartments may be maintained by mesenchymal cells located within the underlying lamina propia (*5*); in the small intestine, by Paneth cells located in the

crypt underneath the +4 position (*6*); and in the colon, by a subset of c-kit positive goblet cells regulated by Notch signalling (*7*).

Tissue-restricted stem cells are considered to be either quiescent or rapidly cycling and there is a great deal of debate as to their actual proliferative capacity (*6*). It has been hypothesised that quiescent bone marrow haematopoietic stem cells (HSCs) have a primary function in repair of injury and tissue damage (*8*). Moreover, it has also been documented that, in adult skin, a niche of quiescent stem cells located in the bulge (or stem cell reservoir) surrounding each hair follicle can be regenerated from engraftments of slow-cycling suprabasal bulge cells. These cells are located above the basal bulge cells between the old and the new hair follicle, and they become quiescent once they reach the niche (*9*). Potten and colleagues (*10*) showed that small intestinal stem cells retain the template DNA strands and lose the newly synthesised DNA strand following second division by labelling intestinal stem cells with tritiated thymidine (^{3}HTdR) and bromodeoxyuridine (BrdU). Long-term administration of BrdU was followed by a long-term cessation in order to remove all BrdU staining from the rapidly dividing cells: proliferating cells dilute the label every time they undergo mitosis, the only cells remaining labelled are the quiescent stem cells (*11*). However in 2007, Hans Clevers and colleagues identified rapidly cycling leucine-rich orphan G protein-coupled receptor (Lgr5, also known as gpr49) positive cells as crypt base columnar cells (CBCs) between the Paneth cells in the mouse small intestine, which appear to cycle rapidly. These cells seem multipotent and have the ability to differentiate into all the different intestinal epithelial cell types (*12*). Since then, several markers have been identified which co-expressed with Lgr5, either supporting the rapidly cycling stem cell theory or arguing for the presence of slow cycling

intestinal stem cells (ISCs). Recently, telomerase reverse transcriptase (mTert) GFP-knock in mice demonstrated multilineage differentiation from a single mTert cell, which can give rise to lgr5-positive cells (*13*). Interestingly the mTert-positive stem cell can also act as a label retaining cell by incorporating DNA synthesis labels for longer than TA cells, suggesting that there is a population of slowly-cycling stem cells that, upon stimulation, begin to proliferate and express lgr5 (*13*). It is possible that stem cell turnover rate may not be self-determined but is actually dictated by the surrounding micro-environment of the niche (*14*). Alterations in the niche, such as chronic inflammation, could initiate a burst of proliferation of either stem cells or their more committed progenitor cells (*2*).

Stem cells in the gastrointestinal tract can be classified according to their anatomical location i.e. oesophageal, gastric, intestinal and colonic, each with their own unique features. Stem cells all produce progeny with a restricted lineage potential. Cheng and LeBlond (*3*) (1974) proposed the Unitarian hypothesis, suggesting that all the differentiated epithelial cell lineages within crypts are derived from a single, multipotent stem cell. Therefore each small intestinal stem cell would have the potential to give rise to enterocytes, enteroendocrine cells, goblet cells and Paneth cells. A single intestinal stem cell has the potential to expand and replace the whole stem cell niche population, known as *niche succession* (*15*). Mutations, either through genetic drift or by conferring a selective advantage over wild type stem cells, will accelerate this process. Once their progeny has taken over the whole crypt, this will become a monocryptal clone through a process known as *monoclonal conversion;* it is thought to be one of the earliest events in the progression to adenoma development (*16, 17*).

Despite remarkable progress that has taken place in the last few years in the field of intestinal stem cell research, there are still many uncertainties regarding the location, proliferation status and differentiation capacity of gastrointestinal stem cells mainly due to the limited number of accepted tissue stem cell markers.

1.2. Intestinal stem cells

The flux of cell proliferation from the base of the intestinal crypt to the villus suggests that stem cells are located towards the base of the crypts yet superior to the Paneth cells (*18*) (*19*). However, recent studies have suggested that CBCs, which were first identified by Cheng and Leblond (*3*), could be the true stem cells, see Figure 1.1 (*6*).

To positively identify a crypt stem cell, a marker must be shown to label cells that are capable of multilineage differentiation. This is the gold standard of stem cell identification in any tissue (*20*).

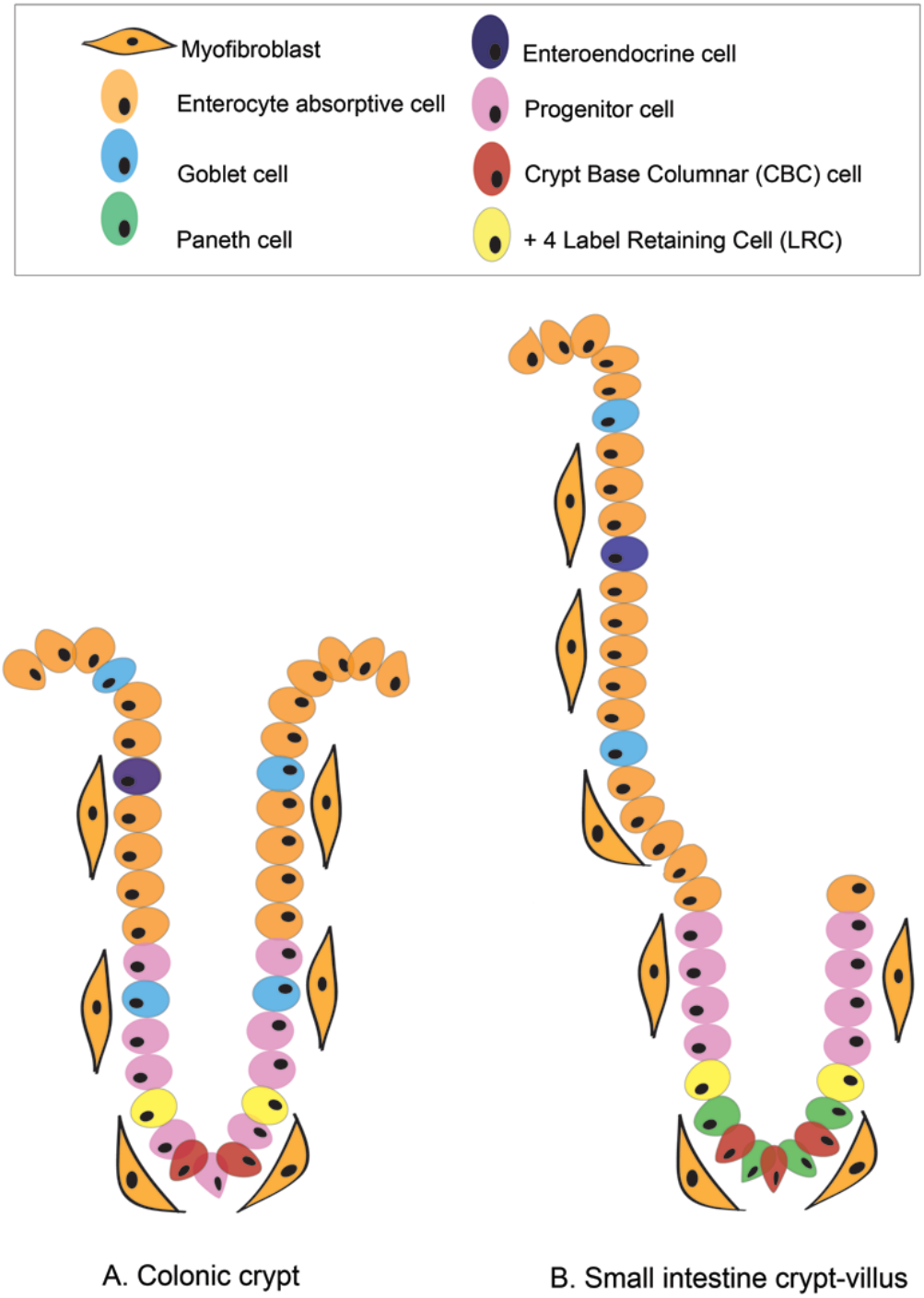

Figure 1.1. **The structure of the human small and large intestinal crypt.** Cartoons representing the colonic crypt (A) and the small intestine crypt-villus (B), with slow cycling label retaining cells (LRC) labelled in yellow and fast dividing crypt base columnar (CBC) cells in red.

1.2.1. Slowly cycling intestinal stem cells

There is some evidence to suggest that the rate at which stem cells proliferate is heterogenous within the intestinal crypt, some quiescent or slowly cycling and some rapidly dividing (*21*). Slowly cycling cells would accrue fewer genetic abnormalities over its life than a fast cycling cell as methylation occurs at mitosis. Stem cells are thought to be capable of retaining nucleotide-binding compounds such as bromo-5'-deoxyuridine. The 'immortal strand' mechanism of preservation is an innate mechanism of genome protection that may also be responsible for label retention in slowly cycling cells. Coupled with the altruistic apoptosis of mutated stem cells, this preservation mechanism would ensure the resistance of epithelial stem cell systems to short exposures to DNA-damaging agents (*22*).

After Potten and colleagues findings (*11*), it became apparent that the most common position for a label retaining cell (LRC) was around cell position +4 , 0 being the cell position at the very base of the crypt.

LRCs have a distinctive program of gene expression and are marked notably by their enriched expression of Bmi1. Bmi1 encodes a chromatin remodelling protein of the polycomb ring finger oncogene group with essential roles in self-renewal of haematopoietic, neuronal and leukaemic cells. Sangiorgi and Capecchi (*23*) found Bmi1 expressed in cells in position +4 and showed their ability to proliferate and differentiate into all the cell lineages of the small intestinal crypt (lineage-tracing), by generating a tamoxifen inducible Bmi1-Cre-ER mouse model. Lessard and Sauvageau

(*24*) also observed that Bmi1 seemed to have a role regulating the proliferative activity in normal stem and progenitor cells, and probably also in leukaemic stem cells.

Other potential stem cell markers have been identified apparently supporting the +4 stem cell hypothesis, however lineage-tracing has not yet been carried out and therefore we must treat these markers as unproven. Potential markers include sFRP5, a Wnt signalling antagonist whose mRNA is present in +4 LRCs (*25*), PTEN (phosphatase and tensin homolog), AKT1 and β-catenin, essential Tcf action cofactor resulting in transcription and expression of target genes leading to cell proliferation (*26, 27*). The EGF receptor antagonist leucine-rich repeats and immunoglobulin-like domains 1 (Lrig1) has been shown to maintain human epidermal stem cells in a quiescent state (*28*) and, in murine epidermis, Lrig1+ cells can give rise to all of the adult epidermal lineages in skin reconstitution assays (*29*). Another marker is doublecortin CaM kinase-like-1 (DCAML-1 or DCLK-1), a microtubule-associated kinase discovered in intestinal epithelial progenitor cells (*30*) and identified in quiescent +4 LRCs in radiation experiments, showing the importance of these cells for tissue renewal (*31*).

1.2.2. Fast dividing intestinal stem cells

In 2007, the intestinal stem cell marker Lgr5 was identified, questioning the previous theory of the location of stem cells and their ability to proliferate (*6*). Barker and colleagues used two knock-in mouse models, lgr5-LacZ and Cre-activatable R26R-LacZ reporter, confirming the expression of lgr5 in CBC cells and labeling them with BrdU; they established that CBC cells cycled on average every day. Crossing both

models they achieved a Cre-activatable lgr5-LacZ model, whose lgr5 positive cells in the small intestine and the colon were capable of generating all cell types of the epithelium. Therefore, via BrdU labeling and lineage tracing, Barker and colleagues proved that stem cells in the small intestine of the mouse can be rapidly proliferating cells (*12*). The *LGR5* and *LGR4* G-protein coupled receptors, as well as their homologues (*32*), have also been shown to be R-spondin receptors, binding the secreted Wnt signalling agonists R-spondins and, therefore, regulating embryonic patterning and stem cell proliferation (*33*).

Later in 2009, prominin-1 (CD133), a five-transmembrane-domain-containing glycoprotein that is expressed on a variety of normal stem cells was present on some cells located at the base of the small intestinal crypts that also co-expressed LGR5 (*34*). These cells were able to generate all intestinal epithelial cell lineages and therefore appear to be small intestinal stem cells (*35*). Furthermore, olfactomedin 4 (OLFM4), a member of the olfactomedin-related protein family that has the ability to bind to cadherins and lectins and can mediate cell adhesion, was identified in a gene expression profile for LGR5-positive cells. CBC cells in the human small intestine and colon have been shown to express high levels of OLFM4, indicating that this gene might also be a marker for intestinal stem cells (*36*).

Interestingly there are a few markers that have been found in lineage in both CBCs and 4+. One example is musashi 1 (Msi1), an RNA-binding protein involved in a unique autocrine signalling pathway activating both the Wnt and Notch pathways (*37*). Msi is known to maintain the proliferation of multipotential neural stem/progenitor cells, to be rapidly downregulated in post-mitotic neurons and to be upregulated in

tumours in the central nervous system (*38*). Another marker is cholecystokinin 2 receptor (CCK-2R), the primary receptor for cholecystokinin (CCK) and amidated gastrin. CCK-2R has been found expressed in colon crypts adjacent to the proliferative zone and its inactivation affected both cell types DCAMKL-1-positive (4+) and LGR5-positive (CBCs) and also colonic crypt fission. These findings suggest that CCK-2R is expressed in the two potential intestinal stem cell types and that it may be a potential target in the treatment or prevention of colorectal cancer (CRC) (*39*). Another possible marker might be cytokeratin CK19, a bile duct marker that may also label intestinal stem cells as lineage-tracing studies found that almost the complete epithelium was labelled by this marker (*40*).

1.2.3. Clonal analysis of the intestinal epithelium

Monoclonal conversion, or clonal replacement, is the process whereby a mutated stem cell that has already established itself in the niche clonally expands to fill the entire crypt. There is a need to assess this process for the identification of stem cells and the location of stem-cell niches in the gastrointestinal tract, as it is essential to the understanding of tumour development in the colon (*41*). Moreover, clonality studies are essential to analyse lineage relationships and assess mutation order and timing in carcinogenesis, in order to establish the origins of colonic adenomas and CRC and also possible targeted therapies. Following the Unitarian hypothesis from Cheng and Leblond (*3*), a considerable body of research has used clonal analysis to study the clonality of small and large intestinal crypts.

Winton and Ponder, in 1990, found the first evidence for clonal mouse small intestinal crypts using whole mounts from heterozygous Dlb-1 locus mice with a peroxidase conjugate of the lectin *Dolichus biflorus* agglutinin (DBA-Px) (*42*). By inducing somatic mutations in individual cells in *Dlb-1*$^{+/+}$ mice, the authors proved the existence of long-lived, pluripotent stem cells that can give rise to all epithelial cell lineages. Later, Bjerknes and Cheng performed chemical mutagenesis in *Dlb-1*$^{-/-}$ mice revealing the existence of a short-lived progenitor cell type generating committed progenitors for the different epithelial lineages (Mix), long-lived mucous and columnar progenitors (M_0 and C_0) and pluripotent stem cells generating additional cell lineages (S) (*43*).

Williams and colleagues studied the loss of O-acetylation of sialomucins using the mild periodic acid-Schiff (mPAS) staining in individuals heterozygous for O-acetyltransferase gene activity in colonic and small intestinal crypts, in patients with or without radiotherapy (*44-46*). These workers concluded that wholly mutated crypts are persistent, that partially mutated crypts are transient and that clonal stabilisation time in the colon is approximately one year in humans. The difference between species and the small and large intestine was attributed to the different number of stem cells in the niche and also to the rates of crypt fission and stem cell cycle time (*46*).

In humans, an extremely rare case of familial adenomatous polyposis (FAP) in an XO/XY patient showed, by *in situ* hybridisation for the Y chromosome, that human small and large intestinal crypts were also clonal (expressing only XO or XY). Interestingly, Novelli and colleagues also observed that at least 76% of human colorectal microadenomas were polyclonal in origin (*47*). Thirlwell and colleagues

confirmed this observation by analysing individually microdissected crypts of the same XO/XY patient individually and of other patients with either familial conditions (FAP or attenuated FAP) or with sporadic adenomas or carcinoma-in-adenomas (*16*). They found microadenoma polyclonality in FAP patients and also in some patients with sporadic lesions. The inherited abnormal genetic background and the local or regional exposure, such as chronic mucosal inflammation, can influence which mutations are selected. Therefore, the most likely cause of adenoma polyclonality could be the interaction between an initiated crypt and its neighbours, mainly due the aberrant epithelial-stromal interactions caused by *APC* mutations and predisposing wild-type non-dysplastic neighbouring crypts to select for an independent epithelial mutation.

Findings in female mice heterozygous for the X-linked gene glucose-6-phosphate dehydrogenase ($G6PD^{+/-}$) suggested that crypts were clonal in origin and that intestinal villi were polyclonal. Polyphenotypic villi were observed by X-linked enzyme histochemistry due to a contribution of epithelial cells from multiple crypts (*48*). Using the same technique on Sardinian females heterozygous for the G6PD Mediterranean mutation (Cys563Thr), Novelli and colleagues showed that clonal patches in the human colon could become relatively large and that human intestinal crypts are clonal (*49*).

Mitochondrial DNA (mtDNA) mutations have been used as markers of clonal expansion allowing analysis of the clonal architecture of individual human epithelial units (*50, 51*). Mitochondria are the major cellular generators of adenosine triphosphate (ATP) and cells contain multiple copies of mitochondrial genomes.

MtDNA is a small 16.6kb self-replicating molecule that encodes 13 proteins of the oxidative phosphorylation pathway, 2 ribosomal RNAs and 22 transfer RNAs (*52*). The mitochondrial genome is especially susceptible to mutation due to its lack of protective histones, its high oxidative stress location and its limited repair mechanisms (*53*). MtDNA mutations are random, increase with age, and they can either affect all copies (homoplasmy) or a portion of the copies (heteroplasmy) of the mitochondrial genome. For a mutation to result in a mutated cellular phenotype, homoplasmy or a high degree of heteroplasmy is necessary (*54*). When using mtDNA mutations to assess niche succession and clonal conversion in humans, it needs to be considered that monoclonal mutated crypts are very rare in patients under 40 years of age. This is due to the time needed for a mutation to occur in a single mitochondrion in an intestinal stem cell and also to the achievement of homoplasmy, in order to have a single mitochondrial DNA-mutated intestinal stem cell. In colonic crypt stem cells, Taylor and colleagues identified homoplasmy of mtDNA mutations using the biomarker of mtDNA defects cytochrome *c* oxidase deficiency (*50*). It has been found subsequently that these cytochrome *c* oxidase deficient mutated crypts can expand clonally by crypt fission, which can have important implications for the biology of the normal human colon (*55*). However, because such mtDNA mutations do not confer a selective advantage they need to expand by the same stochastic process as wild type intestinal stem cells, hence, only around 15% of the crypts are mutated by the time individuals reach the age of 80 (*41*).

Original findings using methylation tags as a lineage-tracing marker suggested that there were multiple stem cells in the colonic crypts that eventually, due to a ‘bottleneck effect’, become related to the closest stem cell ascendant (*56*). Kim and

Shibata used methylation patterns to determine if adjacent adult crypts have similar methylation patterns at CpG sites compared to widely separated crypts (*57*). No evidence was found to prove that directly adjacent or branched crypts are more highly related than the widely separated ones. This lack of similar methylation patterns between closely related crypts indicates that methylation patterns diverge rapidly during ageing in long-lived adult human colonic crypts.

Microsatellites, also known as simple sequence repeats (SSR) or short tandem repeats (STRs), are widely dispersed, hypervariable regions of repetitive DNA sequences composed of 2-6 base pairs. Because of their polymorphic nature and inheritance in a Mendelian codominant manner, microsatellites have been previously used as clonal markers allowing distinction between chromosomes. The loss of heterozygosity (LOH) of microsatellites has been extensively studied to assess tumour suppressor loss in tumour development and to investigate genetic instability in the non-tumour epithelium surrounding areas of cancer in order to track mutated clones and to determine the risk of tumour regrowth (*58-60*). However, more than one microsatellite must display LOH in order to be considered a reliable clonal marker, as loss of only one microsatellite might be due to a field defect or coincidence. Therefore monoclonal proliferation will be ensured when multiple and consistent microsatellite markers along the same gene or region of interest with LOH are demonstrated (*61*). Frumkin and colleagues studied the clonal origin of a mouse lymphoma by performing cell lineage reconstitution, genotyping 120 microsatellite loci from microdissected single cells from the tumour (*62*). Their reconstructed cancer cell lineage tree revealed a monoclonal origin for the carcinoma in a tumour founder cell and a clustering of the

tumour cancer cells and metastasis cells on the same subtree and, therefore, presenting a very similar microsatellite pattern.

Field cancerisation is the process whereby a single clone can expand, preconditioning a large field of epithelium to undergo neoplastic transformation and ultimately develop into cancer. Such fields do not necessarily present a change in cell phenotype but constitute a distinct biological stage in epithelial carcinogenesis (*63*). Recent studies on long-standing Crohn's disease patients have revealed that field cancerisation occurs in the large intestinal epithelium accounting for the extensive spread of pre-tumour clones in non-tumour epithelium throughout the colon and showing that dysplastic epithelium is an unreliable marker for cancer risk (*64*). We can conclude that the initiation of colorectal tumourigenesis is more complex than previously thought and that this complexity is likely to be representative of the overall tumourigenic process in the gastrointestinal tract.

1.3. Gastric stem cells

The human gastric mucosa is divided into cardiac zone, corpus zone (including the fundus) and the antral or pyloric zone (Figure 1.2). There are different types of gastric glands: corpus glands (found in the fundus and corpus) and antral or pyloric glands (found in both cardiac and antral zones) (*65*). The corpus glands contain acid producing parietal cells and pepsin producing chief cells, whereas the pyloric glands consist of mucus secreting cells and are responsible for gastrin hormone production.

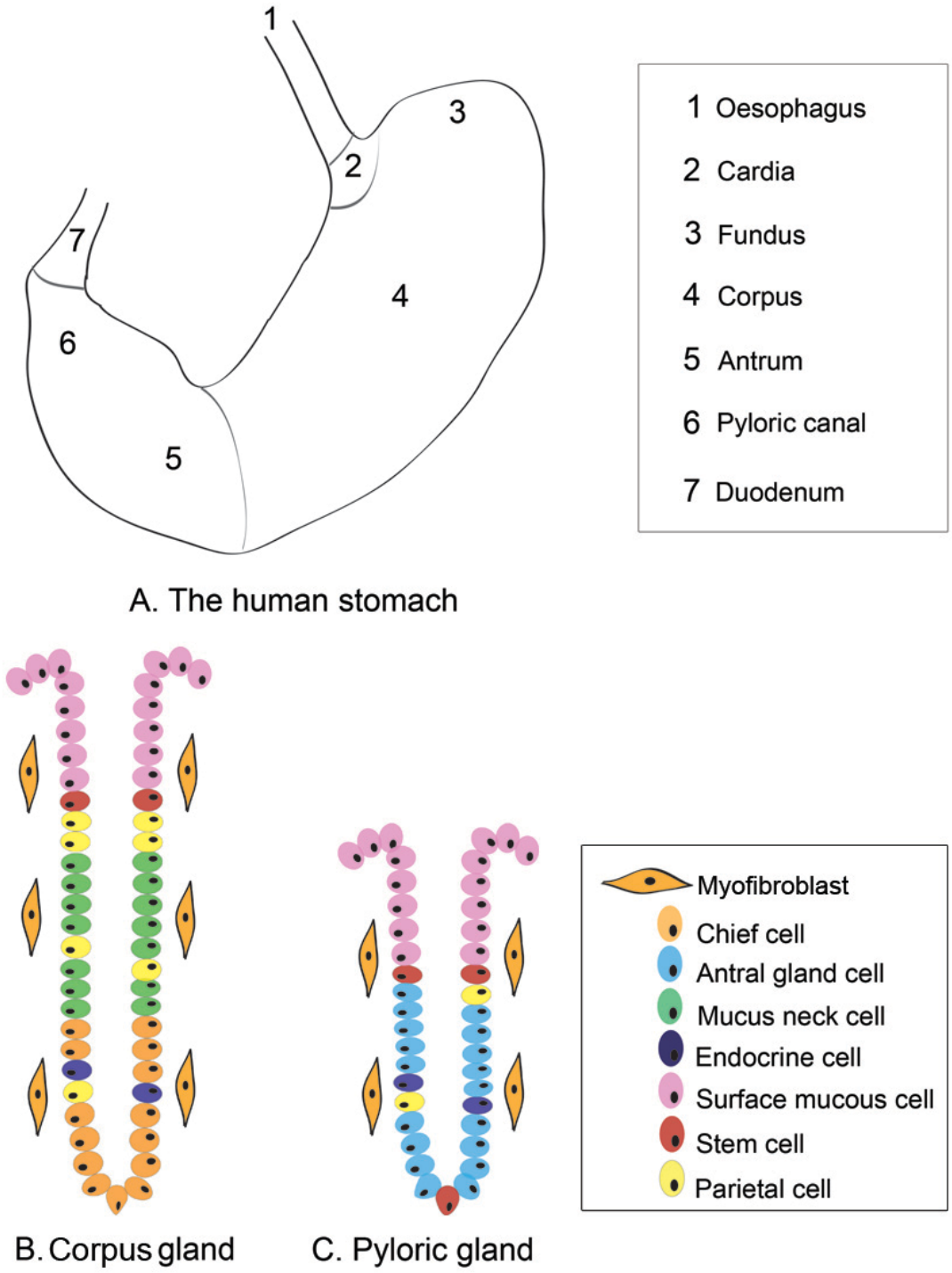

Figure 1.2. **The structure of the human stomach and the gastric corpus and pyloric glands.** Cartoons representing the human stomach (A), the corpus (B) and the pyloric (C) glands, with gastric stem cells labelled in red.

Human and mouse gastric epithelial stem cells are thought to be located around the isthmus/neck region of gastric glands, an area above the neck and underneath the pit of the gland (*30, 66*). This is based on the fact that there is bidirectional migration of proliferating cells up towards the pit and down the gland base. Gastric stem cells are capable of differentiating into foveolar surface cells (or surface mucous cells) forming the gastric pit, and parietal cells (or oxyntic cells) and chief cells (or zymogenic cells) lining the gland, see Figure 1.2 (*67*).

1.3.1. Gastric progenitor and stem cell markers

Gastric stem cells, like intestinal stem cells, are believed to be located within a niche maintained by mesenchymal cells. However, even though several possible stem cell markers have been found in the small intestine and colon, only a few have been found to label gastric stem or progenitor cells. One example is DCLK-1, which has been found to label single cells in the isthmal stem cell niche of gastric glands within the corpus (central) region of the stomach of adult mice (*30*). Giannakis and colleagues observed using a multilabel immunohistochemical study solitary DCLK-1-positive cells in the isthmus region positioned next to fast-dividing BrdU-positive progenitor cells. These cells did not express any gastric differentiation lineage markers and seemed to be produced by pre-neck cell progenitors, characterised by cored secretory granules and giving rise to the zymogenic cell lineage (*66*). These findings suggest that DCLK-1 is not only an intestinal stem cell marker, but also a marker of adult gastric stem cells.

Qiao and colleagues (*68*) identified a gastric progenitor cell (GPC) population using Villin$^{\beta\text{-gal}/+}$ transgenic mice. They observed one to two villin-positive cells in the lower third of the pyloric glands, located at or below the isthmus region, and showed that these GPCs have the ability to re-populate entire glands. Their BrdU study suggested that this cell population is also quiescent, indicating that villin might be a useful marker for slow cycling stem or progenitor cells.

When Barker and colleagues confirmed *Lgr5* expression in CBC cells in the small intestine and colon in their two knock-in mouse models, Lgr5-LacZ and Cre-activatable R26R-LacZ reporter, they also found *Lgr5* expression at the bottom of antral glands (*6*). Barker and colleagues later found *Lgr5* expression in both human and mouse embryonic stomachs throughout the developing gastric glands (*69*). The results from their *Lgr5-EGFP-ires- CreERT2* mice revealed that Lgr5-positive cells were found in the pylorus regions. These observations indicate that there are rapidly diving stem or progenitor cells that can repopulate the epithelium of the antrum and pyloric canal and that *Lgr5* is a marker for stem or progenitor cells in the stomach.

Quante and colleagues (*67*) showed that trefoil factor family 2 (*TFF2*) mRNA transcript expression (TTE) labels a multilineage gastric progenitor cell for parietal, mucus neck and zymogenic cell lineages in gastric corpus glands using a TFF2-BAC-CreERT2 transgenic mouse model. Even though these TTE progenitor cells cannot differentiate into pit cells or neuroendocrine cells in the corpus, *TTF2* can be used as a marker for oxyntic gastric gland progenitor cells.

1.3.2. Clonal analysis of the gastric epithelium

In 1998, initial studies suggested that human gastric glands were polyclonal in origin by showing X-chromosome-linked inactivation of the HUMARA gene. These studies revealed that even though pyloric (antrum) glands appear homotypic and are thus monoclonal, 50% of fundic (oxyntic) glands are actually heterotypic and therefore polyclonal (*70*). Subsequently, other clonality studies analysing mutations in mtDNA showed that, like in the normal human colon, mtDNA mutations also establish themselves in stem cells within the normal human gastric corpus gland. These cells have the ability to differentiate into all gastric cell lineages, producing a new clonal gastric gland via niche succession and *monoclonal conversion* (*71*). McDonald and colleagues also demonstrated that mtDNA mutated gastric glands can divide by fission, leading to clonal patches sharing the same mtDNA mutation. CCO-deficient partially mutated glands are also observed, revealing the presence of multiple stem cells within the gastric gland.

During field cancerisation in the stomach, Gutierrez-Gonzalez and colleagues showed that over time the field could become genetically diverse, suggesting that gastric cancers can arise from a subclone of the founding original mutation (*72*). These workers proved that intestinal metaplasia (IM) of the stomach can clonally expand by crypt fission and that dysplasia arises from a single mutated IM gland. Hence, IM is field cancerisation of the human stomach and gastric cancer develops through progression of the initial founder mutation.

1.4. Oesophageal stem cells

The oesophagus is lined with stratified squamous epithelium that can be divided histologically into two layers, a differentiated layer composed of multiple layers of flattened and differentiated squames (keratinocytes) and a generative basal layer. This second layer is formed by a single layer of cells that adhere to the basement membrane followed by a variable number of cell layers above this (the epibasal or suprabasal layer). In humans, the lamina propia underneath this luminal surface of the oesophagus invaginates the epithelium at regular intervals dividing anatomically the basal layer into interpapillary basal layer (IBL) and papillary basal layer (PBL), see figure 1.3 (*73*).

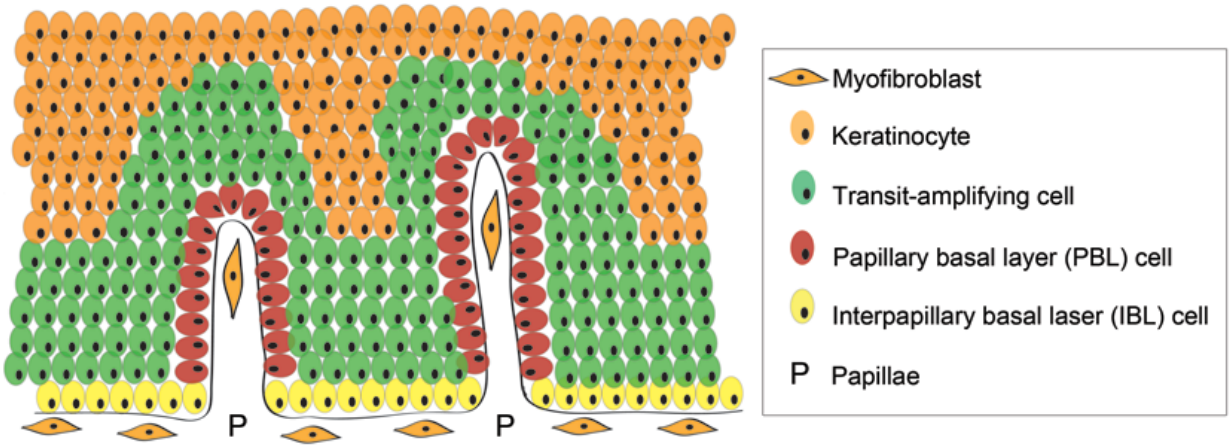

Figure 1.3. **The basic structure of human oesophageal epithelium.** Cartoon representing the human stratified oesophageal epithelium, with papillary basal layer (PBL) cells labelled in red and interpapillary basal layer (IBL) cells labelled in yellow.

Using a transgenic mouse model, Jones and colleagues suggested that the oesophageal epithelium is maintained by a single progenitor cell that divides stochastically with the same probability of generating proliferating or differentiating cells (*74*). After

wounding, the authors observed that these single progenitors have the ability to switch between homeostatic and regenerative behaviour without the need for a slow-cycling stem cell pool.

Oesophageal stem cells are thought to reside and be restricted to the basal layer (*75*). Seery and Watt (*76*) observed that the IBL was enriched with slow proliferating cells and had a high proportion of asymmetrical mitoses, whereas cells in the PBL seemed to undergo symmetrical mitosis and divided frequently. Using fluorescence-activated cell sorting (FACS) and an *in vitro* study these authors had shown that stem cells in the oesophagus reside in the IBL and that transit-amplifying cells reside in the PBL. Cells are thought to migrate from the basal layer towards the oesophageal lumen and this is associated with initiation of differentiation followed by expression of differentiation markers (*77*).

1.4.1. Oesophageal progenitor and stem cell markers

The isolation and characterisation of oesophageal stem cells remains elusive as definitive progenitor or stem cell markers still remain to be found. Moreover, the stratified squamous epithelium of the oesophagus and the epidermis come from different embryological origins and exhibit different functions. Hence, stem cell markers from the epidermis cannot be related to the oesophageal epithelium. For example, some findings have suggested that adhesion molecules such as the β1 integrin subunit might be a marker for keratinocytes given the high levels expressed in stem cells of the epidermis (*78*). However, the slow-dividing IBL stem cell expresses low levels of this marker (*76*).

The ability to exclude Hoechst 33342 DNA binding dye mediated by the ABCG2 transporter was first used to isolate stem cells as a side population (SP) in the haematopoietic system. This HSC SP was shown to rescue lethally irradiated mice and to differentiate into both myeloid and lymphoid lineages (*79*). By using the Hoechst 33342 dye efflux test, Kalabis and colleagues (*80*) isolated a SP from the oesophageal epithelium of previously BrdU-treated mice. A fraction of this SP was BrdU+ and was localised to the oesophageal basal cell compartment. Furthermore, the fraction of this SP expressed the bone marrow stem cell marker, CD34, formed colonies and matured into differentiated epithelium in an organotypic (3D) cell culture. This suggests that the CD34-positive fraction has the capacity for self-renewal, can participate in epithelial regeneration and also that CD34 is a potential candidate as an oesophageal stem cell marker.

Croagh and colleagues observed three independent populations within the basal layer of the mouse oesophagus, based on the expression of α_6 integrin and transferrin receptor (CD71) obtained by FACS (*81*). They found that the $\alpha_6^{bri}CD71^{dim}$ population (high α_6 integrin combined with low CD71) had a slower turnover rate, maintaining BrdU expression the longest, and that it could regenerate the other two cell populations in the tissue reconstitution assay. These observations suggest that the $\alpha_6^{bri}CD71^{dim}$ population can self-renew and has an increased long-term proliferative capacity, indicating that high α_6 integrin and low CD71 levels might serve as markers of oesophageal progenitor or stem cell markers.

1.5. Stem cells in cancer in the gastrointestinal tract

Self-renewal, or the capability of a stem cell to maintain its own population, is thought to become dysregulated within a tumour (*82*). This has lead to the theory that there is a population of stem-like cells within tumours: the so-called cancer stem cell, which refers to the capacity of a subpopulation of cancer cells that can initiate tumourigenesis (*83*). If we also subscribe to the mutation and selection theory of cancer development, the longer a proliferative cell survives, the greater the chance of accruing increasing numbers of genetic abnormalities which can be passed on to its progeny. The tissue stem cell is a long-lived cell and is considered the prime suspect as the tumour-initiating cell of many tumours (*84*). The cancer stem cell (CSC) theory was first proposed by Julius Cohnheim in 1867 and evidence demonstrated first by Hamburger and Salmon (1977) (*85*) who showed that only 1 in 1,000 to 1 in 5,000 cells from a cancer were able to grow macroscopic colonies on soft agar. Some 17 years later John Dick and colleagues were the first to show *in vivo* that acute myeloid leukaemia (AML) could be induced in SCID mice by transplantation of a subset of AML cells. They were able to identify an AML-initiating cell occurring with a frequency of 1 in 250,000 peripheral blood cells and show that the initiating cell produces colony-forming cells with cell-surface-marker expression CD34+ CD38- (*86*). Later studies have suggested that a similar model exists for solid tumours, however, some may conform to the clonal evolution model, in which a dominant population of proliferating cells drives tumorigenesis (*87, 88*). These two models are not mutually exclusive, as CSCs themselves undergo clonal evolution as shown for leukaemia stem cells (*89*).

Kirkland, in 1988, observed that a single human rectal adenocarcinoma cell was capable of generating tumours with columnar, mucous and endocrine cells lineages upon xenotransplantation in nude mice (*90*). Therefore, this study showed that all epithelial lineages are clonal. Since, Vermeulen and colleagues (*91*) performed a similar experiment and observed that the single cells responsible for reconstituting the original tumour contained expression of proposed markers for stem cell populations. This study showed that tumour heterogeneity might also be due to the multipotential characteristics of CSCs, instead of necessarily being caused by the presence several CSCs in a tumour (*92*). The CSC hypothesis may therefore need to be specific for different tumour-types, depending on the origin of the CSC and the changes that occur during tumour progression (*93*) (e.g. the epithelial-mesenchymal transition (EMT), characterised by the acquisition of motility, invasiveness, and self-renewal traits (*94*)).

However, there is great debate within those who subscribe to the CSC theory of cancer development as to how common CSCs actually are. In the past, CSCs have been considered to be very rare, but it now appears that many combined factors may have greatly underestimated their frequency (*93*). The CSCs ratio obtained from immunodeficient mice transplantation experiments can be increased by enriching the number of CSCs selected and by providing them with a niche, after transplantation. This can be done by firstly selecting cells expressing either the ATP-Binding Cassette (ABC) transporter genes, the largest family of membrane transport proteins, and the aldehyde dehydrogenase (ALDH) gene family, responsible for the oxidation of aldehydes to carboxylic acids and therefore the ability to induce drug inactivation. Furthermore, the use of matrigel facilitated tumour growth of human melanoma

ABCB5 enriched circulating tumour cells (CTC) in NOD/SCID *Il2rγ*$^{-/-}$ mice (*95*), proving that a niche-like environment improves CTC detection in assays.

1.5.1. Cancer stem cell markers in the gastrointestinal tract

Two CSC markers have emerged as the most useful for identification purposes in a variety of systems. CD44 is the major ubiquitously expressed cell surface receptor for hyaluronic acid (HA) and is a known downstream target of the Wnt/β-catenin pathway. It is known to undergo complex alternative splicing and participate in cellular functions such as lymphocyte activation, recirculation and homing, haematopoiesis and tumour metastasis. CD44 was the first marker identified for a solid tumour in breast cancer, forming a subpopulation of tumourigenic cells when highly expressed and associated with low levels of CD24 (*96*). It has since been observed in hepatocellular carcinoma (*97*), in sporadic and hereditary gastric cancer (*98*) and used for isolating a population of gastric cancer cells with increased resistance to chemotherapy and radiotherapy induced cell death (*99*). It has also been found to label the CSC capable of generating multilineage differentiation in CRC combined with CD166, CD29, CD24, LGR5, nuclear B-catenin and prominin-1 (CD133) (*91*).

The pentaspan transmembrane glycoprotein prominin-1 (CD133) has also been identified as an alternative cancer stem cell marker for many tumours. The CD133 protein is thought to function in maintaining stem cell properties by suppressing differentiation (*20*). It has been observed in neuroblastoma (*100*), endometrial cancer (*101*) and in a minority of cells in hepatocellular carcinoma (*102*). Even though

CD133 has been previously observed in CSC in CRC (*91*), Shmelkov and colleagues (*103*) found that CD133 was expressed in differentiated epithelial cells and that both CD133-positive and CD133-negative metastatic colon CSCs can initiate tumours. Similarly, another study carried out by Lugli and colleagues in a large archival cohort of patients showed inconclusive data related to the presence or absence of CD133 in CRC (*104*). Therefore, although CD133 might be used in combination with other markers to identify CSCs, these findings suggest that CD133 expression is not restricted to somatic and cancer stem cells (*105*).

Schepers and colleagues observed that the crypt stem cell marker Lgr5 also marked a subpopulation of 5 to 10% of adenoma cells, which were responsible for generating further Lgr5-positive cells as well as all other adenoma cell types (*106*). Several other stem cell markers could be viable CSC markers. However putative markers still require further studies for a consensus to be reached as many experiments have only been carried out in immunodeficient animal models. Nevertheless, it is thought that targeting specific CSCs will allow the development of a much more effective treatment for cancer when restricted CSC markers are finally identified (*107*) (*108*).

1.5.2. Models of neoplastic development

There are two conflicting models of neoplastic development in colorectal adenomas; and both consider that the founder mutation occurs in stem cells of the colonic crypt. The ‘bottom-up’ hypothesis suggests that a clone of cells is produced by expansion of a mutated stem cell in the base of the crypt. This occurs either stochastically or due to selective advantage, and is followed by the colonisation of the entire crypt by this

dysplastic epithelium to form a clonal monocryptal adenoma (*47*). It was demonstrated that the "bottom-up histogenesis" (*109*) occurred when Barker and colleagues showed that Lgr5-positive cells comprise the tumour initiating cell population (*110*) and Tian and collagues proved that Bmi-positive cells can repopulate the Lgr5 population after tissue damage in intestinal cancer in mice (*111*). The *crypt fission index* (proportion of crypts in fission) is up-regulated in colorectal adenomas, colorectal hyperplastic polyps and other cases of genomic instability such as ulcerative colitis (UC) and Crohn's disease (*112*).

The 'top-down' hypothesis suggests that the mutated stem cells are located between the crypt orifices, in an intracryptal zone. From this area, it is thought that the dysplastic tissue spreads laterally and downwards into the adjacent crypts. It has been suggested that the stem cells might migrate to the intracryptal zone once the mutation is acquired before undergoing adenomatous spread (*113*). This has been observed in larger adenomas where evidence suggested an overspill of dysplastic tissue or an adenomatous field effect on neighbouring crypts. Recently, Schwitalla and colleagues used a mouse model to prove that Lgr5-negative enterocytes had the ability to dedifferentiate and reacquire stem cell properties by re-expressing Lgr5, supporting the 'top-down' hypothesis (*114*). Thus, the 'bottom-up' mechanism of clonal expansion occurs to form a monocryptal adenoma, which followed by the 'top-down' mechanism as the clone spreads into the adjacent crypts in larger adenomas (*27, 115*).

1.6. The adenoma-carcinoma sequence

The principle generally held in cancer biology is that of the mutation and selection theory (*116*). Dating back to the 1970s, it suggests that clonal selection in the primary tumour drives cancer progression and metastasis (*117*). Morson and colleagues observed that even though not all benign adenomatous polyps or villous adenomas progress into CRC, the majority of colon and rectum cancers arise from previous adenomas (*118*). This concept was then termed the adenoma-carcinoma sequence (*119*), which is now accepted as the underlying process behind the majority of cancers (*120*). For a summary of the adenoma-carcinoma sequence (*121*), see Figure 1.4.

The "Vogelgram", or multistep cancer progression model of CRC, defined the genetic process behind the development and spread of neoplasia. This model is based on the order and the accumulative effect of the multiple mutations of oncogenes and tumour suppressor genes (TSGs) that lead from normal epithelium to pre-invasive neoplasms and finally to malignant tumours (*122*). It has since been adopted as a model for many other cancers (*123-126*).

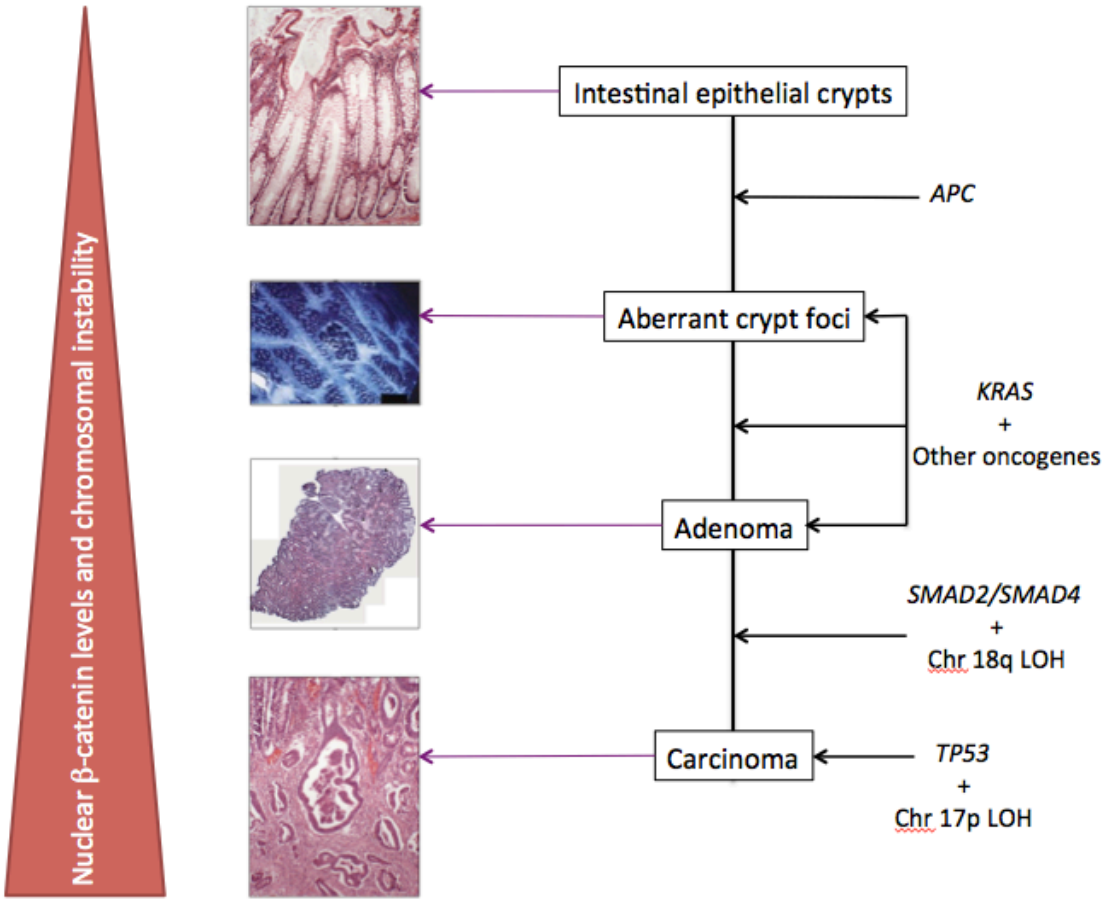

Figure 1.4. **The adenoma-carcinoma sequence leading to colorectal carcinomas. Figure adapted from Fodde and colleagues (*121*).** *APC* mutations have been observed as the earliest genetic alteration in colorectal cancer development, followed by *KRAS*, *SMAD2/SMAD4* and *TP53* mutations. LOH of chromosomes 18q and 17p has been found to occur simultaneously. Nuclear β-catenin levels have been shown to increase with chromosomal instability as malignancy progresses.

1.7. Genes involved in gastrointestinal cancers

1.7.1. The *Wnt* signalling pathway

The *Wnt* signalling pathway plays a crucial role in regulating cellular processes involved in development, differentiation, and adult tissue homeostasis (*127*). Wnts are a large family of secreted glycoproteins with 19 isoforms identified in humans. They have been found in many species including *Drosophila*, where is it known as the

wingless (Wg) gene, the best characterized Wnt gene. Aberrant signaling in this pathway has been associated to mutations in *Axin*, *Adenomatous Polyposis Coli* (*APC) and CTNNB1* (β-catenin), where β-catenin is central in the signaling cascade.

Under normal conditions, in the absence of Wnt signaling, cytoplasmic β-catenin is recruited into a destruction complex where it interacts with APC and Axin, and undergoes serial serine phosphorylation by the glycogen synthase kinase-3 β (GSK-3β) and casein kinase 1α (CK1α). The marked protein is then degraded via the ubiquitin-proteasome pathway resulting in low levels of cytoplasmic β-catenin and forcing the transcription factors lymphoid enhancer factor (LEF) and T-cell factor (TCF) to interact with their corepressor Grouchos in the nucleus in order to repress Wnt-specific target genes (*128*). However, when present, canonical Wnt ligands bind to Frizzled membrane receptors and LRP5-LRP6 co-receptors in the plasma membrane leading to the phosphorylation of LRP5 or LRP6 and the formation of the Dishevelled polymer. Amongst other roles, this polymer will mediate the translocation of Axin to the plasma membrane and will inactivate the destruction complex. The stabilization of β-catenin will lead to an increase of β-catenin in the cytoplasm followed by a translocation of β-catenin into the nucleus where it will displace Grouchos and will form a transcriptionally active complex with Tcf-4 (a member of the TCF/LEF family), and other co-activators. This will lead to the transcription and expression of Wnt target genes responsible for cell proliferation, such as the protooncogene MYC and cyclin D1 (*26, 129*). Wnt signaling has been found to play an important role in cancers of the gastrointestinal tract (*130*).

1.7.1.1. Adenomatous Polyposis Coli

APC is a classified tumour suppressor gene (TSG), known to be located in the long arm of chromosome 5, between positions q21 and q22. Loss of control of the *Wnt* signalling pathway due to mutation of the tumour suppressor *APC* is known to be an early event in colorectal adenocarcinoma formation, particularly familial adenomatous polyposis (FAP) associated with one or more genes on chromosome 5q21 (*131*). FAP results from a germline inherited mutation on an *APC* allele followed by a subsequent 'second hit' on the other allele, rendering the tumour suppressor inactive. Miyoshi and colleagues observed that over 60% of the somatic mutations observed in their cohort of FAP patients were clustered in a small region of exon 15 in the *APC* gene known as the mutation cluster region (MCR) (*132*). The inability of the APC protein destruction complex to degrade cytosolic β-catenin leads to over-transcription of target genes. This will cause the formation of multiple bowel adenomas (*27*).

Sivak and colleagues observed that gastric cancer risk is at least ten times higher in FAP patients than in the general population (*133*). Two studies by Horii, Nakatsuru and colleagues using ribonuclease (RNAse) protection analysis coupled with PCR sequencing revealed that a high proportion of very well differentiated gastric adenocarcinomas (GAs) and signet-ring cell carcinomas exhibited mutations in the *APC* gene, suggesting that *APC* plays a role in gastric carcinogenesis in these two types of cancer, but not in poorly differentiated GAs (*134, 135*). However another study by Fang and colleagues observed *APC* mutations in 33% of intestinal-type GA, independent of grade of differentiation, tumor size, depth of invasion or node

metastasis. They observed, however, that diffuse gastric cancers have a much lower frequency of *APC* mutations (*136*).

1.7.1.2. β-catenin

As mentioned in 1.7.1, β-catenin is a ubiquitous intracellular protein with an essential role in the Wnt canonical pathway. However, it is also very important for intercellular adhesion by linking the cytoplasmic domain of cadherin to α-catenin, resulting in the anchoring of the adhesion complex to the cytoskeleton (*137*). *CTNNB1* mutations have been observed in several types of cancer, such as colorectal, endometrial, hepatocellular, ovarian, prostate, intestinal gastric cancer and uterine endometrioid carcinoma (*138-141*).

Park and colleagues observed that over a quarter of the intestinal-type GAs in their cohort presented mutations in the *CTNNB1* gene. All of the mutations they observed were missense mutations clustered in a region of exon 3 responsible for encoding the GSK-3β phosphorylation consensus region of the *CTNNB1* gene. Their findings revealed no *CTNNB1* mutations in hereditary-diffuse gastric cancer patients (*142*). However, Clements and colleagues observed that 23% of intestinal-type gastric tumours and 38% of diffuse-type tumours presented mutations in *CTNNB1* (*143*). Tong and colleagues also found one *CTNNB1* mutation in a diffuse-type cancer but observed a very low frequency of *CTNNB1* mutations in intestinal-type gastric cancer (*144*). Therefore, the frequency of *CTNNB1* mutations seems variable between cohorts, but it is apparent that *CTNNB1* mutations and the canonical *Wnt*-pathway activation contribute to gastric carcinogenesis.

1.7.2. The *TP53* signalling pathway

The tumour protein gene (*TP53*) is a 20kb gene located on the short arm of chromosome 17 (17p13.1). It encodes a tumour suppressor protein, a transcription factor which functions as a gatekeeper for cell division and growth. Most of the downstream targets of p53 are responsible for: inhibiting cyclin-cyclin-dependent kinases and inducing cell cycle arrest (p21, WAF1 and Clip1); DNA damage repair (GADD45); apoptosis (Bax); and blocking mitogenic growth factor signalling (IGF-BP3) (*145*). Mdm2, another p53 downstream target, is responsible for the inactivation of p53-mediated transcription, forming a negative auto-regulatory loop and causing p53 to undergo ubiquitin-mediated proteolysis in the cytoplasm (*146*).

The p53 protein is activated by DNA damage caused UV light exposure, ionising radiation, chemical damage and hypoxia or genotoxic stress. Once activated it leads to DNA repair and cell cycle arrest and p53 protein activation can eventually result in apoptosis or cellular senescence. P53 becomes active after phosphorylation at its N-terminus and is stabilized by $p19^{ARF}$ which blocks the Mdm2-mediated degradation and neutralizes the inhibition of p53 by Mdm2. Tao and colleagues observed via heterokaryon assays that this process most likely occurs by $p19^{ARF}$ inhibition of nuclear-cytoplasmic export of Mdm2 (*146*).

1.7.2.1. TP53 in cancer

Most *TP53* gene mutations are clustered in exons 5-8, known to be responsible for the p53 DNA binding domain, which prevent DNA binding and disrupt the transcription

of p53 downstream targets. These mutations are found in over 50% of human cancers. For instance, *TP53* mutations have been observed in up to 70% of CRC and they are thought to be one of the late events in CRC development (*147*). Loss of p53-mediated apoptosis is considered to be an important step in the progression from colorectal adenoma to carcinoma and is consistent with the view that transformed cells have less efficient cell cycle checkpoint controls (*148, 149*). Nevertheless, Galandiuk and colleagues recently published a study on field cancerisation on long-standing Crohn's disease patients and showed *TP53*, *CDKN2A* and *K-RAS* mutations as possible independent initiating events in colon cancer development (*64*).

TP53 is mutated in over 33% of gastric cancers. Tamura and colleagues originally postulated that *TP53* mutations occur late in the development of gastric cancer and that these mutations are associated with DNA ploidy alterations in the tumours (*150*). However, Renault and colleagues observed that allelic loss of 17p13 chromosomal regions occurred in the later stages of GA and that *TP53* mutations had preceded such chromosomal loss (*151*). Shiao and colleagues, using PCR sequencing, showed that 37.5% of a cohort of intestinal metaplasia (IM) cases, 58.3% of dysplasia cases and almost 67% of GA cases displayed *TP53* mutations. These workers suggested that *TP53* mutations occurred as an early event in gastric carcinogenesis (*152*). Correa and Shiao then went on to establish the phenotypic and genotypic events in gastric carcinogenesis where they concluded that *TP53* mutations probably occur after IM onset (*153*).

A study by Flejou and colleagues showed a higher incidence of *TP53* mutations in GA of the cardia than that of the antrum. This suggested that GA of the cardia might be

related to oesophageal adenocarcinoma (OA) and therefore have different clinical and epidemiological characteristics than GA of the body and antrum (*154*). Another study by Hanazono and colleagues labelled cardiac carcinomas as OAs, and body or antrum carcinomas as GAs. *TP53* mutations were found in all cancer types, showing that 37.5% of cardiac samples and 44.4% of body and antrum samples were mutated. The authors also noted that immunohistochemical analysis (IHC) of p53 did not correlate with *TP53* mutations (*155*). This lack of correlation was also found in a study assessing the relationship between *TP53* mutations and IHC staining in hepatocellular carcinoma (*156*). *TP53* mutations have been found in Barrett's oesophagus (BO), a premalignant condition that increases the risk of developing OA by 30- to 40-fold. Different studies have shown that *TP53* mutations occur at a high rate in OA and *TP53* has been implicated in the malignant transformation of BO to OA through a metaplasia-dysplasia-carcinoma sequence (*157-159*).

Finally, *TP53* mutations are also common genetic events in the pathogenesis of oesophageal squamous cell cancer (OSCC) (*160*). LOH of areas on chromosome 17q have been observed in a high proportion of OSCCs (*161*). LOH of chromosome 17q25.2 - 25.3 has been linked to tylosis, an autosomal-dominant trait associated with a high risk of oesophageal SCC (*162*). Recently, Blaydon and colleagues have identified the underlying cause for tylotic oesophageal cancer (TOC) to be the inactive rhomboid protease *RHBDF2*, also known as *iRhom2 (163)*.

1.7.3. The *CDKN2A* signalling pathway

The *CDKN2A* or $p16^{INK4A}$ gene belongs to a small family of tumour suppressor genes that can alternatively splice, generating $p15^{INK4B}$, $p19^{ARF}$ (or *ARF*) and $p16^{INK4A}$. The gene is located in a small 35kb locus on chromosome 9. Both related isoforms, $p15^{INK4B}$ and $p16^{INK4A}$, are cyclin-dependent kinase inhibitors that function as inhibitors for cyclin-dependent kinases 4 and 6 (CDK4 and CDK6), and thus render the retinoblastoma (Rb) protein inactive. This inactivation will block the transcription of important cell-cycle regulatory proteins, which suggests that both INK4 isoforms and $p19^{ARF}$ carry out an important role regulating the cell cycle, especially in cell cycle G1 progression (*164*) (see explanation in 1.7.2).

Alterations in the *CDKN2A* tumour suppressor gene have been observed in many tumours either as LOH, point mutation or methylation of its promoter. In the gastrointestinal tract, this has mainly been shown in gastric cancer (*165*), OA (*166*), oesophageal SCC (*167*) and occasionally in intestinal cancer (*64*).

1.8. Cancers of the small intestine, colon and rectum

CRC is a major cause of morbidity and mortality throughout the world, being the third most common cancer in men and the second in women. It accounts for 8% of all cancer deaths, and it is the fourth most common cause of death from cancer (*168*). Even though the incidence for small intestinal cancer has increased over the past decades, its overall incidence is much lower than that of CRC (*169*). Potten and colleagues provide a possible explanation for this much lower incidence by identifying

an innate mechanism of genome protection in the slow cycling small intestinal stem cells (*10*). Another explanation might be the higher incidence of 'spontaneous apoptosis' observed in the small intestinal epithelium, which is associated with the stem cell position in the crypt and is both DNA damage and p53 independent (*149*). Nevertheless, recent studies analysing the hierarchical clustering of array comparative genomic hybridization (ACGH) datasets of 85 microsatellite stable (MSS) adenocarcinomas from the stomach, colorectum and small bowel have revealed that small bowel adenocarcinomas (SMAs) are more similar to colorectal adenocarcinomas than GAs (*170*). These findings, based on genome-wide DNA copy number aberrations, may provide insight into the treatments for MSS SMAs similar to that of colorectal adenocarcinomas.

1.9. Gastric cancer

Gastric cancer is a major cause of morbidity and mortality throughout the world, being the fourth most common cancer in the world and the second leading cause of cancer death in both sexes worldwide (9.7% of the total deaths from 2008) (*168*). The Lauren classification (*171*) divides gastric cancer into 2 major histologic types: intestinal or diffuse. Tumours are described by this system on the basis of microscopic configuration and growth pattern. Hence, the majority of the cases are sporadic in nature and belong to the intestinal type of GAs. This histological variant is associated with a sequential chain of events initiated by chronic inflammation that can eventually lead to the replacement of normal gastric glands by glands of an intestinal crypt phenotype, known as intestinal metaplasia (IM) (*153*). However, diffuse-type cancers

have noncohesive tumor cells diffusely infiltrating the stroma of the stomach and often exhibit deep infiltration of the stomach wall with little or no gland formation (*171*).

1.9.1. *CDH1* mutations in hereditary diffuse gastric cancer

In diffuse-type gastric cancers, a minority of cases (10%) exhibit familial clustering. Only 1-3% of all cases show evidence of inherited susceptibility to the disease and these are diagnosed with hereditary diffuse gastric cancer (HDGC) (*172*). Germline mutations in the cell-cell adhesion protein E-cadherin (*CDH1*) are considered to be the most important cause of HDGC. E-cadherin is a type I classical cadherin (see Figure 1.5). Classical cadherins share a conserved histidine-alanine-valine (HAV) tripeptide motif in their first extracellular domain (*173*), which has been shown to initiate an important step in cadherin mediated adhesion (*174*). Another highly conserved sequence across all species is the one responsible for Ca^{2+} binding sites. Haussinger and colleagues, using NMR spectrometry, demonstrated that a single amino acid substitution in a calcium-binding domain could abolish cell adhesion, proving therefore that such domains are crucial for cell adhesion by cadherins (*175*). The intracellular domain of E-cadherin interacts with β-catenin, α-catenin and p120 catenin and forms a cytoplasmic cell adhesion complex, thereby forming links with the actin cytoskeleton (see Figure 1.5) (*176, 177*).

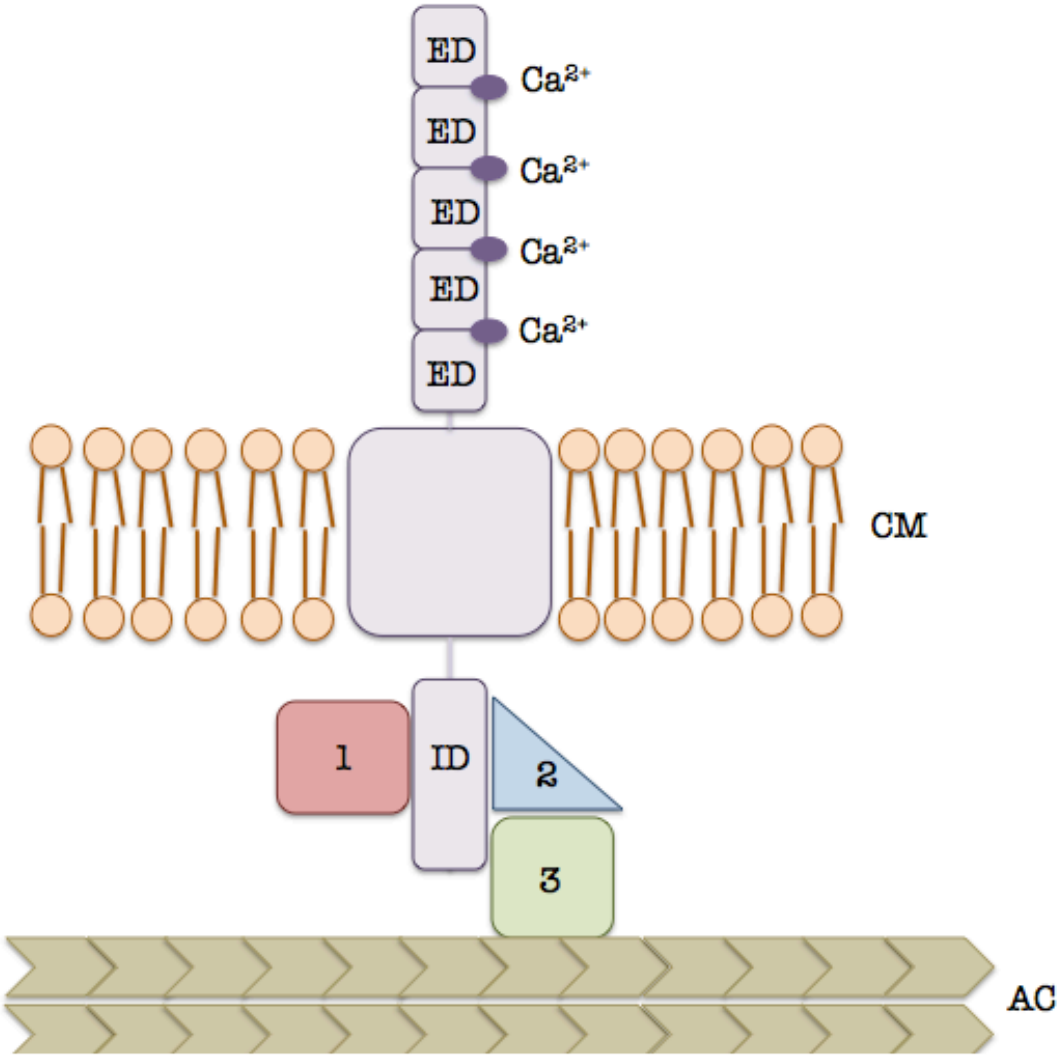

Figure 1.5. **Schematic illustration of interaction between E-cadherin and actin cytoskeleton.** E-cadherin is seen on purple in the cytoplasmic membrane, the interactions in the adherens junctions occur between the external domains of E-cadherin homodimers. CM, cytoplasmic membrane; ED, extracellular domain; ID, intracellular domain; Ca^{2+}, Calcium; AC, actin cytoskeleton; 1, p120; 2, β-catenin; 3, α-catenin.

E-cadherin is the central component of epithelial cell-cell adhesion and is required for the maintenance of the integrity of epithelial layers (*178*). During cancer development, some adherent epithelial tumour cells can acquire the ability to invade the extracellular matrix having undergone epithelial-mesenchymal transition (EMT); this process occurs in most types of cancer (*179*). Undergoing such a transition involves changes in the cadherin-mediated cell-cell adhesion, the actomyosin-mediated contraction due to

intercellular signaling and internalization of E-cadherin can then be targeted for degradation (*180*).

HDGC is characterised as an autosomal dominant cancer syndrome where the second hit is usually methylation of the *CDH1* gene, but can also occur through LOH (*181*). Hence, *CDH1* is a classic tumour suppressor gene (*182*). Nevertheless, not all *CDH1* mutations cause complete inactivation of E-cadherin and *CDH1* germline mutations present with incomplete penetrance (*183*), carriers having a 70% lifetime risk of developing HDGC (*184*). *CDH1* germline mutations are an indication for total gastrectomy in these patients (*185*).

1.9.2. The gastric adenocarcinoma premalignant pathway

GA has been associated with risk factors such as chronic inflammation and *Helicobacter pylori* infection (*186*). These risks are thought to initiate the progression to GA by the initial transition from normal gastric mucosa to atrophic gastritis. The phenotypic step-wise progression has been studied extensively and all the histological steps have been characterised (Figure 1.6) (*153*).

Normal gastric epithelium exhibits very low levels of inflammatory cell infiltration and these are normally present in the lamina propria surrounding the gastric glands (Figure 1.6). However, gastritis is characterized by increased infiltration of the lamina propria that can either be due to acute (polymorphonuclear neutrophils) or a chronic (mononuclear leukocytes) inflammation (Figure 1.6). Two types of gastritis have been characterized: non-atrophic gastritis (NAG), in which the gastric gland structure is

preserved, and atrophic gastritis, in which the gastric glands become damaged and the specialized glandular tissue is lost (*187*). Atrophic gastritis can either have a multifocal, known as multifocal atrophic gastritis (MAG), or a diffuse pattern in gastric tissue and it is associated with the presence of spasmolytic polypeptide-expressing metaplasia (SPEM), which is a form of mucous metaplasia or pseudopyloric metaplasia (*188*). Atrophic gastritis represents a recognizable step in the precancerous cascade (*187*).

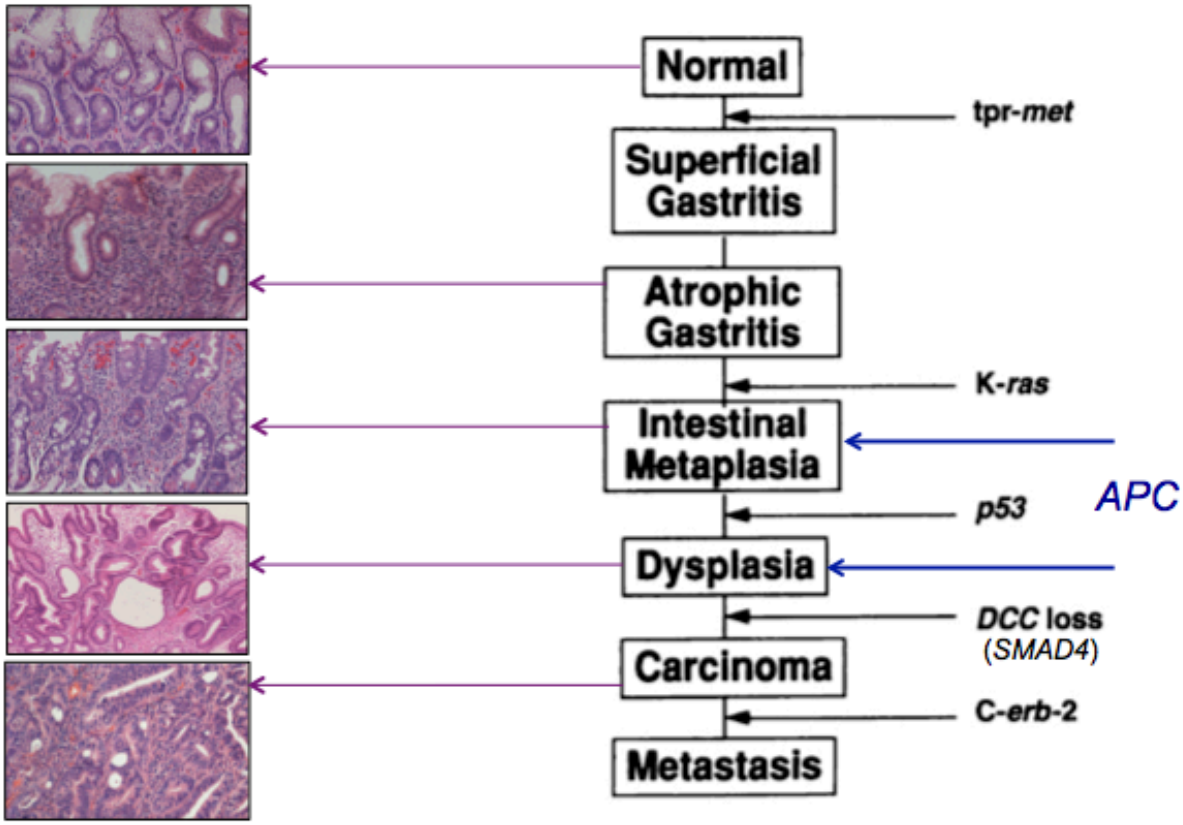

Figure 1.6. **The currently accepted metaplasia-dysplasia-carcinoma pathway in the development of Gastric Adenocarcinoma.** This pathway was published in 1994 by Correa and colleagues (*153*). The involvement of *APC* was not specified at the time, therefore, *APC* is marked here in blue at the stages where it has seen to be mutated since (*72*).

The most frequent cause of gastritis and peptic ulcers is chronic colonization of the human stomach by the Gram-negative bacterium, *H. pylori.* The pathogenicity of *H. pylori* depends on the virulence of the infecting strain, as strains containing the 40kb-long cytotoxic associated gene (cag) pathogenicity island (PAI) induce more severe inflammatory reactions. The most virulent protein responsible for *H. pylori*-induced gastric inflammation and gastric malignancy is the *H. pylori* cytotoxin-associated gene A (cagA), which is injected into the host cells disrupting epithelial cell functions. Together with *H. pylori,* cag PAI is responsible for the general inflammatory stress within the gastric mucosa inducing cell growth and a tissue repair response (*189*) that leads to the activation of multiple oncogenic pathways in epithelial cells. These pathways include NF-kappaB, activator protein-1, PIK3CA, signal transducers and activators of transcription 3, Wnt/B-catenin and cyclooxygenase 2 (*190*). *H. pylori* infection also induces epigenetic changes that affect gene expression and play an important role in cell differentiation. The epigenetic changes include DNA methylation and histone modification, which have been found to play critical roles in oncogenic transformation by increasing significantly the risk of developing GA (*191*).

1.9.3. Intestinal metaplasia in the human stomach

GA was first linked to IM in 1938 when Bonne and colleagues compared gastric specimens from Malay patients, with a low frequency of GA, and Chinese immigrants, with a high frequency of GA, and observed that the Chinese patients presented a much higher frequency of ‘goblet cell metaplasia’ (*187*). IM has been classified into two main types according to enzyme histochemistry and the histopathology of the gastric epithelium: the complete type (or small intestinal, designated type I), and the

incomplete type (or colonic, designated types both II and III). Types II and III of IM were thought to differ in the mucins secreted by columnar cells: type II secreting neutral and acid sialomucins and type III secreting sulfomucins, although it is now thought that the difference might be related to the processes of mucin glycosylation rather than to the pattern of mucin expression (*192*).

In a study involving 160 patients from a high risk GA area in Colombia, Gong and colleagues observed that *KRAS* mutations occur very early in the development of gastric cancer and suggested that IM can contain the same genetic abnormalities as the associated preneoplastic lesions (*193*). Therefore, IM might be a premalignant condition from which a carcinoma can develop. Using cytochrome c oxidase (CCO) enzyme histochemistry and mtDNA sequencing of individual cells, McDonald and colleagues later observed that human intestinal metaplastic glands are clonal and that they clonally expand by crypt fission (*71*). By microdissecting individual IM and dysplastic glands, Gutierrez-Gonzalez and colleagues then showed that in the human stomach intestinal metaplastic glands clonally expand by field cancerisation and give rise to an entire dysplastic lesion (*72*).

1.9.4. Dysplasia and gastric adenocarcinoma

Dysplasia is characterised by a neoplastic phenotype, displaying cells with enlarged, heterochromatic nuclei that undergo mitosis frequently. Dysplasia presents a disrupted architecture, showing bifurcating, branching or irregularly shaped gastric glands. In the western world, dysplasia is considered non-invasive and therefore the cells remain within the boundaries of the lamina propria. There are two types, low-grade and high-

grade dysplasia, the latter having more malignant potential and greatly predisposing an individual to cancer development (*187*). Once neoplastic cells penetrate the surrounding stroma the lesion has become invasive: GA has developed and metastasis can follow.

There is a need to establish which genes are possible targets of mutation and whether the mutations are pathogenic during the process of invasion and metastasis. Alpizar-Alpizar and colleagues recently observed, using immunohistochemistry, that urokinase plasminogen activator receptor (uPAR) is expressed in approximately 50% of gastric cancer cells in both the intestinal and the diffuse type. uPAR was expressed in macrophages and neutrophils in both types. This receptor facilitates the degradation of the extracellular matrix (ECM) and can activate other matrix degrading proteins. Even though uPAR expression did not vary according to the differences seen in incidence and mortality rates according to geographical regions, these workers noted that uPAR was expressed at higher levels in patients infected with *H.pylori (194).*

Several genes have been studied as possible targets of mutation in the associated gastric cancer CSCs. Koshikawa and colleagues observed that the ErbB family of epidermal growth factor (EGF) receptors play a role in mediating enhanced heparin-binding EGF (HB-EGF) activity by membrane type 1-matric metalloproteinase (MT1-MMP) converting HB-EGF into a heparin-independent growth factor with enhanced mitogenic activity (*195*). The authors of this study showed that when both HB-EGF and MT1-MMP are expressed in human gastric cancer cells, the invasive growth of the cancer cells could be supported, resulting in costimulation of tumour cell growth. Another potential target is ERas, a member of the Ras family, which was found to be expressed using immunohistochemistry in approximately 40% of human GA

specimens (*196*). Kubota and colleagues suggest that ERas may play a crucial role in gastric cancer cell survival and metastasis to the liver via down-regulation of E-cadherin. Moreover, monocyte chemoattractant protein 1 (MCP-1) has been observed in human GA and expression found to play a major role in monocyte and lymphocyte migration, and in macrophage infiltration due to MCP-1 secretion. Even though *H.pylori* has been reported to stimulate MCP-1 secretion from gastric mucosa, Mutoh and colleagues suggest that IM and GA might themselves induce MCP-1 expression independently of *H. pylori* infection (*197*).

There are also other cancer-associated events that might lead to human gastric cancer. For instance, Zhi and colleagues suggest that cancer-associated fibroblasts (CAFs) are positively correlated with metastatic potential in human GA (*198*). Using immunohistochemistry and real time-PCR for CAF specific proteins, CAFs have been found to play a prominent role in promoting tumour growth, invasion and metastasis and to be frequently present in gastric cancer tissues. Other findings suggest that mesenchymal stem cells (MSC)-like cells are components of the tumour microenvironment and provide proof for the origin of CAFs, and that both MSC-like cells and CAFs could be potential targets for gastric cancer diagnosis and therapy (*199*).

1.9.5. Genetic instability in gastric adenocarcinoma

Nearly 75% of all reported mutations in GA occur in *TP53, APC, CTNNB1, K-RAS, CDKN2A, PIK3CA* and *PTEN* (summary found in Table 1.1) (*135, 152, 153, 200, 201*). However, two recent exome sequencing studies found that *ARID1A*, a member

of the SWI-SNF chromatin remodeling family, is very commonly mutated in GA with microsatellite instability (MSI). The *ARID1A* mutations were associated with a better prognosis and negatively related to *TP53* mutations (*202*). Moreover, the authors found that the genes involved in cell-adhesion were also frequently mutated with *FAT4*, a cadherin family gene, having the highest mutation rate amongst them (*203*).

Genes commonly mutated	Function	Percentage of mutation in COSMIC	References
TP53	TSG, functions as a gatekeeper for cell division and growth	33.3%	(*151, 152, 154, 204, 205*)
APC	TSG, part of the *Wnt* signalling pathway, targets β-catenin for degradation and plays a crucial role in development, differentiation, and adult tissue homeostasis	18%	(*135, 136, 142, 206, 207*)
CTNNB1	β-catenin is a ubiquitous intracellular protein with an essential role in the Wnt canonical pathway. Also very important for intercellular adhesion	9%	(*141-143*)
KRAS	Oncogene, crucial role in cell division regulation	7%	(*193, 208, 209*)
CDKN2A	TSG, inhibitor for cyclin-dependent kinases 4 and 6 and important in cell cycle regulation	7%	(*165, 201, 210*)
PIK3CA	Oncogene, heterodimeric lipid kinase that plays a crucial role in cell growth, survival, apoptosis, proliferation, motility and adhesion.	12%	(*200, 211-213*)
PTEN	TSG, crucial for cell cycle regulation	7%	(*214-216*)
ARID1A	AT-rich interactive domain-containing protein 1A, member of the SWI/SNF chromatin remodelling family, possible TSG	11%	(*202, 203*)
FAT4	Cadherin family gene, possible TSG in breast cancer and GA, key role in vertebrate core planar cell polarity	--	(*203*)

Table 1.1. **The most commonly mutated genes in gastric adenocarcinoma development.** TSG, tumour suppressor gene.

1.10. Oesophageal cancer

Oesophageal cancer is a major cause of morbidity and mortality throughout the world, being the eight most common cancer worldwide and the sixth most common cause of death from cancer (5.4% of the total). These values include both types of oesophageal cancer, oesophageal adenocarcinoma (OA) and oesophageal squamous cell cancer (OSCC), and both cancers appear to be two to four times more common in men than women. OSCC has a higher prevalence in Eastern Asian and Southern African countries (*168*).

1.10.1. Barrett's Oesophagus

Barrett's oesophagus (BO) occurs when the normal oesophageal stratified squamous epithelium is replaced by columnar-cell metaplasia in response to inflammation and ulceration provoked by duodeno-gastroesophageal reflux (GORD) (*217*). As mentioned in 1.7.2.1, OA can arise from progression through a metaplasia-dysplasia-carcinoma sequence (MCS) and the presence of Barrett's oesophagus increases the risk of OA. The size of this excess risk is difficult to quantify. The lowest estimate is 0.12% per annum by 0.12% (*218*) but other studies have found significantly greater risks. Publication bias is a problem but a risk of around 0.4-0.5% per annum is widely accepted for endoscopically visible and histologically confirmed Barrett's oesophagus. The incidence of oesophageal adenocarcinoma has risen at an alarming rate over the past four decades in many regions of the Western world, and there are indications that the incidence of this disease is on the rise in Asia. Nevertheless, BO rarely progresses to OA and the incidence increase in OA is thought to be partly due to increases in the

prevalence of known risk factors such as obesity, alcohol, cigarette smoking, GORD and a poor diet (*219*).

Neoplastic progression to OA is thought to be due to an accumulation of genetic defects within the Barrett's glands and the driving forces are thought to be genomic instability, disruption of the regulatory pathways and the evolution of the mutated clones modulated either by host, environmental risk or protective factors (*220*). Findings by the Reid group in Seattle suggested that such genetic defects expand to encompass the entire field of Barrett's oesophagus, known as a *selective sweep to fixation* (*166, 221*). However, Leedham and colleagues have demonstrated that clonal heterogeneity exists within fields of Barrett's epithelium and that multiple independent clones are present (Figure 1.7). Findings by Leedham *et al* indicate that there may be a competitive interaction between these clones in the progression to cancer, but to date only mathematical models suggest that such competition exists. Their data also suggested that wild type squamous gland ducts of the oesophagus might be the potential source for a progenitor cell susceptible to mutation and hence responsible for the conversion of stratified squamous epithelium into BO. The ducts may also provide a progenitor cell that might be able to expand and create neo-squamous islands (*157*). Moreover, Nicholson and colleagues observed, using cytochrome c oxidase (CCO) histochemistry, that Barrett's glands are clonal, they contain multiple stem cells and that are most likely to expand clonally by crypt fission (*222*). These workers also observed that a CCO mutated cell could give rise to both squamous and glandular epithelium, corroborating that squamous gland ducts may be the source of progenitor cells in the oesophagus.

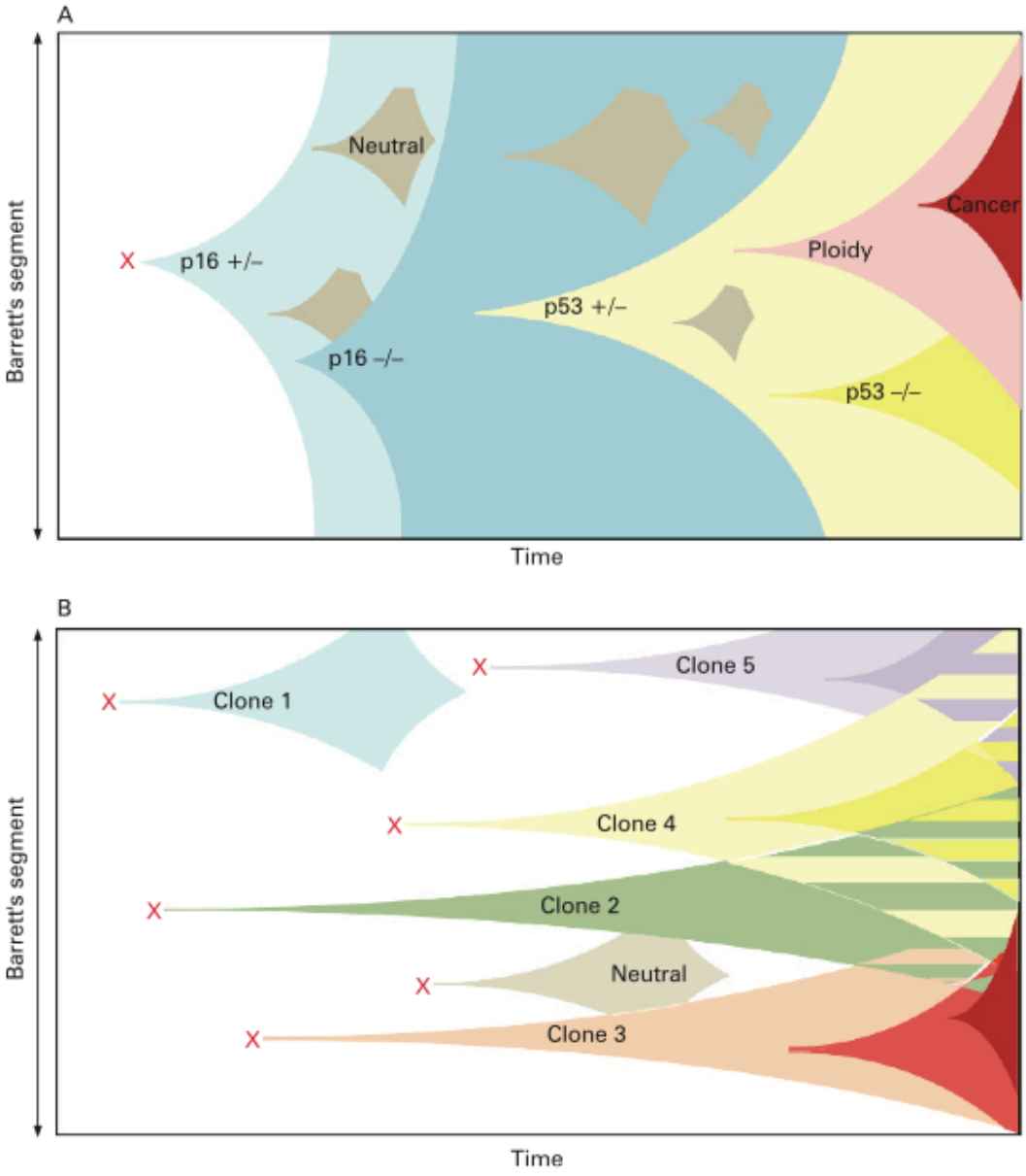

Figure 1.7. **Clonal evolution models for Barrett's oesophagus from Leedham and colleagues (*157*).** (A) Selective sweep to fixation model from Reid and colleagues (*221*). (B) Clonal interference model proposed by Leedham and colleagues showing genetic heterogeneity within Barrett's segments.

1.10.2. Genetic instability in Barrett's oesophagus and oesophageal adenocarcinoma

Even though the mechanisms are currently unclear, mutations in TSGs such as *TP53* and *CDKN2A* are implicated in the development of BO and play a role in neoplastic progression to OA (*223*). Wong and colleagues findings suggest that *CDKN2A* mutations enhance the clonal expansion ability of Barrett's mucosa, creating a field in which other abnormalities arise, which can then lead to OA (*224*). Other TSGs which have been invoked in the development of BO associated adenocarcinomas include c-erbB2, Rb, BRCA1, Smad4, DCC and hMSH2 (*161*).

Members of the Wnt signalling pathway have been shown to play a crucial role in controlling the balance between squamous and glandular differentiation (*73*). The role of these pathways in the pathogenesis of BO and adenocarcinoma is still unclear. However, many reports have also detected reduced expression of cadherins and catenins in tumours, including those of the gastrointestinal tract. These proteins are known to maintain the adult tissue architecture, E-cadherin being expressed in most epithelia and probably co-expressed with P-cadherin in the basal layers of the stratified epithelium. However, as seen in other tissues, E-cadherin expression is further downregulated as BO progresses to oesophageal adenocarcinoma. Although present in OA, E-cadherin expression is usually absent in both BO and dysplasia (*225*).

1.10.3. Oesophageal squamous cell carcinoma

OSCC is the most common oesophageal cancer worldwide. Some of the different histopathological steps that can be seen in the course of OSCC development are: oesophagitis (marked by neutrophil and eosinophil infiltration of the epithelium); and basal cell hyperplasia (BCH, marked by the increased thickness of the basal layer), followed by low-grade and high-grade dysplasia. Dysplasia is marked by atypical cells in the lower part of the epithelium ascending as the grade of dysplasia becomes more severe. Carcinoma *in-situ* can also be observed, where the full thickness of the epithelium presents atypical cells but there is no invasion. Eventually OSCC can develop when neoplastic cells invade the muscularis.

There has been great controversy in the identification of the histopathological steps that lead to OSCC development and, to date, it is still not widely accepted that histological oesophagitis or atrophy have a higher prevalence in the high versus low risk populations (*226, 227*). Wang and colleagues showed in a 13 year prospective study that the only histopathological lesions associated with an increased risk of oesophageal SCC development were squamous cell dysplasia and carcinoma *in-situ* (*228*).

The squamous epidermis is thought to be analogous to the squamous oesophagus. Clayton and colleagues have shown that clones in the epidermis can expand progressively over time and that asymmetrical division occurs in the vast majority of epidermal progenitor cell divisions (*229*). This suggests a new model of epidermal homeostasis involving only one type of progenitor cell, which could undergo both

symmetric and asymmetric divisions to ensure epidermal homeostasis. Nicholson and colleagues observed patches of CCO deficient cells ranging from around 30μm to about 1mm in the normal squamous epithelium. They suggested that if Clayton's observations are applicable to their findings then it is possible that lateral replacement of the stem cell pool along the basal layer of the squamous epithelium occurs and that a process analogous to niche succession also takes place in the normal oesophagus (*222*). Mandard and colleagues found in the same patient two different histological oesophagitis patches with two independent *TP53* mutations where a different *TP53* mutation was also present later in the cancer. All of these mutations were functional and occurred in the DNA binding domain of p53. These findings suggested that field cancerisation occurs in the oesophagus prior to malignant transformation and that, regardless of the controversy questioning oesophagitis as a crucial histopathological step towards OSCC, it may be a target for early detection of OSCC (*162*).

1.10.4. Genetic instability in oesophageal squamous cell carcinoma

OSCC has mainly been associated with: mutations and LOH of the TSG *TP53*; mutations, LOH and promoter methylation of $p15^{INK4b}$ and $p16^{INK4a}$ respectively; reduced *Rb* expression and *cyclin D1*; mutations in the *ras* pathway and *Notch1* signalling pathway; and *EGFR* and *c-myc* gene amplifications (*162, 167, 230-233*). Recently, the *nuclear factor erythroid-related factor 2* gene (*NRF2*, also known as *NFE2L2*), known to encode a transcription factor that induces the expression of antioxidant enzymes upon oxidative stress, has also been found to be mutated in a high percentage of OSCCs (*234*). *NRF2* mutations have been associated with tumour recurrence and poor prognosis due to resistance conferred to stressors, including anti-

cancer therapy. Kim and colleagues observed, via PCR sequencing, that all of the mutations were near or within the NRF2-KEAP1 interaction motifs, inactivating the KEAP1-mediated degradation of NRF2. However, no *KEAP1* mutations were found (*235*). These authors also observed *NRF2* mutations in skin squamous cancers and noted an increase in nuclear NRF2 in both OSCCs and skin squamous cancers, indicating that *NRF2* mutations play a role in the development of both cancer types. DeNicola and colleagues showed that, in murine embryonic fibroblasts, oncogenic alleles of *Kras*, *BRaf* and Myc increased transcription of Nrf2 thereby elevating the antioxidant program and reducing the ROS intracellular levels (*236*). Hence, increased NRF2 antioxidant and cellular detoxification program, either by a mutation preventing NRF2-degradation or by a mutated oncogene, represents a previously unappreciated mediator of oncogenesis.

1.10.5. Tylosis with oesophageal cancer

Tylosis with oesophageal cancer (TOC) is a rare familial syndrome inherited in an autosomal-dominant manner. Symptoms include palmoplantar keratoderma (PPK), oral keratosis and follicular papules and it can be associated with a high risk for oesophageal SCC development (up to a 95% by the age of 65) (*237-239*). Rhomboids are intramembrane serine proteases, which typically contain six or seven transmembrane domains (TMD) classified into four subgroups: Secretase A and B, Presenilin-Associated-Rhomboid-Like (PARL) and iRhoms (*240*). The gene responsible for TOC was recently identified as the inactive rhomboid protease *RHBDF2*, also known as *iRhom2* (*163*). iRhoms are predicted to localise to the endoplasmic reticulum (ER) membrane (*241*) although in the epidermis and

oesophagus RHBDF2 is also localised at the plasma membrane (*163*). The TOC mutations have been found clustered in the highly conserved extended N-terminal domain of *RHBDF2*, suggesting an important function for this region of the RHBDF2 protein (see Figure 1.8) (*242*).

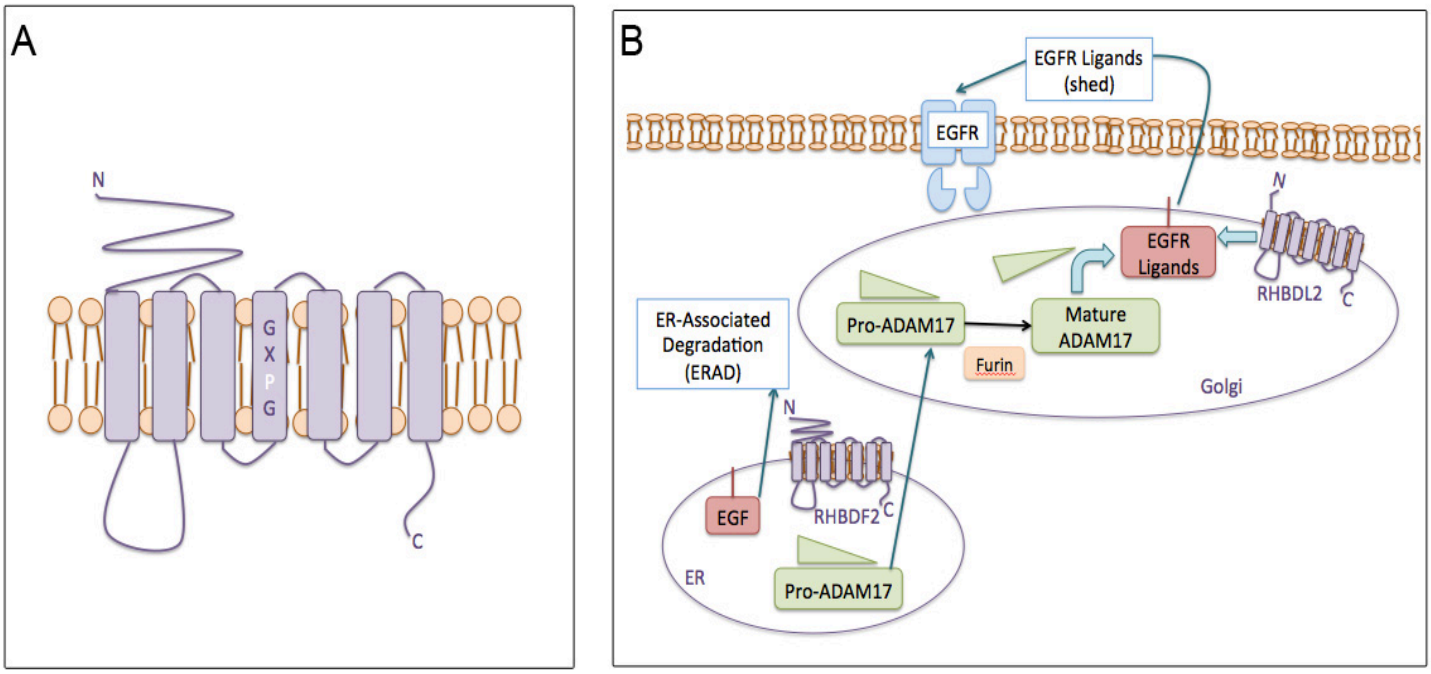

Figure 1.8. **RHBDF2 structure and working model of RHBDF2 and ADAM17 interaction in tylosis with oesophageal cancer.** (A) Topology model illustrating the protein structure of human RHBDF2; highlighted is the fourth transmembrane domain and the lack of catalytic residues in inactive Rhomboid proteins. (B) Working model of the function of RHBDF2 in the ER and translocating Pro-ADAM17 into the Golgi as well as the role of ADAM17 and RHBDL2. Adapted from Etheridge et al (*242*).

The Secretase A type Rhomboid RHBDL2 is the active Rhomboid relative of iRhom1 and RHBDF2 (*240*). RHBDL2 is known to be responsible for EGF cleavage independently of ADAM (A Desintegrin And Metalloprotease) family members (*243*).

Both iRhom1 and RHBDF2 lack the catalytic residues present in active Rhomboid proteases and, instead, they present an invariant proline residue that is N terminal to the expected location of the catalytic serine (i.e., GPx replacing the GxS rhomboid catalytic motif) (Figure 1.8 A) (*244, 245*). Using immunoprecipitation, Zettl and colleagues showed that human iRhom1 and mouse RHBDF2 interact directly with the RHBDL2 ligand EGF in the ER and they were both found to target EGF for ER-associated degradation (ERAD) (*245*). Keratinocytes from TOC patients are unresponsive to exogenous EGF; but, in the absence of exogenous EGF cell migration and proliferation are maintained whereas both are significantly reduced in control keratinocytes (*163*). These results suggest that EGF levels might be higher in TOC patients and that human RHBDF2 also plays a physiological role in EGF signaling (*163, 242*).

By generating RHBDF2 knock-out mice ($RHBDF2^{-/-}$), studies by both Adrian and McIlwan showed that RHBDF2 is critical for the TNFα convertase (TACE) ADAM17 maturation and trafficking from the endoplasmic reticulum (ER) (*243, 246*). Lack of activated ADAM17 in the cell membrane prevents the cleavage-mediated activation of TNFα, leading to a severe reduction of TNFα levels in $RHBDF2^{-/-}$ mice. Overall, these findings suggest that RHBDF2 binds to ADAM17 in the ER and is crucial for the trafficking of ADAM17 from the ER into the Golgi, where ADAM17 undergoes furin-mediated cleavage activation before trafficking to the cell surface (*243*). Unpublished data suggests that the *RHBDF2* gain of function TOC mutations leads to an increased level of ADAM17-mediated shedding of EGF signalling molecules in TOC cells (*242*). This increased activation would account, in part, for the unresponsiveness of TOC keratinocytes to exogenous EGF and also for the

hyperproliferative epidermal phenotype observed in tylotic patients (*242*). The epidermal hyperproliferation observed in the areas undergoing frequent wound healing might be due to the excessive ADAM17 activation, as observed in TOC, because wound healing is mediated, in part, via EGFR signalling in keratinocytes (*247*).

Hence, RHBDF2 appears capable of regulating EGFR signalling through two separate pathways by controlling the shedding of pro-EGF targeting for ERAD and also by controlling the rate of that shedding through the regulation of ADAM17 maturation and transit from the ER into the Golgi.

1.11. Hypothesis and Aims

The high incidence of gastrointestinal cancers in the general population and the presence of premalignant dysplastic precursor lesions in the gastrointestinal tract make the gastrointestinal tract an ideal environment for the study of cancer clonality and clonal expansion. Moreover, the model proposed by Nowell on clonal evolution in neoplasia, caused by further accumulation of mutations in the subclones of the original cancer as a result of genetic instability, still needs to be studied in further detail in gastrointestinal cancers. Therefore, the main areas of interest for this project are pre-malignant lesions and gastric adenocarcinoma of the human stomach, and dysplastic lesions and invasive squamous cell cancer of the oesophagus.

Project 1: Clonal expansion in the human stomach

McDonald and colleagues established that intestinal metaplastic glands in the stomach are clonal and contain multiple stem cells, which are able to spread by fission (*248*). These workers suggested that the mechanism of gland fission causes field cancerisation in the stomach. Following on from this work, the hypothesis of the first project presented here is that gastric adenocarcinoma progresses through a series of genetic events arising from a founder mutation.

The aims of this project were:

1. To demonstrate the clonal origins of dysplasia from IM
2. To determine the clonal architecture of GA
3. To assess clonal expansion in HDGC

Project 2: Clonal expansion in oesophageal squamous cell cancer

Nicholson and colleagues observed clonal patches in the normal squamous oesophagus ranging from around 30μm to about 1mm (*222*). They suggested that if Clayton's observations are applicable to their findings then it is possible that lateral replacement of the stem cell pool along the basal layer of the squamous epithelium occurs and that a process analogous to niche succession also takes place in the normal oesophagus (*222, 229*). Moreover, Mandard and colleagues observed the expansion of independent *TP53* mutated clones in an oesophageal squamous cell cancer patient in areas of oesophagitis and cancer. These workers suggested that field cancerisation occurs prior to malignant transformation in the human oesophagus (*162*). Following on from this

work, the hypothesis of the second part of the project presented here was that oesophageal squamous cell cancer occurs by a process of field cancerisation of the oesophagus.

The aims of this project were:

1. To assess the mutation frequencies of genes known to be involved in the development of OSCC
2. To determine the clonal architecture of OSCC

Project 3: Investigating *iRhom2* and *ADAM17* in sporadic and tylosis oesophageal squamous cell cancer

Tylosis with oesophageal cancer (TOC) is a rare familial syndrome inherited in an autosomal-dominant manner, which can be associated with a high risk for oesophageal SCC development (up to a 95% by the age of 65) (*237-239*). Blaydon and colleagues identified the mutation responsible for TOC as the inactive rhomboid protease *RHBDF2* (*iRhom2)* (*163*). The protein has been found to localize to the ER and to promote ER-associated degradation of RHBDL2 ligands such as EGF (*245*).

RHBDF2 knock-out mice ($RHBDF2^{-/-}$) studies showed that RHBDF2 is critical for the TNFα convertase (TACE) ADAM17 maturation and trafficking from the endoplasmic reticulum (ER) to the golgi (*243, 246*). *RHBDF2* mutations seen in TOC appear to be gain of function mutations, as EGF dysregulation was observed in TOC keratinocytes (*163*). Following on from this work, the hypothesis of this project is to investigate if

TOC associated *RHBDF2* mutations persist during tumour progression in TOC and to determine RHBDF2 localisation in the oesophageal tumour.

The aims of this project are:

1. To characterise the mutational state of *RHBDF2* in sporadic OSCC
2. To determine if *RHBDF2* germline gain of function mutations persist during tumour progression in TOC
3. To assess the localisation of RHBDF2 and ADAM17 in sporadic OSCC and TOC

2. Materials and Methods

2.1. Patients

2.1.1. Patients from Chapter 3.2.1

Intestinal metaplastic and dysplastic formalin-fixed paraffin-embedded and frozen specimens were obtained from patients undergoing resection for either GA or high-grade dysplasia and from pathology archives. A total of 23 patient specimens were used in this study. Ethical approval was sought and obtained as per United Kingdom Human Tissue Act (2006 from UCH, reference 07/Q1604/17) and Hikone Municipal Hospital (Japan) regulations. The histology of each specimen was confirmed by 2 pathologists (N.A.W. and M.R.J.). All specimens showed IM surrounding or in between large areas of dysplasia (or early gastric cancer) and this was consistent through multiple blocks from each patient.

2.1.2. Patients from Chapter 3.2.2

Intestinal metaplastic, dysplastic and gastric adenocarcinoma formalin-fixed paraffin-embedded specimens were obtained from patients undergoing resection for GA and from pathology archives. A total of 51 patient specimens (age range 29-85) were used in this study. Ethical approval was sought and obtained as per United Kingdom Human Tissue Act (2006 from UCH, reference 07/Q1604/17). The histology of each specimen was confirmed by 2 pathologists (N.A.W. and M.R.J.). All specimens

showed gastric adenocarcinoma and this was consistent through multiple blocks from each patient.

2.1.3. Patients from Chapter 3.2.3

Normal gastric epithelium and hereditary diffuse-gastric cancer formalin-fixed paraffin-embedded specimens were obtained from patients undergoing full gastrectomy and from pathology archives. A total of 5 patient specimens from 2 different families (age range 22-59) were used in this study. Ethical approval was sought and obtained as per United Kingdom Human Tissue Act (2011 from the Royal London Hospital, reference 11/L0/1613). The histology of each specimen was confirmed by 2 pathologists (N.A.W. and J.C.A.). All specimens considered for this study showed diffuse-gastric cancer areas and this was consistent through multiple blocks from each patient.

2.1.4. Patients from Chapter 4 and Chapter 5

Normal oesophageal squamous epithelium, low grade dysplasia, high grade dysplasia and oesophageal squamous cell cancer formalin-fixed paraffin-embedded specimens were obtained from patients undergoing oesophageal resection and from pathology archives. A total of 34 patient specimens were used in this study. Ethical approval was sought and obtained as per United Kingdom Human Tissue Act (2006 from UCH, reference 07/Q1604/17; 2011 from the Royal London Hospital, reference 11/L0/1613; and MREC 02/8/1). The histology of each specimen was confirmed by a minimum of 2 pathologists (N.A.W., M.R.J. and J.C.A.). All specimens considered for this study

showed oesophageal squamous cell carcinoma areas and this was consistent through multiple blocks from each patient.

2.2. Tissue macrodissection

Five serial sections from paraffin blocks (4μm) of each specimen were prepared. All sections were cut onto normal glass slides and were either left overnight at 37°C or incubated for 2 hours at 65°C. The slides were dewaxed and then first slide for each patient was stained with Haematoxylin and Eosin (H&E) and mounted (see full methods in 2.7.1). Suitable cancer areas for dissection were identified using the H&E slide. The same areas were identified on slides 2-5 and dissected using needle macrodissection (BD Microlance 3, NJ, USA) and immersed in 30-50 μl of proteinase K solution (Arcturus Bioscience, Mt View, California, USA). Negative control tubes containing proteinase K solution and no macrodissected material were included. Tubes were then centrifuged at 4.5 *g* for 1 min and incubated at 65°C during 16hours, followed by a 10 min incubation at 95°C, which denatured the proteinase K. The tubes were centrifuged at 4.5 *g* for 1 min and the lysate was either used for PCR or stored at -20°C.

2.3. Laser-capture microdissection

Seven serial sections from paraffin blocks of each specimen were prepared. Section 1 (4μm) was cut onto a normal glass slide, and section 2-7 (6μm) were cut onto P.A.L.M. MembraneSlide 1.0 PEN slides (Zeiss Microimaging, Munich, Germany). All sections were either left overnight at 37°C or incubated for 2 hours at 65°C. The

slides were dewaxed and then the normal slide for each patient was stained with H&E and mounted (see full methods in 2.7.1). The P.A.L.M. membrane slides were stained with methylene green (2%; Sigma, Poole, UK) and then air-dried. Suitable crypts or cancer areas for dissection were firstly identified on the H&E slide and were then located on the P.A.L.M. membrane slides (slides 2-7). Individual crypts or cancer areas were cut out from the laser capture slides and catapulted into the adhesive caps of eppendorfs using the P.A.L.M. Laser Microdissection system. Catapulted sections on the cap were immersed in 14 μl of proteinase K solution (Arcturus Bioscience, Mt View, California, USA). Negative control tubes containing proteinase K solution and no laser capture material were included. Tubes were then centrifuged at 4.5 *g* for 1 min and incubated at 65°C during 16hours, followed by a 10 min incubation at 95°C, which denatured the proteinase K. The tubes were centrifuged at 4.5 *g* for 1 min and the lysate was either used for PCR or stored at -20°C.

2.4. Genomic PCR Sequencing

The needle macrodissected lysate was used to screen for mutations via nested PCR reactions in a variety of genes according to the cancer type. The total gene list that we screened for is: *APC* (adenomatous polyposis coli mutation cluster region), *TP53* (exons 5–8), *KRAS* (codons 12 and 13), *CTNNB1* (B-catenin, exon 11), *CDKN2A* (p16, exon 2), *PTEN* (phosphatase and tensin homolog exons 5, 6, and 8), *PIK3CA* (exons 9 and 20), *NRF2* (exon 2) and *RHBDF2* (exons 5 and 6). Primer and reaction conditions are shown in Table 6.1 in the Appendix. After nested PCR reactions the samples were run on a 1% Agarose Gel (Ultrapure Agarose, Invitrogen) made with 10% TBE Buffer (Electran, VWR). All successful reactions were then subjected to an

ExoSAP-IT reaction following manufacturer protocol (Affymetrix) in order to remove any excess of nucleotides and primers from the PCR product. The samples were subsequently sequenced using BigDye Terminator v3.1 reaction mix (Applied Biosystems) and 5x Sequencing Buffer (Applied Biosystems) following manufacturer protocol. Purification of sequencing products for capillary electrophoresis was performed using ethanol/EDTA precipitation. All samples were mixed with 2.5μl of 125mM EDTA pH:6 (Sigma-Aldrich, USA) and 30μl of 100% ethanol. After a 15 minute incubation the mixture was centrifuged in the plate spinner at 4000rpm for 30 minutes. The supernatant with unincorporated dyes and primers was subsequently removed by inverting the plate and spinning the samples at 800rpm for 20 seconds. The pellet was washed by adding 120μl of 70% ethanol into each sample and spinning the samples at 4000rpm for 10 minutes. The supernatant removal process was then repeated and samples were loaded onto the ABI PRISM TM 3130xl Genetic Analyser by adding 10μl of deionized Hi-Di Formamide (stored at -20C, Applied Biosystems) and sealing the well with a 3100 Genetic Analyser plate septa 96-well (Applied Biosystems).

All of the genes screened for account for approximately 75% of all somatic mutations previously reported in either gastric adenocarcinomas or oesophageal squamous cell carcinoma according to the catalogue of somatic mutations in cancer (COSMIC) database (www.sanger.ac.uk/genetics/cgp/cosmic). Most mutations within the COSMIC database have been identified in cancer specimens and may be late events in the dysplasia:carcinoma sequence. After a mutation was detected in tissue lysate, every laser-captured area would then be screened individually for that mutation using the nested PCR protocol.

2.5. Microsatellite Loss of Heterozygosity Analysis

Microsatellite Loss of heterozygosity (LOH) analysis was performed on individual cancer areas lysates using a multiplexed microsatellite assay. Eleven highly polymorphic microsatellites, located on chromosomes 3p (*FHIT*), 5q (*APC*), 9q (*CDKN2A*), 17p (*TP53*), 17q, and 18q (*SMAD4*), were amplified in 3 separate reactions using a multiplex PCR kit (Qiagen, Crawley, UK). Constitutional DNA was extracted from normal smooth muscle. Marker accession numbers and primer and reaction details are shown in Table 6.2 in the Appendix. Primers were tagged at the 5' end with either a FAM (tetrachloro-6-carboxyfluorescin) or a HEX (hexachloro-6-carboxyfluorescin) fluorescent marker. Successfully amplified PCR products were analyzed on an ABI 3100 Genetic analyser (Applied Biosystems) by adding 7.6μl of deionized formamide (stored at -20C, Applied Biosystems) and 0.4μl of ROX500 (Applied Biosystems) to each sample and sealing the well with a 3100 Genetic Analyser plate septa 96-well (Applied Biosystems). LOH was calculated measuring the area under curve using Peak Scanner software (Applied Biosystems). LOH was then considered present if the area under 1 allelic peak was more than twice that of the other, after normalizing the peak areas relative to the constitutional DNA.

2.6. DNA preparation and pyrosequencing

As per personal communication, Dr J. Risk, Dr A.Ellis and Dr J.K Field performed these experiments at the Department of Molecular & Clinical Cancer Medicine, Institute of Translational Medicine. For full methods please refer to Blaydon *et al* (*163*).

DNA was extracted from frozen tumour tissue taken from surgical resections from patients 33 and 34 using resin-binding technology (Nucleon kit from Scotlab) and ethanol precipitation. These two samples were assessed for LOH at the listed microsatellites (D17S515, D17S929, D17S186, D17S1839, D17S1603, D17S785, D17S801 and D17S1790) using pyrosequencing. PCR primers and a pyrosequencing primer were designed to cover the c.557T>C *RHBDF2* mutation site. Hot-start PCR was carried out with 50 ng/ml of DNA template in each reaction (PCR conditions: 94C for 5 min; 35 cycles of 94C for 30 s, 65C for 40 s, and 72C for 30 s; and a final extension of 72C for 10 min). Confirmation of PCR product quality and freedom from contamination was established on 2% agarose gels with ethidium bromide staining. Pyrosequencing was carried out with the PSQ 96MA System (Biotage), including Single-Stranded Binding Protein (PyroGold reagents), according to the manufacturers' protocol.

Primers Used for Pyrosequencing Assay:

- Forward primer (biotin-labelled): GGACCCTAATGGCTCTGCTT
- Reverse primer: ATGTCCATCTCCTCCGGGT
- Pyrosequencing primer: GCCAGCGGATCCACA

2.7. Histological staining and immunohistochemistry

2.7.1. Haematoxylin and Eosin staining

The slides were dewaxed in xylene (twice for 2 minutes) and rehydrated through decreasing ethanol concentrations (100%, 100%, 90% and 70%) to water. Slide 1 was

stained with Haematoxylin (1-5 minutes), 1% Acid Alcohol (2 seconds) and Eosin (2 minutes) and then mounted with Eukitt quick-hardening mounting medium (FLUKA BioChemika, Sigma-Aldrich, USA).

2.7.2. AB-PAS staining

This staining was performed using the Leica Autostainer for special staining by the BICMS pathology department. In brief, the slides were dewaxed in xylene, rehydrated in IMS, stained in 1% Alcian Blue pH:2.5 for 30 minutes, washed, treated with 1% Periodic Acid solution for 5 minutes, washed, stained in Schiffs Reagent for 10 minutes and washed. Finally, the slides were stained in Gills Haematoxylin for 2 minutes, washed, dipped in 1% Acid Alcohol, dehydrated in IMS, cleared in Xylene and finally mounted in DPX.

2.7.3. E-cadherin staining

This staining was performed using the Leica Autostainer for special staining by the BICMS pathology department. The E-cadherin primary antibody (NCL-L-E-Cad, Leica Biosystems) was used at the recommended concentration, 1:25, for 30 minutes at 25 °C after epitope retrieval at pH 6. After the staining procedure, the slides were then dehydrated and mounted in DPX.

2.7.4. RHBDF2 staining

The BICMS pathology department optimised the RHBDF2 primary antibody (HPA018080, Sigma). They later performed the staining on all slides. In brief, the slides were dewaxed in xylene, rehydrated in IMS and pretreated in a pH 6 Buffer for 25 minutes in the microwave. The primary antibody was used at a concentration of 1:100 followed by an RTU kit and 2 component DAB procedure. The slides were then dehydrated and mounted in DPX.

2.7.5. ADAM17 staining

The BICMS pathology department optimised the ADAM17 primary antibody (ab2051, Abcam). They later performed the staining on all slides. In brief, the slides were dewaxed in xylene, rehydrated in IMS and pretreated in a pH 8.1 Buffer for 35 minutes in the microwave. The primary antibody was used at a concentration of 1:100 followed by vector RTU and 2 component DAB procedure. The slides were then dehydrated and mounted in DPX.

3. Clonal expansion in the human stomach

3.1. Introduction

Gastric carcinoma is the fourth most common cancer and the second leading cause of cancer death worldwide (*168*). Most cases (90%) are sporadic in nature and belong to an intestinal type of cancer (*172*), called gastric adenocarcinoma (GA). However, a minority of cases show evidence of inherited susceptibility to the disease and are diagnosed with hereditary diffuse gastric cancer (HDGC) (*172*).

GA is thought to be the culmination of a sequential chain of events initiated by chronic inflammation. The replacement of normal gastric glands by glands of an intestinal crypt phenotype, intestinal metaplasia (IM), was first linked to GA in 1938, when a high frequency of GA was observed in Chinese patients with high incidence of 'goblet cell metaplasia' (*249*). The development of IM, as a result of *Helicobacter pylori* infection, is now known to be a major risk factor for GA.

Work published by our laboratory has shown that human IM glands are clonal and expand by crypt fission (*248*); IM might represent field cancerisation in the human stomach (*72, 248*). Moreover, the fields of dysplasia associated with GA could potentially be initiated by multiple mutational events or by the clonal expansion of one single dysplastic gland carrying a single mutation. Other recent work published by our laboratory has indicated that familial adenomatous polyposis (FAP)–associated colorectal adenomas as well as some sporadic lesions are polyclonal (*16*) and we have independent results that Barrett's oesophagus may originate from multiple clones (*157*); it remains to be seen if polyclonality also occurs in GA.

The current dogma for GA development proposes a stepwise progression through the Metaplasia-Dysplasia-Carcinoma sequence (MCS) and that the mutation and selection theory of cancer development also holds true for GA (*187*). Furthermore, the dogma proposes that as a stem cell acquires more mutations, its progeny becomes more likely to develop into a neoplasm (*153*). This has led to the hypothesis that specific genes become mutated at specific stages in the progression to cancer. Whether it is possible to establish an order of mutations in which specific genetic events occur during the MCS in the development of GA remains open to question (*64*).

The part played by field cancerisation, the process by which a field of phenotypically-normal epithelial cells is preconditioned for neoplastic development, in GA development remains unclear (*250*). Clones of cells with mutations that confer a selective advantage have the potential to develop into carcinoma within a field; following surgical removal of the primary carcinoma any mutated clones remaining in unresected fields will provide a reservoir for the possible development of recurrent tumours.

The clonal origin of many tumours is unclear because of incorrect assumptions made especially in the application of X-inactivation analysis of tumours. This was demonstrated by *in situ* hybridization in an XO/XY mosaic individual that proved the polyclonal origin of colonic microadenomas (*49*). Nowell, in 1976, proposed a model of clonal evolution in neoplasia where tumours originate from a single cell. This model, thought to fit most cancer types, proposed that the originating mutated clone acquired further mutations as a result of genetic instability and eventually led to a tumour composed of subclones with a higher selective advantage to that of the original

tumour initiating clone (*88*). However, differences in the clonal origin of cancer in different organs can be due to a number of factors, including different mutation rates, clonal competition, undetected founder mutations or to underlying chronic diseases or germline mutations, each of which can influence field cancerisation (*251*).

To date, many markers of genetic progression of gastrointestinal tumours have been identified, such as *Kirsten rat sarcoma viral oncogene homolog* (*KRAS)*, *Adenomatous polyposis coli* (*APC)* and *Tumour protein 53* (*TP53)* (*252*). These progression markers, or driver mutations in cancer development, are currently used to assess the mutational status of gastrointestinal cancer patients, and are associated with the heterogeneity in tumour sizes and the rate of tumour development (*253*). Nevertheless, previous studies have not taken under consideration the spatial distribution of mutations or the different mutated populations within the tumour, which can be carried out by microdissection using laser-capture microdissection (LCM) techniques.

Therefore, to understand the clonal origins and progression of dysplasia and GA, the presence of single or multiple clones in pre-neoplastic and malignant epithelium needs to be assessed alongside clonal analysis of the lineage relationships and mapping of the expansion of mutated clones within the tumour. This will provide insight into the stepwise progression model, namely the order of mutations, proposed for GA development (*153, 187*).

HDGC is caused by germline mutations in the cell-cell adhesion protein E-cadherin (*CDH1*) (*254*). This protein is the central component of epithelial cell-cell adhesion and, hence, is required for the maintenance of the integrity of epithelial layers (*178*).

HDGC is characterised as an autosomal dominant cancer syndrome where the second hit is normally methylation of the *CDH1* gene, leading to E-cadherin loss and cancer development (*181*). However, not all *CDH1* mutations cause complete inactivation of E-cadherin and *CDH1* germline mutations present with incomplete penetrance, having a 70% lifetime risk of developing HDGC (*184*). Therefore, *CDH1* germline mutations are an indication for total gastrectomy in these patients (*185*).

Khayat and colleagues used FISH and immunohistochemistry on 20 gastric cancer samples to suggest that *TP53* deletion, chromosome 17 aneusomy and *TP53* mutations may be implicated in the development of diffuse and intestinal-type gastric carcinomas (*204*). Ranzani and colleagues suggested that *TP53* mutations might be a transitional step between metaplasia and dysplasia in GA, but that such mutations may be a late event in diffuse-type gastric carcinoma leading to tumour progression (*205*). Their results were obtained from PCR-sequencing and immunohistochemistry. Shiao and colleagues also suggested that *TP53* mutations, including gene silencing by methylation, played an important role during gastric carcinogenesis regardless of histology (*255*). The identification of mutations and methylation changes in *CDH1* is very difficult to assess and previous studies have shown that *TP53* mutations are relatively common in HDGC. Therefore, in order to assess clonal expansion in diffuse gastric carcinomas in this study the presence or absence of *TP53* mutations was investigated.

3.1.1. Hypothesis and Aims

The hypothesis for this project is: GA progresses through a series of genetic events arising from a founder mutation.

The aims of this study were:

1. To demonstrate the clonal origins of dysplasia from IM
2. To determine the clonal architecture of GA
3. To assess clonal expansion in HDGC

3.2. Results

3.2.1. The clonal origins of dysplasia from intestinal metaplasia

In order to investigate the origins of dysplasia within the human stomach, areas of dysplasia from each patient was needle macrodissected and screened for mutations in genes commonly mutated in GA, (for full methods see 2.1.1, 2.2 and 2.4): *APC* (MCR region), *CTNNB1*, *KRAS*, *CDKN2A*, *TP53* and *PTEN*. Overall, these genes account for approximately 75% of all somatic mutations previously reported in GA, according to the catalogue of somatic mutations in cancer (COSMIC) database (www.sanger.ac.uk/genetics/cgp/cosmic, 16/05/2013). From the 23 patients screened, 3 showed a mutation common to both metaplasia and dysplasia (Table 3.1). Interestingly, 20 patients did not present any mutations in the dysplasia (*72*).

Table 3.1. **Only three patients had lesions with mutations in the dysplasia.** This table shows the mutations found in the dysplastic gastric epithelium of 3 out of the 23 patients screened. Dr Lydia Gutierrez-Gonzalez carried out the work on patient 3 and the data is presented in Gutierrez-Gonzalez *et al* (*72*).

Patient	Gene mutated	Mutation
Patient 1	*APC*	c.4683insA
Patient 2	*APC*	c.4667insA
Patient 3	*TP53*	c.G643A

In order to determine how dysplasia originates and spreads in the human stomach, LCM was performed on individual hyperplastic, metaplastic and dysplastic glands. Nested PCR sequencing was then carried out for the region in the mutation cluster region (MCR) of *APC*.

All hyperplastic glands were *APC*-wild type (for patients 1 and 2) and *TP53*-wild type (in the case of patient 3, see Table 3.2). The vast majority of IM glands were also wild type (83.3%-95.8%); however, IM glands were occasionally found to contain the mutation that was present in the dysplasia (4.2%-16.6%). All high-grade dysplasia (HGD) glands were mutated (Table 3.2).

Table 3.2. **Most metaplastic glands are wild type and all dysplastic glands are mutated.** Summary table of the data collected from patients 1, 2 and 3 via laser-capture microdissection of individual gastric glands with varying histology: hyperplastic; metaplastic; and dysplastic glands.

	Hyperplastic		Metaplastic		Dysplastic	
Patient	Wild type (%)	Mutated (%)	Wild type (%)	Mutated (%)	Wild type	Mutated (%)
1	10 (100)	0	35(83.3)	7 (16.6)	0	22(100)
2	15 (100)	0	73 (93.6)	5 (6.4)	0	67 (100)
3	14 (100)	0	49 (95.8)	3 (4.2)	0	158(100)

The set of experiments presented here was performed using tissue from patients 1 and 2. Every individually microdissected gland was mapped according to both its phenotype and its genotype. Tissue from patient 1 showed an *APC* mutation c.4683insA; strips of gastric epithelium from this patient can be seen in Figures 3.1, 3.2 and 3.3. Tissue from patient 2 presented with an *APC* mutation c.4667insA; three strips of gastric epithelium from this patient can be seen in Figure 3.4.

Wild type (WT) microdissected hyperplastic and IM glands were observed next to large areas of *APC*-mutated HGD glands (Figures 3.1 and 3.2). All of the figures include the previous serial section to the post-LCM section stained with haematoxylin and eosin to act as a guide for laser capture, and the highlighted areas are then seen in higher power. The corresponding raw data indicating the phenotype and the matching genotype for each gland can be found in Tables 3.3 and 3.4.

WT hyperplastic and IM glands were again found to surround areas of mutated HGD glands in a third strip of gastric epithelium from patient 1 (Figure 3.3). However, one

IM gland showed the same *APC*-mutation found in the HGD, the *APC* mutation c.4683insA. The corresponding raw data is given in Table 3.5.

All HGD glands from patient 2 showed the c.4667insA mutation and were, therefore, all clonal. The IM glands surrounding the fields of HGD were found to be WT (Figure 3.4). The corresponding raw data is presented in Table 3.6.

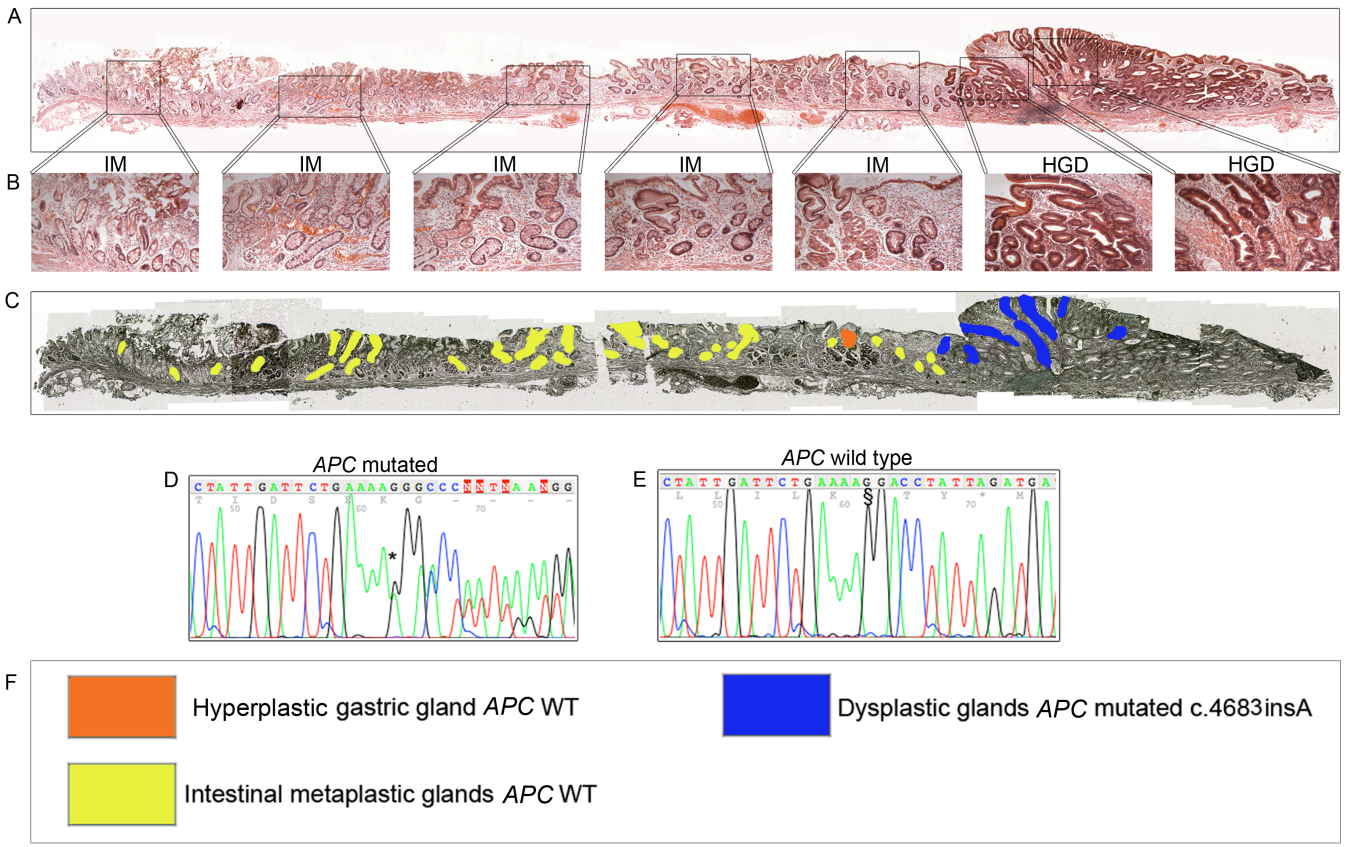

Figure 3.1. **Wild type intestinal metaplastic glands are found adjacent to large areas of mutated dysplastic glands in a strip of gastric epithelium from patient 1.** (A) A H&E of an entire section of gastric mucosa showing gastritis, intestinal metaplasia (IM) and high grade dysplasia (HGD) from patient 1. (B) Higher power of highlighted areas, showing from left to right five areas of IM and two areas of HGD. (C) Serial section showing post laser-capture microdissection (LCM). The space left by the LCM in the glands has been coloured to reflect the genotype. Yellow areas represent *APC* wild type (WT) IM glands and dark blue areas represent *APC* mutated dysplastic glands. (D and E) Two representative traces showing the *APC* mutation c.4683insA (D) and an *APC* WT trace (E). (F) Key for patient 1 on post LCM section.
Note: The H&E staining had become oxidised when the pictures were taken.

Table 3.3. **Association of the identified mutation with histology shows wild type intestinal metaplastic glands adjacent to large areas of mutated dysplastic glands in a strip of gastric epithelium from patient 1, block 6 strip 1.** WT, wild type.

Patient 1 Block 6:1	**Histology**	c.4683insA ***APC***
1	Metaplastic	WT
2	Metaplastic	WT
3	Metaplastic	WT
4	Metaplastic	WT
5	Metaplastic	WT
6	Metaplastic	WT
7	Metaplastic	WT
8	Metaplastic	WT
9	Metaplastic	WT
10	Metaplastic	WT
11	Metaplastic	WT
12	Metaplastic	WT
13	Metaplastic	WT
14	Metaplastic	WT
15	Metaplastic	WT
16	Metaplastic	WT
17	Metaplastic	WT
18	Metaplastic	WT
19	Metaplastic	WT
20	Metaplastic	WT
21	Metaplastic	WT
22	Metaplastic	WT
23	Metaplastic	WT
24	Metaplastic	WT
25	Metaplastic	WT
26	Metaplastic	WT
27	Metaplastic	WT
28	Metaplastic	WT
29	Metaplastic	WT
30	Dysplastic	MUTATED
31	Dysplastic	MUTATED
32	Dysplastic	MUTATED
33	Dysplastic	MUTATED
34	Dysplastic	MUTATED
35	Dysplastic	MUTATED
36	Dysplastic	MUTATED
37	Hyperplastic	WT

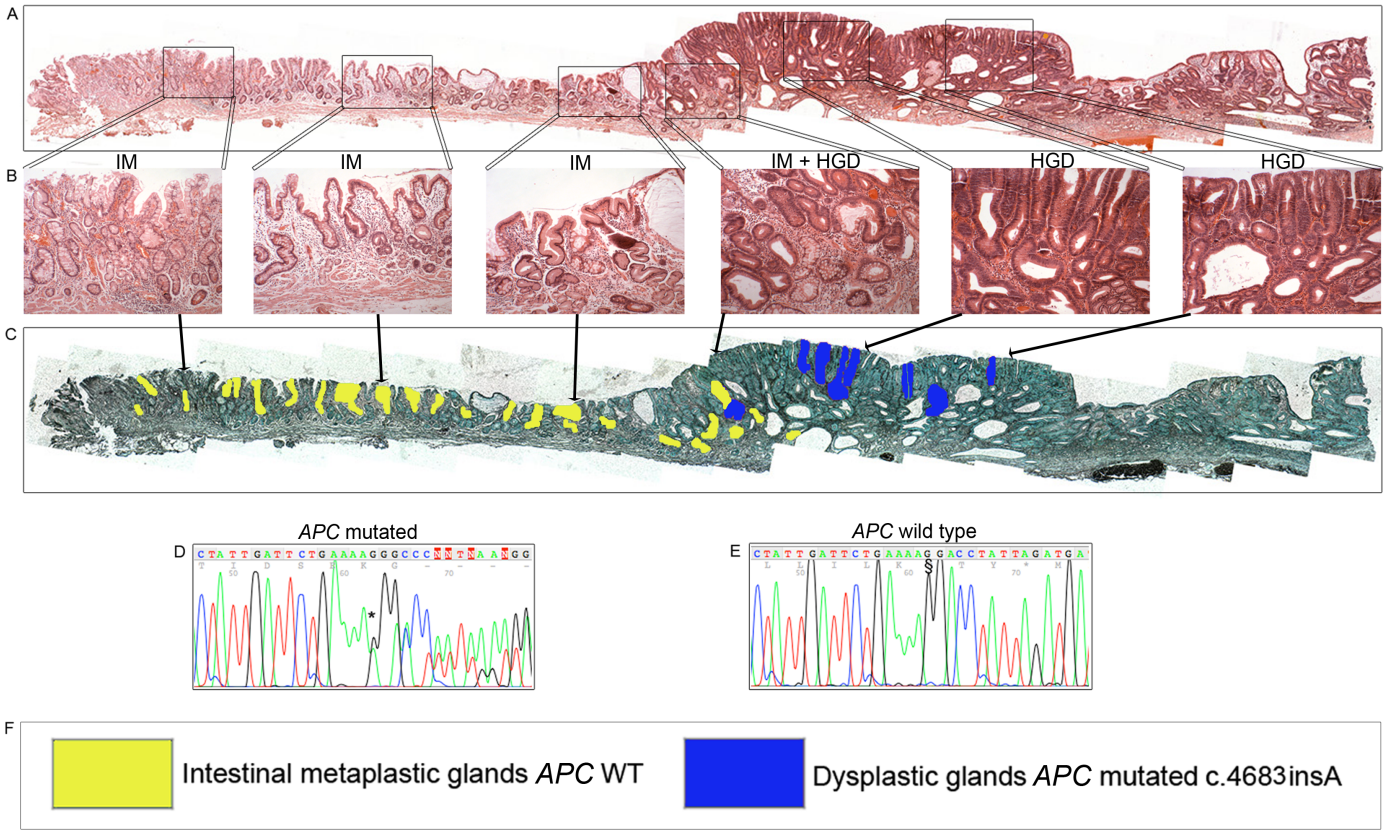

Figure 3.2. **Wild type intestinal metaplastic glands are found adjacent to large areas of mutated dysplastic glands in a second strip of gastric epithelium from patient 1.** (A) A H&E of an entire section of gastric mucosa showing gastritis, intestinal metaplasia (IM) and high grade dysplasia (HGD) from patient 1. (B) Higher power of highlighted areas, showing from left to right three areas of IM, and area of IM and HGD and two areas of HGD. (C) Serial section showing post laser-capture microdissection (LCM). Yellow areas represent *APC* WT IM glands and dark blue areas represent *APC* mutated HGD glands. (D and E) Two representative traces showing the *APC* mutation c.4683insA (D) and an *APC* WT trace (E). (F) Key for patient 1 on post LCM section.

Note: The H&E staining had become oxidised when the pictures were taken.

Table 3.4. **Association of the identified mutation with histology shows wild type intestinal metaplastic glands adjacent to large areas of mutated dysplastic glands in a second strip of gastric epithelium from patient 1, block 8 strip 3.** WT, wild type; --, denotes insufficient DNA to obtain results.

Patient 1 Block 8:3	**Histology**	c.4683insA ***APC***
1	Metaplastic	WT
2	Metaplastic	WT
3	Metaplastic	WT
4	Metaplastic	WT
5	Metaplastic	WT
6	Metaplastic	WT
7	Metaplastic	WT
8	Metaplastic	WT
9	Metaplastic	WT
10	Metaplastic	WT
11	Metaplastic	WT
12	Metaplastic	WT
13	Metaplastic	WT
14	Metaplastic	WT
15	Metaplastic	WT
16	Metaplastic	WT
17	Metaplastic	WT
18	Metaplastic	WT
19	Dysplastic	MUTATED
20	Metaplastic	WT
21	Metaplastic	WT
22	Metaplastic	WT
23	Metaplastic	WT
24	Metaplastic	--
25	Metaplastic	WT
26	Dysplastic	MUTATED
27	Dysplastic	MUTATED
28	Dysplastic	MUTATED
29	Dysplastic	MUTATED
30	Dysplastic	MUTATED
31	Dysplastic	MUTATED

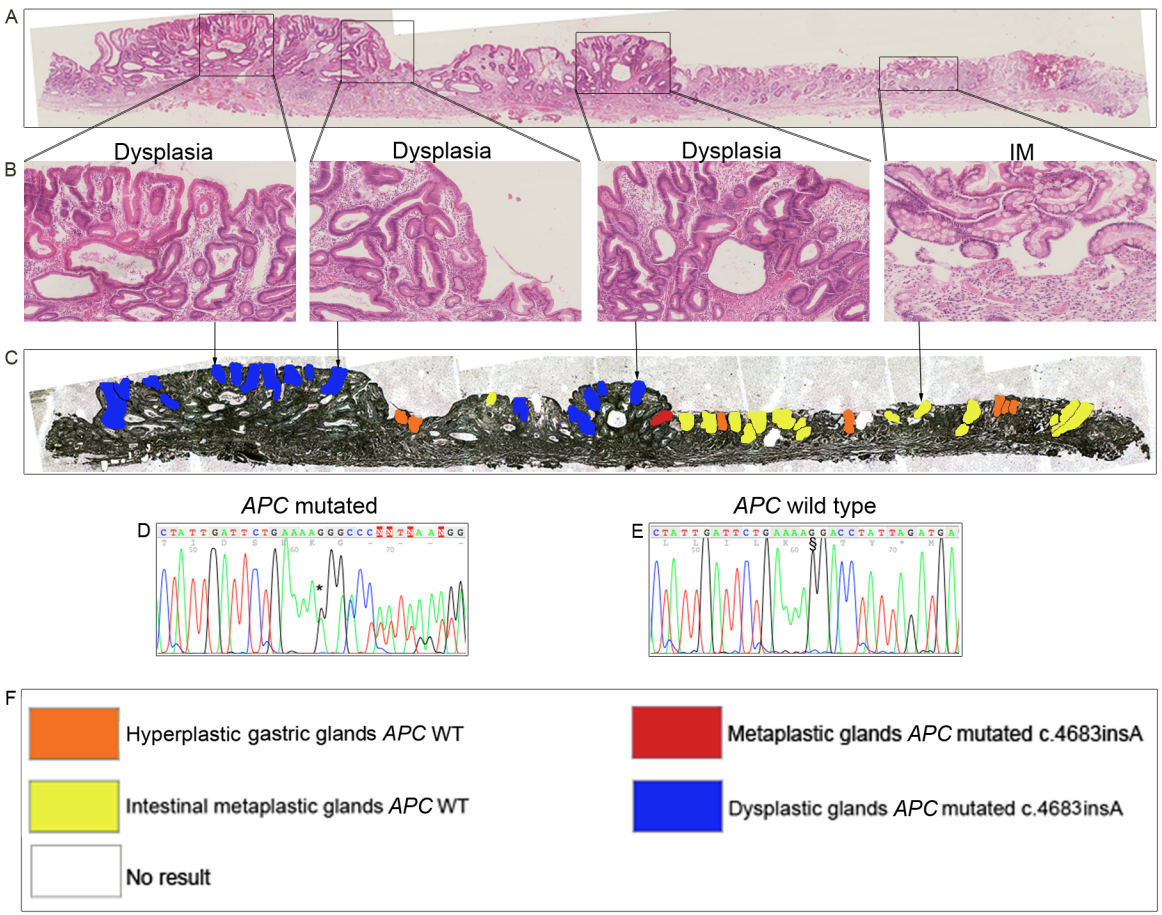

Figure 3.3. **The clonal origins of dysplasia from intestinal metaplasia in a third strip of gastric epithelium from patient 1.** (A) A H&E of an entire section of gastric mucosa showing gastritis, intestinal metaplasia (IM) and high grade dysplasia (HGD) from patient 1. (B) Higher power of highlighted areas, showing from left to right three areas of HGD and an area of IM. (C) Serial section showing post laser-capture microdissection (LCM). Orange areas represent *APC* WT hyperplastic glands, yellow areas represent *APC* WT IM glands, white areas denote insufficient DNA for a successful PCR-sequencing result, red areas represent *APC* mutated IM glands and dark blue areas represent *APC* mutated dysplastic glands. (D and E) Two representative traces showing the *APC* mutation c.4683insA (D) and an *APC* WT trace (E). (F) Key for patient 1 on post LCM section.

Table 3.5. **Association of the identified mutation with histology suggests the clonal origins of dysplasia from intestinal metaplasia in a third strip of gastric epithelium from patient 1, block 9 strip 2.** Dr Lydia Gutierrez-Gonzalez obtained the remaining of the sequencing data for this block (*72*). WT, wild type.

Patient 1 Block 9:2	**Histology**	c.4683insA ***APC***
1	Dysplastic	MUTATED
2	Dysplastic	MUTATED
3	Dysplastic	MUTATED
4	Dysplastic	MUTATED
5	Metaplastic	WT
6	Dysplastic	MUTATED
7	Dysplastic	MUTATED
8	Metaplastic	WT
9	Metaplastic	WT
10	Metaplastic	WT
11	Metaplastic	WT
12	Metaplastic	WT
13	Metaplastic	WT
14	Hyperplastic	WT
15	Metaplastic	MUTATED
16	Metaplastic	WT
17	Metaplastic	WT

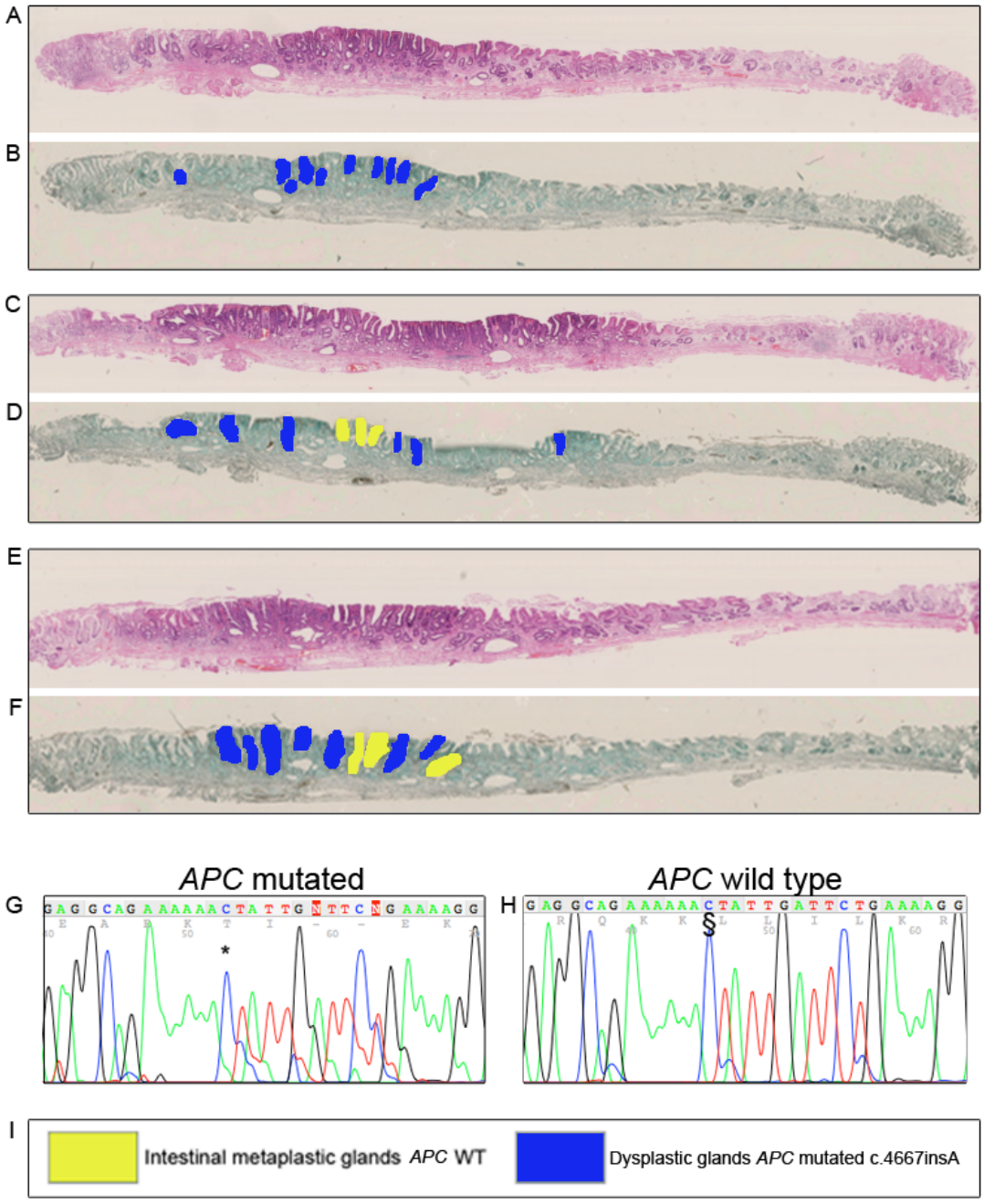

Figure 3.4. **Analysis of sequential strips of gastric epithelium from patient 2 suggests that large areas of dysplasia are clonal.** (A, C, E) H&E pictures of entire sections of gastric mucosa showing gastritis, intestinal metaplasia (IM) and high grade dysplasia (HGD) from patient 2. (B, D, F) serial sections showing post laser-capture microdissection (LCM). Yellow areas represent *APC* WT IM glands and dark blue areas represent *APC* mutated HGD glands. (G and H) Two representative traces showing the *APC* mutation c.4667insA (G), an *APC* WT trace (H). (I) Key for patient 2 on post LCM section.

Table 3.6. **Association of the identified mutation with histology suggests that large areas of dysplasia are clonal in sequential strips of gastric epithelium from patient 2, block A20-1 strips 4, 6 and 7.** WT, wild type.

Patient 2 Block A20-1: 4	**Histology**	c.4667insA ***APC***
1	Metaplastic	WT
2	Dysplastic	MUTATED
3	Dysplastic	MUTATED
4	Metaplastic	WT
5	Dysplastic	MUTATED
6	Dysplastic	MUTATED
7	Dysplastic	MUTATED
8	Dysplastic	MUTATED
9	Dysplastic	MUTATED
10	Metaplastic	WT
Block A20-1: 6	**Histology**	c.4667insA ***APC***
1	Dysplastic	MUTATED
2	Dysplastic	MUTATED
3	Dysplastic	MUTATED
4	Metaplastic	WT
5	Metaplastic	WT
6	Metaplastic	WT
7	Dysplastic	MUTATED
8	Dysplastic	MUTATED
9	Dysplastic	MUTATED
Block A20-1: 7	**Histology**	c.4667insA ***APC***
1	Dysplastic	MUTATED
2	Dysplastic	MUTATED
3	Dysplastic	MUTATED
4	Dysplastic	MUTATED
5	Dysplastic	MUTATED
6	Dysplastic	MUTATED
7	Dysplastic	MUTATED
8	Dysplastic	MUTATED
9	Dysplastic	MUTATED
10	Dysplastic	MUTATED

3.2.2. Clonal expansion in gastric adenocarcinoma

Common cancer-associated mutations are found in gastric adenocarcinomas and occur as a single event

To assess the clonal architecture of GA within the human stomach, one carcinoma area from 51 GA patients was needle macrodissected and screened for mutations in genes commonly associated with cancer: *APC* (MCR region); *CTNNB1*; *KRAS*; *CDKN2A*; *TP53*; *PTEN;* and *PIK3CA*. From these 51 GA patients, 31.4% (16/51) had a single mutation in the cancer (Table 3.7, see Table 7.3 in Appendix for full summary of the clinicopathological features).

Next, we compared the frequencies of mutations found in GA with those previously reported in the COSMIC database (www.sanger.ac.uk/genetics/cgp/cosmic 16/05/2013) to confirm we had sufficient coverage of known mutations (see Table 3.8 for full details on the patients presenting mutations). The frequency of mutation for each gene was: *APC,* 6.5% (3/46); *CDKN2A,* 2.6% (1/38); *TP53,* 23.4% (11/47); *CTNNB1,* 2.2% (1/46); 1 in *KRAS,* 2.3% (1/43); *PTEN,* 0% (0/51); and *PIK3CA,* 0% (0/24). All of our mutation frequencies were comparable to previous reports in the COSMIC database (Figure 3.5) (*256*). Even though the majority of mutations found in *TP53* (7 out of the 11 mutations) occurred in exon 8, there has been no previously published correlation between specific exon 8 mutations and GA. Therefore, this high mutation frequency in exon 8 may be either cohort-specific or due to an increased hotspot in *TP53* exon 8 in GA.

It is important to note that during the course of the screening, some DNA samples were exhausted and, unfortunately, some of the blocks were unavailable and could not be retrieved from UCH. The white areas in Table 3.7 represent insufficient DNA to obtain results. Therefore, the percentages of mutations per genes seen in Figure 3.5 were calculated for the total number of patients for which there was enough DNA; samples with insufficient DNA were excluded. The screening for *PIK3CA* was not included in Table 3.7 or in Figure 3.5 because there was only enough DNA to do the nested-PCR sequencing for approximately 50% of the samples.

Interestingly, only 1 GA (1.96%, 1/51) showed two independent functional mutations (*TP53* and *CTNNB1*). This indicated that either a functional mutation occurs as a single event in the development of GA or that other genes not included in the screening may play an important role in the development of GA. This lack of mutations in a large percentage of the cohort was also found when assessing clonal expansion in patients with dysplasia in 3.2.1.

Table 3.7. **Summary of mutations in genes selected from the COSMIC database for gastric adenocarcinoma.** Screening of 51 gastric adenocarcinomas (GA) for mutations within genes accounting for 75% of known mutations in GA (*256*): *APC*, *CTNNB1*, *KRAS*, *CDKN2A*, *TP53* and *PTEN*. White denotes insufficient DNA to obtain results; light grey stands for WT and dark blue stands for mutated sample. The red rectangles highlight the six samples analysed by laser-capture microdissection.

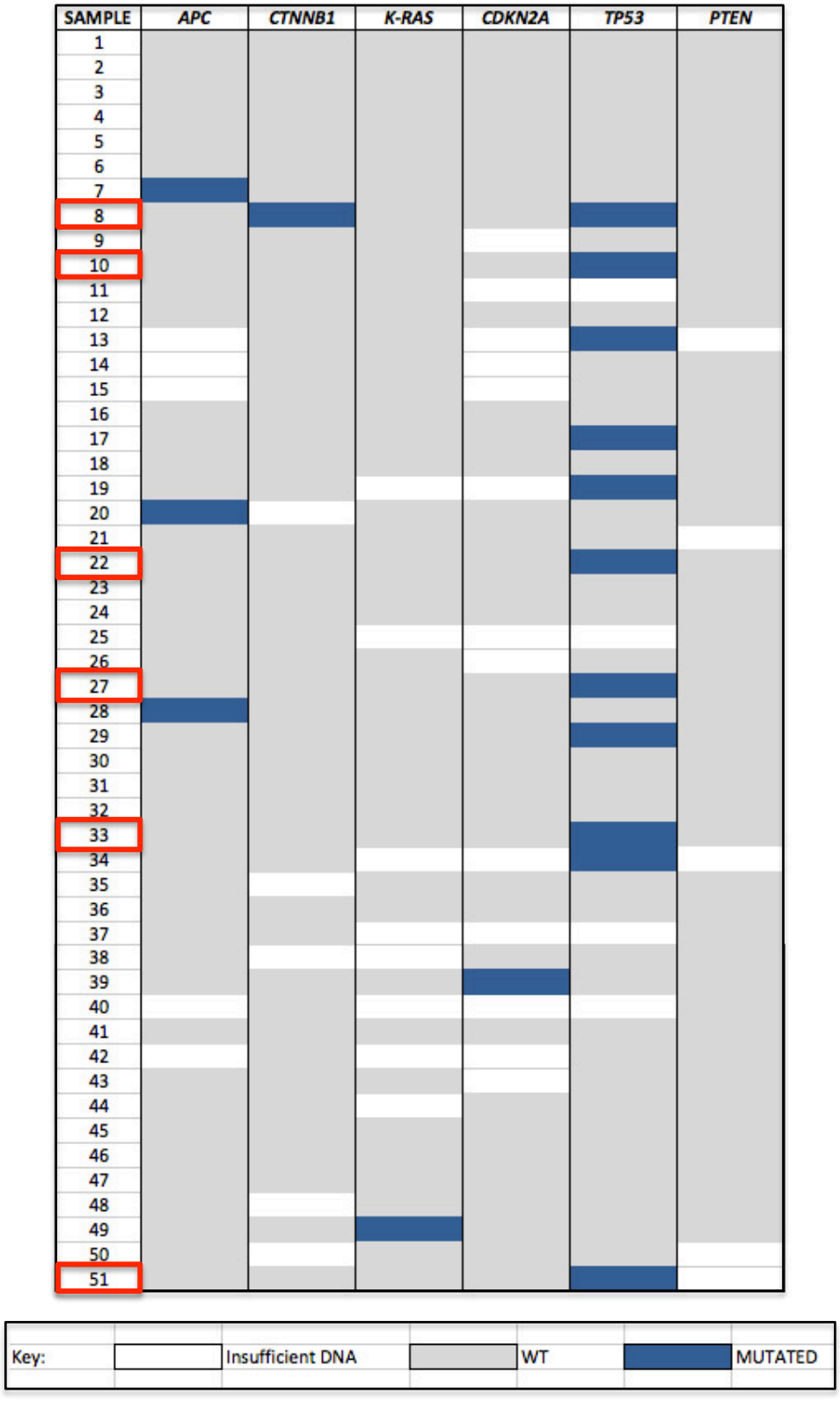

Table 3.8. **Summary of mutations identified in a cohort of gastric adenocarcinoma.** 31.4% (16/51) of patients presented a single mutation in gastric adenocarcinoma and only one sample (1.96%, 1/51) had two mutations. The patients highlighted in red denote the six samples analysed by laser-capture microdissection.

Patient	Gene	Mutation
7	*APC*	c.G4729A p.Glu1576Lys
8	*CTNNB1*	c.A121G p.Thr41Ala
8	*TP53*	c.G743A p.Arg248Gln
10	*TP53*	c.C493T,p.Gln165 Stop
13	*TP53*	c.C916T p.Arg306STOP
17	*TP53*	c.A488G p.Tyr163Cys
19	*TP53*	c.C916T p.Arg306STOP
20	*APC*	c.C4123A His1375Tyr
22	*TP53*	c.C455T p.Pro152Leu
27	*TP53*	c.G818A p.Arg273His
28	*APC*	c.C4285T p.Gln1429STOP
29	*TP53*	c.C844G p.Arg282Gly
33	*TP53*	G14439A INTRON SPLICE SITE
34	*TP53*	c.G882T p.Glu294Asp
39	*CDKN2A*	c.G207C p.Glu69Asp
49	*KRAS*	c.G38A p.Gly13Glu
51	*TP53*	c.G824A p.Cys275Tyr

A

	APC	
	Total	%
COSMIC	117/645	18
Data	3/46	6.5
Chi-square with Yates correction	3.270	
P value	0.0706	

B

	CTNNB1	
	Total	%
COSMIC	143/1514	9
Data	1/46	2.2
Chi-square with Yates correction	2.016	
P value	0.1556	

C

	KRAS	
	Total	%
COSMIC	193/2793	7
Data	1/43	2.3
Chi-square with Yates correction	0.770	
P value	0.3802	

D

	TP53	
	Total	%
COSMIC	1066/3203	33.3
Data	11/47	23.4
Chi-square with Yates correction	1.618	
P value	0.2034	

E

	CDKN2A	
	Total	%
COSMIC	42/602	7
Data	1/38	2.6
Chi-square with Yates correction	0.495	
P value	0.4817	

F

	Total	%
Total patients	51	100%
Patients with mutations	16	31.4%
Patients with multiple mutations	1	1.96%

Figure 3.5. **Mutation frequencies are comparable to reports for gastric adenocarcinoma held in the COSMIC database.** Statistical analysis of results obtained from the screening of 51 gastric adenocarcinoma patients. (A-E) Tables show the frequency of mutations within *APC* (A), *CTNNB1* (B), *KRAS* (C), *TP53* (D) and *CDKN2A* (E) in our patient cohort compared with the COSMIC database (*256*). (F) Table showing the percentages of mutated samples. *P* value was obtained by Chi-square test using Yates correction (two-tailed).

Gastric adenocarcinoma is clonal

To assess clonal expansion in GA, six patients were selected and analysed by LCM. These were patients 8, where the GA showed two independent functional mutations, 10, 22, 27, 33 and 51 (see mutational details for the patients highlighted in red in Table 3.8). LCM was then performed for areas of chronic gastritis, IM, dysplasia and carcinoma, where present in the available tissue for each patient (see Table 3.9).

Table 3.9. **Randomly selected patients for laser-capture microdissection.** List of the blocks of gastric epithelium used for laser-capture microdissection from the six patients selected randomly.

Patient	Genes mutated	Block number	Histopathological phenotypes present
8	*TP53* + *CTNNB1*	6	Gastritis and IM
		7	GA
		8	GA
10	*TP53*	5	Gastritis , IM and GA
22	*TP53*	6	GA
27	*TP53*	3	Squamous epithelium, gastritis, IM, GA
		5	Gastritis and GA
33	*TP53*	5	Gastritis, IM and GA
		6	Gastritis, IM and HGD
51	*TP53*	5	Gastritis, IM, HGD and GA

Dissected gastritic and IM areas from patient 8 were WT, although most dissected IM areas showed LOH for microsatellite markers D17S1832, D17S1176, D17S1678, D17S1881 and D17S1506E for *TP53* at the 17p locus (Figure 3.6). The associated poorly differentiated GA had three different populations of cells with specific mutations within the carcinoma: WT *TP53* and WT *CTNNB1*; mutated *TP53* and WT *CTNNB1*; and mutated *TP53* and mutated *CTNNB1* (Figure 3.8). A consecutive

specimen of gastric mucosa from patient 8, again with a poorly differentiated GA, showed two of the different populations of cells within the carcinoma: WT *TP53* and WT *CTNNB1*; and mutated *TP53* and mutated *CTNNB1* (Figure 3.9). All three populations of cells present LOH for the same markers in the cancer as in the IM (see Figure 3.7 for representative traces showing controls and LOH traces for the 5 microsatellite markers for patient 8). The raw data associating the identified mutations and LOH status for each microdissected area with histology can be found in Figure 3.7 and Tables 3.10 and 3.11, respectively.

A specimen of gastric epithelium from patient 10 presented areas of chronic gastritis, IM, GA and muscle with a high level of GA infiltration (Figure 3.10). Microdissected areas of chronic gastritis and IM were WT and did not show LOH for markers at the 17p and 17q loci. All areas of GA and invaded muscle were mutated; they all presented LOH for microsatellite markers D17S1881 and D17S250 (see Figure 3.11 for representative traces showing controls and LOH traces, and for the corresponding raw data). Due to the reduced number of informative microsatellite markers in chromosome 17 for this patient, LOH was only recorded when the two informative markers were lost in each individual area.

A poorly differentiated adenocarcinoma from patient 22 had two different populations of cells harbouring WT *TP53* or mutated *TP53* (Figure 3.12); both populations showed LOH for microsatellite markers D17S1881, D17S1506E, D17S1176 and D17S250 from the 17p and 17q chromosomal region (see Figure 3.13 for representative traces showing controls and LOH traces, and for the corresponding raw data).

Dissected gastritis and muscle areas from patient 27 were WT, but all GA areas were *TP53* mutated (Appendix Figure 7.16). Another specimen of gastric epithelium from this patient showed that benign areas (gastritis and muscle) and pre-neoplastic lesions (IM) were WT; however, all GA areas were *TP53* mutated (Appendix Figure 7.17). Patient 27 was not informative for any microsatellite marker on the 17p locus. The raw data associating the identified *TP53* mutation for each microdissected area with histology can be found in the appendix in the corresponding Tables 7.4 and 7.5.

TP53 mutations could also be found in GA microdissected areas but not in those IM areas dissected from patient 33 (Figure 3.14). LOH was observed for microsatellite markers D17S1678 and D17S1176 mapped to the 17p locus in most GA areas. There was one IM area that also presented LOH for both markers (see Figure 3.15 for representative traces showing controls and LOH traces, and for the corresponding raw data). The *TP53* mutation could not be found in any HGD or any benign areas in a consecutive specimen of gastric mucosa from patient 33 (Figure 3.16; see Table 3.12 for the corresponding raw data). Once again, due to the limited number of informative microsatellite markers in chromosome 17 for this patient, LOH could only be identified when the two informative markers were lost in each individual area.

A strip of gastric epithelium from patient 51 displaying chronic gastritis, IM, HGD and GA was examined. The chronic gastritis and IM areas were found to be *TP53* WT, whereas the areas with HGD and GA were all *TP53* mutated. Chronic gastritis and IM did not show LOH, but some GA did show LOH for microsatellite markers D17S1832 and D17S1506E for *TP53* from the 17p locus (Figure 3.17; see Figure 3.18 for

representative traces showing controls and LOH traces, and for the corresponding raw data).

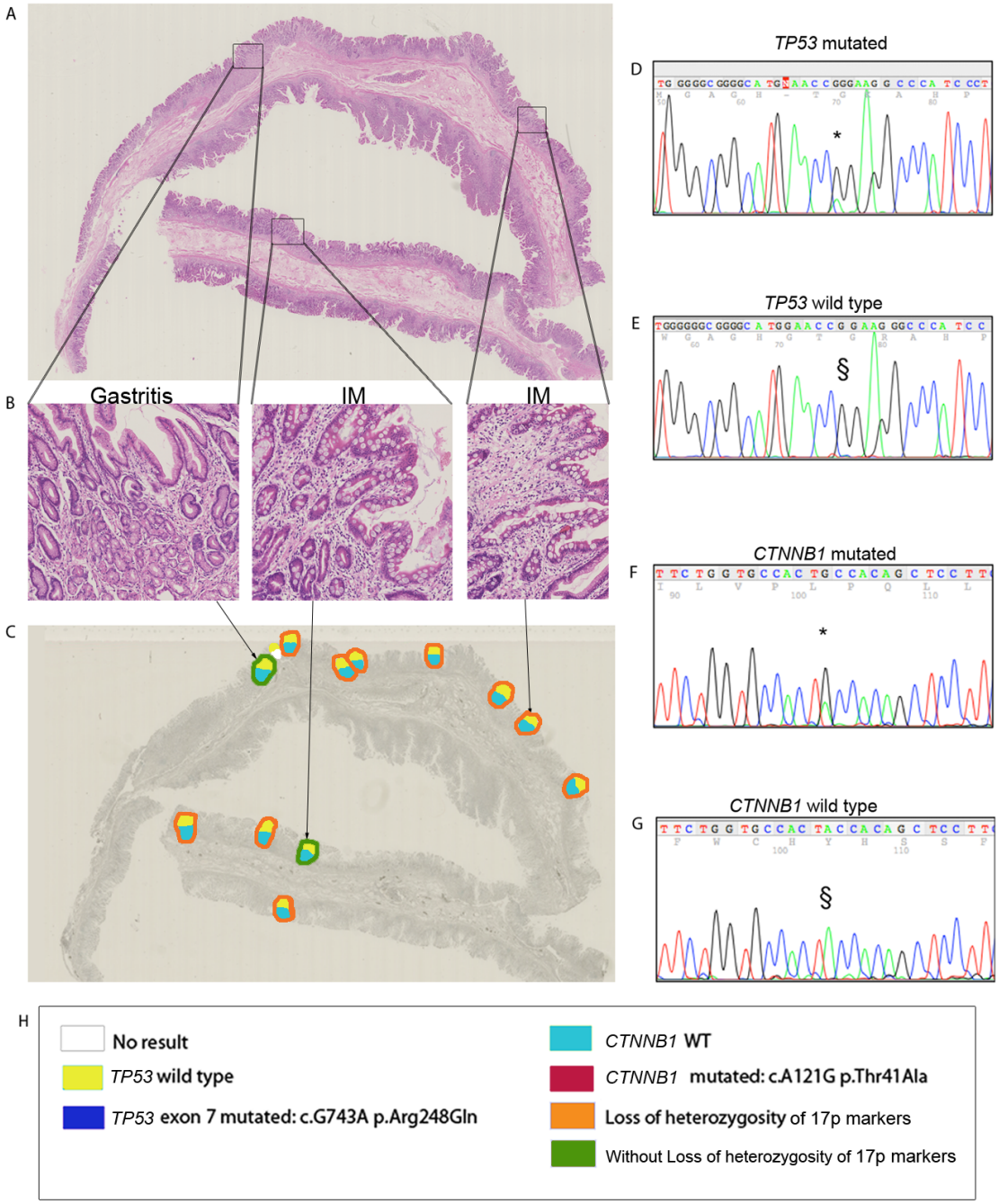

Figure 3.6. **Intestinal metaplastic glands are wild type but show loss of heterozygosity for microsatellites at 17p in patient 8.** (A) A H&E of an entire section of gastric mucosa showing normal epithelium and intestinal metaplasia (IM) from patient 8, specimen block 6. (B) Higher power of highlighted areas, showing from left to right gastritis and two areas of IM. (C) Serial section showing post laser-capture microdissection (LCM). Yellow areas are *TP53* WT and light blue areas are *CTNNB1* WT. Areas with loss of heterozygosity (LOH) at 17p for markers D17S1832 (180bp), D17S1881 (210bp), D17S1506E (150bp), D17S1678 (120bp) and D17S1176 (80bp) are distinguished by an orange border and areas without LOH by a green border. (D, E, F and G) Four representative traces showing the *TP53* mutation c.G743A (D), a *TP53* WT trace (E), the *CTNNB1* mutation c.A121G (F), and a *CTNNB1* WT trace (G). (H) Key for patient 8 on post LCM section.

A

Patient 8:6	Histology	*TP53*	*CTNNB1*	D17S1832	D17S1881	D17S1506E	D17S1678	D17S1176
1	IM	WT	WT	LOH	+	LOH	LOH	+
2	IM	WT	WT	LOH	LOH	LOH	LOH	+
3	IM	WT	WT	+	LOH	LOH	+	+
4	Gastritis	WT	WT	LOH	LOH	LOH	LOH	LOH
5	IM	WT	WT	LOH	+	LOH	LOH	+
6	IM	WT	WT	+	LOH	LOH	LOH	+
7	IM	WT	WT	ND	LOH	ND	LOH	ND
8	Gastritis	WT	WT	+	+	ND	+	+
9	IM	WT	WT	LOH	LOH	LOH	LOH	LOH
10	IM	WT	WT	+	+	+	LOH	+
11	IM	WT	WT	+	LOH	LOH	LOH	+
12	IM	WT	WT	+	+	+	+	+

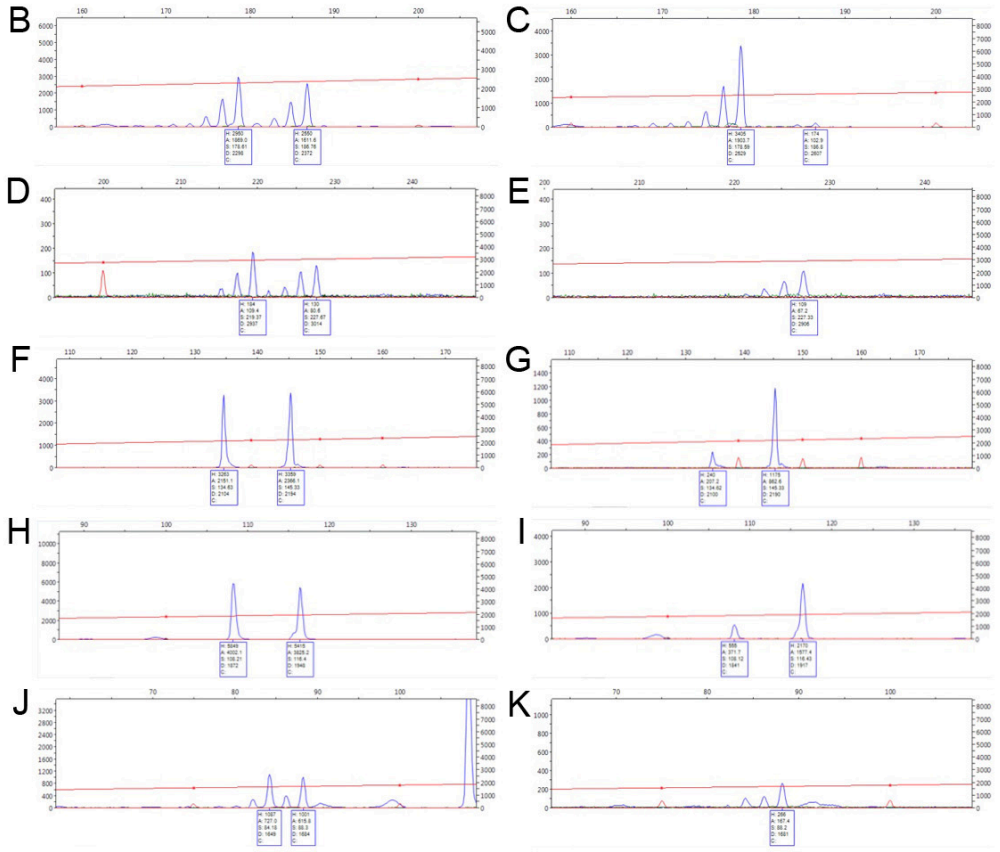

Figure 3.7. **Association of identified mutations with histology and loss of heterozygosity shows intestinal metaplastic glands are wild type but show loss of heterozygosity for microsatellites at 17p in patient 8.** (A) This table corresponds to the laser-capture microdissection data presented in Figure 3.6, tissue from patient 8, specimen block 6. (B, D, F, H and J) Five representative traces showing controls where both alleles are present (+) and (C, E, G, I and K) five representative traces where loss of heterozygosity (LOH) has occurred for markers D17S1832 (180bp) (B, C), D17S1881 (210bp) (D, E), D17S1506E (150bp) (F, G), D17S1678 (120bp) (H, I) and D17S1176 (80bp) (J, K) at 17p from patient 8. An enlarged version of traces B to K can be seen in Figures 7.1 to 7.5 in the Appendix. WT, wild type; +, both alleles are present in chromosome 17; ND, not determined due to insufficient DNA; LOH was calculated by measuring the area under the curve of the samples compared to that of a normalized control (gastritis or muscle epithelium areas from the same patient). LOH was considered when the area under the curve was <0.5 or >2.0.

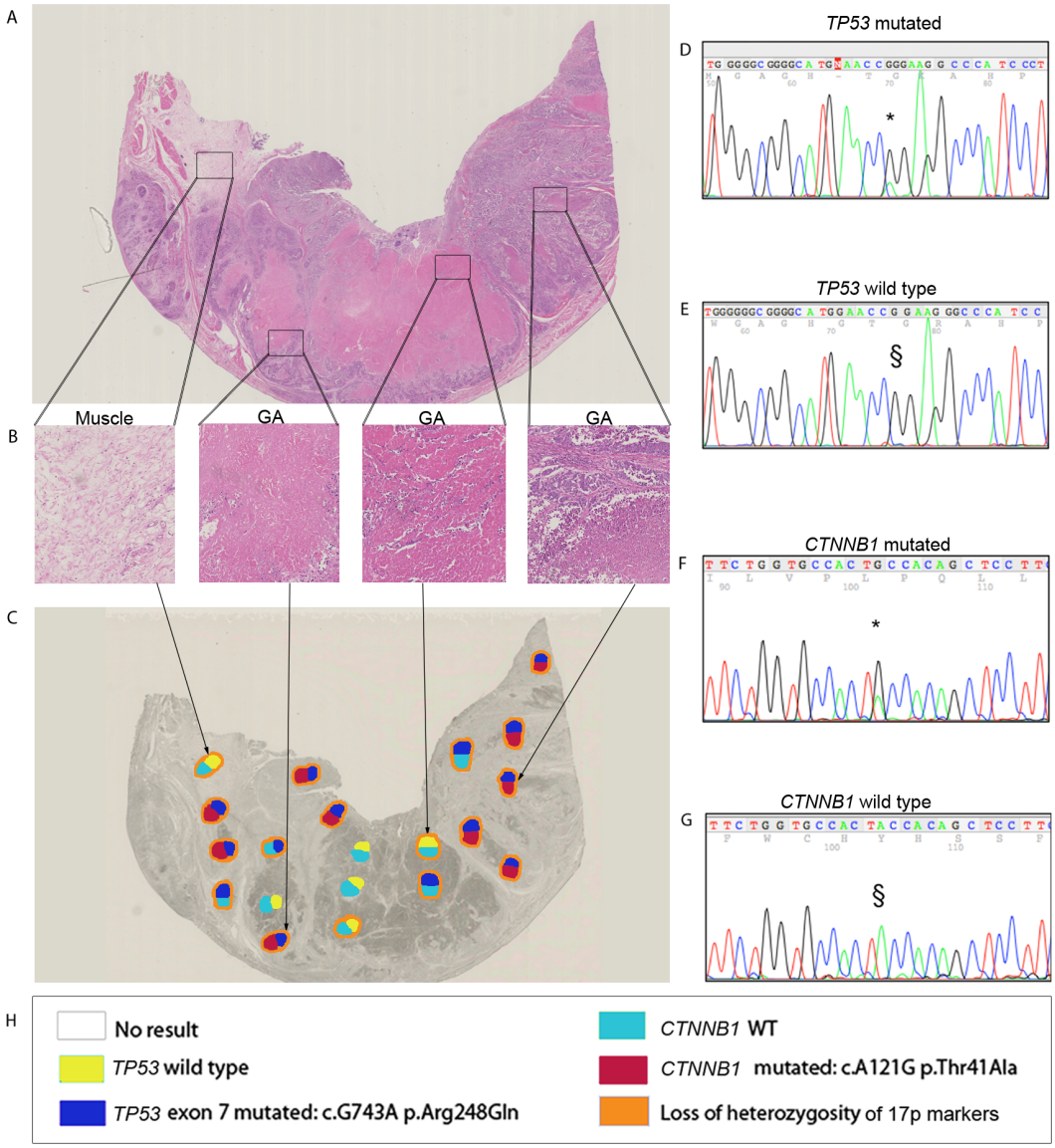

Figure 3.8. **Clonal ordering of mutations in gastric adenocarcinoma shows clonal evolution in patient 8.** (A) A H&E of an entire section of gastric mucosa showing a poorly differentiated gastric adenocarcinoma (GA) from patient 8, specimen block 7. (B) Higher power of highlighted areas showing from left to right a muscle area and three areas of highly necrotic GA. (C) Serial section showing post laser-capture microdissection (LCM). Yellow areas are *TP53* WT whereas dark blue areas are positive for the *TP53* mutation c.G743A. Light blue areas are *CTNNB1* WT whereas dark red areas are positive for the *CTNNB1* mutation c.A121G. Areas with loss of heterozygosity (LOH) at 17p for markers D17S1832 (180bp), D17S1881 (210bp), D17S1506E (150bp), D17S1678 (120bp) and D17S1176 (80bp) are distinguished by an orange border. (D, E, F and G) Four representative traces showing the *TP53* mutation c.G743A (D), a *TP53* WT trace (E), the *CTNNB1* mutation c.A121G (F), and a *CTNNB1* WT trace (G). (H) Key for patient 8 on post LCM section.
NOTE: Large areas of necrosis were present in the adenocarcinoma, these could account for the WT genotype of some of the *TP53* and *CTNNB1* GA areas.

Table 3.10. **Association of identified mutations with histology and loss of heterozygosity shows clonal evolution in gastric adenocarcinoma in patient 8.** This table corresponds to the laser-capture microdissection data presented in Figure 3.8, tissue from patient 8, specimen block 7. The representative traces showing controls where both alleles are present (+) and samples where loss of heterozygosity (LOH) has occurred for markers D17S1832 (180bp), D17S1881 (210bp), D17S1506E (150bp), D17S1678 (120bp) and D17S1176 (80bp) at 17p from patient 8 is shown in Figure 3.7. An enlarged version of traces B to K can be seen in Figures 7.1 to 7.5 in the Appendix.

Patient 8:7	Histology	*TP53*	*CTNNB1*	D17S1832	D17S1881	D17S1506E	D17S1678	D17S1176
1	Muscle	WT	WT	LOH	ND	ND	LOH	ND
2	GA	MUTATED	MUTATED	LOH	LOH	+	LOH	ND
3	GA	MUTATED	MUTATED	LOH	ND	LOH	LOH	LOH
4	GA	MUTATED	WT	LOH	ND	ND	LOH	LOH
5	GA	MUTATED	MUTATED	LOH	LOH	LOH	LOH	LOH
6	GA	MUTATED	MUTATED	LOH	LOH	LOH	LOH	
7	GA	MUTATED	WT	+	ND	LOH	LOH	LOH
8	GA	WT	WT	ND	ND	ND	ND	ND
9	GA	MUTATED	MUTATED	LOH	LOH	LOH	LOH	LOH
10	GA	WT	WT	LOH	ND	LOH	LOH	ND
11	GA	WT	WT	ND	ND	ND	ND	ND
12	GA	MUTATED	WT	ND	ND	LOH	ND	ND
13	GA	WT	WT	LOH	ND	ND	ND	ND
14	GA	WT	WT	ND	ND	ND	ND	ND
15	GA	MUTATED	WT	LOH	ND	LOH	ND	ND
16	GA	MUTATED	MUTATED	LOH	ND	+	LOH	ND
17	GA	MUTATED	MUTATED	LOH	LOH	+	LOH	LOH
18	GA	MUTATED	MUTATED	LOH	LOH	+	LOH	ND
19	GA	MUTATED	MUTATED	LOH	LOH	LOH	LOH	LOH
20	GA	MUTATED	MUTATED	LOH	LOH	LOH	LOH	LOH

NOTE: WT, wild type; +, both alleles are present in chromosome 17; ND, not determined due to insufficient DNA; LOH was calculated by measuring the area under the curve of the samples compared to that of a normalized control (gastritis or muscle epithelium areas from the same patient). LOH was considered when the area under the curve was <0.5 or >2.0.

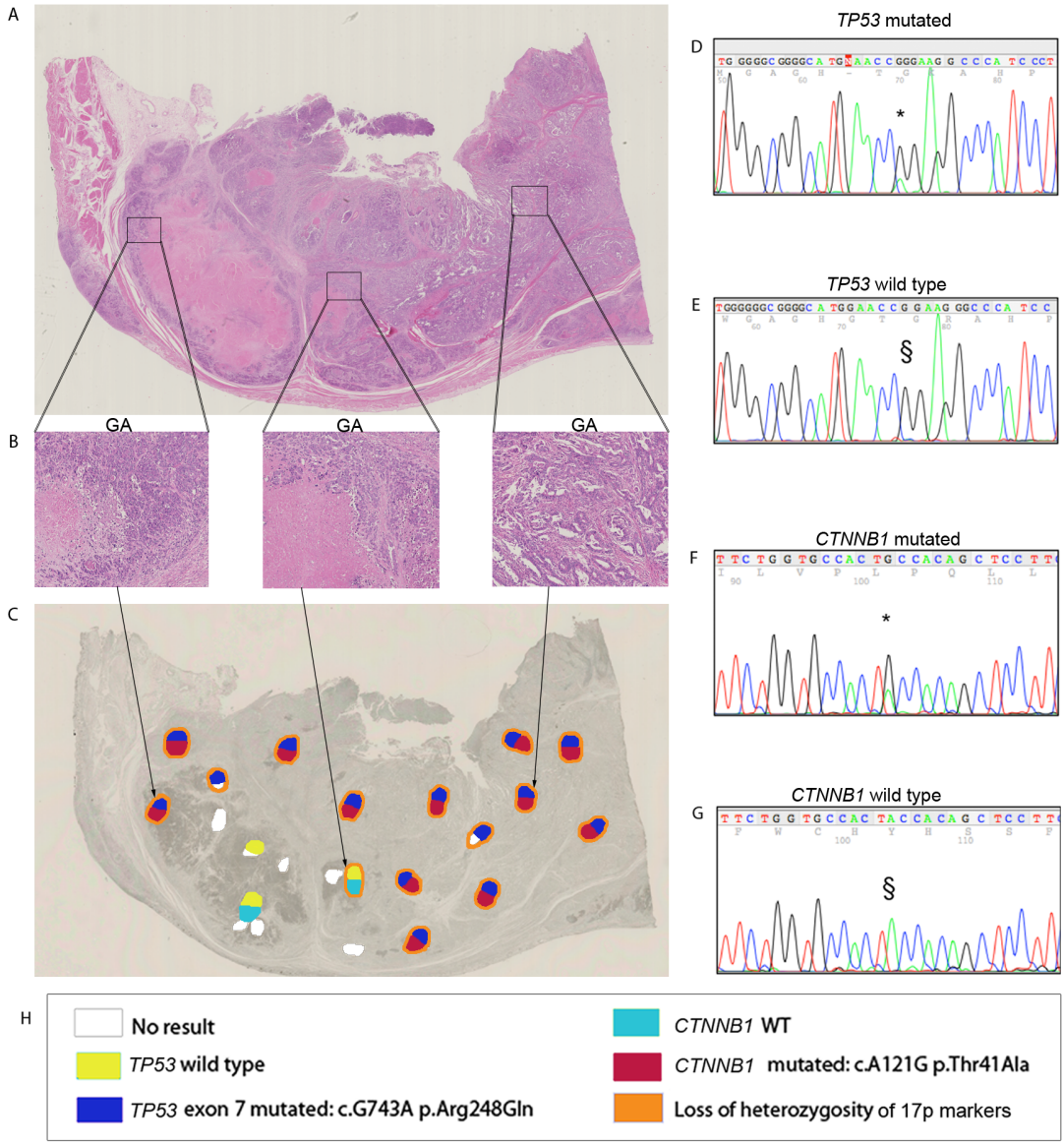

Figure 3.9. **Clonal ordering of mutations in a sequential specimen of gastric adenocarcinoma shows again clonal evolution in patient 8.** (A) A H&E of an entire section of gastric mucosa showing a poorly differentiated gastric adenocarcinoma (GA) from patient 8, specimen block 8. (B) Higher power of highlighted areas, showing three areas of highly necrotic GA. (C) Serial section showing post laser-capture microdissection (LCM). The space left by the LCM areas have been coloured to reflect the genotype. Yellow areas are *TP53* WT whereas dark blue areas are positive for the *TP53* mutation c.G743A. Light blue areas are *CTNNB1* WT whereas dark red areas are positive for the *CTNNB1* mutation c.A121G. Areas with loss of heterozygosity (LOH) in 17p for markers D17S1832 (180bp), D17S1881 (210bp), D17S1506E (150bp), D17S1678 (120bp) and D17S1176 (80bp) are distinguished by an orange border. (D, E, F and G) Four representative traces showing the *TP53* mutation c.G743A (D), a *TP53* WT trace (E), the *CTNNB1* mutation c.A121G (F), and a *CTNNB1* WT trace (G). (H) Key for patient 8 on post LCM section.

Table 3.11. **Association of identified mutations with histology and loss of heterozygosity shows clonal evolution in a sequential specimen of gastric adenocarcinoma in patient 8.** This table corresponds to the laser-capture microdissection data presented in Figure 3.9, tissue from patient 8, specimen block 8. The representative traces showing controls where both alleles are present (+) and samples where loss of heterozygosity (LOH) has occurred for markers D17S1832 (180bp), D17S1881 (210bp), D17S1506E (150bp), D17S1678 (120bp) and D17S1176 (80bp) at 17p from patient 8 is shown in Figure 3.7. An enlarged version of traces B to K can be seen in Figures 7.1 to 7.5 in the Appendix.

Patient 8:8	Histology	*TP53*	*CTNNB1*	D17S1832	D17S1881	D17S1506E	D17S1678	D17S1176
1	GA			ND	ND	ND	ND	ND
2	GA			ND	ND	ND	ND	ND
3	GA	MUTATED	MUTATED	+	ND	LOH	LOH	ND
4	GA	WT		ND	ND	ND	ND	ND
5	GA	MUTATED		ND	ND	LOH	LOH	ND
6	GA	WT	WT	ND	ND	ND	ND	ND
7	GA	MUTATED	MUTATED	LOH	LOH	LOH	LOH	LOH
8	GA			ND	ND	ND	ND	ND
9	GA	WT	WT	LOH	ND	LOH	ND	ND
10	GA	MUTATED	MUTATED	LOH	LOH	LOH	LOH	LOH
11	GA	MUTATED	MUTATED	LOH	LOH	LOH	LOH	+
12	GA	MUTATED	MUTATED	LOH	ND	LOH	LOH	ND
13	GA	MUTATED	MUTATED	LOH	LOH	LOH	LOH	LOH
14	GA	MUTATED		LOH	LOH	ND	LOH	LOH
15	GA	MUTATED	MUTATED	LOH	LOH	LOH	LOH	+
16	GA	MUTATED	MUTATED	LOH	LOH	LOH	LOH	LOH
17	GA	MUTATED	MUTATED	LOH	LOH	LOH	LOH	LOH
18	GA	MUTATED	MUTATED	+	ND	+	LOH	ND
19	GA	MUTATED	MUTATED	LOH	LOH	LOH	LOH	LOH
20	GA	MUTATED	MUTATED	LOH	LOH	+	LOH	ND

NOTE: WT, wild type; Grey coloured area denotes no result from PCR reaction; +, both alleles are present in chromosome 17; ND, not determined due to insufficient DNA; LOH was calculated by measuring the area under the curve of the samples compared to that of a normalized control (gastritis or muscle epithelium areas from the same patient). LOH was considered when the area under the curve was <0.5 or >2.0.

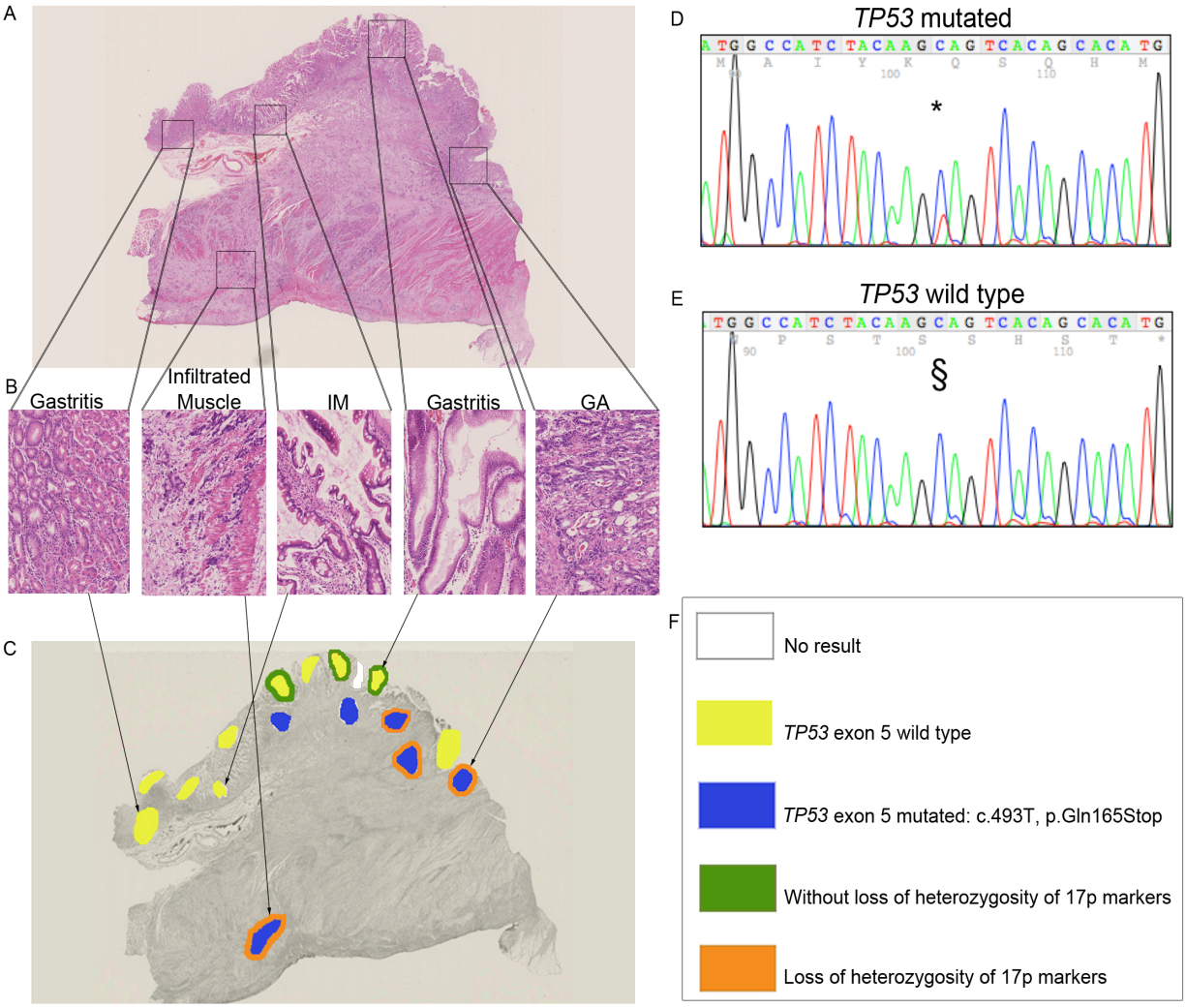

Figure 3.10. ***TP53* mutations could be found in gastric adenocarcinoma but not in intestinal metaplastic glands in patient 10.** (A) A H&E showing areas of gastritis, intestinal metaplastic glands (IM) and gastric adenocarcinoma (GA). (B) Higher power of highlighted areas showing from left to right an area of gastritis, invasive GA within the muscle, IM, another area of gastritis and GA. (C) Serial section showing post laser-capture microdissection (LCM). Yellow areas are *TP53* WT whereas dark blue areas are positive for the *TP53* mutation c.C493T. Areas with LOH at 17p for markers D17S1881 (210bp) and D17S250 (140bp) are distinguished by an orange border and areas without LOH by a green border. (D, E) Two representative traces showing the *TP53* mutation c.C493T (D) and a *TP53* WT trace (E). (F) Key for patient 10 on post LCM section.

A

Patient 10	Histology	*TP53*	D17S1881	D17S250
1	Gastritis	WT	LOH	+
2	Gastritis	WT	LOH	+
3	Gastritis	WT	LOH	+
4	IM	WT	LOH	+
5	Gastritis	WT	ND	ND
6	GA	MUTATED	LOH	+
7	Gastritis	WT	+	+
8	Gastritis	WT	ND	ND
9	GA	MUTATED	LOH	+
10	Gastritis	WT	ND	+
11	Gastritis		ND	ND
12	Gastritis	WT	+	+
13	GA	MUTATED	LOH	LOH
14	Gastritis	WT	LOH	+
15	GA	MUTATED	LOH	LOH
16	GA	MUTATED	LOH	LOH
17	Muscle	MUTATED	LOH	LOH

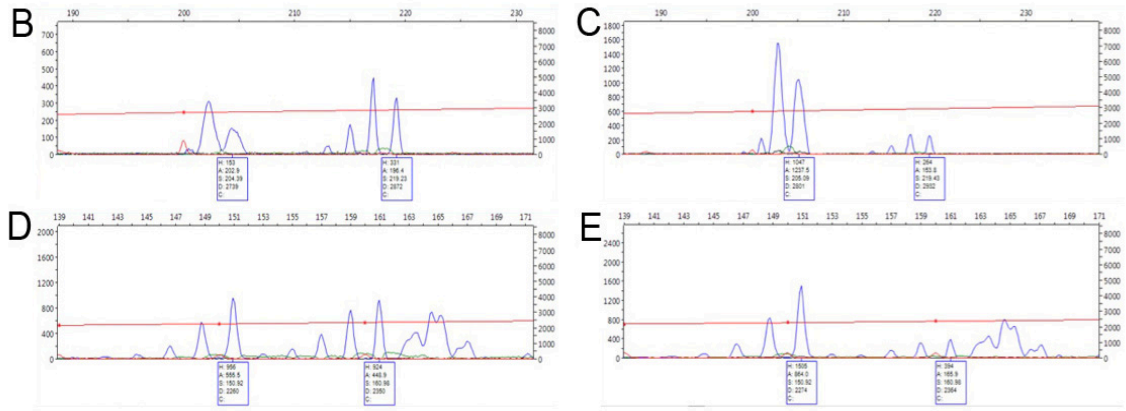

Figure 3.11. **Association of the identified mutation with histology and loss of heterozygosity shows *TP53* mutations could be found in gastric adenocarcinoma but not in intestinal metaplastic glands in patient 10.** (A) Table corresponding to the laser-capture microdissection data presented in Figure 3.10, from patient 10. (B and D) Two representative traces showing controls where both alleles are present (+) and (C and E) two representative traces where loss of heterozygosity (LOH) has occurred for markers D17S1881 (210bp) (B, C) and D17S250 (140bp) (D, E) at 17p from patient 10. An enlarged version of traces B to E can be seen in Figures 7.6 and 7.7 in the Appendix. WT, wild type; +, both alleles are present in chromosome 17; ND, not determined due to insufficient DNA; LOH was calculated by measuring the area under the curve of the samples compared to that of a normalized control (gastritis or muscle epithelium areas from the same patient). LOH was considered when the area under the curve was <0.5 or >2.0.

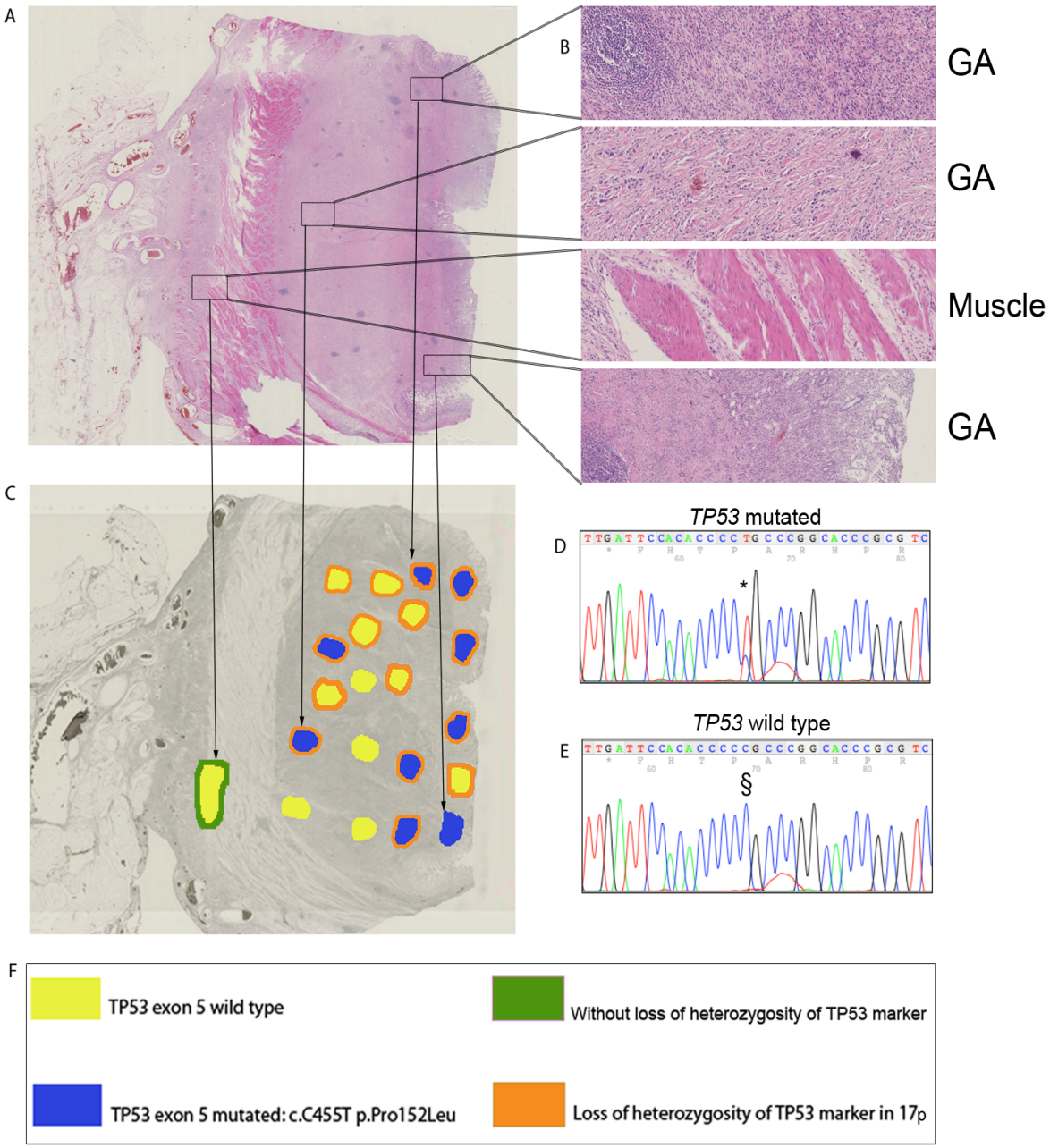

Figure 3.12. **Wild type and mutated clones demonstrate a clonal relationship in patient 22.** (A) A scanned H&E picture of an entire section of gastric mucosa showing a poorly differentiated gastric adenocarcinoma (GA). (B) Higher power of highlighted areas, showing from top to bottom two areas of poorly differentiated GA, a muscle area and another poorly differentiated GA area. (C) Serial section showing post laser-capture microdissection (LCM). Yellow areas are *TP53* WT whereas dark blue areas are positive for the *TP53* mutation c.C455T. Areas with loss of heterozygosity (LOH) at 17p for markers D17S1881 (210bp), D17S1506E (150bp), D17S1176 (80bp), and D17S250 (140bp) are distinguished by an orange border and areas without LOH by a green border. (D, E) Two representative traces showing the *TP53* mutation c.C455T (D) and a *TP53* WT trace (E). (F) Key for patient 22 on post LCM section.

A

Patient 22	Histology	*TP53*	D17S1881	D17S1506E	D17S1176	D17S250
1	GA	MUTATED	+	LOH	ND	LOH
2	GA	MUTATED	LOH	LOH	LOH	LOH
3	GA	MUTATED	LOH	LOH	LOH	+
4	GA	WT	LOH	LOH	LOH	+
5	GA	MUTATED	+	LOH	+	+
6	GA	MUTATED	ND	LOH	LOH	+
7	GA	MUTATED	LOH	LOH	ND	+
8	GA	WT	LOH	ND	ND	+
9	GA	WT	LOH	LOH	+	+
10	GA	MUTATED	LOH	LOH	LOH	LOH
11	GA	WT	ND	LOH	LOH	+
12	GA	WT	LOH	LOH	LOH	LOH
13	GA	WT	ND	LOH	ND	ND
14	GA	WT	ND	+	ND	ND
15	GA	WT	LOH	LOH	ND	ND
16	GA	WT	LOH	+	LOH	ND
17	GA	WT	LOH	+	LOH	+
18	GA	MUTATED	LOH	+	LOH	+
19	GA	MUTATED	LOH	+	LOH	LOH
20	GA	WT	ND	ND	ND	ND
21	Muscle	WT	ND	LOH	+	+

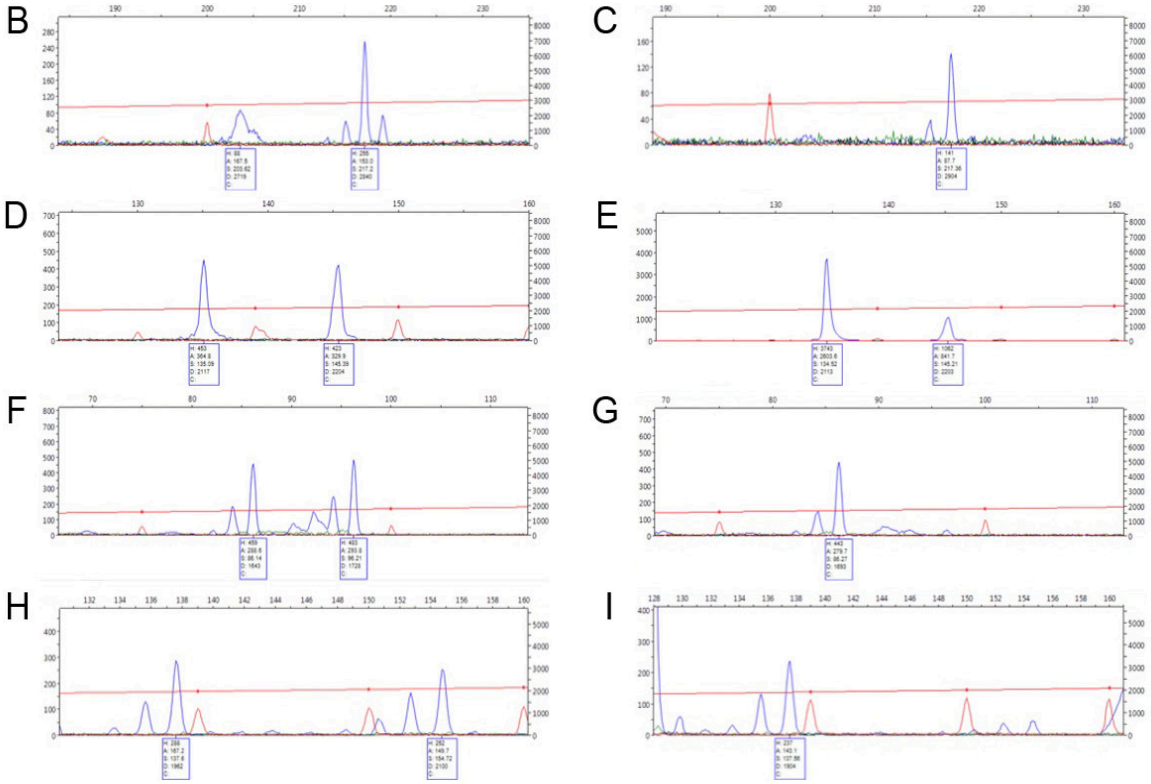

Figure 3.13. **Association of identified mutations with histology and loss of heterozygosity shows that wild type and mutated clones demonstrate a clonal relationship in patient 22.** (A) This table corresponds to the laser-capture microdissection data presented in Figure 3.12, from patient 22. (B, D, F and H) Four representative traces showing controls where both alleles are present (+) and (C, E, G and I) four representative traces where loss of heterozygosity (LOH) has occurred for markers D17S1881 (210bp) (B, C), D17S1506E (150bp) (D, E), D17S1176 (80bp) (F, G) and D17S250 (140bp) (H, I) at 17p from patient 22. An enlarged version of traces B to I can be seen in Figures 7.8 to 7.11 in the Appendix. WT, wild type; +, both alleles are present in chromosome 17; ND, not determined due to insufficient DNA; LOH was calculated by measuring the area under the curve of the samples compared to that of a normalized control (gastritis or muscle epithelium areas from the same patient). LOH was considered when the area under the curve was <0.5 or >2.0.

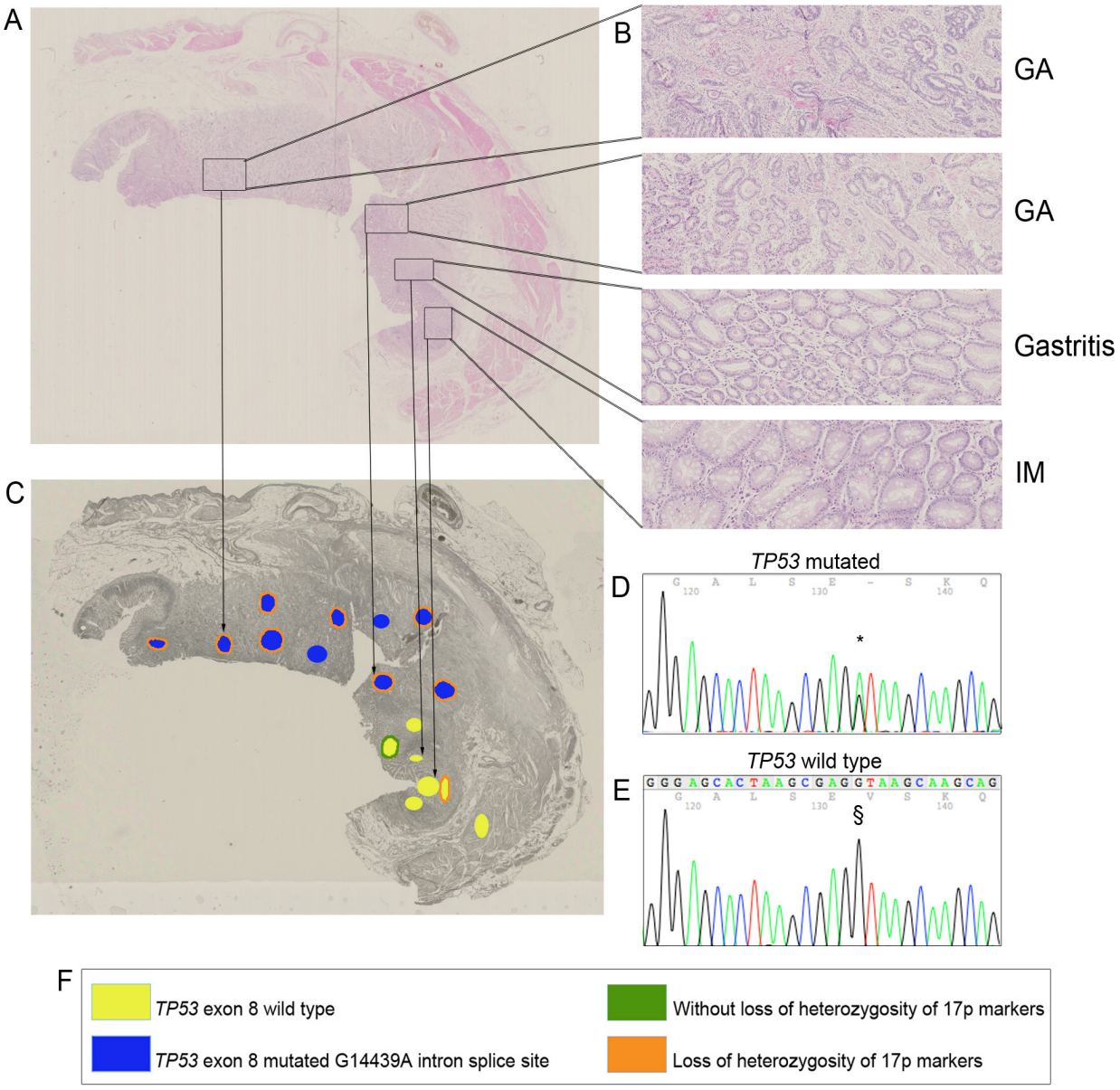

Figure 3.14. ***TP53* mutations found in gastric adenocarcinoma but not in intestinal metaplastic glands in patient 33.** (A) A H&E of an entire section of gastric mucosa showing a poorly differentiated gastric adenocarcinoma (GA) with areas of gastritis and intestinal metaplasia (IM) from patient 33, specimen block 5. (B) Higher power of highlighted areas, showing from top to bottom two areas of poorly differentiated GA, an area of gastritis and an area of IM. (C) Serial section, showing post laser-capture microdissection (LCM). Yellow areas are *TP53* WT whereas dark blue areas are positive for the *TP53* mutation G14439A. Areas with loss of heterozygosity (LOH) at 17p for markers D17S1678 (120bp) and D17S1176 (80bp) are distinguished by an orange border and areas without LOH by a green border. (D, E) Two representative traces showing the *TP53* mutation c G14439A (D) and a *TP53* WT trace (E). (F) Key for patient 33 on post LCM section.

A

Patient 33:5	Histology	*TP53*	D17S1678	D17S1176
1	GA	MUTATED	LOH	LOH
2	GA	MUTATED	LOH	LOH
3	GA	MUTATED	LOH	LOH
4	GA	MUTATED	ND	LOH
5	GA	MUTATED	LOH	LOH
6	GA	MUTATED	LOH	LOH
7	GA	MUTATED	LOH	+
8	GA	MUTATED	LOH	LOH
9	GA	MUTATED	LOH	LOH
10	GA	MUTATED	LOH	LOH
11	Gastritis	WT	LOH	+
12	Gastritis	WT	+	+
13	Gastritis	WT	LOH	ND
14	IM	WT	LOH	+
15	IM	WT	LOH	LOH
16	IM	WT	LOH	ND
17	Muscle	WT	LOH	+

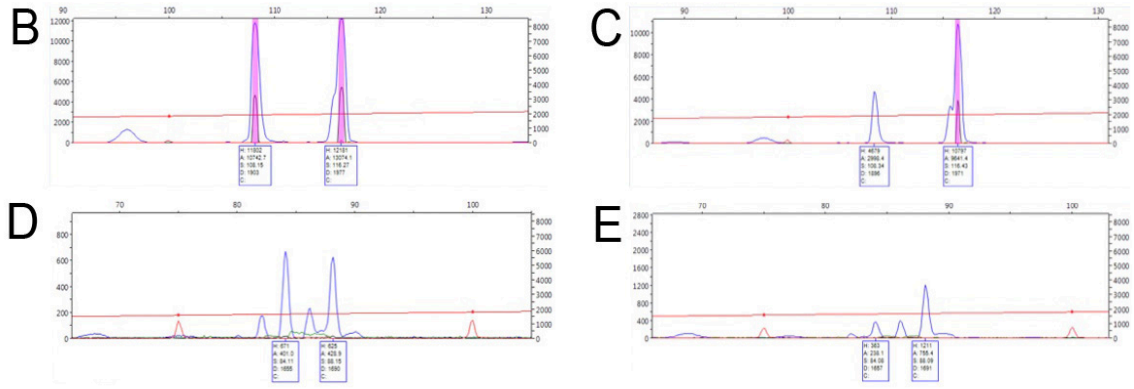

Figure 3.15. **Association of identified mutations with histology and loss of heterozygosity shows that *TP53* mutations were found in gastric adenocarcinoma but not in intestinal metaplastic glands in patient 33.** (A) This table corresponds to the laser-capture microdissection data presented in Figure 3.14, tissue from patient 33, specimen block 5. (B and D) Two representative traces showing controls where both alleles are present (+) and (C and E) two representative traces where loss of heterozygosity (LOH) has occurred for markers D17S1678 (120bp) (B, C) and D17S1176 (80bp) (D, E) in 17p from patient 33. An enlarged version of traces B to E can be seen in Figures 7.12 and 7.13 in the Appendix. WT, wild type; +, both alleles are present in chromosome 17; ND, not determined due to insufficient DNA; the purple vertical line on the traces denotes a high concentration of PCR product; LOH was calculated by measuring the area under the curve of the samples compared to that of a normalized control (gastritis or muscle epithelium areas from the same patient). LOH was considered when the area under the curve was <0.5 or >2.0.

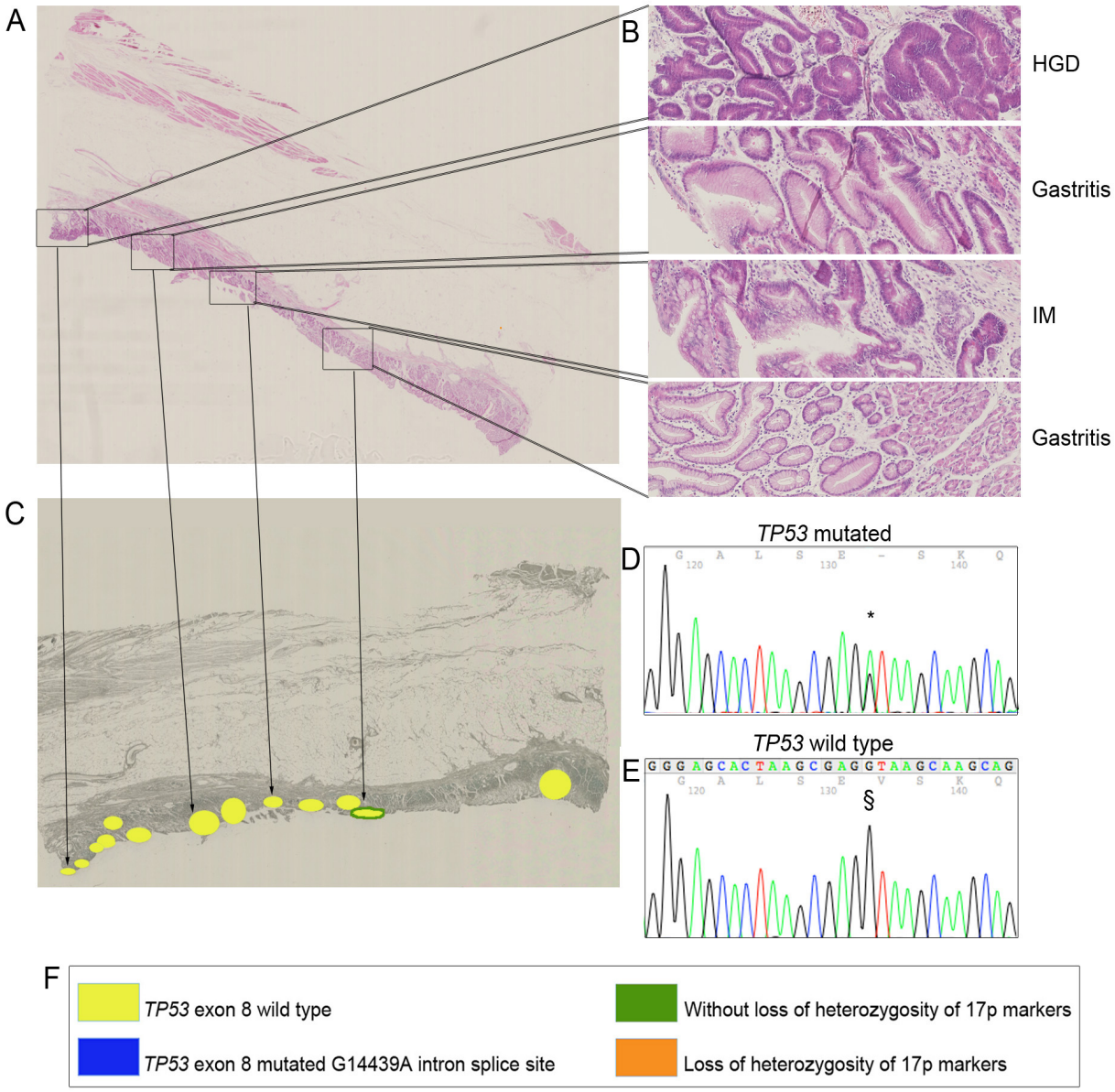

Figure 3.16. ***TP53* mutations were not found in high grade dysplasia or intestinal metaplasia in patient 33.** (A) A H&E picture of an entire section of gastric mucosa showing high grade dysplasia (HGD), and areas of gastritis and intestinal metaplasia (IM) from patient 33, specimen block 3. (B) Higher power of highlighted areas, showing from top to bottom an area of HGD, an area of gastritis, an area of IM and another area of gastritis. (C) Serial section, showing post laser-capture microdissection (LCM). Yellow areas are *TP53* WT. Areas with loss of heterozygosity (LOH) at 17p for markers D17S1678 (120bp) and D17S1176 (80bp) are distinguished by an orange border and areas without LOH by a green border. (D, E) Two representative traces showing the *TP53* mutation c G14439A (D) and a *TP53* WT trace (E). (F) Key for patient 33 on post LCM section.

Table 3.12. **Association of identified mutations with histology and loss of heterozygosity shows that *TP53* mutations were not found in high grade dysplasia or intestinal metaplasia in patient 33.** This table corresponds to the laser-capture microdissection data presented in Figure 3.16, from patient 33 specimen block 3. The representative traces showing controls where both alleles are present (+) and samples where loss of heterozygosity (LOH) has occurred for markers D17S1678 (120bp) and D17S1176 (80bp) at 17p from patient 33 is shown in Figure 3.15. An enlarged version of traces B to E can be seen in Figures 7.12 and 7.13 in the Appendix.

Patient 33:3	Histology	*TP53*	D17S1678	D17S1176
1	HGD	WT	LOH	ND
2	HGD	WT	LOH	ND
3	HGD	WT	LOH	ND
4	HGD	WT	LOH	ND
5	HGD	WT	LOH	ND
6	HGD	WT	LOH	ND
7	Gastritis	WT	LOH	ND
8	Gastritis	WT	LOH	ND
9	IM	WT	LOH	ND
10	IM	WT	LOH	ND
11	Gastritis	WT	+	+
12	Gastritis	WT	ND	ND
13	Gastritis	WT	ND	ND

NOTE: WT, wild type; +, both alleles are present in chromosome 17; ND, not determined due to insufficient DNA; the purple vertical line on the traces denotes a high concentration of PCR product; LOH was calculated by measuring the area under the curve of the samples compared to that of a normalized control (gastritis or muscle epithelium areas from the same patient). LOH was considered when the area under the curve was <0.5 or >2.0.

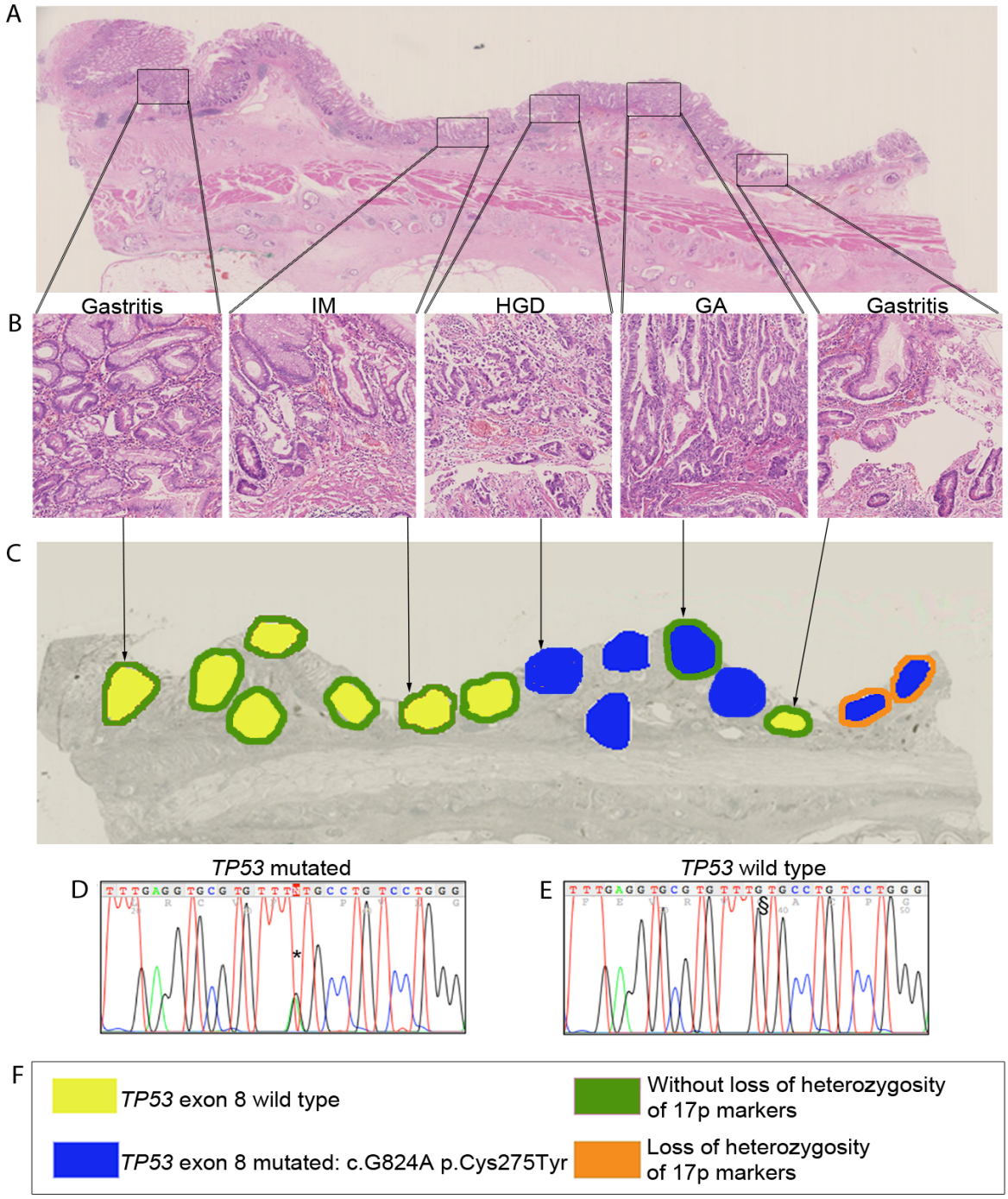

Figure 3.17. ***TP53* mutations were found in high grade dysplasia and in gastric adenocarcinoma but not in intestinal metaplasia in patient 51.** (A) A H&E picture of an entire section of gastric mucosa showing gastritis, intestinal metaplasia (IM), high grade dysplasia (HGD) and gastric adenocarcinoma (GA) from patient 51. (B) Higher power of highlighted areas showing from left to right gastritis, IM, HGD, GA and an area of IM within GA. (C) Serial section, showing post laser-capture microdissection (LCM). Yellow areas are *TP53* WT whereas dark blue areas are positive for the *TP53* mutation c.G824A. Areas with loss of heterozygosity (LOH) at 17p for markers D17S1832 (180bp) and D17S1506E (150bp) are distinguished by an orange border and areas without LOH by a green border. (D, E) Two representative traces showing the *TP53* mutation c.G824A (D) and a *TP53* WT trace (E). (F) Key for patient 51 on post LCM section.

A

Patient 51	Histology	*TP53*	D17S1832	D17S1506E
1	GA	MUTATED	LOH	LOH
2	GA	MUTATED	LOH	LOH
3	Gastritis	WT	+	+
4	GA	MUTATED	LOH	+
5	GA	MUTATED	+	+
6	HGD	MUTATED	LOH	ND
7	GA	MUTATED	LOH	ND
8	HGD	MUTATED	LOH	ND
9	IM	WT	+	ND
10	IM	WT	+	ND
11	IM	WT	+	ND
12	IM	WT	+	ND
13	Gastritis	WT	+	ND
14	Gastritis	WT	+	ND
15	Gastritis	WT	+	ND

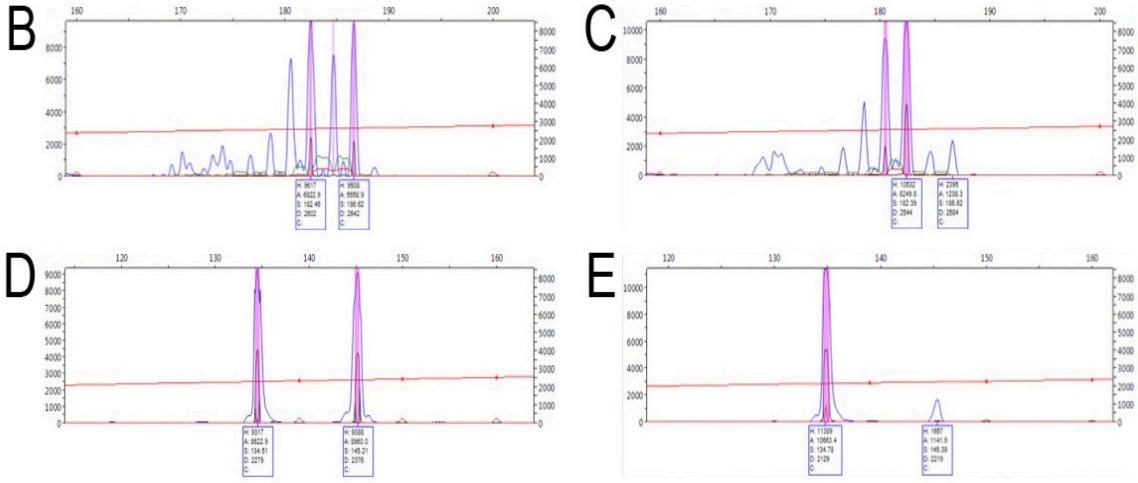

Figure 3.18. **Association of identified mutations with histology and loss of heterozygosity shows that *TP53* mutations were found in high grade dysplasia and in gastric adenocarcinoma but not in intestinal metaplasia in patient 51.** (A) Table corresponding to the laser-capture microdissection data presented in Figure 3.17, tissue from patient 51. (B and D) Two representative traces showing controls where both alleles are present (+) and (C and E) two representative traces where loss of heterozygosity (LOH) has occurred for markers D17S1832 (180bp) (B, C) and D17S1506E (150bp) (D, E) at 17p from patient 51. An enlarged version of traces B to E can be seen in Figures 7.14 to 7.15 in the Appendix. WT, wild type; +, both alleles are present in chromosome 17; ND, not determined due to insufficient DNA; the purple vertical line on the traces denotes a high concentration of PCR product; LOH was calculated by measuring the area under the curve of the samples compared to that of a normalized control (gastritis or muscle epithelium areas from the same patient). LOH was considered when the area under the curve was <0.5 or >2.0.

Gastric adenocarcinoma demonstrates genetic heterogeneity through clonal evolution

Six phylogenetic trees were used to summarise the data for patients 8, 10, 22, 33 and 51 (Figure 3.19 B, C, D, E and F respectively) and patient 27 (Appendix Figure 7.18). A schematic representation of the location of the microsatellite markers used for LOH analysis has also been included (Figure 3.19A).

In the case of patient 8 it is probable that at some point in the development of IM, LOH of *TP53* markers develops (Figure 3.19B) and as the mutated clone spreads, a *TP53* exon 7 mutation and eventually a *CTNNB1* mutation are acquired through clonal evolution. The data presented indicated that the three populations observed are clonal and, by inference, that GA is clonal with new mutations acquired through the evolution of the carcinoma clones due to the bottleneck effect. It is likely, therefore, that a founder mutation caused the transition from IM to dysplasia and to GA. This may have occurred either before or after the development of LOH. Our findings suggested that LOH occurred during the IM and that this was followed by a mutation in an unidentified gene during either the IM or the dysplasia that led to GA development.

The phylogenetic tree of patient 10 demonstrated that LOH might occur during the development of IM, since one of the microsatellite markers has already been lost in the dissected IM area of this patient. Because GA areas and carcinoma-infiltrated muscle areas present the same *TP53* mutation, the data suggested that GA is clonal and that as

the carcinoma becomes more invasive the *TP53* mutated clone persisted (Figure 3.19C).

In the case of patient 22, a *TP53* mutation arose during clonal expansion, which probably led to further progression of the carcinoma. The data suggested that the two carcinoma areas are clonal and, therefore, that GA is clonal (Figure 3.19D).

The data from patient 27 suggests again that GA is clonal, as all GA areas in the two consecutive specimens present the same *TP53* mutations (Appendix Figure 7.18).

All pre-malignant areas appear WT in patient 33. However, the data suggested that LOH occurred in the IM and also that another unknown mutation in a gene that was not included in our screening was likely to have caused the transition from IM to dysplasia and to GA (Figure 3.19E).

In the case of patient 51 a *TP53* mutation developed at some point in the HGD (Figure 3.19F), giving the clone the potential to progress to a carcinoma, which was then followed by LOH for *TP53* at 17p. This showed that a mutation present in cells within a dysplastic area can clonally expand to form an associated carcinoma and, in this case, the GA is therefore clonal.

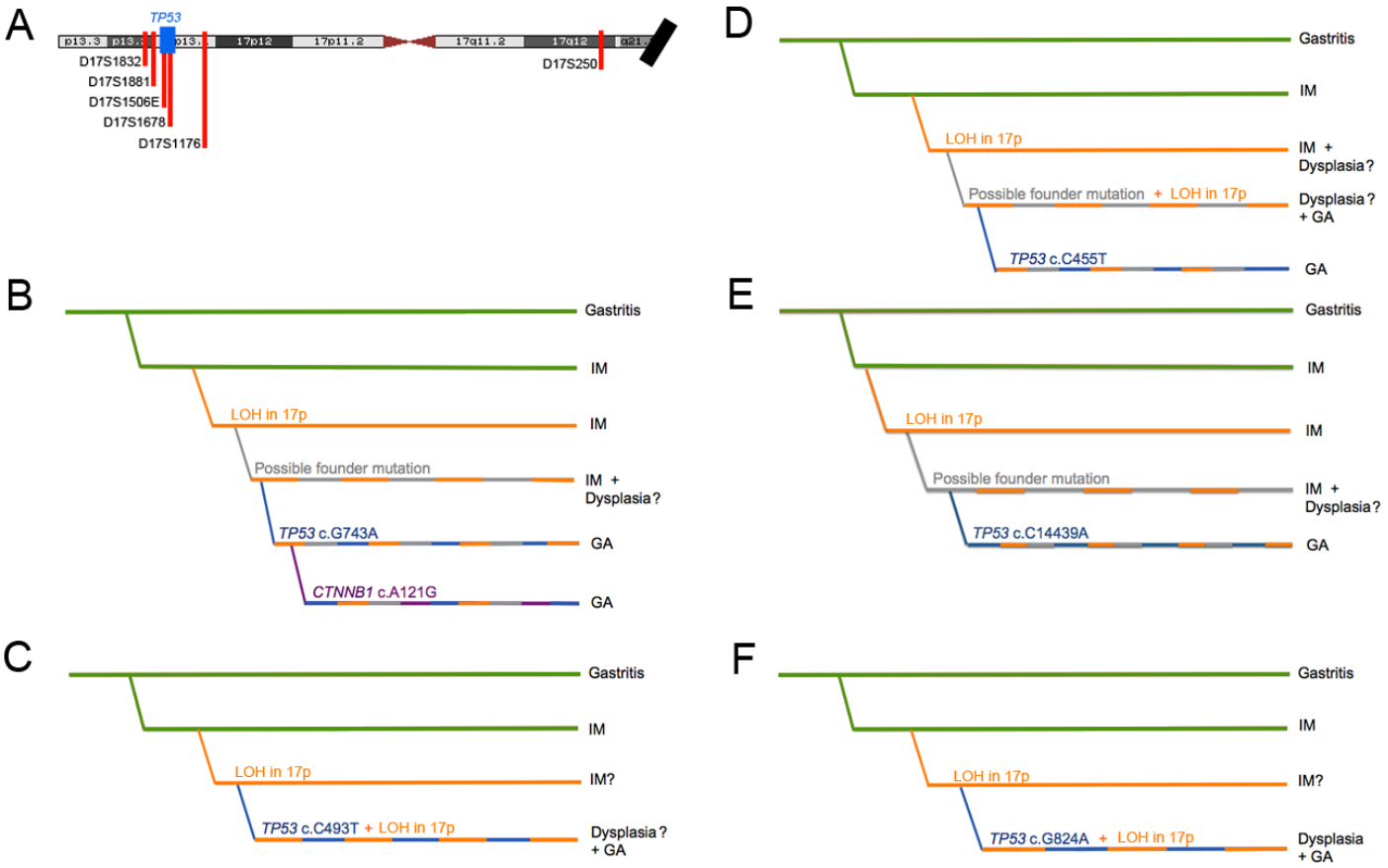

Figure 3.19. **Phylogenetic trees provide evidence for a monoclonal origin for gastric adenocarcinoma.** (A) Schematic representation of the location of the microsatellites used for loss of heterozygosity (LOH) analysis for chromosome 17. (B-F) Phylogenetic trees representative of patients 8 (B), 10 (C), 22 (D), 33 (E) and 51 (F), the data has been interpreted from the experimental data found in figures 3.6 to 3.18. Tree branches represent either phenotypic or genotypic changes. The wild type genotype is coloured in green, LOH is coloured in orange and *TP53* mutations are coloured in dark blue. Cumulative mutations are represented by different coloured lines and a "?" has been used to highlight likely genotypic and phenotypic events previous to GA development in the five patients.

3.2.3. Clonal expansion in hereditary diffuse gastric cancer

To assess clonal expansion in HDGC within the human stomach, areas of HDGC from 5 patients from 2 different families were microdissected by LCM and screened for mutations in *TP53* in exons 5, 6, 7 and 8 (see Table 3.13 for full patient summary). These patients could not be screened by needle macrodissection due to the small size of the clusters of signet ring cells forming the diffuse-type tumours. Each of these individuals had a germline mutation in the *CDH1* gene responsible for cell-cell adhesion. Individuals from family A carried a c.1565+2dupT mutation in intron 10 and those from family B had the familial splicing mutation c.G832A.

This study was performed using tissues from two patients from family A, who had both been found to carry the familial c.1565+2dupT mutation in intron 10:

- **Patient A3**: 22 year old female where 69 diffuse-type tumours had been found ranging between 1 to 7 mm. An ovarian mature cystic teratoma with no gastric tissue had also been found in this patient.

- **Patient A4**: 43 year old female where 16 diffuse-type tumours had been found ranging between 1 to 4 mm. Ectopic duodenal tissue and granulomatous lymphadenitis was also observed in this patient. Patient A4 is patient A3's aunt.

The study was also performed using tissues from three patients from family B, who had all been found to carry the familial splicing mutation c.G832A:

- **Patient B1**: 22 year old male where 267 diffuse-type tumours had been found ranging between 1 to 3 mm. IM was also present in the cardia area of the stomach in this patient.

- **Patient B4**: 33 year old female where 47 diffuse-type tumours had been found ranging from 1 to 2 mm. Leiomyomata and fundic gland polyps were also observed in this patient. Patient B4 is patient B1's second cousin.

- **Patient B5**: 59 year old female where 80 diffuse-type tumours had been found ranging from 1 to 3 mm. Gastrointestinal stromal tumours (GIST) positive for *C-KIT* mutations and granulomatous lymphadenitis were also observed in this patient. Patient B5 is patient B4's mother and patient B1's second aunt.

Table 3.13. **Summary of patients carrying E-cadherin mutations from families A and B.** The two families present two different germline mutations in *CDH1*, c.1565+2dupT in family A and c.G832A in family B.

Patient	Family	*CDH1* mutation	Gender	Age	Relationship	Number HDGC
A3	A	c.1565+2dupT	F	22	niece	69
A4	A	c.1565+2dupT	F	43	aunt	16
B1	B	c.G832A	M	22	second cousin + nephew	267
B4	B	c.G832A	F	33	second cousin + daughter	47
B5	B	c.G832A	F	59	mother + second aunt	80

E-cadherin immunohistochemistry (IHC) and Alcian Blue and Periodic acid-Schiff staining were performed on tissues from these five patients. The HDGC area from patient A3 seemed to present a low level of expression of E-cadherin protein even though the *CDH1* germline mutation had been confirmed (Figure 3.21 C and G). On the other hand, all HDGC areas from patients A4 and B5 were negative for E-cadherin expression by IHC (Figure 3.23 C and G; and Figure 3.29 C and G, respectively). HDGC areas from Patients B1 and B4 showed a mixture of HDGC E-cadherin negative areas and HDGC areas with a low level of expression of E-cadherin positive (Figure 3.25 C and G; and Figure 3.27 C and G, respectively) (see full percentages in Table 3.14).

Table 3.14. **E-cadherin protein can be found expressed at a low level in the membrane of signet ring cells in some hereditary diffuse gastric cancer areas.** This has been observed in patients presenting a *CDH1* germline mutation.

Patient	HDGC *CDH1* negative areas	HDGC *CDH1* positive areas
A3	0	1 (100%)
A4	1 (100%)	0
B1	1 (50%)	1 (50%)
B4	4 (66.67%)	2 (33.33%)
B5	3 (100%)	0

In summary, all HDGC areas were WT for *TP53* exons 5, 6, 7 and 8 in these five patients. Only the largest HDGC areas were microdissected and analysed by nested-PCR sequencing. No mutated areas were found and therefore LOH was not assessed.

The results for the field cancerisation study using *TP53* mutations from HDGC areas from patients A3, A4, B1, B4 and B5 are shown in figures 3.20, 3.22, 3.24, 3.26 and

3.28. The raw data associating the genotype of each dissected area to the histology and the high power images compiling the summary of the IHC results are found in the corresponding Figures 3.21, 3.23, 3.25, 3.27 and 3.29.

The lack of *TP53* mutations on the largest HDGC areas from these patients indicates that none of these patients showed *TP53* mutations. However, it is possible that these mutations might be a later step in the development of diffuse-type gastric carcinoma as Ranzani and colleagues (*205*) have suggested. Moreover, it could also be possible that field cancerisation does not occur in diffuse-type gastric cancers - it has never been reported. Nevertheless, it is most likely that the germline mutation acts as the field-cancerisation event, which then probably leads to the methylation of the WT *CDH1* allele, loss of function and to genetic instability.

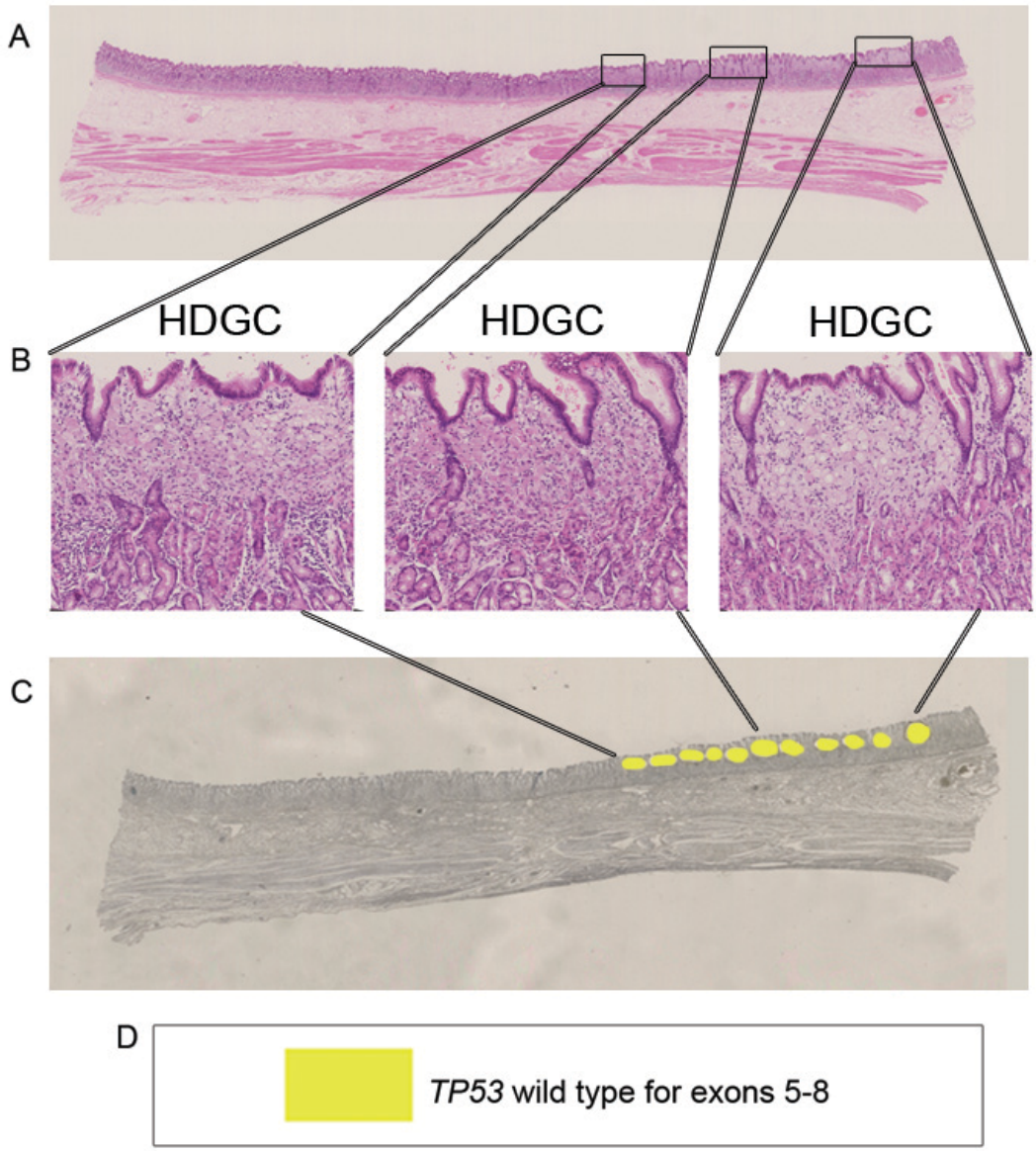

Figure 3.20. **Field cancerisation was not observed when using *TP53* mutations as a clonal marker in HDGC tissue from patient A3.** (A) Gastric mucosa showing a strip of gastric epithelium with areas of hereditary diffuse gastric cancer (HDGC) from patient A3, which presents a c.1565+2dupT mutation in intron 10 of the *CDH1* gene. (B) Higher power of highlighted regions showing three different areas of HDGC. (C) Serial section, showing post laser-capture microdissection (LCM). All areas were WT for *TP53* exons 5, 6, 7 and 8 and are all coloured in yellow. (D) Key for patient A3 on post LCM section.

A

Patient A3	*TP53* exon 5	*TP53* exon 6	*TP53* exon 7	*TP53* exon 8
1	WT	WT	WT	WT
2	WT	WT	WT	WT
3	WT	WT	WT	WT
4	WT	WT	WT	WT
5	WT	WT	WT	WT
6	WT	WT	WT	WT
7	WT	WT	ND	WT
8	WT	WT	ND	WT
9	WT	WT	WT	WT
10	WT	WT	WT	WT
11	WT	WT	WT	WT
12	WT	WT	WT	WT

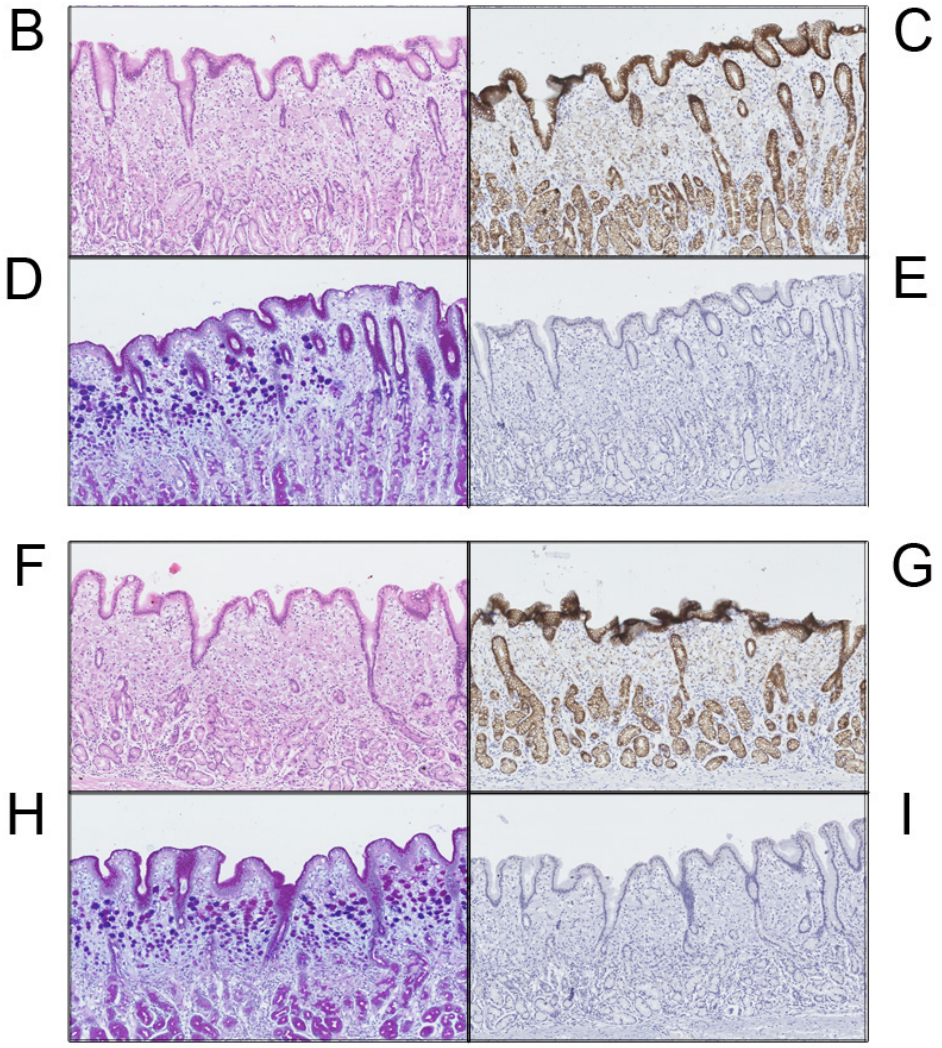

Figure 3.21. **Screening for *TP53* exons 5 to 8 mutations and E-cadherin immunohistochemistry in HDGC tissue from patient A3.** This figure shows that all hereditary diffuse gastric cancer areas are *TP53* wild type but that some areas still express very low levels of E-cadherin despite carrying a germline mutation and having a signet ring cell phenotype in patient A3. (A) This table corresponds to the laser-capture microdissection data presented in figure 3.20 for *TP53* exons 5, 6, 7 and 8, tissue from patient A3. (B-I) High power (x10) images of two hereditary diffuse gastric cancer (HDGC) areas in patient A3 showing haematoxylin and eosin staining (H&E) (B, D); E-cadherin immunohistochemistry (C, G); Alcian Blue and Periodic acid-Schiff stain (D, H); and the immunohistochemistry negative control for each area (E, I). WT, wild type; ND, not determined due to insufficient DNA.

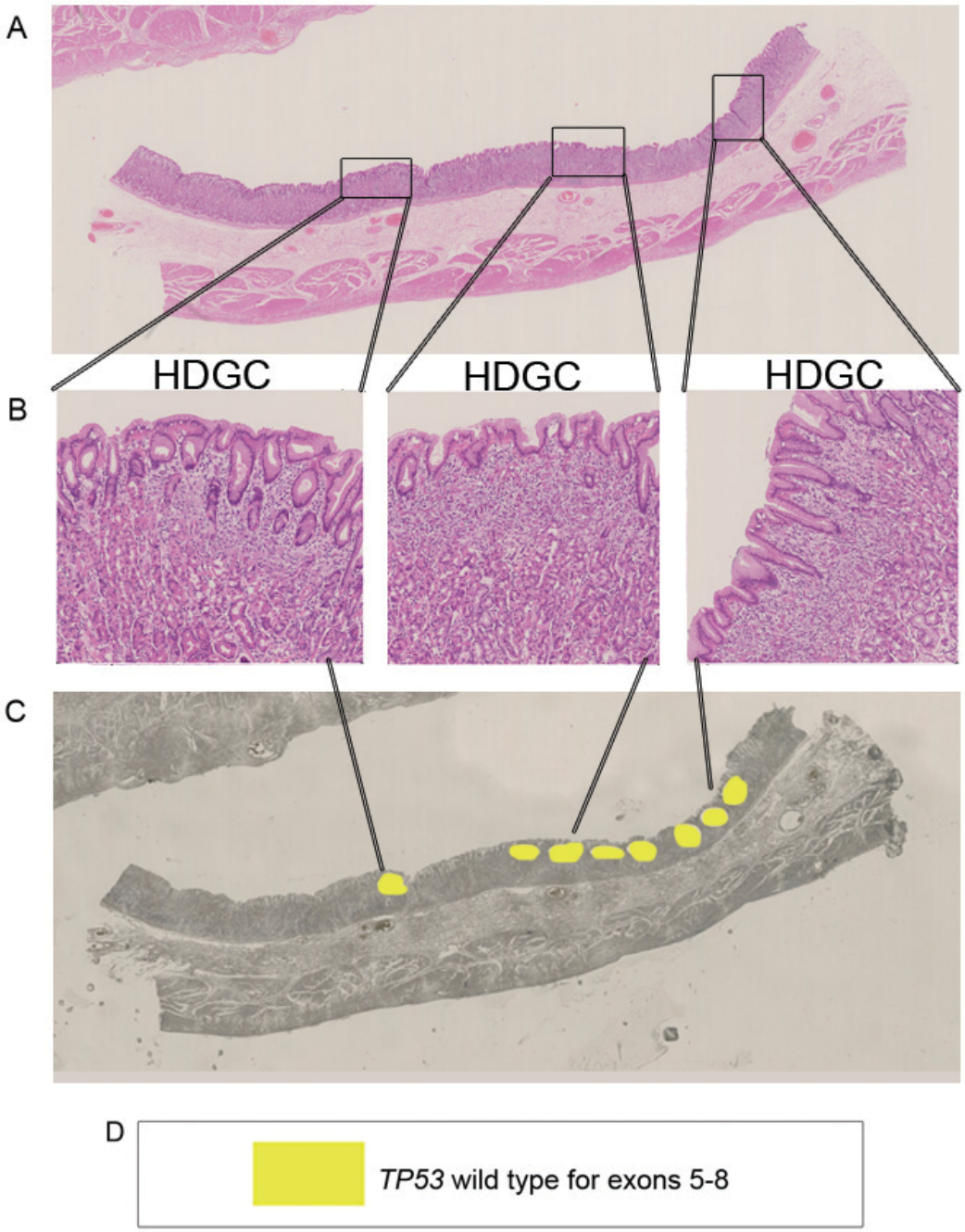

Figure 3.22. **Field cancerisation was not observed when using *TP53* mutations as a clonal marker in HDGC tissue from patient A4.** (A) Gastric mucosa showing a strip of gastric epithelium with areas of diffuse gastric cancer from patient A4, which presents a c.1565+2dupT mutation in intron 10 of the *CDH1* gene. (B) Higher power of highlighted regions showing three different areas of hereditary diffuse gastric cancer (HDGC). (C) Serial section, showing post laser-capture microdissection (LCM). All areas were WT for *TP53* exons 5, 6, 7 and 8 and are all coloured in yellow. (D) Key for patient A4 on post LCM.

A

Patient A4	*TP53* exon 5	*TP53* exon 6	*TP53* exon 7	*TP53* exon 8
1	WT	WT	WT	WT
2	WT	WT	WT	WT
3	WT	WT	WT	WT
4	WT	WT	WT	WT
5	WT	WT	WT	WT
6	WT	WT	WT	WT
7	WT	WT	WT	WT
8	WT	WT	WT	WT

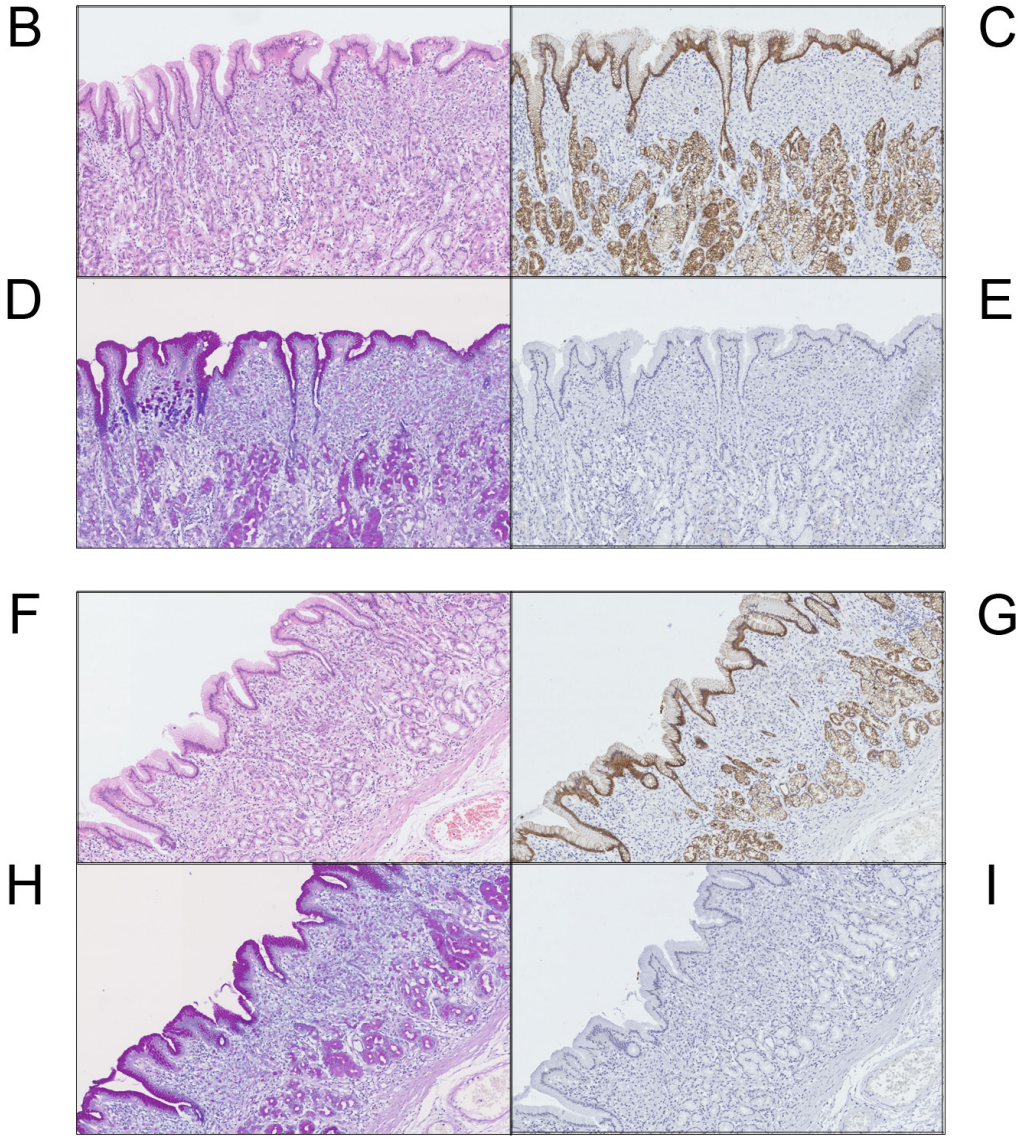

Figure 3.23. **Screening for *TP53* exons 5 to 8 mutations and E-cadherin immunohistochemistry in HDGC tissue from patient A4.** This figure shows that all hereditary diffuse gastric cancer areas are *TP53* wild type and that none of these areas express E-cadherin in patient A4. (A) This table corresponds to the laser-capture microdissection data presented in figure 3.20 for *TP53* exons 5, 6, 7 and 8, tissue from patient A4. (B-I) High power (x10) images of two hereditary diffuse gastric cancer (HDGC) areas in patient A3 showing haematoxylin and eosin staining (H&E) (B, D); E-cadherin immunohistochemistry (C, G); Alcian Blue and Periodic acid-Schiff stain (D, H); and the immunohistochemistry negative control for each area (E, I). WT, wild type.

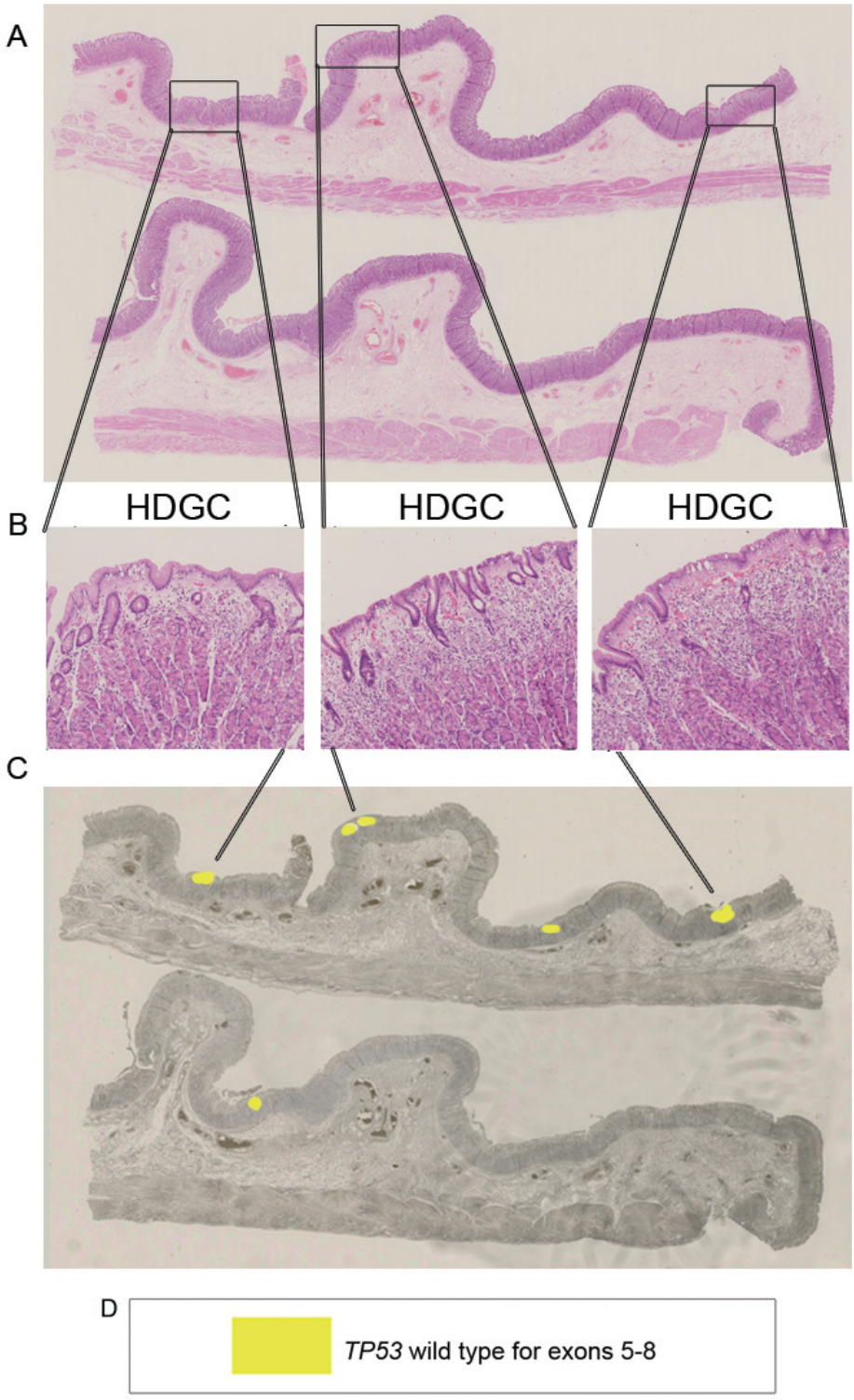

Figure 3.24. **Field cancerisation was not observed when using *TP53* mutations as a clonal marker in HDGC tissue from patient B1.** (A) Gastric mucosa showing a strip of gastric epithelium with areas of diffuse gastric cancer from patient B1, which presents a c.G832A mutation in intron 10 of the *CDH1* gene. (B) Higher power of highlighted regions showing three different areas of hereditary diffuse gastric cancer (HDGC). (C) Serial section, showing post laser-capture microdissection (LCM). All areas were WT for *TP53* exons 5, 6, 7 and 8 and are all coloured in yellow. (D) Key for patient B1 on post LCM.

A

Patient B1	*TP53* exon 5	*TP53* exon 6	*TP53* exon 7	*TP53* exon 8
1	WT	WT	WT	WT
2	WT	WT	WT	WT
3	WT	WT	WT	WT
4	WT	WT	WT	WT
5	WT	WT	WT	WT
6	WT	WT	WT	WT

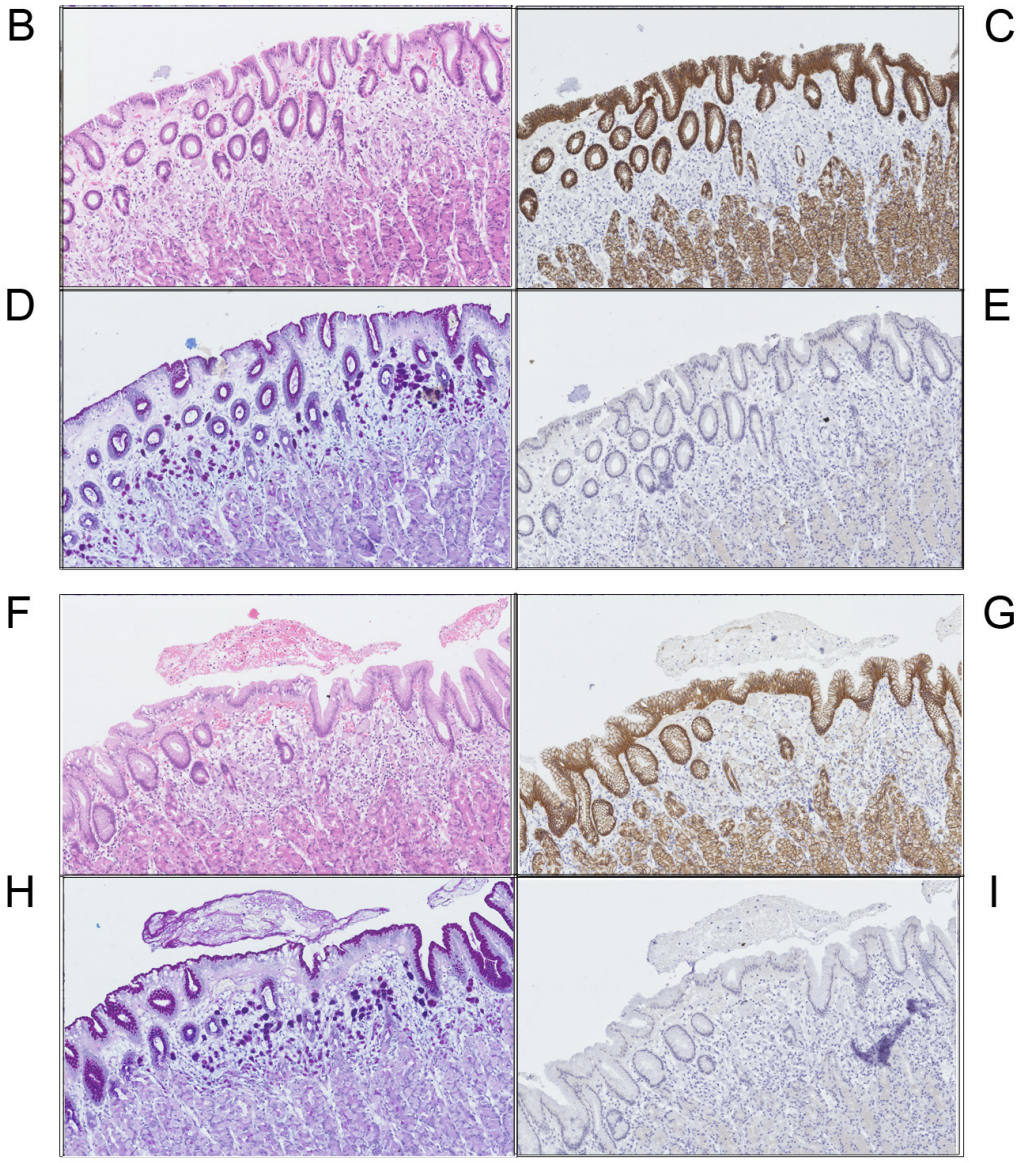

Figure 3.25. **Screening for *TP53* exons 5 to 8 mutations and E-cadherin immunohistochemistry in HDGC tissue from patient B1.** This figure shows that all hereditary diffuse gastric cancer areas are *TP53* wild type but that some areas still express faint levels of E-cadherin despite carrying a germline mutation and having a signet ring cell phenotype. (A) This table corresponds to the laser-capture microdissection data presented in figure 3.20 for *TP53* exons 5, 6, 7 and 8, tissue from patient B1. (B-I) High power (x10) images of two hereditary diffuse gastric cancer (HDGC) areas in patient A3 showing haematoxylin and eosin staining (H&E) (B, D); E-cadherin immunohistochemistry (C, G); Alcian Blue and Periodic acid-Schiff stain (D, H); and the immunohistochemistry negative control for each area (E, I). WT, wild type.

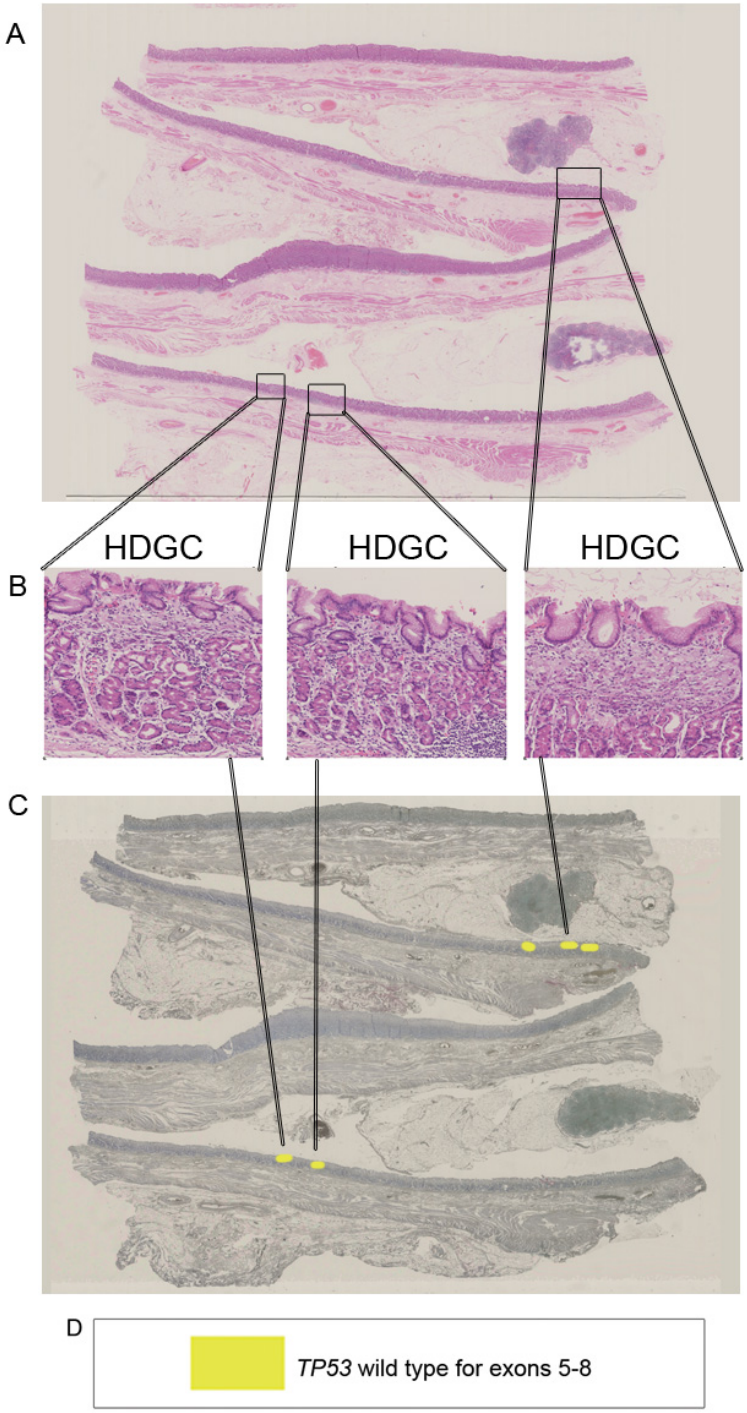

Figure 3.26. **Field cancerisation was not observed when using *TP53* mutations as a clonal marker in HDGC tissue patient B4.** (A) Gastric mucosa showing a strip of gastric epithelium with areas of diffuse gastric cancer from patient B4, which presents a c.G832A mutation in intron 10 of the *CDH1* gene. (B) Higher power of highlighted regions showing three different areas of hereditary diffuse gastric cancer (HDGC). (C) Serial section, showing post laser-capture microdissection (LCM). All areas were WT for *TP53* exons 5, 6, 7 and 8 and are all coloured in yellow. (D) Key for patient B4 on post LCM.

A

Patient B4	*TP53* exon 5	*TP53* exon 6	*TP53* exon 7	*TP53* exon 8
1	WT	WT	ND	WT
2	WT	WT	WT	WT
3	WT	WT	WT	WT
4	WT	WT	ND	WT
5	WT	WT	WT	WT

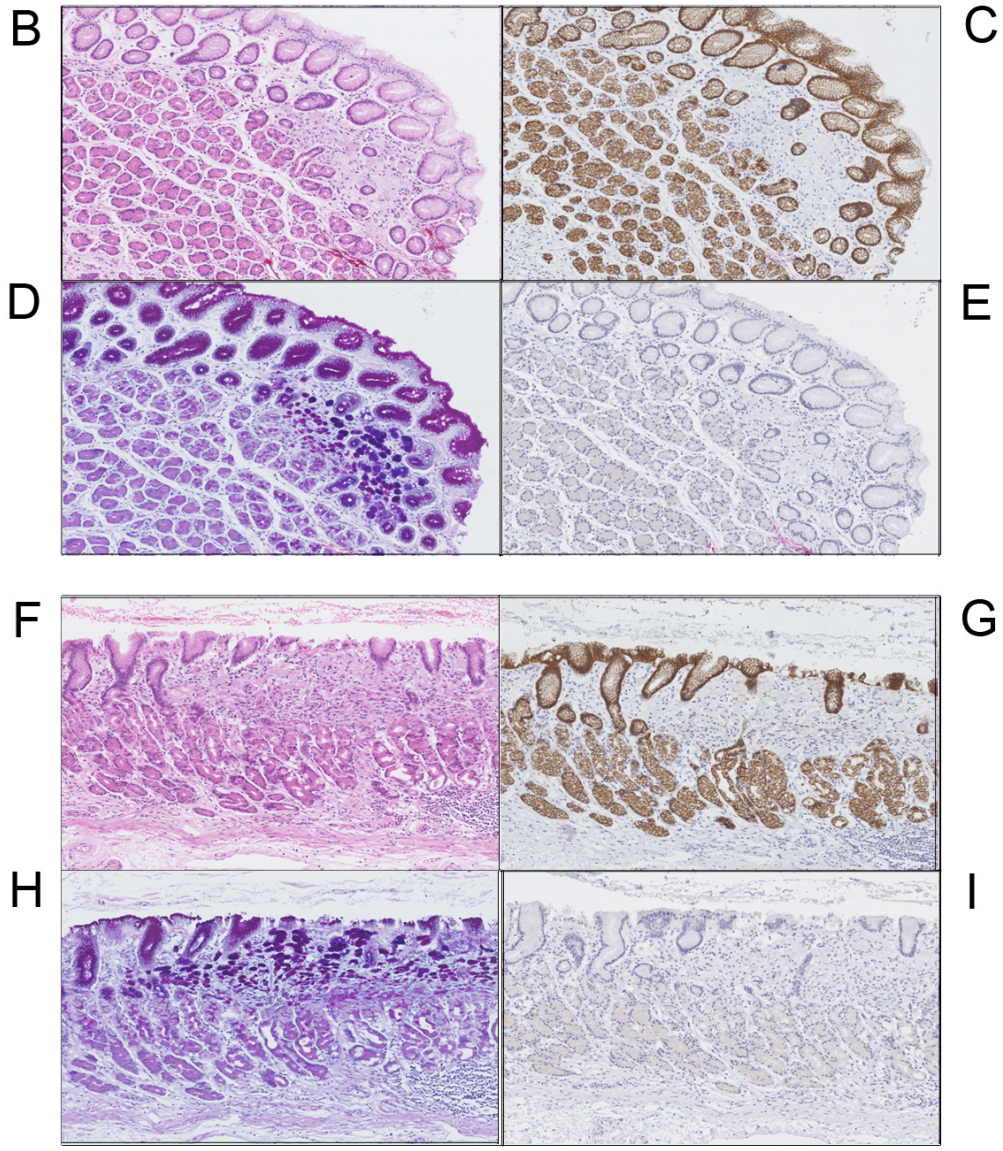

Figure 3.27. **Screening for *TP53* exons 5 to 8 mutations and E-cadherin immunohistochemistry in HDGC tissue from patient B4.** This figure shows that all hereditary diffuse gastric cancer areas are *TP53* wild type but that some areas still express very low levels of E-cadherin despite carrying a germline mutation and having a signet ring cell phenotype in patient B4. (A) This table corresponds to the laser-capture microdissection data presented in figure 3.20 for *TP53* exons 5, 6, 7 and 8, tissue from patient B4. (B-I) High power (x10) images of two hereditary diffuse gastric cancer (HDGC) areas in patient A3 showing haematoxylin and eosin staining (H&E) (B, D); E-cadherin immunohistochemistry (C, G); Alcian Blue and Periodic acid-Schiff stain (D, H); and the immunohistochemistry negative control for each area (E, I). WT, wild type; ND, not determined due to insufficient DNA.

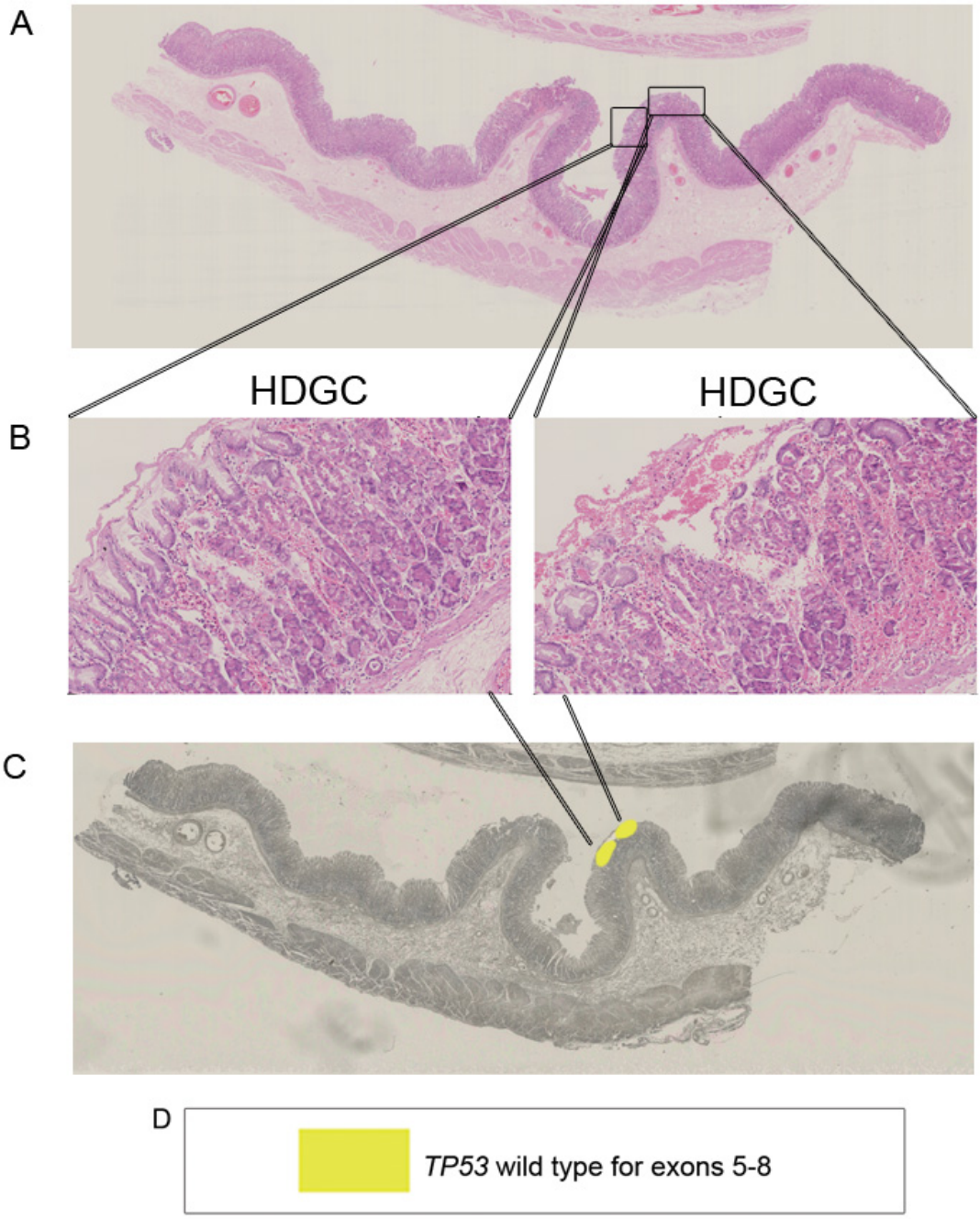

Figure 3.28. **Field cancerisation was not observed when using *TP53* mutations as a clonal marker in HDGC tissue from patient B5.** (A) Gastric mucosa showing a strip of gastric epithelium with areas of diffuse gastric cancer from patient B5, which presents a c.G832A mutation in intron 10 of the *CDH1* gene. (B) Higher power of highlighted regions showing two different areas of hereditary diffuse gastric cancer (HDGC). (C) Serial section, showing post laser-capture microdissection (LCM). All areas were WT for *TP53* exons 5, 6, 7 and 8 and are all coloured in yellow. (D) Key for patient B5 on post LCM.

A

Patient B5	*TP53* exon 5	*TP53* exon 6	*TP53* exon 7	*TP53* exon 8
1	WT	WT	WT	WT
2	WT	WT	WT	WT

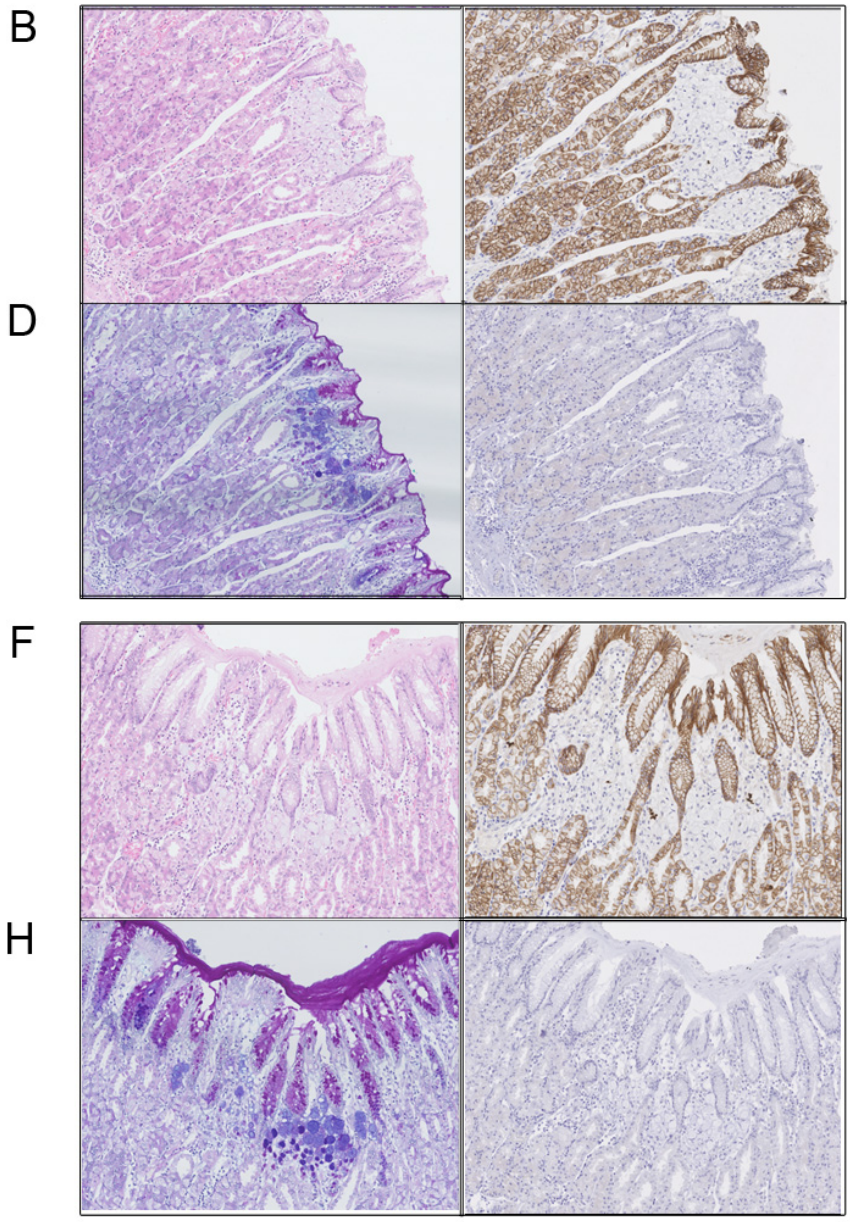

Figure 3.29. **Screening for *TP53* exons 5 to 8 mutations and E-cadherin immunohistochemistry in HDGC tissue from patient B5.** This figure shows that all hereditary diffuse gastric cancer areas are *TP53* wild type and that none of these areas express E-cadherin. (A) This table corresponds to the laser-capture microdissection data presented in figure 3.20 for *TP53* exons 5, 6, 7 and 8, tissue from patient B5. (B-I) High power (x10) images of two hereditary diffuse gastric cancer (HDGC) areas in patient A3 showing haematoxylin and eosin staining (H&E) (B, D); E-cadherin immunohistochemistry (C, G); Alcian Blue and Periodic acid-Schiff stain (D, H); and the immunohistochemistry negative control for each area (E, I). WT, wild type.

3.3. Discussion

As had previously been published by McDonald and colleagues, IM glands are clonal and expand by crypt fission (*248*). Large fields of IM in the human stomach have previously been linked to a higher incidence of GA (*187*). Moreover, another study observed the same genetic mutations in IM and in the associated preneoplastic lesions found in the follow-up biopsies (*193*). However, previous genetic studies had analysed large areas of tissue or biopsies and could not rule out the presence of other clones, since the large number of cells can mask genetic heterogeneity. Therefore there was a need to assess the mutational status of IM and the associated dysplastic lesions on a gland-by-gland basis, since there was limited evidence for IM being an immediate precursor to dysplasia.

The results from our study show that all glands within an entire region of dysplasia contain a founder mutation and, therefore, that the lesion is clonal (Figures 3.1, 3.2 and 3.4). The total percentage of mutated IM glands was very small, ranging from 4.2% to 16.6% of all IM glands (Table 3.2) (*72*). This indicated that when a mutation occurred in IM, cellular expansion can take place rapidly and dysplasia follows after that, thereby forming very large clonal lesions. IM can therefore be perceived as field cancerisation of the human stomach, as it seems to predispose large areas of epithelium to progress into more malignant preneoplastic lesions and also to promote genetic instability.

We have screened for mutations in the genes that account for approximately 75% of all somatic mutations reported previously for GA in the COSMIC database (*256*).

Originally, tumour tissue from 23 patients was included in our study on the clonal origins of dysplasia from IM (*72*). Nevertheless, only 3 out of the 23 (13%) patients presented with single identifiable functional mutations in the dysplasia. In the study on clonal expansion in GA, 31.4% of the patients presented with functional mutations and only 1 patient (1.96%) presented two functional mutations. Overall, the mutation frequencies obtained were comparable to those from previous reports (Figure 3.5). The absence of mutations in a large proportion of our GA patients (68.6%) could also indicate that other mutated genes, such as *ARID1A* and *FAT4* (*202, 203*), may play an important role in GA development. Further exome sequencing studies will hopefully reveal novel target genes pertinent to the development of carcinoma of the stomach.

To study clonal expansion in GA tissue from 6 patients presenting with detectable mutations were studied by LCM of the FFPE specimens, which showed varied histology including gastritis, IM, dysplasia and carcinoma. The data suggested that during field cancerisation a mutation arises in IM followed by the development of dysplasia, which then becomes the focus of subsequent mutations (Figure 3.19). Clonal expansion within the dysplasia eventually leads to progression to an adenocarcinoma. In the carcinoma tissue from patients 8, 22 and 33 it appears that a founder mutation in an unknown gene must have taken place previously or at the same time as the LOH, since a WT *TP53* population was found with the same LOH pattern present in the *TP53* mutated population. Both WT and mutated populations are clonal and have evolved through clonal evolution, as suggested in Nowell's model of clonal evolution (*88*). Moreover, HGD and GA are clonal as they display the same *TP53* mutation in Patient 51 (Figure 3.19).

Our results, here and previously (*72*), differ from those obtained from the clonal origin of Barrett's lesions (*157*) and colorectal microadenomas (*16*). Leedham and colleagues observed different mutations in different populations in metaplasia and dysplasia within Barrett's oesophagus: the Barrett's glands were a mosaic of multiple genetically distinct independent clones (*157*). Clonal analysis on a crypt-by-crypt basis in familial and sporadic adenomas, and in carcinoma-in-adenomas suggested that colorectal adenomas can be polyclonal and that clonal evolution takes place throughout adenoma development (*16*). In contrast, Galandiuk and colleagues analyzed tumours from Crohn's disease patients by LCM, which produced similar findings to those reported here (*64*). They detected a mutation within non-tumour tissue that was also found in the presenting tumour, suggesting a clonal relationship between the tumour and the surrounding pre-neoplastic mucosa due to field cancerisation. Overall, it would appear that different underlying pre-neoplastic conditions, such as FAP (*16*) or Crohn's (*64*), lead to different modes of clonal evolution. Interestingly, both studies (*16, 64*) revealed an absence of a clear order of genetic events for the development of tumours in FAP and Crohn's patients, in contrast to the hypothesis that the genetic events described in the adenoma-carcinoma sequence always occurred in a defined sequence in the development of colorectal carcinomas (*121*).

The usual mutational events established for GA development during the MCS (*153*) do not fit the results from either of our two LCM mutation screening studies (*72*). Correa and colleagues proposed a stepwise progression towards GA by compiling results from several different studies and not by detection of specific mutations in a cohort of GA tumours as conducted here. Our results indicated that the specific genetic events

described during the MCS might not be true for GA. Mutations do not occur at specific stages during tumour development and we have not observed an accumulation of driver mutations during tumourigenesis in our GA patient cohort. Indeed, if the Correa hypothesis were correct then one would expect to find more cases with multiple mutations and all GA would present with the same mutation signature (Figure 3.30).

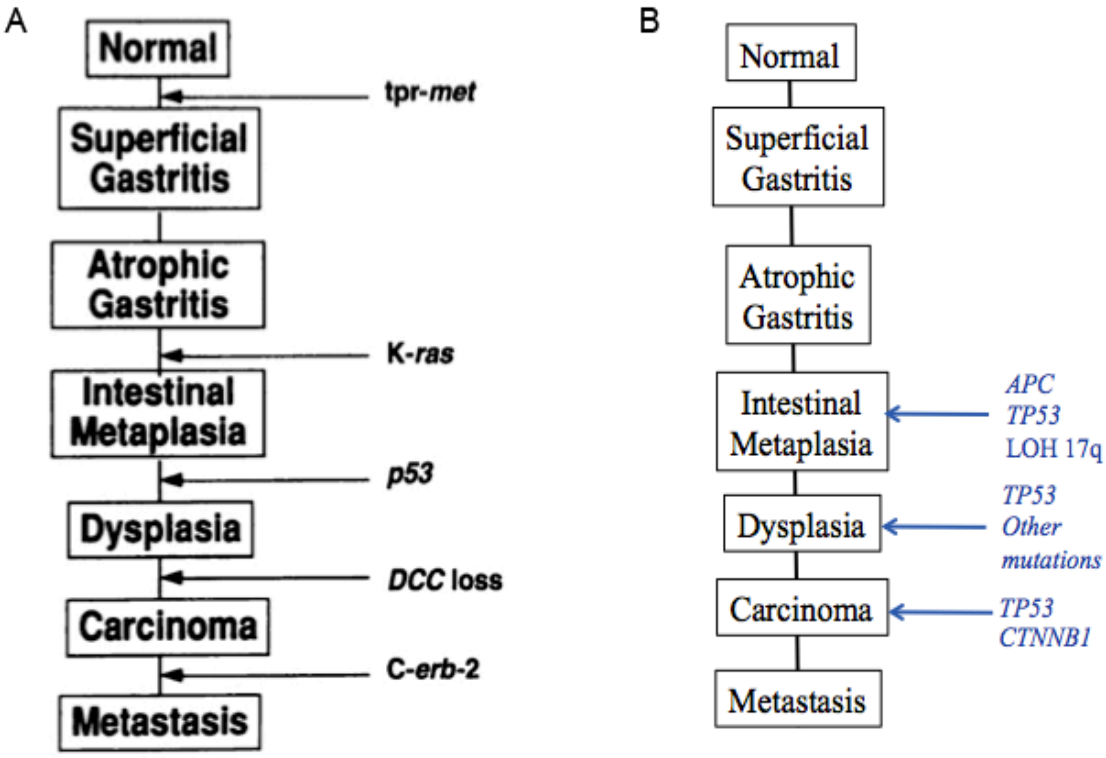

Figure 3.30. **Comparison between the phenotypic and genotypic events.** Figures show a comparison between the observation of Correa and colleagues (*153, 187*) (A) that supports an order of mutations during the Metaplasia-Dysplasia-Carcinoma sequence (MCS) and the mutational events observed in the studies of the clonal origins of dysplasia from intestinal metaplasia (*72*) and the clonal architecture of GA (B).

Our study shows that field cancerisation and mutated pre-malignant clones can drive tumour progression. This is very relevant clinically, since lesions such as IM are not removed at surgery unless the carcinoma has already developed. Our study would

suggest that the increased surveillance based on mutational screening of biopsy specimens might form part of a patient management regime for GA in the future.

In summary, the proposal that the monoclonal origin of GA from one progenitor cell, which subsequently acquires genetic heterogeneity through clonal evolution, fits with the current study on the clonal origins of dysplasia and clonal expansion in GA (*72*). This study is the most exhaustive carried out in a large cohort of patients and we have observed different populations within the same tumour and established the mutational status of individual tumour areas. However, the phylogenetic trees produced for the lesions investigated will only be complete when deep sequencing and validation studies are undertaken.

The results from these two studies indicated that it was possible that an event similar to field cancerisation occurred in HDGC. Mutations in the *TP53* gene have been previously reported in HDGC, although the mutations were suggested to occur at a later stage leading to tumour progression (*205*). When the largest lesions were located in 5 members of the two families, these areas were LCM and analysed for mutations in exons 5, 6, 7 and 8 of *TP53*. Nevertheless, the results obtained were negative and no *TP53* mutations could be observed in any HDGC lesion. This suggested that either field cancerisation does not occur in HDGCs or that, because all of these patients have a germline *CDH1* mutation, field cancerisation might be due to events such as promoter methylation of the wild type *CDH1* allele. *CDH1* methylation is thought to be the second hit mutation in over 50% of diffuse gastric carcinoma cases (*257*), hence, *TP53* mutations might arise after field cancerisation has occurred in a background where one of the alleles is mutated and the other silenced.

Immunohistochemistry results for E-cadherin staining in these patients revealed that 3 out of the 5 patients (60%) presented some signet ring areas positive for E-cadherin membranous staining but with the same mucin production as that of the E-cadherin negative areas (seen by AB-PAS staining). E-cadherin background staining was not observed in any of the negative control serial sections and, therefore, it was deemed that none of the positive signet ring cell areas were due to antibody artefact. Nevertheless, the epitope for the mouse-monoclonal antibody corresponds to the N-terminal external region of E-cadherin, which would not be affected by either of the mutations found in family A or B. These results could suggest that incomplete *CDH1* methylation might be sufficient for the formation of signet ring diffuse carcinoma areas or that *CDH1* might become partially unmethylated once the tumour areas have formed. Moreover, normal membranous immunohistochemical staining for E-cadherin has been previously shown in samples with or without *CDH1* methylation (*258*). In conclusion, the faint membrane staining observed in some of the patients with a *CDH1* germline mutation was probably due to the fact that immunohistochemical staining was less sensitive than PCR in detecting subpopulations of cells with gene methylation and hence downregulation of E-cadherin.

Overall, these three studies highlight the importance of clonal expansion in carcinoma development in gastric epithelium. Cancer screening of commonly mutated genes and the analysis of clonal evolution through microdissection will keep revealing the underlying mechanism of clonal expansion in cancer; such as in sporadic and tylotic oesophageal squamous cell carcinoma.

4. Clonal expansion in oesophageal squamous cell cancer

4.1. Introduction

Barrett's oesophagus (BO) occurs when oesophageal stratified squamous epithelium is replaced by columnar-cell metaplasia and it increases the risk of OA to at least 0.12% per annum (and possibly more) (*218*). There have been many studies analysing neoplastic progression from BO to OA, which is considered to occur due to the accumulation of genetic defects within the Barrett's glands and environmental factors such as GORD, diet, smoking and alcohol (*219, 220*). There are currently two clonal evolution models proposed for BO: the selective sweep to fixation model detailed by the Reid group (*221*) and the clonal interference model proposed by Leedham and colleagues (*157*) (see Figure 1.7). Nicholson and colleagues observed that Barrett's glands are clonal, contain multiple stem cells and are likely to divide by crypt fission (*222*). The possibility that different mutated stem cells could be involved in the formation of a pre-neoplastic lesion is important in order to assess clonal competition. However, it is the identification of mutated clones within pre-neoplastic lesions that is crucial, since these clones have the potential to expand by crypt fission and to cause OA development.

Leedham and colleagues have also suggested that WT squamous ducts of the oesophagus might be the potential source for a progenitor cell that could give rise to both stratified squamous epithelium and columnar-cell metaplasia (*157*). Nicholson and colleagues corroborated that squamous gland ducts might be the source of progenitor cells in the oesophagus when they observed a CCO deficient patch containing both squamous and glandular epithelium (*222*).

Oesophageal cancer is a major cause of morbidity and mortality throughout the world, and the most common type is OSCC (*168*). The different histopathological steps observed in the course of OSCC development are: oesophagitis; basal cell hyperplasia (BCH) followed by low-grade and high-grade dysplasia; carcinoma *in-situ*; and OSCC can develop when neoplastic cells invade the muscularis. Currently, no pre-neoplastic histopathological lesions are considered to represent field cancerisation in OSCC (*228*). However, Nicholson and colleagues suggested that lateral replacement of the stem cell pool occurs along the basal layer of the squamous epithelium (*222*), which might lead to the spread of preconditioned phenotypically-normal squamous epithelial cells that will eventually cause tumour development. Furthermore, Mandard and colleagues observed two independent patches of oesophagitis containing two different *TP53* mutations. Interestingly, only one of the *TP53* mutations was found later in the associated OSCC (*162*). Similar to BO, findings by both Mandard and Nicholson suggested that field cancerisation could indeed occur in stratified squamous epithelium, leading to OSCC development.

The observation of polyclonal lesions within the metaplasia and dysplasia in Barrett's oesophagus (BO) by Leedham *et al* (*157*) has lead to three different hypothesis explaining the origin and maintenance of genetic diversity in BO (*251*); previously explained in section 3.3. Even though OSCC does not arise as a result from GORD, it is possible that inflammatory events such as chronic oesophagitis might increase the mutation rate. It is also possible that a mutation might spread through field cancerisation in OSCC or that multiple clones might arise in fields of oesophagitis leading to clonal competition. However, Shima and colleagues analysis of needle

microdissected areas within 16 OSCC tumours revealed homogeneous LOH patterns mixed with either genetic progression or divergence (*259*). Both of these processes occurred through clonal evolution: it was suggested that the initial homogenous clone might have acquired further LOH of other microsatellite markers as the neoplasm evolved. Following on from Mandard's and Nicholson's work, these results suggest that OSCC might be clonal and that it would progress through clonal evolution.

Therefore, to understand clonal expansion and progression in oesophageal squamous cell dysplasia (OSCD) and OSCC, the presence of single or multiple clones presenting somatic mutations in genes involved in OSCC development needs to be assessed in pre-neoplastic and malignant epithelium. This might be expected to give insight into the process of field cancerisation and clonal expansion in OSCC.

4.1.1. Hypothesis and Aims

The hypothesis for the project presented here is that OSCC occurs by a process of field cancerisation of the oesophagus.

The aims of this project are:

1. To assess the mutation frequencies of genes known to be involved in the development of OSCC
2. To determine the clonal architecture of OSCD and OSCC

4.2. Results

Common cancer-associated mutations are found in oesophageal squamous cell carcinoma and occur mostly as a single event

To assess the clonal architecture of OSCC, areas of carcinoma or dysplasia from 34 patients were needle macrodissected and screened for mutations in genes commonly mutated in OSCC (for full methods see sections 2.1.4, 2.2 and 2.4). The most commonly mutated genes were *TP53*, *CDKN2A* and *NRF2*, according to the catalogue of somatic mutations in cancer (COSMIC, 16/05/2013) database (*256*). Patient 1 was removed from the screening due to insufficient DNA to obtain PCR results. From the 33 remaining patients, 36.36% (12/33) presented with mutations in the cancer (see Table 4.1 and Table 7.6 in the appendix).

Next, we compared the frequencies of mutations found in OSCC with those reported previously in the COSMIC database to confirm we had sufficient coverage of known mutations (see Table 4.1 for full details on the patients presenting mutations). The frequency of mutation for each gene was: *TP53,* 27.27% (9/33); *CDKN2A,* 9.09% (3/33); and *NRF2*, 12.12% (4/33). On correction of multiple testing using the Bonferroni adjustment (r=3), the significant *P* value was lowered to 0.01667. Therefore, the number of *TP53* mutated samples is not statistically significant and the mutation frequencies observed were comparable to previous reports in the COSMIC database (Figure 4.1) (*256*).

Interestingly, only 2 OSCC (6.06%, 2/33) presented with two independent functional mutations (*TP53* and *NRF2*; and *CDKN2A* and *NRF2*). This low incidence of OSCC patients with mutations indicated either that most functional mutations occur as a single event or that other genes not included in this screening may be involved in the premalignant pathway that eventually leads to OSCC.

Table 4.1. **Summary of mutations in genes selected from the COSMIC database for oesophageal squamous cell carcinoma.** Screening of 33 oesophageal squamous cell carcinomas (OSCC) for genes detailed in the COSMIC database (16/05/2013) that account for mutations in over 70% of OSCCs (*256*): *TP53*, *CDKN2A* and *NRF2* (or *NFE2L2*). Light grey stands for WT and dark blue stands for mutated samples, where the mutations found are written in bold. Patient 1 was removed from the screening due to insufficient DNA to obtain PCR results. The red rectangles highlight the three samples analysed by laser-capture microdissection.

Patient	*TP53*	*CDKN2A*	*NRF2*
2			
3			
4	**c.G818A Arg273His**		**c.T70C Trp24Arg**
5			
6			
7		**c.C203G Ala68Gly**	**c.62-65del**
8			
9			**c.G85C Asp29His**
10			
12	**c.451insC**		
13	**c.C916T Arg306STOP**		
14			
15			
16			
17	**c.C832A Pro278Thr**		
18	**c.633delT**		
19	**c.761-767del**		
20			
21			
22	**c.A659G Tyr220Cys**		
23			
24			**c.A230G Asp77Gly**
25			
26	**c.G856A Glu286Lys**		
27			
28	**c.C493T Gln165STOP**		
29			
30			
31			
32			
33			
34			

	WILD TYPE
	MUTATED

A

	TP53	
	Total	%
COSMIC	821/1670	49
Data	9/33	27.27
Chi-square with Yates correction	5.225	
P value	0.0223	

C

	NRF2	
	Total	%
COSMIC	29/160	18
Data	4/33	12.12
Chi-square with Yates correction	0.337	
P value	0.5618	

B

	CDKN2A	
	Total	%
COSMIC	132/645	20
Data	3/33	9.09
Chi-square with Yates correction	1.884	
P value	0.1699	

D

	Total	%
Total patients	33	100%
Patients with mutations	12	36.36%
Patients with multiple mutations	2	6.06%

Figure 4.1. **Mutation frequencies are comparable to reports for oesophageal squamous cell carcinoma held in the COSMIC database.** Statistical analysis of results obtained from the screening of 33 oesophageal squamous cell carcinoma patients. (A-C) Tables show the frequency of mutations within *TP53* (A), *CDKN2A* (B) and *NRF2* (C) in our patient cohort compared with the COSMIC database (*256*). (D) Table showing the percentages of mutated samples. *P* value was obtained by Chi-square test using Yates correction (two-tailed). After using the Bonferroni adjustment (r=3) the significant *P* value was lowered to 0.01667, therefore the number of *TP53* mutated samples is not statistically significant.

Oesophageal squamous cell dysplasia and carcinoma are clonal

To assess clonal expansion in OSCC, three patients were selected and analysed by LCM. These were patient 4, where the OSCC showed two independent functional mutations: a *TP53* exon 8 (c.G818A p.Arg273His) and an *NRF2* (c.T70C p.Trp24Arg) mutations; patient 26, where the OSCC showed a *TP53* exon 5 mutation (c.G856A p.Glu286Lys); and patient 28, where the oesophageal squamous cell dysplasia had a *TP53* exon 5 mutation (c.C493T Gln165Stop). LCM was then performed for

hyperplastic, dysplastic and carcinoma areas, when present in the available tissue for each patient (see Table 4.2).

Table 4.2. **Randomly selected patients for laser-capture microdissection.** List of the blocks of oesophageal epithelium used for laser-capture microdissection from the three patients selected randomly. Oesophageal squamous cell carcinoma, OSCC.

Patient	Genes mutated	Block	Histopathological phenotypes present
4	*TP53* + *NRF2*	B	Hyperplasia, dysplasia and OSCC
26	*TP53*	H	Hyperplasia and OSCC
		J	Hyperplasia and OSCC
		L	OSCC
28	*TP53*	7	Dysplasia, focal OSCC and infiltrated ducts
		8	Dysplasia and infiltrated ducts
		9	Dysplasia and focal OSCC

A specimen of oesophageal epithelium from patient 4 had muscle, hyperplastic and dysplastic areas that were WT for both *TP53* and *NRF2* (Figure 4.2). The surrounding invasive OSCC only showed one population of cells, mutated *TP53* and mutated *NRF2* within all areas of carcinoma (Figure 4.2). OSCC dissected area 14 appeared WT for both *TP53* and *NRF2*; however, this was due to the high levels of keratinisation and inflammatory cells present in that carcinoma area, which meant that the sample had extremely low numbers of carcinoma cells (see Table 4.3).

The dissected muscle and hyperplastic areas from patient 26 were WT in the three consecutive specimens of oesophageal epithelial mucosa (Figures 4.3, 4.4 and 4.5). Areas of highly invasive OSCC with elevated levels of keratinisation were present in the same specimens and these had the *TP53* mutation c.G856A (Figures 4.3, 4.4 and

4.5). However, around 4.6% of carcinoma areas (3/65) did not show the mutation. This again seemed to be due to the high levels of keratinisation and inflammatory cells within the carcinoma, which diluted the quantity of OSCC cells present in samples 14 (specimen block H), 15 (specimen block J) and 18 (specimen block L). The raw data linking the identified mutations to each microdissected area with the relevant histology can be found in Tables 4.4, 4.5 and 4.6, respectively.

All muscle areas microdissected from three consecutive blocks from patient 28 were WT for *TP53* (Figures 4.6, 4.7 and 4.8). Areas of dysplasia, focal invasive OSCC and infiltrated oesophageal ducts showed the *TP53* mutation c.C493T. Nevertheless, around 3% of dysplastic areas (3/98) found amongst fields of *TP53* mutated dysplasia appeared *TP53* WT. This lack of mutations could either be due to poor DNA quality and artefact during the PCR reaction, sample contamination with surrounding inflammatory cells, LOH of the *TP53* mutated allele or the actual lack of mutation within these specific dysplastic areas. The raw data linking the identified *TP53* mutation for each microdissected area with the histology can be found in Tables 4.7, 4.8 and 4.9, respectively.

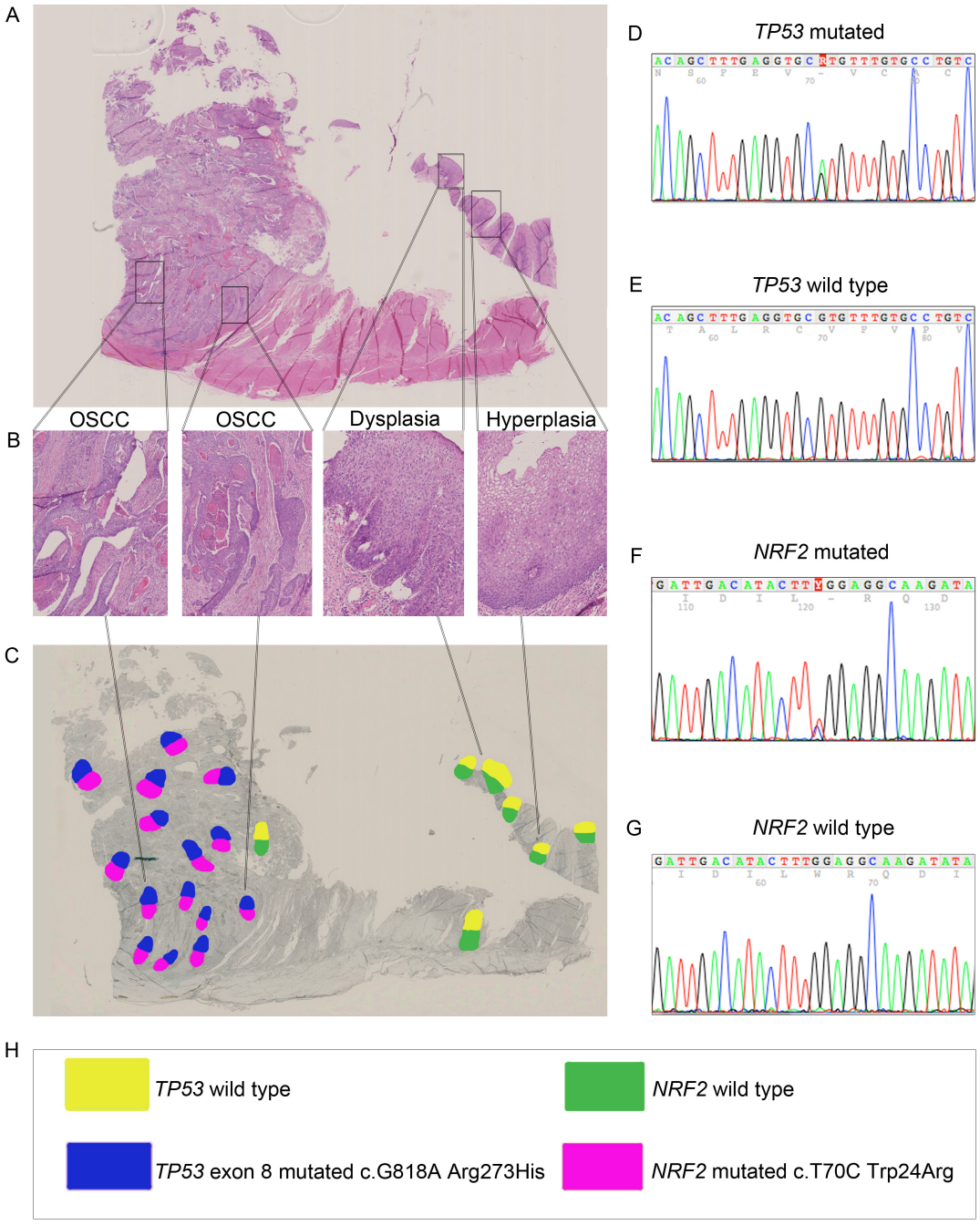

Figure 4.2. ***TP53* and *NRF2* mutations were found in all areas of oesophageal squamous cell carcinoma but not in dysplasia or hyperplasia in patient 4.** (A) A H&E of an entire section of oesophageal mucosa showing a moderately well differentiated oesophageal squamous cell carcinoma (OSCC) with dysplasia and hyperplasia; tissue from patient 4. (B) Higher power of highlighted areas showing from left to right two areas of OSCC, an area of dysplasia and an area of hyperplasia. (C) Serial section showing post laser-capture microdissection (LCM). Yellow areas are *TP53* WT whereas dark blue areas are positive for the *TP53* mutation c.G818A. Light green areas are *NRF2* WT whereas pink areas are positive for the *NRF2* mutation c.T70C. (D, E, F and G) Four representative traces showing the *TP53* mutation c.G818A (D), a *TP53* WT trace (E), the *NRF2* mutation c.T70C (F), and a *NRF2* WT trace (G). (H) Key for patient 4 on post LCM section.

Table 4.3. **Association of the identified mutations with histology shows *TP53* and *NFR2* mutations were found in all areas of oesophageal squamous cell carcinoma but not in dysplasia or hyperplasia in patient 4.** This table corresponds to the laser-capture microdissection data presented in Figure 4.2, tissue from patient 4. WT, wild type.

Patient 4	Histology	*TP53*	*NRF2*
1	Hyperplasia	WT	WT
2	Dysplasia	WT	WT
3	Hyperplasia	WT	WT
4	Hyperplasia	WT	WT
5	Hyperplasia	WT	WT
6	OSCC	MUTATED	MUTATED
7	OSCC	MUTATED	MUTATED
8	OSCC	MUTATED	MUTATED
9	OSCC	MUTATED	MUTATED
10	OSCC	MUTATED	MUTATED
11	OSCC	MUTATED	MUTATED
12	OSCC	MUTATED	MUTATED
13	OSCC	MUTATED	MUTATED
14	OSCC	WT	WT
15	OSCC	MUTATED	MUTATED
16	OSCC	MUTATED	MUTATED
17	OSCC	MUTATED	MUTATED
18	OSCC	MUTATED	MUTATED
19	OSCC	MUTATED	MUTATED
20	OSCC	MUTATED	MUTATED
21	OSCC	MUTATED	MUTATED
22	Muscle	WT	WT

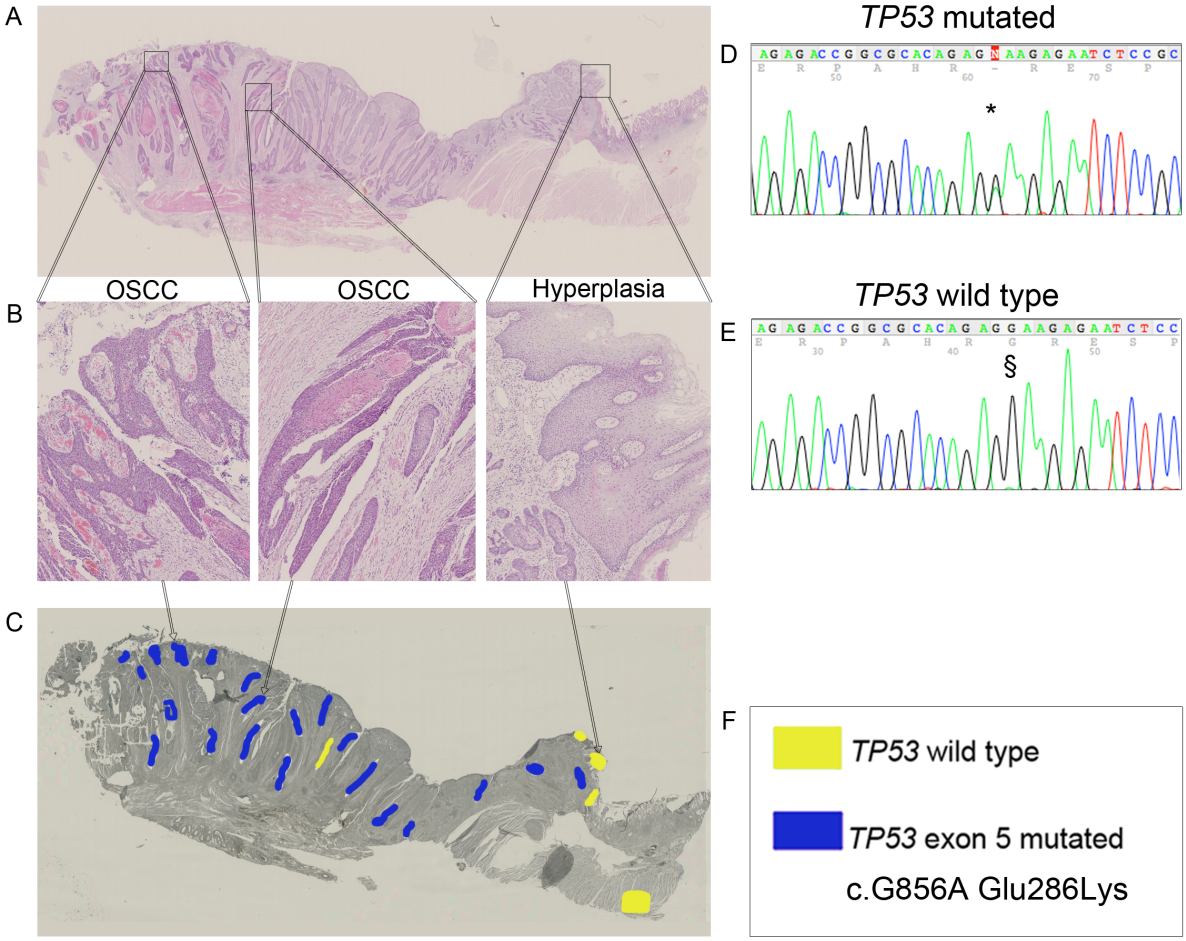

Figure 4.3. ***TP53* mutations were found in all areas of oesophageal squamous cell carcinoma but not in hyperplasia in patient 26.** (A) A H&E of an entire section of oesophageal mucosa showing a poorly differentiated oesophageal squamous cell carcinoma (OSCC) with hyperplasia, tissue from patient 26, specimen block H. (B) Higher power of highlighted areas showing from left to right two areas of OSCC and an area of hyperplasia. (C) Serial section showing post laser-capture microdissection (LCM). Yellow areas are *TP53* WT whereas dark blue areas are positive for the *TP53* mutation c.G856A. (D and E) Two representative traces showing the *TP53* mutation c.G856A (D) and a *TP53* WT trace (E). (F) Key for patient 26 on post LCM section.

Table 4.4. **Association of the identified mutation with histology shows *TP53* mutations were found in all areas of oesophageal squamous cell carcinoma but not in hyperplasia in patient 26.** This table corresponds to the laser-capture microdissection data presented in Figure 4.3, tissue from patient 26, specimen block H. WT, wild type.

Patient 26:H	Histology	*TP53*
1	OSCC	MUTATED
2	OSCC	MUTATED
3	OSCC	MUTATED
4	OSCC	MUTATED
5	OSCC	MUTATED
6	OSCC	MUTATED
7	OSCC	MUTATED
8	OSCC	MUTATED
9	OSCC	MUTATED
10	OSCC	MUTATED
11	OSCC	MUTATED
12	OSCC	MUTATED
13	OSCC	MUTATED
14	OSCC	WT
15	OSCC	MUTATED
16	OSCC	MUTATED
17	OSCC	MUTATED
18	OSCC	MUTATED
19	OSCC	MUTATED
20	OSCC	MUTATED
21	OSCC	MUTATED
22	Hyperplasia	WT
23	Hyperplasia	WT
24	Hyperplasia	WT
25	OSCC	MUTATED
26	Muscle	WT

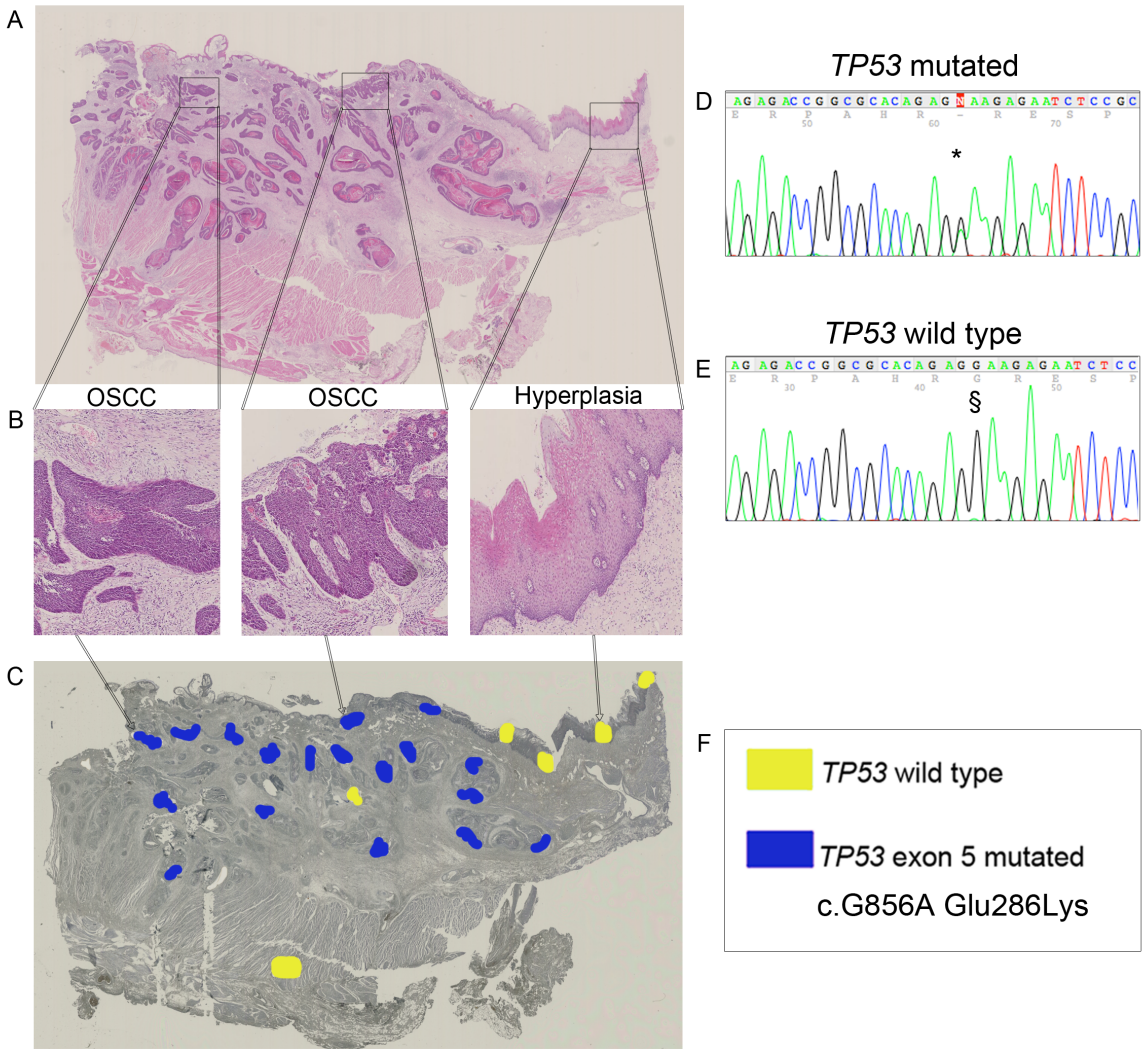

Figure 4.4. ***TP53* mutations were found in all areas of oesophageal squamous cell carcinoma but not in hyperplasia in patient 26.** (A) A H&E of an entire section of oesophageal mucosa showing a poorly differentiated oesophageal squamous cell carcinoma (OSCC) with hyperplasia, tissue from patient 26, specimen block J. (B) Higher power of highlighted areas showing from left to right two areas of OSCC and an area of hyperplasia. (C) Serial section showing post laser-capture microdissection (LCM). Yellow areas are *TP53* WT whereas dark blue areas are positive for the *TP53* mutation c.G856A. (D and E) Two representative traces showing the *TP53* mutation c.G856A (D) and a *TP53* WT trace (E). (F) Key for patient 26 on post LCM section.

Table 4.5. **Association of the identified mutation with histology shows *TP53* mutations were found in all areas of oesophageal squamous cell carcinoma but not in hyperplasia in patient 26.** Table corresponding to the laser-capture microdissection data presented in Figure 4.4, tissue from patient 26, specimen block J. WT, wild type.

Patient 26:J	Histology	*TP53*
1	Hyperplasia	WT
2	Hyperplasia	WT
3	Hyperplasia	WT
4	Hyperplasia	WT
5	OSCC	MUTATED
6	OSCC	MUTATED
7	OSCC	MUTATED
8	OSCC	MUTATED
9	OSCC	MUTATED
10	OSCC	MUTATED
11	Muscle	WT
12	OSCC	MUTATED
13	OSCC	MUTATED
14	OSCC	MUTATED
15	OSCC	WT
16	OSCC	MUTATED
17	OSCC	MUTATED
18	OSCC	MUTATED
19	OSCC	MUTATED
20	OSCC	MUTATED
21	OSCC	MUTATED
22	OSCC	MUTATED
23	OSCC	MUTATED
24	OSCC	MUTATED

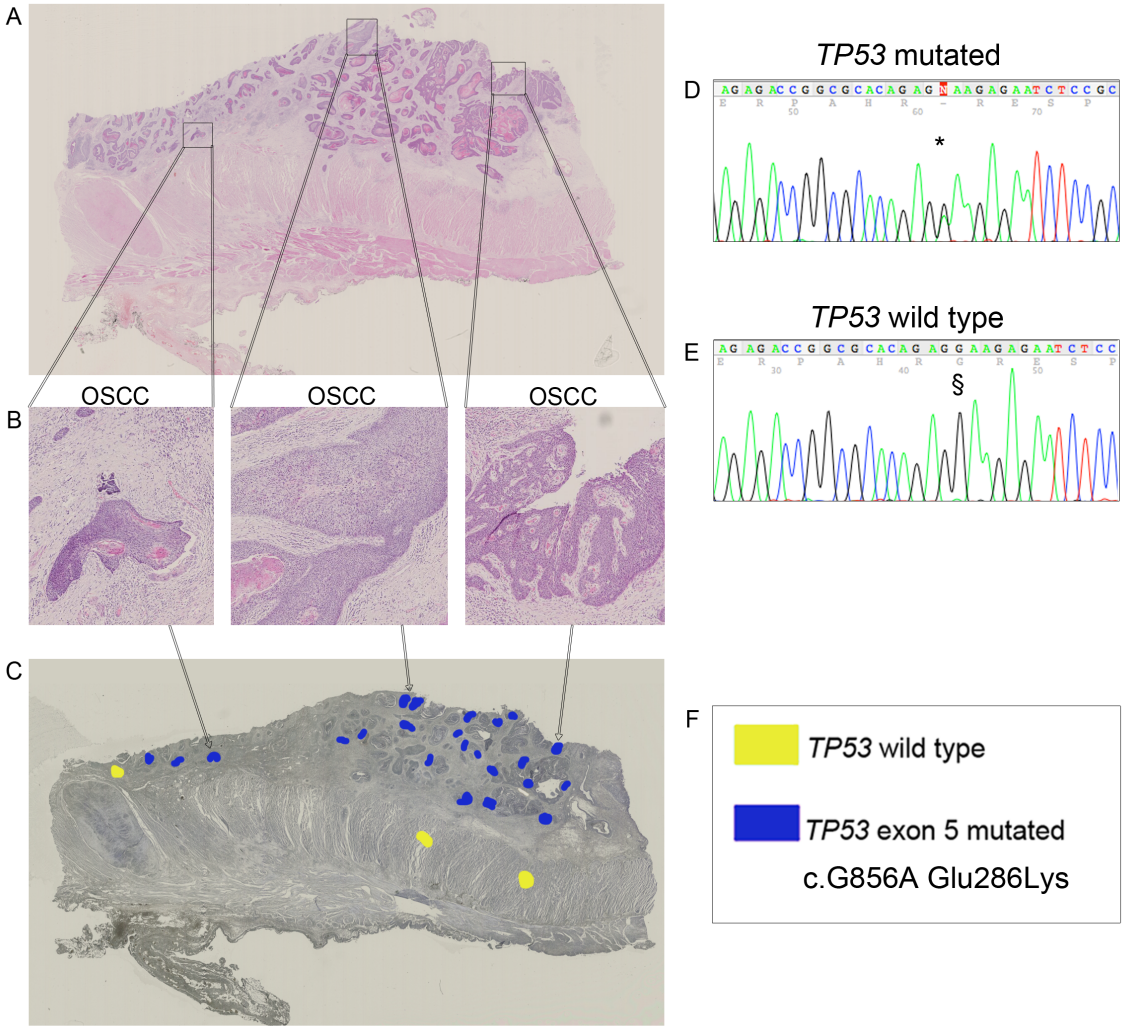

Figure 4.5. ***TP53* mutations were found in all areas of oesophageal squamous cell carcinoma in patient 26.** (A) A H&E of an entire section of oesophageal mucosa showing a poorly differentiated oesophageal squamous cell carcinoma (OSCC), tissue from patient 26, specimen block L. (B) Higher power of highlighted areas showing three areas of OSCC. (C) Serial section showing post laser-capture microdissection (LCM). Yellow areas are *TP53* WT whereas dark blue areas are positive for the *TP53* mutation c.G856A. (D and E) Two representative traces showing the *TP53* mutation c.G856A (D) and a *TP53* WT trace (E). (F) Key for patient 26 on post LCM section.

Table 4.6. **Association of the identified mutation with histology shows *TP53* mutations were found in all areas of oesophageal squamous cell carcinoma in patient 26.** This table corresponds to the laser-capture microdissection data presented in Figure 4.5, tissue from patient 26, specimen block L. WT, wild type.

Patient 26:L	Histology	*TP53*
1	OSCC	MUTATED
2	OSCC	MUTATED
3	OSCC	MUTATED
4	OSCC	MUTATED
5	OSCC	MUTATED
6	OSCC	MUTATED
7	Muscle	WT
8	OSCC	MUTATED
9	OSCC	MUTATED
10	OSCC	MUTATED
11	OSCC	MUTATED
12	OSCC	MUTATED
13	OSCC	MUTATED
14	OSCC	MUTATED
15	OSCC	MUTATED
16	Muscle	WT
17	OSCC	MUTATED
18	OSCC	WT
19	OSCC	MUTATED
20	OSCC	MUTATED
21	OSCC	MUTATED
22	OSCC	MUTATED
23	OSCC	MUTATED
24	OSCC	MUTATED
25	OSCC	MUTATED
26	OSCC	MUTATED

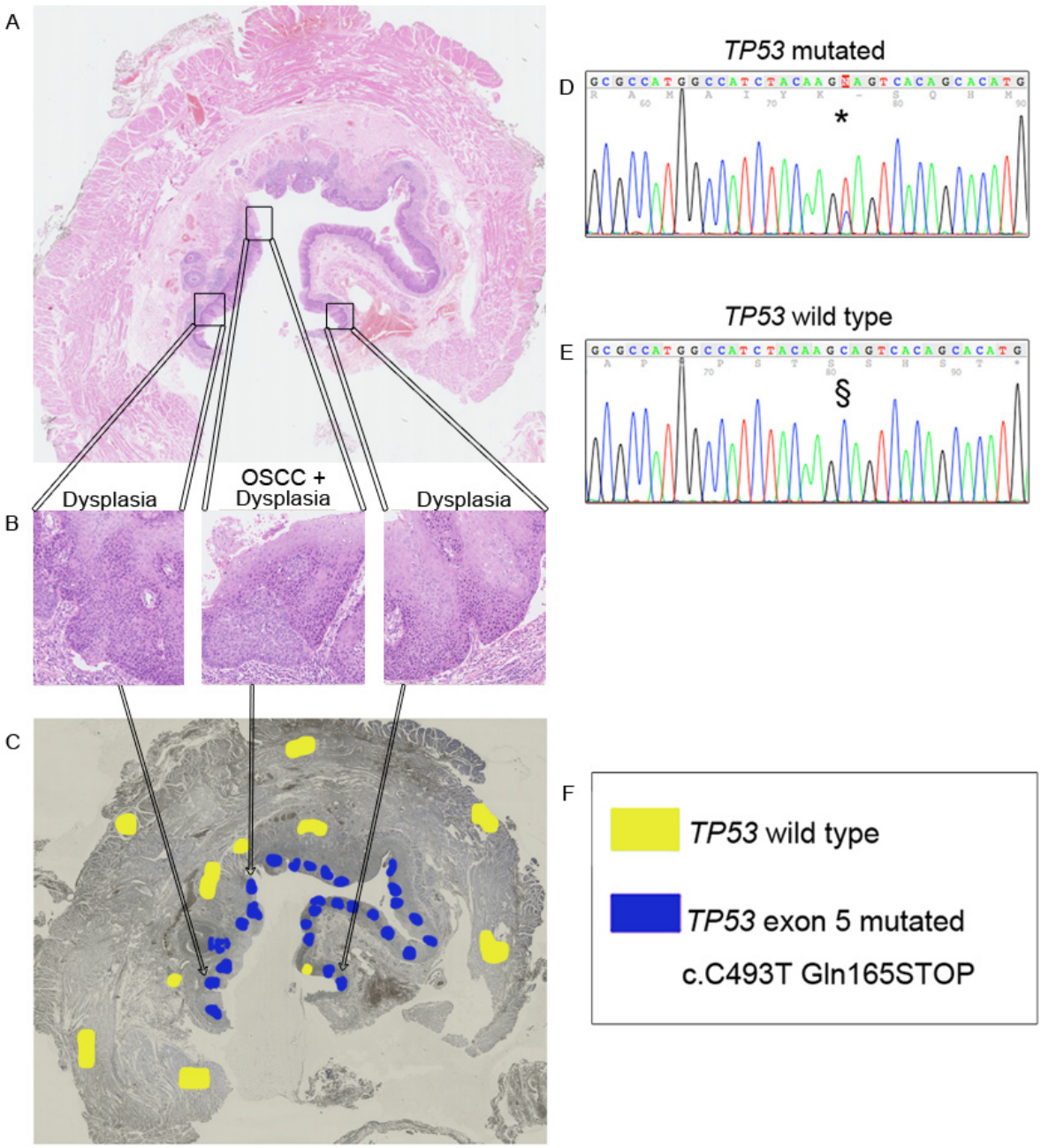

Figure 4.6. ***TP53* mutations were found in all dysplastic areas, in focal areas of invasive oesophageal squamous cell carcinoma and in infiltrated oesophageal ducts in patient 28.** (A) A H&E of an entire section of oesophageal mucosa showing dysplasia and small areas of invasive oesophageal squamous cell carcinoma (OSCC), tissue from patient 28, specimen block 7. (B) Higher power of highlighted areas showing from left to right an area of dysplasia, an area of dysplasia with a small invasive island of OSCC and another area of dysplasia. (C) Serial section showing post laser-capture microdissection (LCM). Yellow areas are *TP53* WT whereas dark blue areas are positive for the *TP53* mutation c.C493T. (D and E) Two representative traces showing the *TP53* mutation c.C493T (D) and a *TP53* WT trace (E). (F) Key for patient 28 on post LCM section.

Table 4.7. **Association of the identified mutation with histology shows *TP53* mutations were found in all dysplastic areas, in focal areas of oesophageal squamous cell carcinoma and in infiltrated oesophageal ducts in patient 28.** This table corresponds to the laser-capture microdissection data presented in Figure 4.6, tissue from patient 28, specimen block 7. WT, wild type.

Patient 28:7	Histology	*TP53*
1	Dysplasia	MUTATED
2	Dysplasia	MUTATED
3	Dysplasia	WT
4	Dysplasia	MUTATED
5	Dysplasia	MUTATED
6	Dysplasia	MUTATED
7	Dysplasia	MUTATED
8	Dysplasia	MUTATED
9	Dysplasia	MUTATED
10	Dysplasia	MUTATED
11	Dysplasia	MUTATED
12	Dysplasia	MUTATED
13	Dysplasia	MUTATED
14	Dysplasia	MUTATED
15	Dysplasia	MUTATED
16	Dysplasia	MUTATED
17	Dysplasia	MUTATED
18	Dysplasia	MUTATED
19	Dysplasia	MUTATED
20	Dysplasia	MUTATED
21	Dysplasia	MUTATED
22	OSCC	MUTATED
23	Dysplasia	MUTATED
24	Dysplasia	MUTATED
25	Dysplasia	MUTATED
26	Dysplasia	MUTATED
27	Dysplasia	MUTATED
28	Dysplasia	MUTATED
29	Muscle	WT
30	Duct	MUTATED
31	Dysplasia	MUTATED
32	Duct	MUTATED
34	Gland	WT
35	Muscle	WT
36	Muscle	WT
37	Gland	WT
38	Muscle	WT
39	Muscle	WT
40	Muscle	WT
41	Muscle	WT
42	Muscle	WT

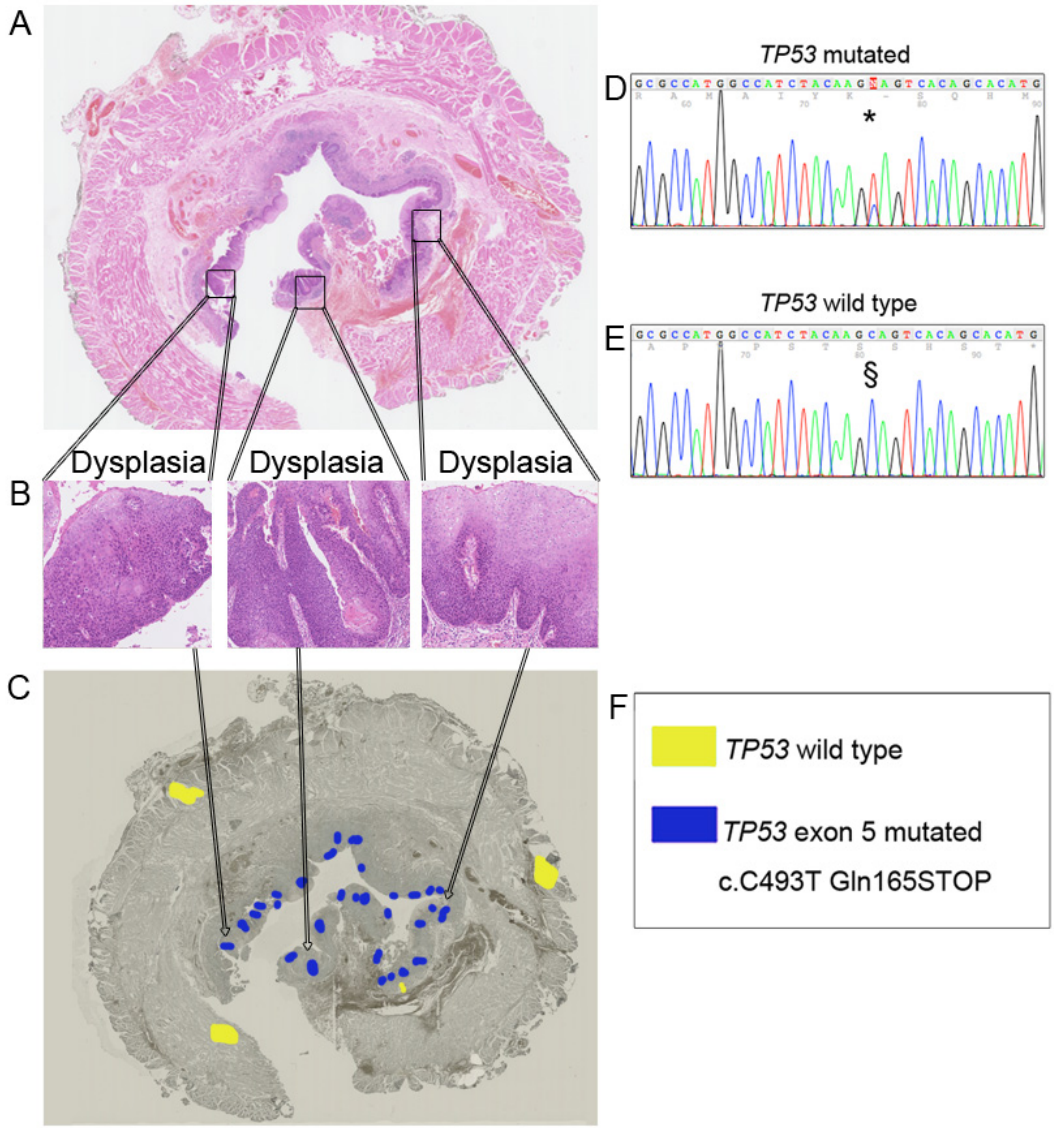

Figure 4.7. ***TP53* mutations were found in all dysplastic areas and in infiltrated oesophageal ducts in patient 28.** (A) A H&E of an entire section of oesophageal mucosa showing dysplasia, tissue from patient 28, specimen block 8. (B) Higher power of highlighted areas showing three areas of dysplasia. (C) Serial section showing post laser-capture microdissection (LCM). Yellow areas are *TP53* WT whereas dark blue areas are positive for the *TP53* mutation c.C493T. (D and E) Two representative traces showing the *TP53* mutation c.C493T (D) and a *TP53* WT trace (E). (F) Key for patient 28 on post LCM section.

Table 4.8. **Association of the identified mutation with histology shows *TP53* mutations were found in all dysplastic areas and in infiltrated oesophageal ducts in patient 28.** This table corresponds to the laser-capture microdissection data presented in Figure 4.7, tissue from patient 28, specimen block 8. WT, wild type.

Patient 28:8	Histology	*TP53*
1	Dysplasia	MUTATED
2	Duct	MUTATED
3	Dysplasia	MUTATED
4	Dysplasia	MUTATED
5	Dysplasia	MUTATED
6	Dysplasia	MUTATED
7	Dysplasia	WT
8	Dysplasia	MUTATED
9	Dysplasia	MUTATED
10	Dysplasia	MUTATED
11	Dysplasia	MUTATED
12	Dysplasia	MUTATED
13	Dysplasia	MUTATED
14	Dysplasia	MUTATED
15	Dysplasia	MUTATED
16	Dysplasia	MUTATED
17	Dysplasia	MUTATED
18	Dysplasia	MUTATED
19	Dysplasia	MUTATED
20	Dysplasia	MUTATED
21	Dysplasia	MUTATED
22	Dysplasia	MUTATED
23	Dysplasia	MUTATED
24	Dysplasia	MUTATED
25	Dysplasia	MUTATED
26	Dysplasia	MUTATED
27	Dysplasia	MUTATED
28	Dysplasia	MUTATED
29	Dysplasia	MUTATED
30	Dysplasia	MUTATED
31	Dysplasia	MUTATED
32	Dysplasia	MUTATED
33	Dysplasia	MUTATED
34	Muscle	WT
35	Gland	WT
36	Muscle	WT
37	Muscle	WT
38	Muscle	WT
39	Muscle	WT

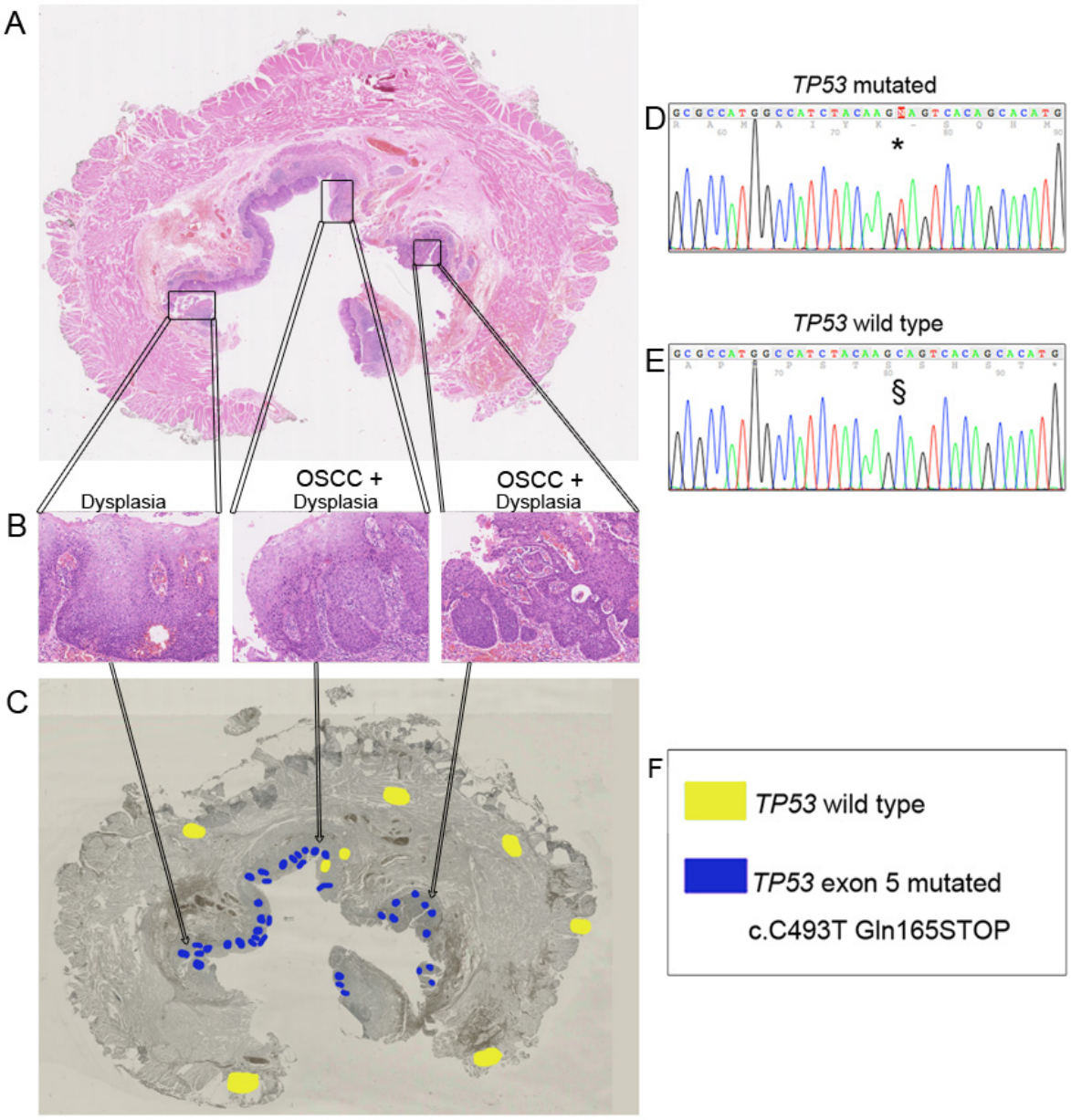

Figure 4.8. ***TP53* mutations were found in all dysplastic areas and in focal areas of invasive oesophageal squamous cell carcinoma in patient 28.** (A) A H&E of an entire section of oesophageal mucosa showing dysplasia and small areas of invasive oesophageal squamous cell carcinoma (OSCC), tissue from patient 28, specimen block 9. (B) Higher power of highlighted areas showing from left to right an area of dysplasia and two areas of dysplasia and OSCC. (C) Serial section showing post laser-capture microdissection (LCM). Yellow areas are *TP53* WT whereas dark blue areas are positive for the *TP53* mutation c.C493T. (D and E) Two representative traces showing the *TP53* mutation c.C493T (D) and a *TP53* WT trace (E). (F) Key for patient 28 on post LCM section.

Table 4.9. **Association of the identified mutation with histology shows *TP53* mutations were found in all dysplastic areas and in focal areas of oesophageal squamous cell carcinoma in patient 28.** This table corresponds to the laser-capture microdissection data presented in Figure 4.8, tissue from patient 28, specimen block 9. WT, wild type.

Patient 28:9	Histology	*TP53*
1	Dysplasia	MUTATED
2	Dysplasia	MUTATED
3	Dysplasia	MUTATED
4	Dysplasia	MUTATED
5	Dysplasia	MUTATED
6	Dysplasia	MUTATED
7	Dysplasia	MUTATED
8	OSCC	MUTATED
9	Dysplasia	MUTATED
10	Dysplasia	MUTATED
11	Dysplasia	MUTATED
12	Dysplasia	MUTATED
13	Dysplasia	MUTATED
14	Dysplasia	MUTATED
15	Gland	WT
16	Dysplasia	WT
17	Dysplasia	MUTATED
18	Dysplasia	MUTATED
19	OSCC	MUTATED
20	Dysplasia	MUTATED
21	Dysplasia	MUTATED
22	Dysplasia	MUTATED
23	Dysplasia	MUTATED
24	Dysplasia	MUTATED
25	Dysplasia	MUTATED
26	Dysplasia	MUTATED
27	Dysplasia	MUTATED
28	Dysplasia	MUTATED
29	Dysplasia	MUTATED
30	Dysplasia	MUTATED
31	Dysplasia	MUTATED
32	Dysplasia	MUTATED
33	Dysplasia	MUTATED
34	Dysplasia	MUTATED
35	Dysplasia	MUTATED
36	Dysplasia	MUTATED
37	Dysplasia	MUTATED
38	Dysplasia	MUTATED
39	Dysplasia	MUTATED
40	Dysplasia	MUTATED
41	Dysplasia	MUTATED
42	Muscle	WT
43	Muscle	WT
44	Muscle	WT
45	Muscle	WT
46	Muscle	WT
47	Muscle	WT

Oesophageal squamous cell dysplasia and carcinoma demonstrate clonal expansion through tumour progression

Three phylogenetic trees were used to summarise the data for patients 4 (A), 26 (B) and 28 (C) (Figure 4.9).

In the case of patient 4 it can be inferred that at some point in the development of oesophageal squamous cell dysplasia both a *TP53* and an *NRF2* mutation must have occurred (Figure 4.9A). As seen in GA (Figure 3.19), one of the mutations occurred first, followed by a second mutation through clonal evolution as the tumour progressed. Because all OSCC areas presented the same *TP53* and *NRF2* mutations, this data indicates that OSCC is clonal, that this clone was likely to have evolved from an original dysplastic mutated clone and that a second mutation was likely to have caused the transition from dysplasia to OSCC.

The phylogenetic tree of patient 26 demonstrated that all OSCC areas had a *TP53* mutation and that this mutation was probably also present in the dysplasia. However, this could not be confirmed experimentally due to a lack of available dysplastic tissue for this particular patient (Figure 4.9B).

In the case of patient 28, a *TP53* mutation arose during clonal expansion in the dysplasia or even at an earlier stage, which probably led to further progression of the carcinoma. The *TP53* mutated clone was also found in the focal OSCC areas surrounding the dysplasia and also in the infiltrated oesophageal ducts. This shows that a mutation present in cells within a dysplastic area can clonally expand to form an

associated carcinoma and, in this case, the oesophageal squamous cell dysplasia and OSCC were therefore clonal (Figure 4.9C).

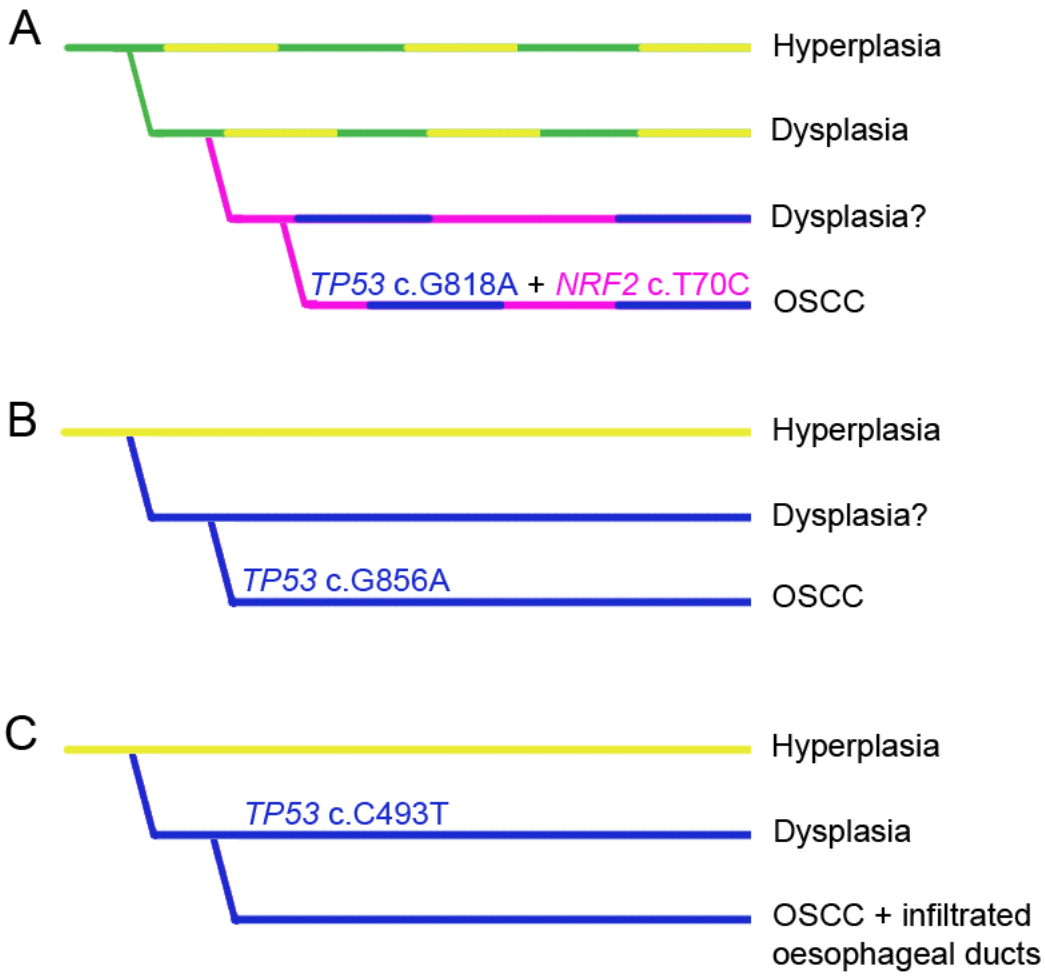

Figure 4.9. **Phylogenetic trees provide evidence for a monoclonal origin for oesophageal squamous cell carcinoma.** (A-C) Phylogenetic trees representative of patients 4 (A), 26 (B) and 28 (C) presenting oesophageal squamous cell carcinoma (OSCC), the data has been interpreted from the experimental data found in Figures 4.2 to 4.8. Tree branches represent phenotypic or genotypic changes. The wild type genotype is coloured in yellow (representing *TP53*) and/or green (representing *NRF2*). *NRF2* mutations are coloured in pink and *TP53* mutations are coloured in dark blue. Cumulative mutations are represented by different coloured lines and a "?" has been used to highlight likely but not proven genotypic and phenotypic events previous to OSCC development in the three patients.

4.3. Discussion

All samples were screened for mutations in the three most frequently mutated genes in OSCC. These genes account for over 70% of all somatic mutations previously reported for OSCC in the COSMIC database (16/05/2013) (*256*). However, from the 33 patients included in our study, 12 (36.36%) presented with a single identifiable functional mutation and only 2 (6.06%) presented two functional mutations. After using the Bonferroni adjustment for multiple testing, all mutation frequencies obtained were comparable to those from previous reports (*260*) (Figure 4.1). The absence of mutations in a large proportion of our OSCC patients (63.64%) could indicate that other mutational events occur at a much higher frequency in OSCC than has been reported previously. These would include LOH at *TP53* locus 17p13.1; LOH and promoter methylation of $p15^{INK4b}$ and *CDKN2A* respectively; reduced *Rb* expression and *cyclin D1*; mutations in the *ras* family and *Notch1* signalling pathway; and *EGFR* and *c-myc* gene amplifications (*162, 167, 230-233, 259, 261*).

This lack of mutations could also be explained by mutational events in genes not yet known to have an effect in sporadic OSCC, such as mutations in the TOC susceptibility gene *RHBDF2*. Von Brevern *et al* have already reported high levels of LOH of microsatellite markers in the 17q region correspondent to *RHBDF2* in sporadic OSCC; however, *RHBDF2* somatic mutations have not yet been reported (*262*). Moreover, there are very few exome sequencing studies for OSCC. Agrawal and colleagues performed a study comparing genetic differences between OAC and OSCC in North American patients, suggesting that different genes are involved in carcinogenesis in both tumour types and that the ethnicity and geographic location of

OSCC patients considerably affects the genes involved in different subtypes of OSCC, as is the case for *Notch1* (*233*). Further exome sequencing studies will hopefully reveal novel target genes pertinent to the development of OSCC.

To study clonal expansion in OSCC, the tissue from 3 patients that had detectable mutations were studied by LCM of FFPE specimens with varied histology, including hyperplasia, dysplasia and carcinoma. The data suggested that during field cancerisation a mutation might arise in a pre-neoplastic area (for example in an area of oesophagitis (*162*)), followed by the development of dysplasia where subsequent mutations will occur via clonal evolution. Clonal expansion within the dysplasia will eventually lead to progression into a squamous cell carcinoma (Figure 4.9). In tissue from patients 4 and 26 OSCC areas contained mutated cells. Whilst, in tissue from patient 28 all dysplastic areas and associated focal OSCC and infiltrated oesophageal ducts were populated by mutated cells. In the case of patient 4 it is likely that a mutation in a gene not included in the screening was responsible for field cancerisation, since the microdissected dysplasia area appeared WT for both *TP53* and *NRF2*. Overall, the LCM data of these patients suggested that OSCD and OSCC were clonal and that clonal expansion occurred as the tumour progressed.

Therefore the results from this study are in agreement with those of Shima and colleagues (*259*): LOH analysis showed that single clones within OSCC fields acquired further loss of microsatellites as the carcinoma evolved. These results were also in agreement with the findings from Mandard *et al* (*162*), who observed a *TP53* mutated clone in an area of oesophagitis which clonally expanded into a squamous cell carcinoma. However, Mandard and colleagues had observed two areas of oesophagitis

containing two different *TP53* mutations. This could be explained by a mutation in an unknown gene that through field cancerisation took over the oesophageal mucosa and then, via clonal evolution, led to genetic divergence in the oesophagitis and finally genetic progression into a carcinoma. Following on from previous work and using data from this study, it seems likely that OSCC is monoclonal in origin and that genetic heterogeneity arises through clonal evolution (*88*). This was observed in the study of clonal expansion in GA (Results Chapter 3), and not because of clonal competition as seen in BO (*157*) and colorectal microadenomas (*16*).

5. Clonal expansion in tylosis with oesophageal cancer

5.1. Introduction

Tylosis with oesophageal cancer (TOC) is a rare familial syndrome inherited in an autosomal-dominant manner (*163*). Symptoms include palmoplantar keratoderma (PPK), oral keratosis and follicular papules and it can be associated with a high risk for oesophageal SCC development (up to a 95% by the age of 65) (*237-239*). Rhomboids are intramembrane serine proteases, which typically contain six or seven transmembrane domains (TMD) classified into four subgroups: Secretase A and B, Presenilin-Associated-Rhomboid-Like (PARL) and iRhoms (*240*). The gene responsible for TOC was recently identified as the inactive rhomboid protease *RHBDF2*, also known as *iRhom2* (*163*). To date, heterozygous missense *RHBDF2* mutations have been found in four different families: from the UK, c.T557C p.Ile186Thr; US, c.T557C p.Ile186Thr; Germany, c.C566T p. Pro189Leu; and Finland, c.A562G p.Asp188Asn (*163, 263*). iRhoms are predicted to localise to the endoplasmic reticulum (ER) membrane (*241*) although in the epidermis and oesophagus RHBDF2 is also localised at the plasma membrane (*163*). The TOC mutations have been found clustered in the highly conserved extended N-terminal domain of *RHBDF2*, suggesting an important function for this region of the RHBDF2 protein (see Introduction Figure 1.8) (*242*).

The Secretase A type Rhomboid RHBDL2 is the active Rhomboid relative of iRhom1 and RHBDF2 (*240*). RHBDL2 is known to be responsible for EGF cleavage independently of ADAM (A Desintegrin And Metalloprotease) family members: thrombomodulin (ThM) in wound healing; and ephrin B3, where cleavage may lead to

intercellular interactions between ephrinB3 and eph receptors (*243, 264, 265*). Both iRhom1 1 and RHBDF2 lack the catalytic residues present in active Rhomboid proteases and, instead, they present an invariant proline residue that is N terminal to the expected location of the catalytic serine (i.e., GPx replacing the GxS rhomboid catalytic motif) (Figure 1.8 A) (*244, 245*). Nevertheless, Zettl and colleagues showed that human iRhom1 and mouse RHBDF2 interact directly with the RHBDL2 ligand EGF in the ER using immunoprecipitation experiments; they were both found to target EGF for ER-associated degradation (ERAD) (*245*). Keratinocytes from TOC patients are unresponsive to exogenous EGF; but, in the absence of exogenous EGF cell migration and proliferation are maintained whereas both are significantly reduced in control keratinocytes (*163*). These results suggest that EGF levels might be higher in TOC patients and that human RHBDF2 also plays a physiological role in EGF signaling (*163, 242*).

Both iRhom1 and RHBDF2 have been reported in the ER and Golgi in cultured cells (*266, 267*). Blaydon and colleagues observed strong plasma membrane expression and some cytoplasmic staining, probably representing the ER and the Golgi, in human stratified squamous epithelium such as the skin and the oesophagus (*163, 242*). These workers suggested that RHBDF2 trafficking or targeting is altered in TOC patients as they had observed that RHBDF2 immunohistochemistry staining was much more diffuse in human stratified skin biopsies from TOC patients compared to healthy controls. To date, no *RHBDF2* mutations have been reported in sporadic OSCC, although Von Brevern and colleagues showed high levels of LOH of microsatellite markers in the 17q region correspondent to *RHBDF2* in sporadic OSCC (*262*). In addition, Blaydon also showed a more cytoplasmic localisation of RHBDF2 in both

tylotic and sporadic OSCC patients suggesting that *RHBDF2* also plays a role in the pathogenesis of sporadic OSCC development (*163*).

Studies on RHBDF2 knock-out mice (RHBDF2$^{-/-}$) revealed a severe reduction of TNFα levels in serum and in bone marrow derived macrophages (BMDMs), suggesting that RHBDF2 is critical for the TNF convertase (TACE) ADAM17 maturation and trafficking from the endoplasmic reticulum (ER) (*243, 246*). Lack of activated ADAM17 in the cell membrane prevents the cleavage-mediated activation of TNFα leading to a severe reduction of TNFα levels in RHBDF2 $^{-/-}$ mice. In support of this suggestion, ADAM17, a member of the membrane-anchored ADAM family of proteases, is widely expressed in somatic tissues and is responsible for the proteolytic cleavage of the majority of known ectodomain shedding events (*268*), including TNFα and five of the seven known ligands of EGFR (*269*). Overall, these findings suggest that RHBDF2 binds to ADAM17 in the ER and is crucial for the trafficking of ADAM17 from the ER into the Golgi, where ADAM17 undergoes furin-mediated cleavage activation before trafficking to the cell surface (*243*). Unpublished data suggests that the *RHBDF2* gain of function TOC mutations leads to an increased level of ADAM17-mediated shedding of EGF signalling molecules in TOC cells (*242*). This increased activation would account, in part, for the unresponsiveness of TOC keratinocytes to exogenous EGF and also for the hyperproliferative epidermal phenotype observed in tylotic patients (*242*). The epidermal hyperproliferation observed in the areas undergoing frequent wound healing might be due to the excessive ADAM17 activation, as observed in TOC, because wound healing is mediated, in part, via EGFR signalling in keratinocytes (*247*).

Hence, RHBDF2 appears capable of regulating EGFR signalling through two separate pathways by controlling the shedding of pro-EGF targeting for ERAD and also by controlling the rate of that shedding through the regulation of ADAM17 maturation and transit from the ER into the Golgi.

5.1.1. Hypothesis and Aims

The hypothesis for the project presented here is to investigate if TOC associated *RHBDF2* mutations persist during tumour progression in TOC and that the localisation of RHBDF2 and ADAM17 plays a key role in oesophageal tumourigenesis.

The aims of this project are:

4. To characterise the mutational state of *RHBDF2* in sporadic OSCC
5. To determine if *RHBDF2* germline gain of function mutations persist during tumour progression in TOC
6. To assess the localisation of RHBDF2 and ADAM17 in sporadic OSCC and TOC

6.3 Results

TOC associated *RHBDF2* mutations are not found in sporadic oesophageal squamous cell carcinomas but are present in oesophageal carcinomas from patients with tylosis

To assess the mutational state of *RHBDF2* in OSCC, areas of carcinoma or dysplasia in tumour tissue from 34 patients were needle macrodissected and screened for

mutations in the highly conserved extended N-terminal domain of *RHBDF2* (exons 5 and 6, for full methods see 2.1.4, 2.2 and 2.4). Patient 1 was removed from the screening due to insufficient DNA to obtain PCR results. From the 33 remaining patients, 30 presented with sporadic OSCC and 3 presented with TOC (these patients are also the ones from Results Chapter 4, see Table 4.1 and Table 7.6 in the appendix). The *RHBDF2* mutations detected in this screening were exclusive to the 3 patients with TOC. Therefore, *RHBDF2* does not appear to be mutated in sporadic OSCC at a high frequency, see Table 5.1.

Table 5.1. **Summary of mutations in inactive rhomboid protein *RHBDF2* in specimens from sporadic and tylosis associated oesophageal squamous cell carcinoma patients.** Screening of 33 oesophageal squamous cell carcinomas (OSCC) for *RHBDF2*. Light grey, WT; dark blue, mutated samples; the mutations found are written in bold. Patient 1 was removed from the screening due to insufficient DNA to obtain PCR results. The red rectangles highlight the three samples analysed by laser-capture microdissection and a "--" has been used to highlight information that was not available.

Patient	Gender	Age	*RHBDF2*
2	M	--	**c.T557C**
3	F	34	
4	--	--	
5	M	60	
6	M	71	
7	M	69	
8	M	69	
9	F	72	
10	F	66	
12	M	57	
13	F	66	
14	F	59	
15	F	78	
16	M	55	
17	M	71	
18	M	71	
19	F	68	
20	M	53	
21	M	65	
22	--	--	
23	--	--	
24	--	--	
25	M	74	
26	F	71	
27	M	64	
28	F	70	
29	M	61	
30	F	72	
31	F	58	
32	F	54	
33	--	--	**c.T557C**
34	--	--	**c.T557C**

	WILD TYPE
	MUTATED

***RHBDF2* germline mutations can be lost in oesophageal carcinomas from patients with tylosis when carcinomas exhibit LOH in 17q**

To assess the clonality of TOC, the three tylotic patients (2, 33 and 34) who all carried the same germline *RHBDF2* mutation (c.T557C p.Ile186Thr) were analysed by LCM for the muscle, dysplastic and carcinoma areas, when present in the available tissue for each patient (see Table 5.2). As TOC is caused by the germline mutation in *RHBDF2*, all laser-captured areas should present the c.T557C mutation unless LOH of the mutated allele had occurred during the clonal expansion of the carcinoma.

Table 5.2. **Oesophageal carcinoma from tylotic patients analysed by laser-capture microdissection.** List of the blocks of oesophageal epithelium used for laser-capture microdissection from the three TOC patients.

Patient	Gene mutated	Block	Histopathological phenotypes and tissue
2	*RHBDF2*	2	OSCC, Muscle
		3	OSCC, Muscle
33	*RHBDF2*	EE	Dysplasia, OSCC, Muscle
34	*RHBDF2*	K	Dysplasia, OSCC, Muscle

Two specimens of oesophageal epithelium from patient 2 had both muscle and OSCC areas available (Figures 5.1 and 5.2). As expected the muscle areas analysed showed the *RHBDF2* mutation. However, there was a mixture of two populations in the carcinoma; one population of cells presenting the *RHBDF2* mutation and a WT population where the mutation appeared to be lost (see Table 5.3).

Dissected muscle, dysplasia and carcinoma areas from patient 33 all had the *RHBDF2* mutation, indicating that there was no LOH of the mutated allele in this patient (Figures 5.3, Table 5.4). All muscle, dysplasia and carcinoma areas microdissected from patient 34 were WT for *RHBDF2,* which indicated there was LOH of the *RHBDF2* mutated allele (Figures 5.4, Table 5.5).

Retrospective studies using extracted DNA from two separate samples of frozen tumour tissue from patient 34 showed the T/C and T/T genotype respectively (*163*). In addition, studies using single-nucleotide polymorphism analysis on patients 33 and 34 revealed genetic instability in the tumour in patient 34 but not in patient 33. LOH data on chromosome 17q25 from the same DNA sample prepared from a frozen tumour resection from patient 34 showed evidence of: retention of heterozygosity (2 markers); loss of the WT allele (3 markers); and loss of the mutated allele (2 markers) (Figure 5.5). These results are consistent with the findings presented here as we found the mutation in all muscle, dysplasia and carcinoma LCM areas of patient 33 (B) but not in those of patient 34 (C).

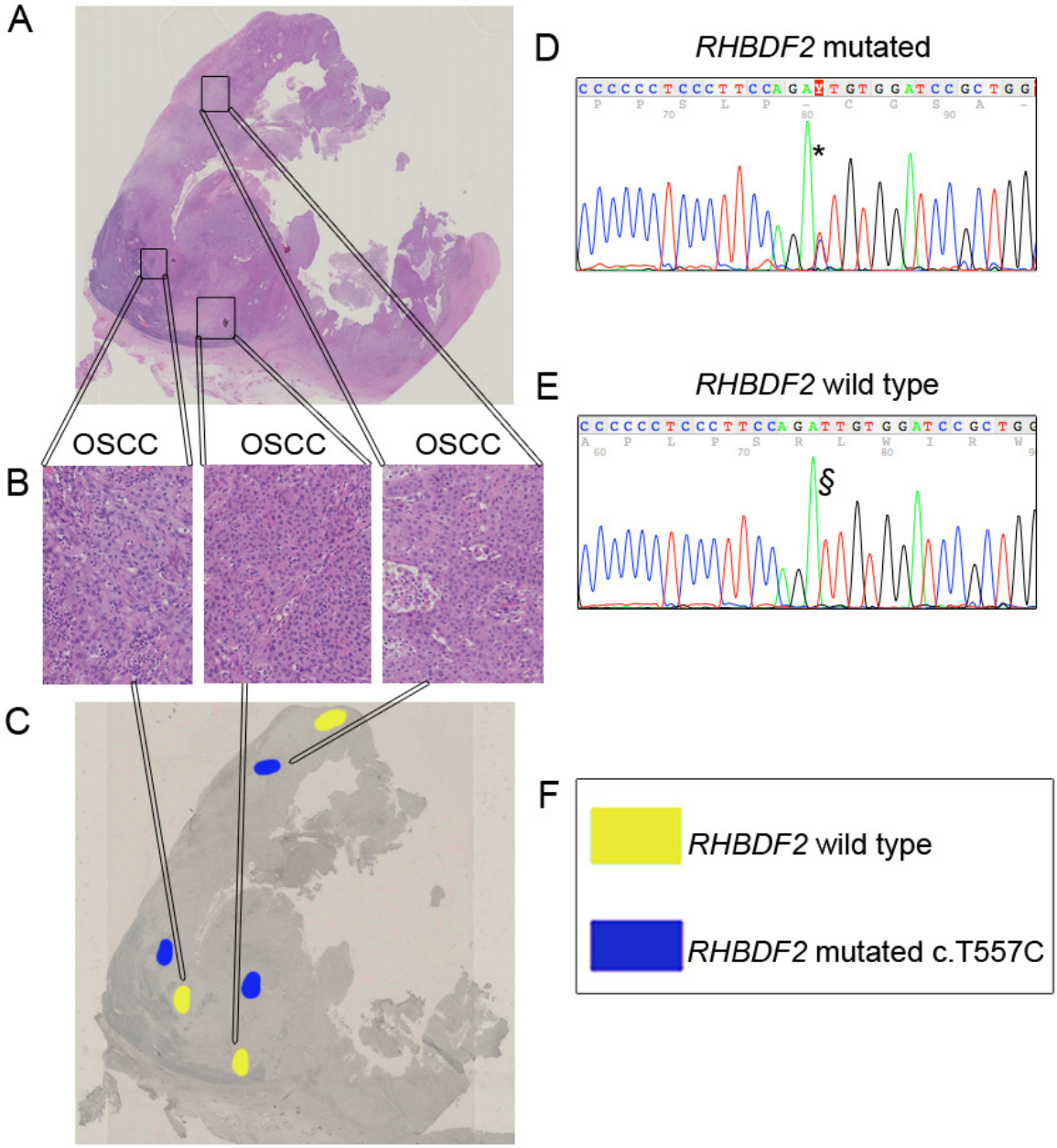

Figure 5.1. **The *RHBDF2* germline mutation was absent from areas of oesophageal squamous cell carcinoma from patient 2 indicating loss of heterozygosity of the mutated allele.** (A) A H&E of an entire section of oesophageal mucosa showing a poorly differentiated oesophageal squamous cell carcinoma (OSCC), tissue from patient 2, specimen block 2. (B) Higher power of highlighted areas showing three areas of OSCC. (C) Serial section showing post laser-capture microdissection (LCM). Yellow areas are *RHBDF2* WT whereas dark blue areas are positive for the *RHBDF2* mutation c.T557C. (D and E) Two representative traces showing the *RHBDF2* mutation c.T557C (D), an *RHBDF2* WT trace (E). (F) Key for patient 2 on post LCM section.

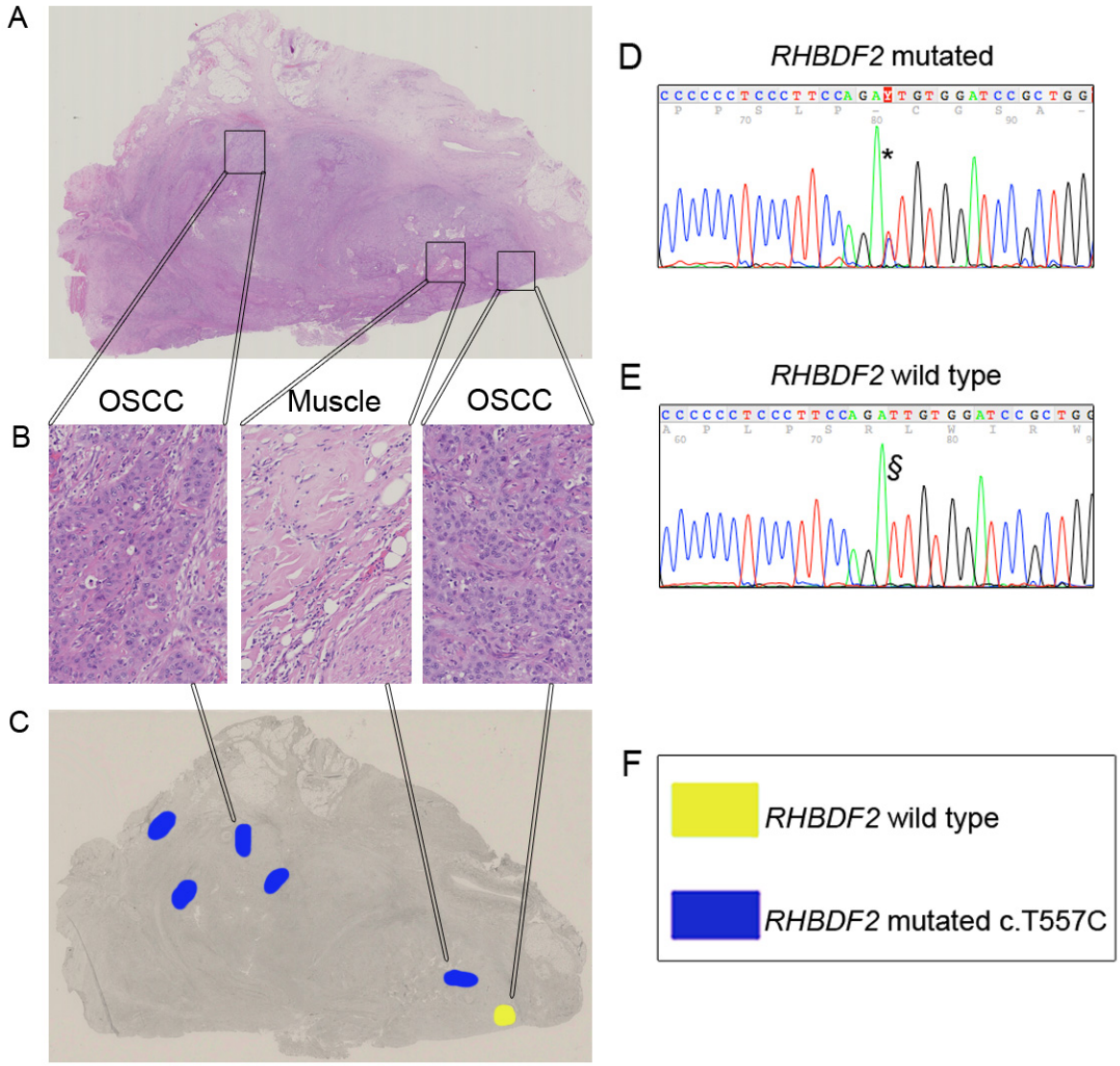

Figure 5.2. **The *RHBDF2* germline mutation was absent from areas of oesophageal squamous cell carcinoma from patient 2 indicating loss of heterozygosity of the mutated allele.** (A) A H&E of an entire section of oesophageal mucosa showing a poorly differentiated oesophageal squamous cell carcinoma (OSCC), tissue from patient 2, specimen block 3. (B) Higher power of highlighted areas showing from left to right an area of OSCC, a muscle area and another area of OSCC. (C) Serial section showing post laser-capture microdissection (LCM). Yellow areas are *RHBDF2* WT whereas dark blue areas are positive for the *RHBDF2* mutation c.T557C. (D and E) Two representative traces showing the *RHBDF2* mutation c.T557C (D), an *RHBDF2* WT trace (E). (F) Key for patient 2 on post LCM section.

Table 5.3. **Association of the germline mutation with histology shows that the *RHBDF2* mutation was absent from areas of oesophageal squamous cell carcinoma from patient 2 indicating loss of heterozygosity of the mutated allele.** These tables correspond to the laser-capture microdissection data presented in Figure 5.1 (A) and 5.2 (B), tissue from patient 2, specimen blocks 2 and 3 respectively. WT, wild type.

A

Patient 2:2	Histology	*RHBDF2*
1	OSCC	WT
2	OSCC	MUTATED
3	OSCC	WT
4	OSCC	MUTATED
5	OSCC	MUTATED
6	OSCC	WT

B

Patient 2:3	Histology	*RHBDF2*
1	OSCC	MUTATED
2	OSCC	MUTATED
3	OSCC	MUTATED
4	OSCC	WT
5	OSCC	MUTATED
6	Muscle	MUTATED

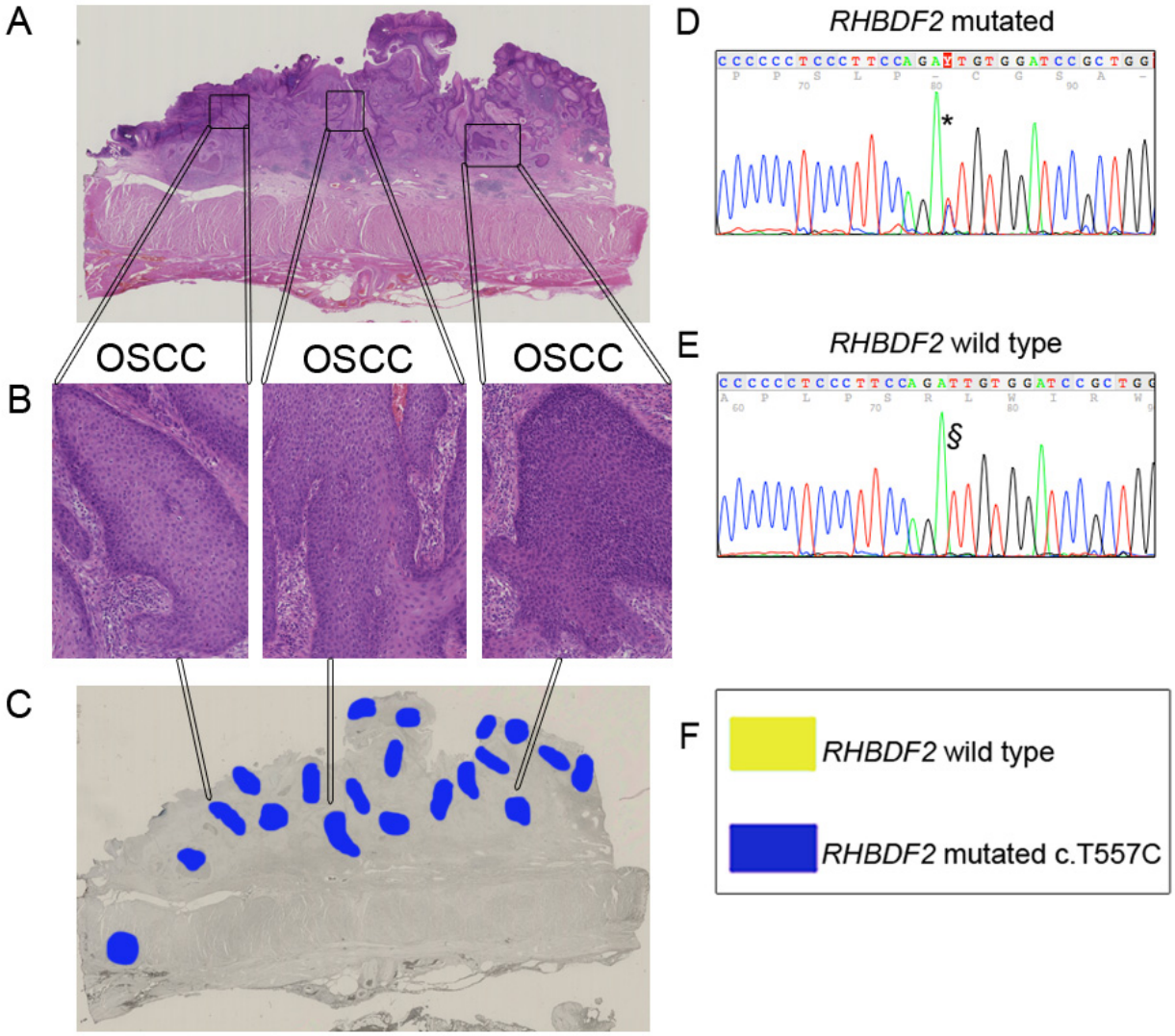

Figure 5.3. **The *RHBDF2* germline mutation was present in all areas of oesophageal squamous cell carcinoma from patient 33 indicating there is no loss of heterozygosity of the mutated allele.** (A) A H&E of an entire section of oesophageal mucosa showing a specimen with oesophageal squamous cell carcinoma (OSCC), tissue from patient 33. (B) Higher power of highlighted areas showing three areas of OSCC. (C) Serial section showing post laser-capture microdissection (LCM). Yellow areas are *RHBDF2* WT whereas dark blue areas are positive for the *RHBDF2* mutation c.T557C. (D and E) Two representative traces showing the *RHBDF2* mutation c.T557C (D), an *RHBDF2* WT trace (E). (F) Key for patient 33 on post LCM section.

Table 5.4. **Association of the germline mutation with histology shows that the *RHBDF2* mutation was present in all areas of oesophageal squamous cell carcinoma from patient 33 indicating there is no loss of heterozygosity of the mutated allele.** This table corresponds to the laser-capture microdissection data presented in Figure 5.3, tissue from patient 33.

Patient 33	Histology	*RHBDF2*
1	OSCC	MUTATED
2	OSCC	MUTATED
3	OSCC	MUTATED
4	OSCC	MUTATED
5	OSCC	MUTATED
6	OSCC	MUTATED
7	OSCC	MUTATED
8	OSCC	MUTATED
9	Dysplasia	MUTATED
10	Dysplasia	MUTATED
11	OSCC	MUTATED
12	OSCC	MUTATED
13	OSCC	MUTATED
14	OSCC	MUTATED
15	OSCC	MUTATED
16	OSCC	MUTATED
17	OSCC	MUTATED
18	OSCC	MUTATED
19	OSCC	MUTATED
20	Muscle	MUTATED

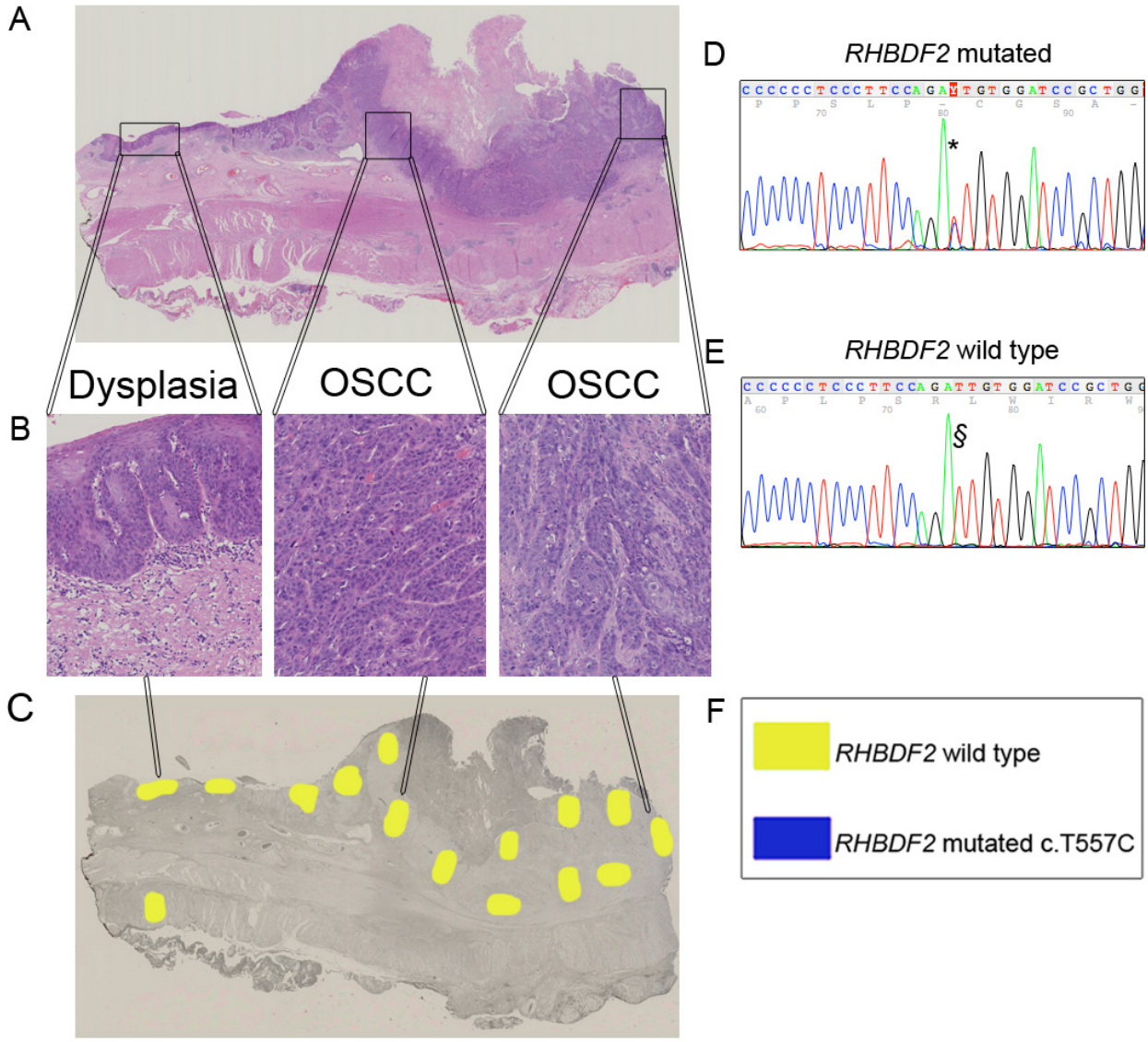

Figure 5.4. **The *RHBDF2* germline mutation was absent from oesophageal squamous cell carcinoma, dysplasia or muscle epithelium obtained from patient 34 indicating loss of heterozygosity of the mutated allele.** (A) A H&E of an entire section of oesophageal mucosa from patient 34 showing a poorly differentiated oesophageal squamous cell carcinoma (OSCC) and areas of dysplastic tissue. (B) Higher power of highlighted areas showing from left to right an area of dysplasia and two areas of OSCC. (C) Serial section showing post laser-capture microdissection (LCM). Yellow areas are *RHBDF2* WT whereas dark blue areas are positive for the *RHBDF2* mutation c.T557C. (D and E) Two representative traces showing the *RHBDF2* mutation c.T557C (D), an *RHBDF2* WT trace (E). (F) Key for patient 34 on post LCM section.

Table 5.5. **Association of the germline mutation with histology shows that the *RHBDF2* mutation was absent from oesophageal squamous cell carcinoma, dysplasia or muscle epithelium obtained from patient 34 indicating loss of heterozygosity of the mutated allele.** This table corresponds to the laser-capture microdissection data presented in Figure 5.4, tissue from patient 34. WT, wild type.

Patient 34	Histology	*RHBDF2*
1	OSCC	WT
2	OSCC	WT
3	OSCC	WT
4	OSCC	WT
5	OSCC	WT
6	OSCC	WT
7	OSCC	WT
8	OSCC	WT
9	OSCC	WT
10	OSCC	WT
11	Dysplasia	WT
12	Dysplasia	WT
13	Dysplasia	WT
14	Dysplasia	WT
15	Muscle	WT

A

B

Patient 33	
D17S515	+
D17S929	+
D17S1864	+
D17S1839	+
D17S1603	+
D17S785	+
D17S801	+
D17S1790	+

C

Patient 34	
D17S515	+
D17S929	Loss WT allele
D17S1864	Loss MUT allele
D17S1839	+
D17S1603	Loss MUT allele
D17S785	Loss WT allele
D17S801	+
D17S1790	Loss WT allele

Figure 5.5. **Single-nucleotide polymorphism analysis reveals genetic instability in patient 34 but not in patient 33.** (A) Schematic representation of the location of the microsatellites used for single-nucleotide polymorphism (SNP) analysis for chromosome 17, seen in tables B and C. (B-C) These tables correspond to the SNP analysis performed on patients 33 (B) and 34 (C) using blood or adjacent normal tissue and frozen tumour tissue by pyrosequencing as given in (*163*). WT, wild type; MUT, mutated; +, both alleles are present in chromosome 17; Loss of mutated and WT allele analysed by SNP analysis. This work was carried out by Dr J. Risk, Dr A.Ellis and Dr J.K Field at the Department of Molecular & Clinical Cancer Medicine, Institute of Translational Medicine.

Investigating RHBDF2 and ADAM17 expression in sporadic and tylotic oesophageal squamous cell carcinoma.

To study the role of *RHBDF2* and *ADAM17* in the pathogenesis of OSCC development, RHBDF2 and ADAM17 IHC was performed on patients presenting either sporadic oesophageal squamous cell dysplasia, OSCC or TOC. As no *RHBDF2* mutations were found in any of the sporadic OSCC patients (Table 5.1) patients 26 and 28 only, from the LCM study on clonal expansion in sporadic OSCC, were selected for IHC (Results Chapter 4). IHC was also performed on tissue from patients 33 and 34 that were part of the LCM study on clonality in TOC.

Even though RHBDF2 and ADAM17 primary antibodies were optimised several times in the pathology department, neither of the antibodies seemed very specific and they both showed a significant amount of background in all samples, which made the analysis extremely difficult. The staining revealed a cytoplasmic localisation of RHBDF2 and ADAM17 in both sporadic and tylotic OSCC, which could represent protein in the ER and the Golgi (Figure 5.6). Both RHBDF2 and ADAM17 showed a similar staining pattern in the OSCC from the different patients, being strong in the 2 to 3 basal cells along dysplastic areas and stronger in areas of OSCC. Nevertheless, the staining seemed much weaker and variable in tylotic associated OSCC (C, D, H and I) than in sporadic oesophageal squamous cell dysplasia and OSCC (M, N, R and S). Due to a lack of better antibodies, no final conclusions could be drawn on a higher expression

level of ADAM17 in TOC specimens, where there is an *RHBDF2* gain of function mutation, compared to sporadic specimens.

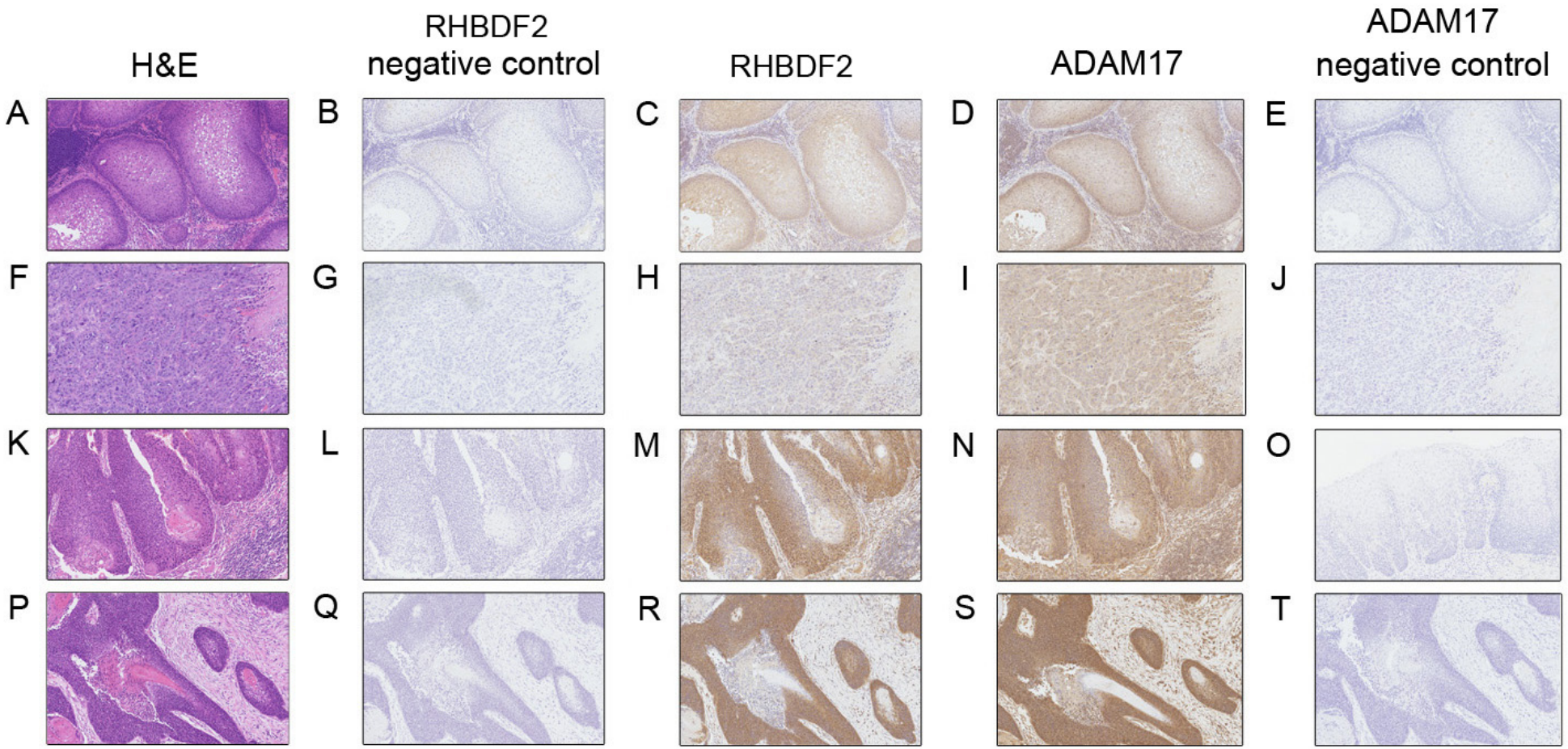

Figure 5.6. **Oesophageal squamous cell dysplasia and carcinoma show cytoplasmic RHBDF2 and ADAM17 expression.** Tylosis-associated oesophageal squamous cell carcinomas (OSCC) show weak and variable cytoplasmic staining for both RHBDF2 and ADAM17 (A-J). In contrast, sporadic OSCC shows strong cytoplasmic staining, again for RHBDF2 and ADAM17 (K-T). There was, however, a high background from both primary antibodies and no final conclusions could be drawn. High power (x10) images of patients 33 (A-E) and 34 (F-J) presenting tylosis associated oesophageal squamous cell carcinomas, patient 28 block 8 presenting sporadic oesophageal squamous cell dysplasia (K-O) and patient 26 block J presenting sporadic oesophageal squamous cell carcinoma (P-T). These include haematoxylin and eosin staining (H&E) (A, F, K and P); the RHBDF2 immunohistochemistry negative control for each patient (B, G, L and Q); RHBDF2 immunohistochemistry (C, H, M and R); ADAM17 immunohistochemistry (D, I, N and S); and the ADAM17 immunohistochemistry negative control for each patient (E, J, O, T).

6.3 Discussion

Both sporadic and tylotic OSCC were screened for the *RHBDF2* gain of function mutations that are known to be responsible for TOC (*163*). However, mutations were only found in the OSCCs from the three TOC patients in the screening, which are germline *RHBDF2* mutations. The other 30 patients with sporadic OSCC were all WT for *RHBDF2*. Hence, there are still no *RHBDF2* mutations reported in sporadic OSCC and mutation of the highly conserved N-terminal domain from *RHBDF2* does not seem crucial for OSCC development in sporadic cases. It is, of course, possible that *RHBDF2* mutations are present in the *RHBDF2* exons that were not sequenced in sporadic OSCC. However, no *RHBDF2* mutations have been reported from the exome sequencing studies published to date in a number of SCC tumour types (*233, 270*).

To study clonal expansion in TOC and determine if *RHBDF2* germline gain of function mutations persist during tumour progression in TOC, tissue from FFPE specimens provided by the three TOC patients were analysed by LCM. These specimens showed varied histology and included dysplasia and carcinoma. The data suggests that there is LOH of the mutated allele on chromosome 17q resulting in the loss of the germline mutation. We observed *RHBDF2* mutated and WT populations of cells in very poorly differentiated OSCC specimens from patient 2. These two populations of cells are within the same carcinoma confirming that LOH can occur during clonal expansion in tumour progression in TOC. Retrospective single-nucleotide polymorphism studies carried out on frozen surgical resections from OSCCs from patients 33 and 34 suggested that in the case of patient 34 LOH occurred on both chromosomes in regions of 17q25, including LOH of two markers in the

mutated allele (Figure 5.5 C). Moreover, DNA from frozen tumour resections also revealed a loss of the *RHBDF2* mutation. These findings were supported by the LCM study, as all patient 33 areas were *RHBDF2* mutated whereas all areas from patient 34 were WT. It can therefore be concluded from both previous studies and the LCM study presented here that, as Von Brevern and colleagues had observed in sporadic OSCC (*262*), OSCC from tylotic patients can also present high levels of LOH of microsatellite markers in the 17q region correspondent to *RHBDF2* during tumour progression.

To investigate the function of RHBDF2 and its relation to ADAM17 in both sporadic and tylotic OSCC, we performed IHC of both proteins in serial sections of two OSCC and two TOC patients. From the study of Blaydon and colleagues (*163*), we expected to find a cytoplasmic localisation of RHBDF2 in both sporadic and tylotic OSCC specimens. We also anticipated that if RHBDF2 facilitates the translocation of ADAM17 from the ER into the Golgi, then ADAM17 staining should be cytoplasmic, as per RHBDF2 (representing the ER and the Golgi), but would also be present in the cell membrane as ADAM17 is a cell surface membrane anchored protease (*243*). However, both primary antibodies stained blood vessels, blood cells, inflammatory cells and muscle even after two rounds of IHC optimisation in the pathology department. According to the analysis carried out with the help of the pathologists, it was concluded that due to the high background staining and the apparent unspecificity of the primary antibodies the staining could not be scored and quantified as previously planned. However, the best possible descriptive analysis of the staining given the circumstance suggested that both RHBDF2 and ADAM17 show a similar cytoplasmic staining pattern, which appeared weak and variable in the TOC samples; and stronger,

but still variable, in the sporadic OSCC samples. ADAM17 IHC did not appear membranous in any of the samples. The connection between a higher expression level of ADAM17 in TOC specimens, where there is an *RHBDF2* gain of function mutation, compared to sporadic specimens, could not be established.

Future work should consist of a quantifying study with new primary RHBDF2 and ADAM17 antibodies on tylotic and sporadic OSCC patients for which the mutation status of *RHBDF2* needs to be previously established. New primary antibodies would be necessary in order to assess the role of the EGFR signalling pathway in wound healing in tylotic patients (*163, 242, 247*).

In summary, it would appear that *RHDBF2* mutations are not crucial for OSCC development in sporadic cases. Clonal analysis of OSCC in tylotic patients has revealed that clonal expansion can lead to LOH of microsatellites in the region of 17q25, hence leading to a loss of the mutated allele of *RHBDF2*. This would fit the data from the LCM study on sporadic OSCC (Results Chapter 4), which suggested that OSCC is monoclonal in origin and that genetic heterogeneity arises through clonal evolution (*88*), as was also observed in the study of clonal expansion in GA (Results Chapter 3). As the loss of the mutated allele of *RHBDF2* does not seem to stop cancer progression, the *RHBDF2* gain of function mutation might be required to initiate OSCC development in tylotic patients but may not be needed for cancer progression. Further studies on the molecular role of *RHBDF2* in combination with *ADAM17* will give more insight into the role of *RHBDF2* in the pathogenesis of OSCC development (*163, 242*).

6. Discussion

6.1 Summary of findings

The somatic mutation theory of carcinogenesis has provided a framework for some of the most important advances in 20th century translational oncology. This theory proposes that tumour clonality is the result of sequential mutations of the progeny of a single stem cell (*271*). Previously, genetic studies have analysed large areas of tissue or biopsies, but could not rule out the presence of other clones or subclones, since the large number of cells used for DNA isolation could mask genetic heterogeneity. Recent improvements based on laser microdissection and isolation of pre-neoplastic and tumour tissue have permitted the work in this thesis and allowed an exploration of clonality and mutation burden, but at a much higher resolution than previously possible in the carcinomas studied here. Implementation of these new technologies has resulted in clonality studies becoming an essential tool for investigations in tumour biology. Here I present a study involving different carcinoma aetiologies and different areas of the gastrointestinal tract; this has afforded some comparison of carcinogenic processes in gastrointestinal malignancies.

Previous publications had linked large fields of IM in the human stomach to a higher incidence of GA and had also observed the same genetic mutations in areas of IM and in the associated preneoplastic lesions present in follow-up biopsies (*153, 187, 193*). Moreover, findings from our laboratory proved that IM glands are clonal and expand by crypt fission (*71*). The results from this study on clonal origins of dysplasia from intestinal metaplasia show that dysplastic glands are also clonal as all glands within an

entire region of dysplasia contain a founder mutation (Figures 3.1, 3.2 and 3.4). Importantly the total percentage of mutated IM glands was very small (Table 3.2) (*72*), indicating that after the occurrence of a mutation in IM, cellular expansion can take place rapidly followed by the formation of dysplastic glands. Hence, large clonal lesions of dysplasia can arise from IM, which can be perceived as field cancerisation of the human stomach.

In order to find dysplastic lesions with mutations in the first project, and subsequently to study clonal expansion in GA, 23 patients specimens and 51 GA tumours, respectively, were screened for genes accounting for approximately 75% of all somatic mutations reported previously for GA in the COSMIC database (16/05/2013) (*256*). Even though our mutation frequencies were comparable to those from previous reports (*256*) (Figure 3.5), the low percentage of mutations found in these specimens indicated that the specific genetic events described by Correa and colleagues (*153*) in the stepwise progression towards GA does not fit with either of the LCM studies in the human stomach presented here (Figure 3.30).

The results from LCM of specimens from 6 patients presenting with GA suggested that during field cancerisation a mutation arises in IM followed by the development of dysplasia where subsequent mutations occur. Hence, clonal expansion within the dysplasia leads eventually to progression to an adenocarcinoma, and HGD and GA are clonal (Figure 3.19). Some of the GA specimens presented WT and mutated *TP53* populations with the same LOH pattern, indicating that a founder mutation in an unknown gene must have taken place previous to the LOH. Therefore, these two

populations are clonal and have evolved through clonal evolution, as suggested in Nowell's model of clonal evolution (*88*).

The observation of field cancerisation in the human stomach in GA suggests that a similar event may also occur in HDGC. However, no *TP53* mutations were found in the LCM study carried out in 5 patients presenting with HDGC. This data suggested that field cancerisation might be due to events such as promoter methylation of the WT *CDH1* allele in HDGC, as it is thought to be the second hit mutation in over 50% of diffuse gastric carcinoma cases (*257*). The immunohistochemistry results for E-cadherin in these patients revealed some signet ring areas positive for E-cadherin, even though the AB-PAS production was the same as that of E-cadherin negative areas and the negative control showed no background staining. However, as normal membranous staining has been observed in *CDH1* methylated cells, the faint positive staining is most likely due to the low sensitivity of the immunohistochemical staining in detecting subpopulations of cells with gene methylation and hence downregulation of E-cadherin.

In order to carry out a similar study to that of GA on clonal expansion in OSCC, a mutation screen was performed on 33 sporadic and tylotic OSCC tumours for genes accounting for approximately over 70% of all somatic mutations previously reported for OSCC in the COSMIC database (16/05/2013) (*256*). After using the Bonferroni adjustment for multiple testing all mutation frequencies obtained were comparable to previous reports (*256*), a low number of tumours presented identifiable mutations. This absence of mutations in a large proportion of our OSCC cohort could indicate that other mutational events in genes not present in the screening occur at a much

higher frequency in OSCC than reported previously. However, when both sporadic and tylotic OSCC specimens were screened for the *RHBDF2* gain of function mutations that are known to be responsible for TOC (*163*), mutations were only found in the OSCCs from the three TOC patients in the screening. Therefore, *RHBDF2* mutations do not seem to be crucial for OSCC development in sporadic cases.

To study clonal expansion in OSCC, as done previously on GA specimens, LCM was carried out on tumour specimens from 3 patients presenting with OSCC. The results show that field cancerisation seems to have occurred in a pre-neoplastic area, followed by the development of OSCD where subsequent mutations occur and leading eventually to OSCC. The LCM data shows that this process occurs via clonal evolution (Figure 4.9), and therefore that OSCD and OSCC are clonal. Hence, these findings are in agreement with those on the clonal origins of GA.

Finally, to study clonal expansion in TOC and determine if *RHBDF2* germline gain of function mutations persist during tumour progression in TOC, three TOC patients were analysed by LCM. The data shows both WT and mutated *RHBDF2* populations in some TOC specimens, suggesting that, during tumour progression and clonal evolution, OSCC from tylotic patients can also show high levels of LOH of microsatellite markers in the 17q region correspondent to *RHBDF2* (*262*). Therefore, there is also a clonal evolution process in tylotic associated OSCC. After analysing the ADAM17 and RHBDF2 immunohistochemistry staining in tylotic and sporadic OSCC specimens, ADAM17 levels did not appear higher in tylotic specimens, where there is an *RHBDF2* germline gain of function mutation.

6.2 Polyclonality, monoclonality and intratumour heterogeneity

In 1976, Peter Nowell postulated the clonal evolution model of cancer where tumours were described to originate from a single cell (*88*). This model applied evolutionary theories to understand tumour growth and treatment failure, as well as the increased tumour aggressiveness that occurs during the advanced stages of most solid tumours. Nowell proposed that the originating mutated clone acquired further mutations as a result of genetic instability and eventually led to a tumour composed of subclones with a higher selective advantage to that of the original tumour-initiating clone.

Tumour morphologic heterogeneity was first observed by David Von Hansemann, in 1890, describing that the first change occurring in cancer is an alteration of the hereditary material of a normal cell at the site where the cancerous process begins (*272*). Recent publications using whole exome sequencing of clear cell renal tumours have revealed a striking inter-tumour heterogeneity in patients with kidney cancer as additional candidate cancer genes have now been identified (*273-276*). This represents an obvious limitation to a homogenous approach in systemic therapy in cancer patients. The recent use of whole-genome sequencing in tumour biopsies in spatial and temporal studies have provided increasing evidence for intratumour heterogeneity (ITH). Examples include studies in breast cancer by Navin and colleagues that used flow-sorted nuclei, whole genome amplification and next generation sequencing or Sector-Ploidy-Profiling. The acquired data indicated that tumours grow by punctuated clonal expansions with few persistent intermediates and it has been used to study new potential pathways of cancer progression. It has also provided information on the

differences in tumour growth organisation in monogenomic and polygenomic tumours (*277, 278*).

Linear models of tumour evolution with sequentially ordered somatic mutations in driver genes followed by clonal sweeps of homogeneous tumour cell expansion seem insufficient to justify the presence of ITH within a primary tumour, and also within metastatic tumour sites (*279*). Therefore, it appears that branched evolutionary tumour growth contributes to ITH. In a tree structure of tumour evolution, an initiating mutation driving tumour growth would occur in the "trunk" of the tumour and most likely be present ubiquitously in all sites of the tumour. Subsequently, later somatic events would appear following the branched separation of subclones and would hereby provide ITH.

The results presented in this thesis suggest that both GA and OSCC have a clonal origin and that they both acquire genetic heterogeneity as the tumours evolve. They also show that tylotic OSCC can present LOH of the chromosome 17q region, responsible for the tylosis *RHBDF2* germline mutation, during tumour progression. Therefore, this data subscribes to the Nowell clonal evolution model of cancer and also supports the increasing evidence that tumours show ITH as the subclones emerge.

Studies on Crohn's disease patients by Galandiuk and colleagues produced similar findings to those reported here (*64*). They detected a mutation within non-tumour tissue that was also found in the presenting tumour, suggesting a clonal relationship between the tumour and the surrounding pre-neoplastic mucosa due to field cancerisation. Nevertheless, these results differ from those obtained from the clonal

origin of Barrett's lesions (*157*), where Leedham and colleagues observed that Barrett's glands were a mosaic of multiple genetically distinct independent clones. These observations are also in contrast to the findings in colorectal microadenomas (*16*), where clonal analysis on a crypt-by-crypt basis suggested that colorectal adenomas can be polyclonal and that clonal evolution takes place throughout adenoma development.

Overall, it would appear that different underlying pre-neoplastic conditions, such as FAP (*16*) or Crohn's (*64*), lead to different modes of clonal evolution. Nevertheless, it is evident that ITH is present throughout the carcinomas mentioned herein and that clonal studies will provide further insight into the dynamics of tumour growth.

6.3 Limitations of the work presented in this thesis

The work presented here was all performed on formalin-fixed paraffin embedded (FFPE) archival tissue. FFPE was preferable in these studies because patient's tissues needed to be collected retrospectively: germline mutations such as *RHBDF2* and *CDH1* needed to be assessed first in the case of TOC and HDGC patients; and the proper orientation in the specimens was necessary to assess the spatial distribution of IM, HGD, GA, HDGC, OSCD and OSCC by LCM for clonal ordering studies. However, the use of FFPE tissue presents major methodological disadvantages that contribute to the limitations of this work. The major limitations are as follows:

1. The small amounts of partially degraded DNA obtained by LCM from FFPE required nested PCR in order to allow the identification of mutations via PCR-sequencing. The

risk of contamination from both unintentionally dissected tissue and artefactual was high, but these were significantly reduced by careful use of LCM and by the use of several negative controls in every PCR reaction. Therefore, whilst risk of contamination was reduced to a minimum, the small amount of available lysate for each sample was a great limitation for this work particularly when either duplication of sequencing or multiple mutated genes were sequenced to verify findings.

2. Data showing genetic alterations encompassed with microsatellite marker analysis of LOH increase greatly the significance of the findings. However, the small amount of DNA obtained from LCM as well as the lack of informative markers in control tissue for some of the patients restricted considerably the application of MS markers and limited mainly the amount of duplication possible.

3. In order to study the clonal origins of the different carcinomas presented here it was important to have identified the founding mutation in the tissue. Even though all HGD, GA, OSCD and sporadic and tylotic OSCC specimens were individually screened for genes accounting for 70-75% of all somatic mutations previously reported for these carcinomas, a low percentage of patients presented with single identifiable functional mutations and a very low percentage (1.96% in GA specimens and 6.06% in OSCC specimens) presented with two functional mutations. The lack of hotspots in other genes related to these carcinomas, such as *ARID1A* and *FAT4* for GA, and LOH, methylation changes and reduced expression, in genes such as $p15^{INK4b}$ and *CDKN2A*, *Rb*, *cyclin D1* and *Notch1* amongst others for OSCC, means that other more advanced sequencing and expression techniques should be used in this type of study; a number were not available at the start of this project or were too expensive to be considered.

Moreover, the specific genetic events described by Correa and colleagues (*153*) in the stepwise progression towards GA did not fit with either of our LCM studies in the human stomach and the data showed mutated and WT *TP53* populations presenting the same LOH signature in GA. Therefore, this data suggests that founding mutations occurring in IM in the human stomach and in gastritis or OSCD in the human oesophagus were possibly missed in this study. However the work of this thesis was a clonality assay, re-assessing previous publications but using a higher resolution of microdissection and a complete screening of most of the known mutated genes in the individual specimens that were collected.

4. The limited number of antibodies available for RHBDF2 and ADAM17 meant that the data obtained from the immunohistochemistry studies performed in sporadic and tylotic OSCC was very poor. Unfortunately, no definite correlation will be established between sporadic and tylotic carcinomas and between the function of *RHBDF2* and *ADAM17* until better molecular tools are in the market.

6.4. Future directions

This work has raised a number of important questions providing the basis for a great deal of further investigation. This section will briefly explore potential future directions:

1. The genes involved in the stepwise progression towards GA (Chapter 3) and towards OSCC (Chapter 4): The use of more advanced deep-sequencing technologies in these samples such as whole-genome sequencing in the dysplasia and carcinoma specimens

would provide further insight into the tree structure of tumour growth of GA and OSCC and would probably allow a re-evaluation of the work presented here.

2. Clonal analysis of IM, HGD, GA, OSCD and sporadic and tylotic OSCC (Chapters 3, 4 and 5): Performing SNP arrays on the LCM samples of different histology following the progression to both carcinomas in the same patients would improve considerably the knowledge of clonal analysis in both GA and OSCC. The tree structure of the carcinoma specimens analysed in this thesis would be much more complete and the study of the clones and subclones present would provide more insight into ITH in the cancers of the gastrointestinal tract.

3. Clonal analysis of HDGC (Chapter 3.3): Performing deep-sequencing in the LCM areas of HDGC and bisulfite sequencing of *CDH1* would clarify if the methylation of *CDH1* is the second hit mutation for the formation of signet ring cells in HDGC in only 50% of the cases and would also highlight the presence of clones and subclones in the progression of HDGC.

4. The relationship between ADAM17 and RHBDF2 (Chapter 5): Further studies using cell cultures and western blotting are currently assessing the individual function of RHBDF2 and ADAM17. Moreover, studies using fresh-frozen tissue have been able to localise RHBDF2 *in vivo* in the oesophagus and in the skin (*163*). Therefore, once better antibodies are available we will be able to assess the relationship *in vivo* retrospectively using FFPE tissue.

6.5. Final conclusions

The work presented in this thesis has improved the resolution of the study of clonality by using somatic gene mutations to analyse the clonality of gastrointestinal pre-neoplastic and neoplastic lesions in the human oesophagus and human stomach. The data presented here has made evident that different underlying inflammatory and pre-neoplastic conditions lead to different modes of clonal evolution, as seen in the colon in FAP (*16*) and Crohn's (*64*) patients and as seen in the oesophagus in Barrett's oesophagus (*157*) and here in OSCD and OSCC. This work has also highlighted that the different organs of origin and the aetiology of the carcinomas mean that different genes are involved in the progression to distinct tumours types. Moreover, the data from the screenings of GA and OSCC has proved that inter-tumour heterogeneity occurs in the gastrointestinal tract as the tumour specimens analysed did not show a cohesive genetic signature, as for example Correa and colleagues had suggested (*153*).

The somatic mutation theory of carcinogenesis seems to hold true for both the progression to GA and OSCC, as both carcinomas seem to evolve from a single mutated stem cell and acquire genetic heterogeneity as the tumours evolve. The mechanism does not currently fit all clonality studies. However, it is possible that future deep-sequencing results will bring into light founder mutations in genes still not known to be involved in certain malignant pathways and that may be crucial during field cancerisation. It is also possible that clonal interaction, cooperation or competition may play an important role in the development of certain pre-malignant conditions and carcinomas, and promote the concept of carcinogenesis as an evolutionary process (*280*).

This study has approached many questions surrounding carcinomas of the human oesophagus and stomach and has contributed significantly to the debate on gastrointestinal carcinogenesis. Increasing evidence of ITH only highlights the need to investigate the primary tumour and metastatic subclones in order to provide a personalised treatment to each patient that would take into consideration the existing mutations and the subclones dynamics to avoid favouring treatment-resistant clones.

7. Appendix

Table 7.1. **Primers and reaction conditions for Genomic PCR sequencing**

Primer	Sequence 5' to 3'	Conditions
APC 1st 1F	GGACAAAGCAGTAAAACCGAAC	**55/1/0**
APC 1st 1R	AACTACATCTTGAAAAACATATTGGA	
APC 1st 2F	AAGTGGTCAGCCTCAAAAGG	**60/3/5**
APC 1st 2R	GCTATTTGCAGGGTATTAGCA	
APC 1st 3F	GATACTCCAATATGTTTTTCAAGATG	**55/1/0**
APC 1st 3R	GCCTGGCTGATTCTGAAGAT	
APC 1st 4F	CCCTGCAAATAGCAGAAATAAAA	**55/2/5**
APC 1st 4R	AACATGAGTGGGGTCTCCTG	
APC 1st 5F	CAGACTGCAGGGTTCTAGTTTATC	**60/2/0**
APC 1st 5R	CATTCCACTGCATGGTTCAC	
APC 1st 6F	CCAAAAGTGGTGCTCAGACA	**60/2/0**
APC 1st 6R	CATGGTTTGTCCAGGGCTAT	
APC 1st 7F	TTTGAGAGTCGTTCGATTGC	**60/1/0**
APC 1st 7R	TCTCTTTTCAGCAGTAGGTGCTT	
APC 1st 8F	CATGCAGTGGAATGGTAAGT	**55/2/0**
APC 1st 8R	GCAGCATTTACTGCAGCTT	
APC 1st 9F	CAAGCGAGAAGTACCTAAAAA	**55/2/0**
APC 1st 9R	TTCTGTATAAATGGCTCATCG	
APC 1st 10F	GGTTCTTCCAGATGCTGATA	**55/1/5**
APC 1st 10R	CTTGGTTTTCATTTGATTCTTT	
APC 1st 11F	AATTAAGAATAATGCCTCCAGT	**55/2/0**
APC 1st 11R	TTTACGTGATGACTTTGTTGG	
APC 1st 12F	CCAAGAGAAAGAGGCAGAAAAA	**55/1/5**
APC 1st 12R	TGATGGTAGAAGTTTGTACACAGG	
APC 2nd 1F	CAAGCAGTGAGAATACGTCCA	**55/1/0**
APC 2nd 1R	TTTCTTGGTTAATAGAAGAAACTTTGC	
APC 2nd 2F	GCCACTTGCAAAGTTTCTTCT	**55/2/5**
APC 2nd 2R	TGCTTCCTGTGTCGTCTGA	
APC 2nd 3F	CAGACGACACAGGAAGCAGA	**60/1/0**
APC 2nd 3R	TGGAACTTCGCTCACAGGAT	
APC 2nd 4F	GAAGATCCTGTGAGCGAAGTTCC	**60/1/0**
APC 2nd 4R	CAAGTCCTCTGGGGTGAGTA	
APC 2nd 5F	AGAATCAGCCAGGCACAAAG	**55/1/0**
APC 2nd 5R	GCAATCGAACGACTCTCAAA	
APC 2nd 6F	CACTATGTTCAGGAGACCCCA	**60/1/0**
APC 2nd 6R	TGGAAGATCACTGGGGCTTA	
APC 2nd 7F	GTGAACCATGCAGTGGAATG	**60/1/0**
APC 2nd 7R	ACTTCTCGCTTGGTTTGAGC	

Table 7.1. continued

Primer	Sequence 5' to 3'	Conditions
APC 2nd 8F	GCTTAGGTCCACTCTCTCTCTT	**60/1/0**
APC 2nd 8R	GGCATTATAAGCCCCAGT	
APC 2nd 9F	CCTAAAAATAAAGCACCTACTGCTG	**60/3/5**
APC 2nd 9R	CACTCAGGCTGGATGAACAA	
APC 2nd 10F	ACATTTTGCCACGGAAAGTA	**55/2/0**
APC 2nd 10R	GGCTGCTCTGATTCTGTTTC	
APC 2nd 11F	CAGGAAAATGACAATGGGAAT	**55/2/0**
APC 2nd 11R	TGGCATGGCAGAAATAATACA	
APC 2nd 12F	GGACCTATTAGATGATTCAGATGATG	**55/2/0**
APC 2nd 12R	ACTTGGTTTCCTTGCCACAG	
p53-5 1st F	CACTTGTGCCCTGACTTTCA	**55/1/5**
p53-5 1st R	GAGCAATCAGTGAGGAATCAGA	
p53-6 1st F	AGAGACGACAGGGCTGGTT	**60/2/5**
p53-6 1st R	TGGAGGGCCACTGACAAC	
p53-7 1st F	TGCTTGCCACAGGTCTCC	**60/1/5**
p53-7 1st R	GGTCAGAGGCAAGCAGAGG	
p53-8 1st F	TTTTTAAATGGGACAGGTAGGA	**60/2/5**
p53-8 1st R	CACCCTTGGTCTCCTCCAC	
p53-5 2nd F	TCTGTCTCCTTCCTCTTCCTACA	**60/1/5**
p53-5 2nd R	AACCAGCCCTGTCGTCTCT	
p53-6 2nd F	CAGGCCTCTGATTCCTCACT	**60/1/0**
p53-6 2nd R	CTTAACCCCTCCTCCCAGAG	
p53-7 2nd F	CTTGGGCCTGTGTTATCTCC	**60/1/5**
p53-7 2nd R	GTGTGCAGGGTGGCAAGT	
p53-8 2nd F	GCCTCTTGCTTCTCTTTTCC	**60/2/0**
p53-8 2nd R	GCTTCTTGTCCTGCTTGCTT	
p16-2A 1st F	GCTTCCTTTCCGTCATGC	**60/2/5**
p16-2A 1st R	CAGGTACCGTGCGACATC	
p16-2B 1st F	CTGTTCTCTCTGGCAGGTCA	**60/2/5**
p16-2B 1st R	TGTGCTGGAAAATGAATGCT	
p16-2A 2nd F	CCTGGCTCTGACCATTCTGT	**60/2/5**
p16-2A 2nd R	CAGCTCCTCAGCCAGGTC	
p16-2B 2nd F	CTTCCTGGACACGCTGGT	**60/2/5**
p16-2B 2nd R	TGGAAGCTCTCAGGGTACAAA	
Kras 1st F	GAGTTTGTATTAAAAGGTACTGGTGGA	**60/2/5**
Kras 1st R	ATCAAAGAATGGTCCTGCAC	
Kras 2nd F	TTTGATAGTGTATTAACCTTAT	**55/2/5**
Kras 2nd R	TATTAAAACAAGATTTACCTC	

Table 7.1. continued

Primer	Sequence 5' to 3'	Conditions
B-cat 1st F	CTTTTTAGTTCTCAAAACTGCA	**55/2.5/0**
B-cat 1st R	CAATGGGTCATATCACAGATTC	
B-cat 2nd F	CAATCTACTAATGCTAATACTG	**55/2.5/5**
B-cat 2nd R	GACTTTCAGTAAGGCAATGAAA	
NRF2 1F	CCACCATCAACAGTGGCATA	**60/2.5/5**
NRF2 1R	TGGGAGAAATTCACCTGTCTC	
NRF2 2F	CATGAGCTCTCTCCTTCCTTTT	**60/2.5/5**
NRF2 2R	TGGGAGAAATTCACCTGTCTC	

NOTE: Naming nomenclature is as follows: gene-exon, polymerase chain reaction round; primer direction. Large exons, consisting of more than 250 nucleotides, were subdivided into separate regions for amplification; a letter following the exon number denotes these regions (eg. p16-2A). For *APC* primers, the numbers do not refer to exons but identify regions of the mutation cluster region. Reaction condition nomenclature is annealing temperature/magnesium concentration (mmol/L)/addition of Q-solution. F: forward; R: reverse.

Table 7.2. **Primers and reaction conditions for Microsatellite Loss of Heterozygosity Analysis**

Primer	Sequence 5' to 3'	Conditions
Multiplex 2		**57/0**
D17S250 F	[FAM]GGAAGAATCAAATAGACAAT	
D17S250 R	GCTGGCCATATATATATTTAAACC	
D17S1832 F	[FAM]ACGCCTTGACATAGTTGC	
D17S1832 R	TGTGTGACTGTTCAGCCTC	
D18S474 F	[FAM]CTCCACCCACTAGATGTCAG	
D18S474 R	ACTTGCTTAAGCCTTGGACT	
D3S1313 F	[FAM]TACTTTCCTTCAGATCCTTGG	
D3S1313 R	AACTAGGGGCCATGAATAAG	
Multiplex 3		**57/0**
D17S1176 F	[FAM]ACTTCATATACATATCACGTGC	
D17S1176 R	TCAATGGAGAATTACGATAGTG	
D17S1678 F	[FAM]TTTGGGTCTTTGAACCCTTG	
D17S1678 R	CCACAACAAAACACCAGTGC	
D17S1881 F	[FAM]CCCAGTTTAAGGAGTTTGGC	
D17S1881 R	TAGGGCAGTCAGCCTTGTG	
Multiplex 4		**57/5**
D9S942 F	[FAM]GCAAGATTCCAAACAGTA	
D9S942 R	CTCATCCTGCGGAAACCATT	
D5S2001 F	[HEX]GCCAAGATGGTCTCGATCTC	
D5S2001 R	TCTGAACAGGTGATGGCAAC	
D17S1506E F	[FAM]TGTGGGATGGGGTGAGATTTC	
D17S1506E R	CTGTTGGTCGGTGGGTTG	
D5S489 F	[HEX]GGGCTTTTGTGTTGTTTCTA	
D5S489 R	GAAAACCCATAACCAGACTTG	

NOTE: Reaction condition nomenclature is annealing temperate/Q-solution used in reaction. Other conditions were performed according to manufacturer's instructions.

Table 7.3. **Summary of clinicopathological features in screened samples.** Gender, age and tumour site information from the screening of 51 gastric adenocarcinomas (GA) for mutations within genes accounting for 85% of known mutations (see COSMIC database) in GA (*256*). (--) stands for patient information not available.

SAMPLE	GENDER	AGE	TUMOUR SITE
1	M	52	GOJ
2	M	79	GOJ
3	M	67	Pyloric
4	F	80	Antrum
5	F	29	Body
6	F	85	Body
7	F	44	Body
8	M	69	Body
9	M	80	Antrum
10	M	48	Antrum
11	M	55	GOJ
12	M	64	Body
13	M	58	Fundus
14	M	45	Antral
15	M	81	Antral
16	F	48	Antral
17	M	76	Antral
18	M	69	Body
19	M	80	Pyloric
20	M	65	Body
21	F	72	Pyoric
22	F	45	Antrum
23	M	80	Body
24	F	69	GOJ
25	M	67	Body
26	M	66	GOJ
27	M	52	Body
28	F	63	GOJ
29	M	64	GOJ
30	M	85	GOJ

Table 7.3. continued

SAMPLE	GENDER	AGE	TUMOUR SITE
31	F	61	Antrum
32	M	48	Antrum
33	M	78	Body
34	F	77	Pyloric
35	M	65	GOJ
36	M	68	GOJ
37	M	60	Pyloric
38	M	71	Antrum
39	F	69	Body
40	F	84	Antrum
41	M	56	Body
42	M	56	GOJ
43	M	61	Body
44	M	77	Antrum
45	M	64	Antrum
46	F	45	Pyloric
47	M	51	Antrum
48	M	53	Distal stomach
49	M	66	Antrum
50	--	--	--
51	--	--	--

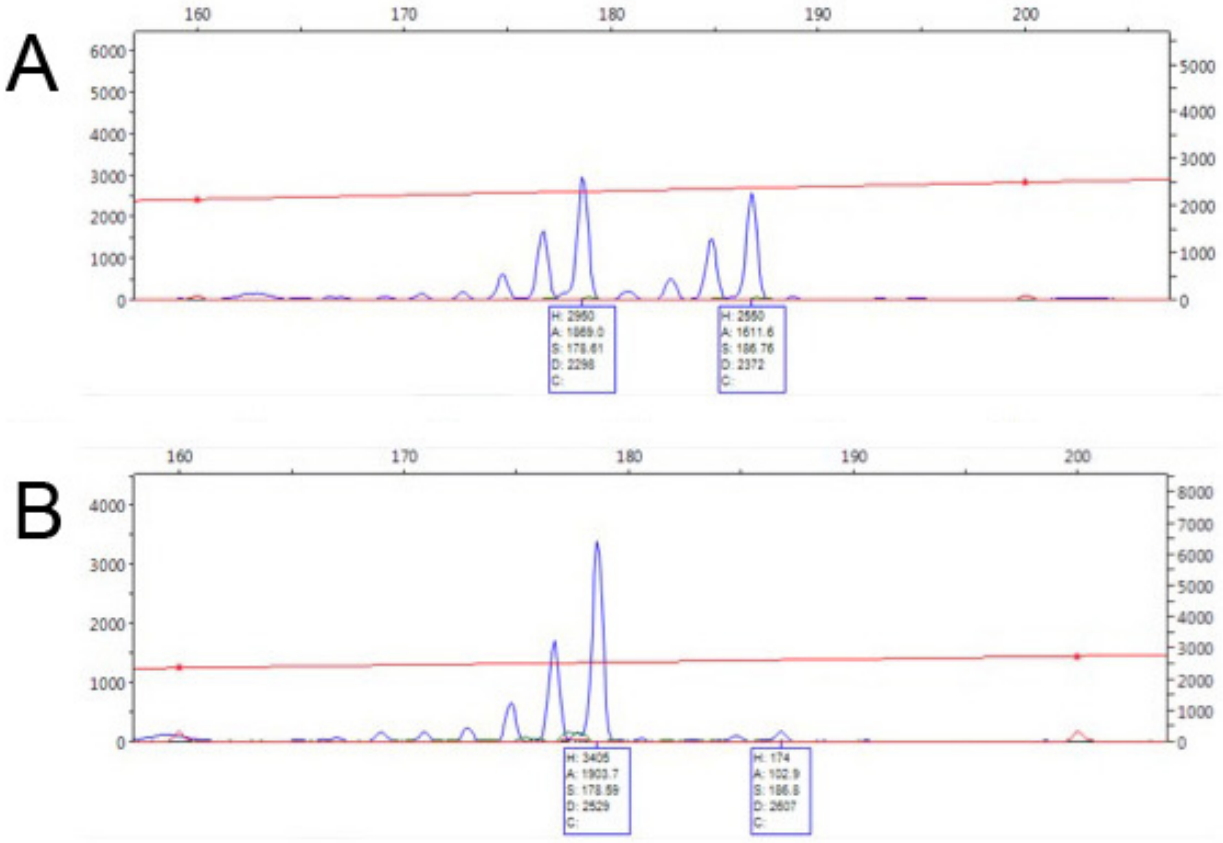

Figure 7.1. **Loss of heterozygosity of microsatellite marker D17S1832 was observed in patient 8.** Two traces (A and B) representative of 17p microsatellite marker D17S1832 from patient 8, specimen blocks 6, 7 and 8, corresponding to figures 3.6 to 3.9. (A) Representative trace of a control sample where both alleles are present; the values for the area under the control peaks are 1869.0 and 1611.6 respectively. (B) Representative trace where loss of heterozygosity (LOH) has occurred for marker D17S1832 (180bp); the values for the area under the sample peaks this example are 1903.7 and 102.9 respectively. LOH was calculated by measuring the area under the curve of the samples compared to that of a normalized control (gastritis or muscle epithelium areas from the same patient). LOH was considered when the area under the curve was <0.5 or >2.0.

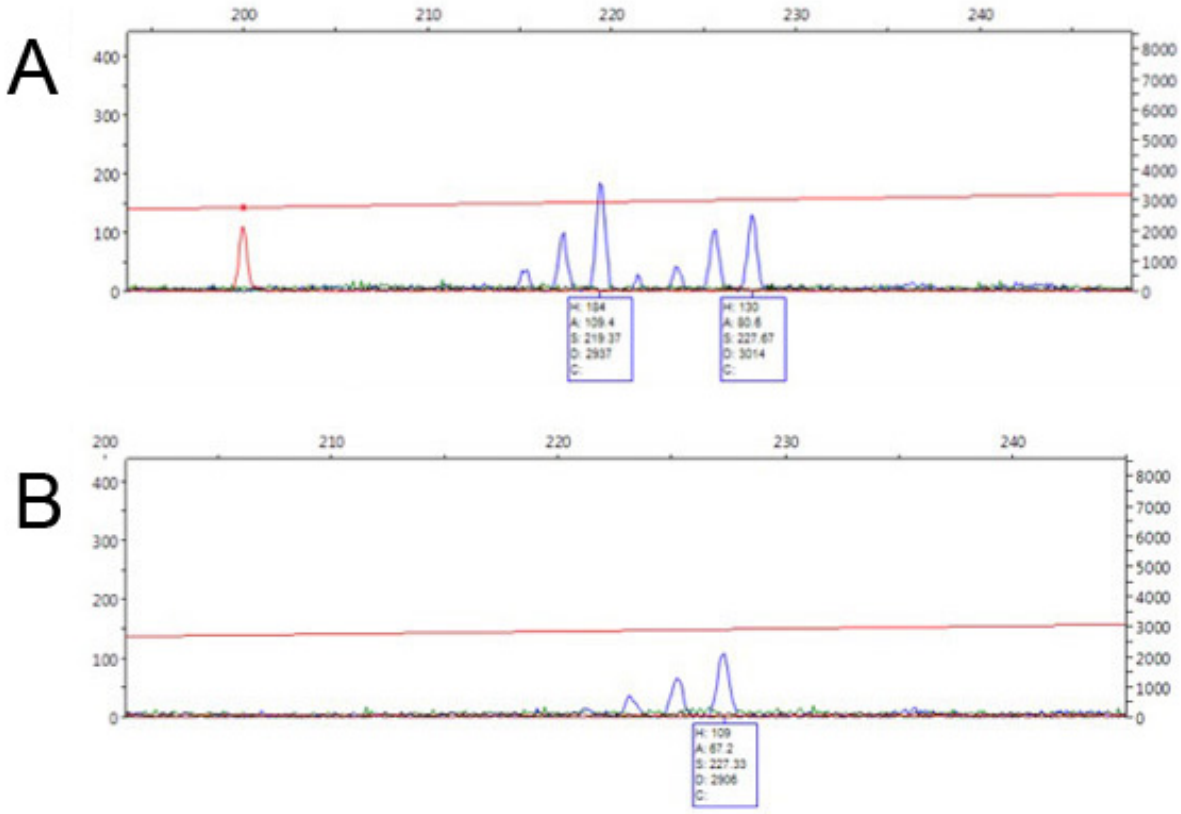

Figure 7.2**. Loss of heterozygosity of microsatellite marker D17S1881 was observed in patient 8.** Two traces (A and B) representative of 17p microsatellite marker D17S1881 from patient 8, specimen blocks 6, 7 and 8, corresponding to figures 3.6 to 3.9. (A) Representative trace of a control sample where both alleles are present; the values for the area under the control peaks are 109.4 and 80.6 respectively. (B) Representative trace where loss of heterozygosity (LOH) has occurred for marker D17S1881 (210bp) the values for the area under the sample peaks this example are 67.2 and 0 respectively. LOH was calculated by measuring the area under the curve of the samples compared to that of a normalized control (gastritis or muscle epithelium areas from the same patient). LOH was considered when the area under the curve was <0.5 or >2.0.

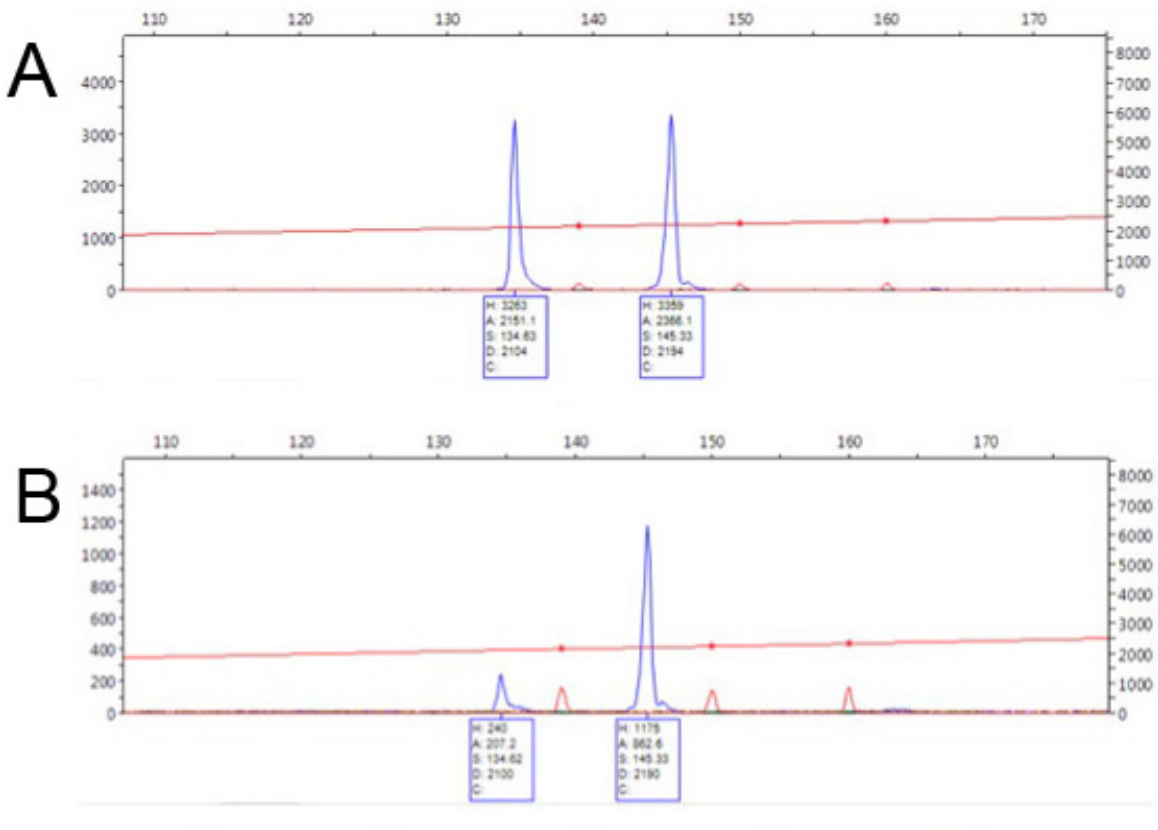

Figure 7.3**. Loss of heterozygosity of microsatellite marker D17S1506E was observed in patient 8.** Two traces (A and B) representative of 17p microsatellite marker D17S1506E from patient 8, specimen blocks 6, 7 and 8, corresponding to figures 3.6 to 3.9. (A) Representative trace of a control sample where both alleles are present; the values for the area under the control peaks are 2151.1 and 2366.1 respectively. (B) Representative trace where loss of heterozygosity (LOH) has occurred for marker D17S1506E (150bp); the values for the area under the sample peaks this example are 207.2 and 862.6 respectively. LOH was calculated by measuring the area under the curve of the samples compared to that of a normalized control (gastritis or muscle epithelium areas from the same patient). LOH was considered when the area under the curve was <0.5 or >2.0.

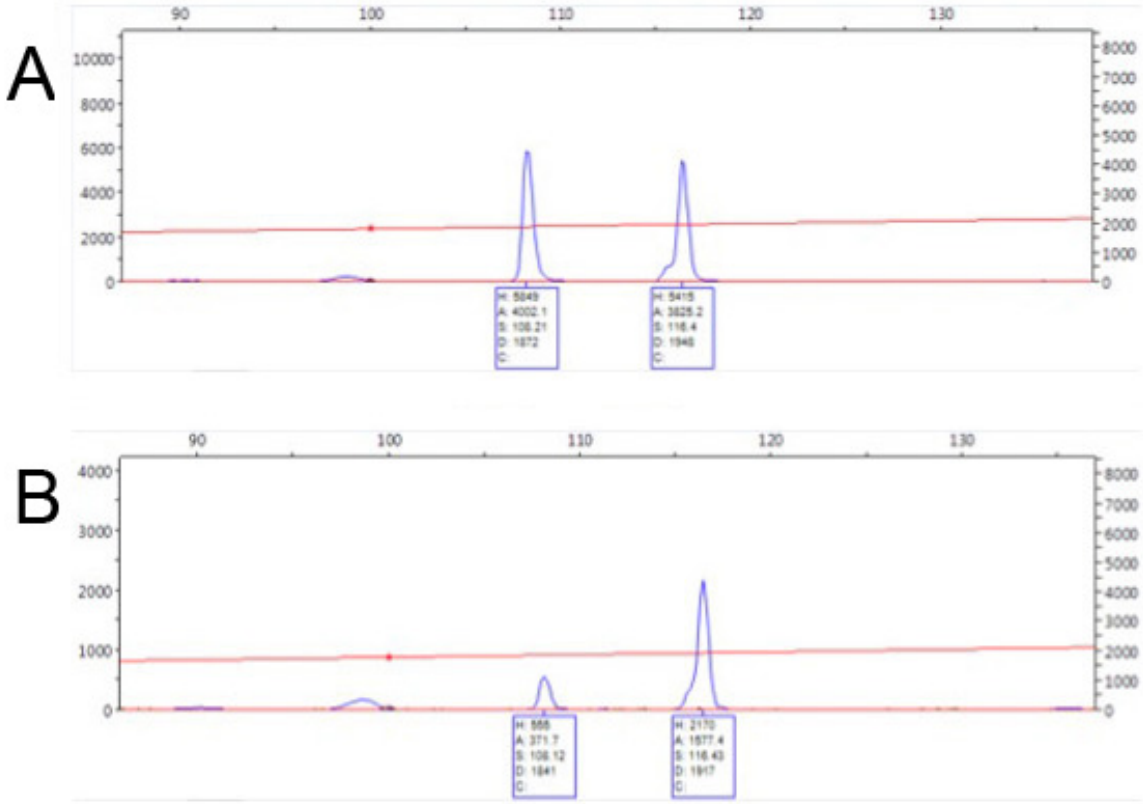

Figure 7.4**. Loss of heterozygosity of microsatellite marker D17S1678 was observed in patient 8.** Two traces (A and B) representative of 17p microsatellite marker D17S1678 from patient 8, specimen blocks 6, 7 and 8, corresponding to figures 3.6 to 3.9. (A) Representative trace of a control sample where both alleles are present; the values for the area under the control peaks are 4002.1 and 3825.2 respectively. (B) Representative trace where loss of heterozygosity (LOH) has occurred for marker D17S1678 (120bp); the values for the area under the sample peaks this example are 371.7 and 1577.4 respectively. LOH was calculated by measuring the area under the curve of the samples compared to that of a normalized control (gastritis or muscle epithelium areas from the same patient). LOH was considered when the area under the curve was <0.5 or >2.0.

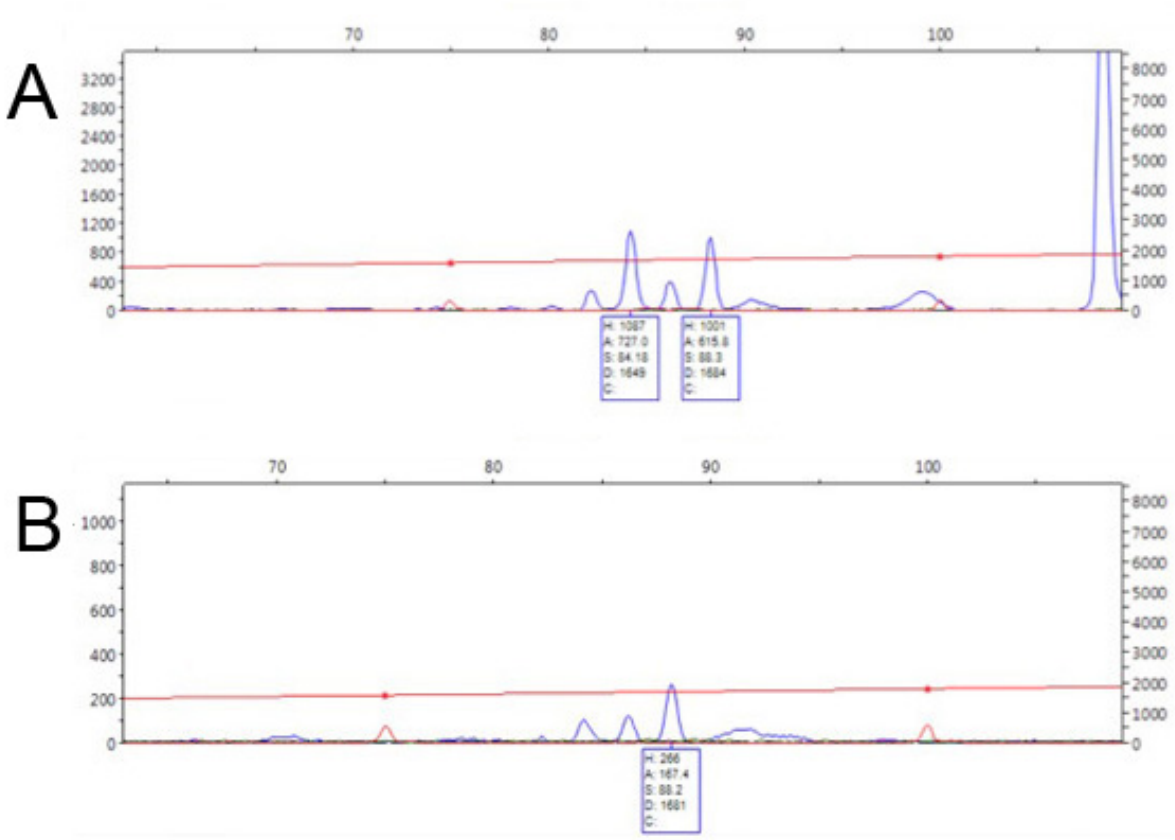

Figure 7.5. **Loss of heterozygosity of microsatellite marker D17S1176 was observed in patient 8.** Two traces (A and B) representative of 17p microsatellite marker D17S1176 from patient 8, specimen blocks 6, 7 and 8, corresponding to figures 3.6 to 3.9. (A) Representative trace of a control sample where both alleles are present; the values for the area under the control peaks are 727.0 and 615.8 respectively. (B) Representative trace where loss of heterozygosity (LOH) has occurred for marker D17S1176 (80bp); the values for the area under the sample peaks this example are 167.4 and 0 respectively. LOH was calculated by measuring the area under the curve of the samples compared to that of a normalized control (gastritis or muscle epithelium areas from the same patient). LOH was considered when the area under the curve was <0.5 or >2.0.

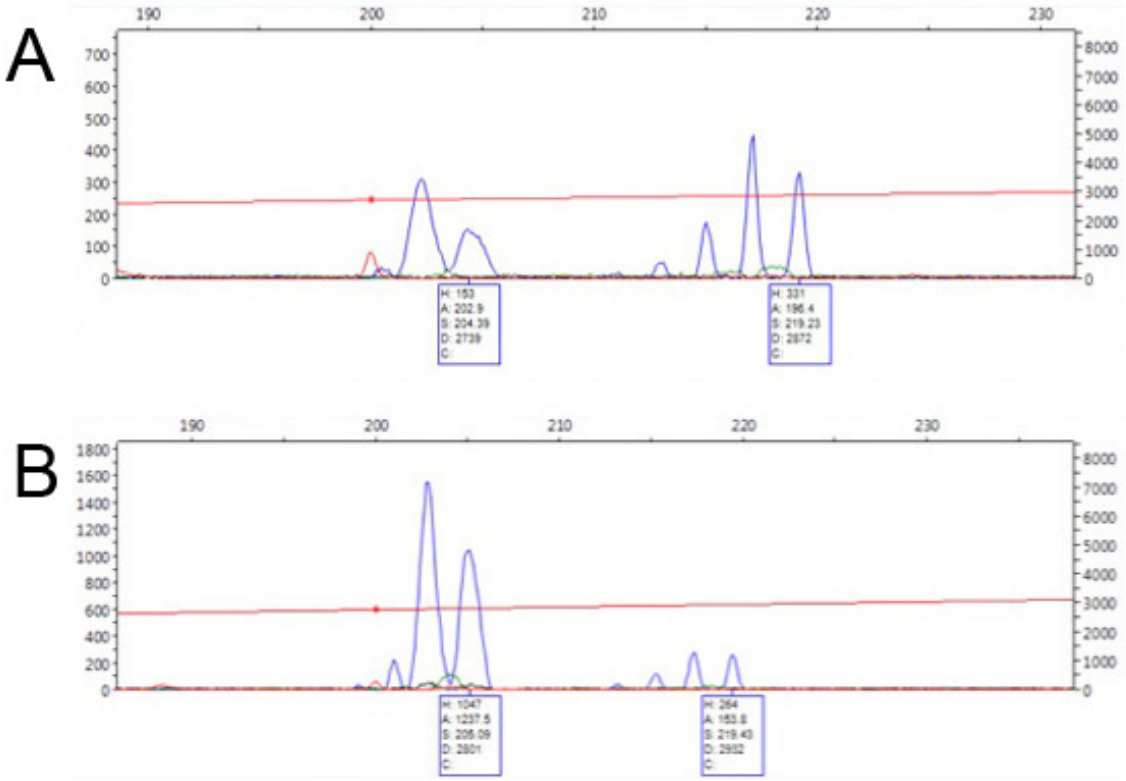

Figure 7.6**. Loss of heterozygosity of microsatellite marker D17S1881 was observed in patient 10.** Two traces (A and B) representative of 17p microsatellite marker D17S1881 from patient 10 corresponding to figures 3.10 and 3.11. (A) Representative trace of a control sample where both alleles are present; the values for the area under the control peaks are 202.9 and 196.4 respectively. (B) Representative trace where loss of heterozygosity (LOH) has occurred for marker D17S1881 (210bp); the values for the area under the sample peaks this example are 1237.5 and 153.8 respectively. LOH was calculated by measuring the area under the curve of the samples compared to that of a normalized control (gastritis or muscle epithelium areas from the same patient). LOH was considered when the area under the curve was <0.5 or >2.0.

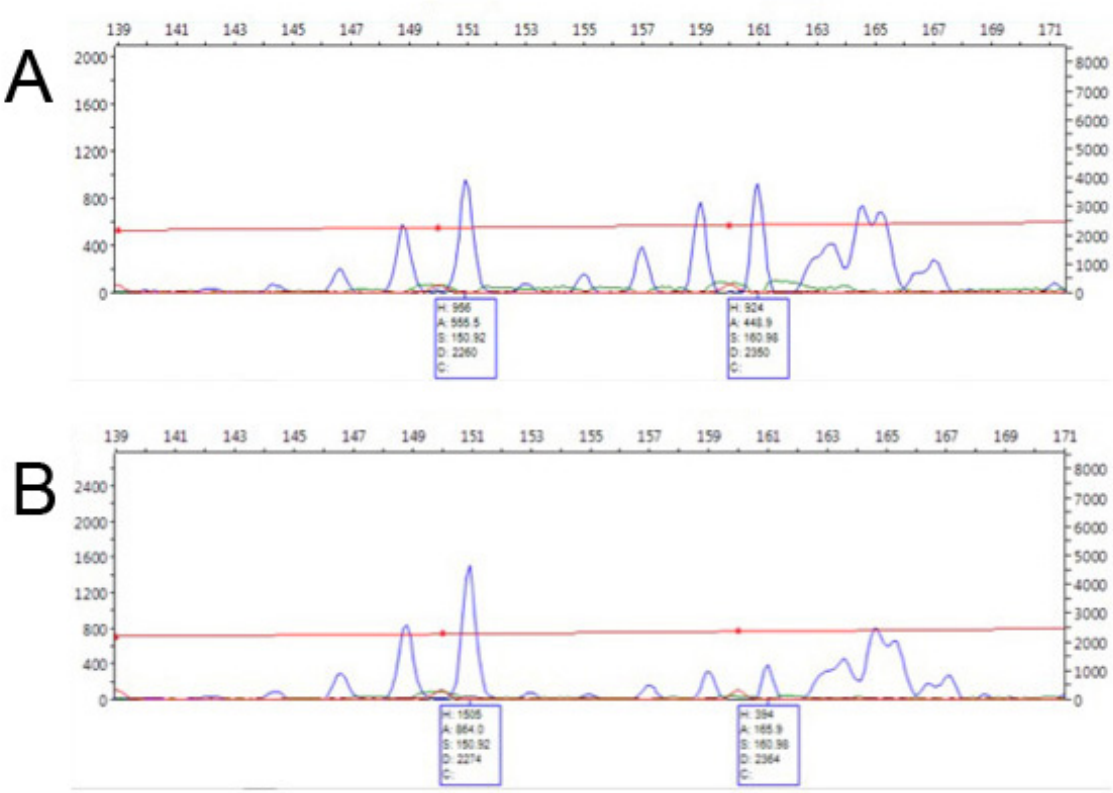

Figure 7.7**. Loss of heterozygosity of microsatellite marker D17S250 was observed in patient 10.** Two traces (A and B) representative of 17q microsatellite marker D17S250 from patient 10 corresponding to figures 3.10 and 3.11. (A) Representative trace of a control sample where both alleles are present; the values for the area under the control peaks are 202.9 and 196.4 respectively. (B) Representative trace where loss of heterozygosity (LOH) has occurred for marker D17S250 (140bp); the values for the area under the sample peaks this example are 1237.5 and 153.8 respectively. LOH was calculated by measuring the area under the curve of the samples compared to that of a normalized control (gastritis or muscle epithelium areas from the same patient). LOH was considered when the area under the curve was <0.5 or >2.0.

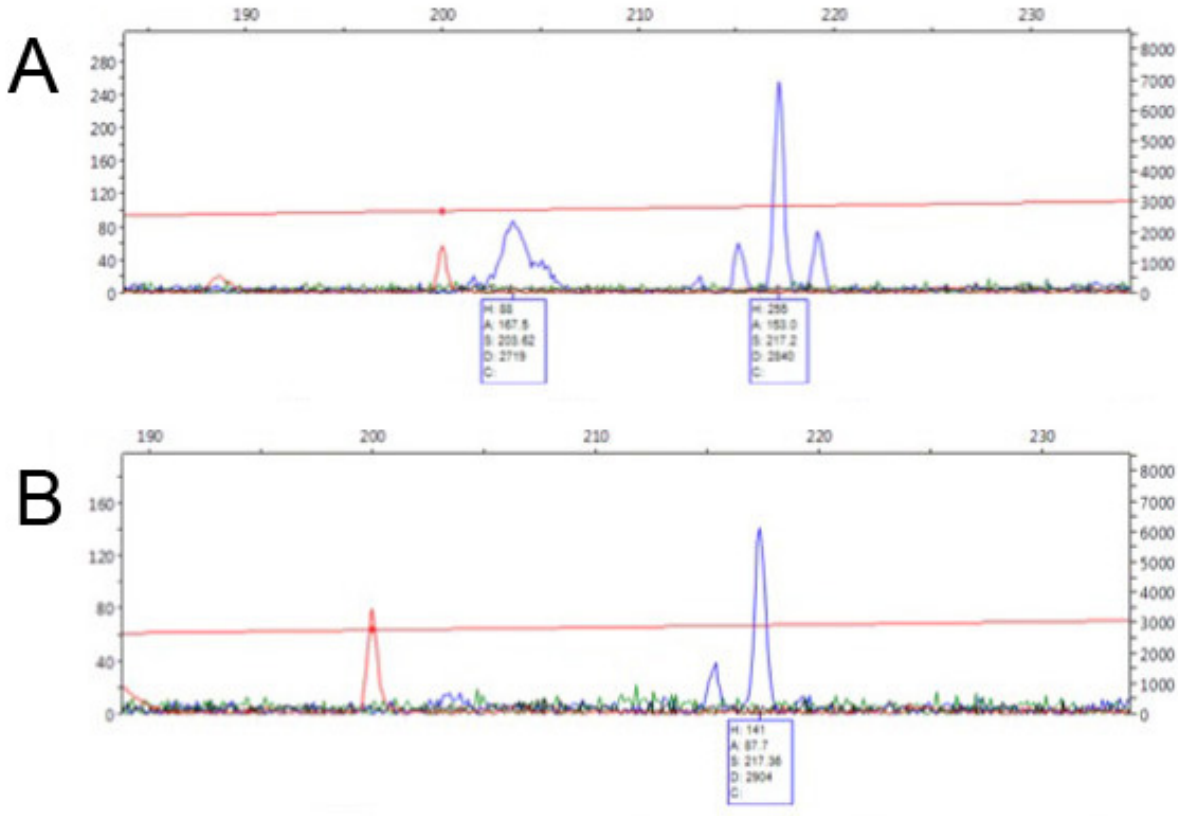

Figure 7.8**. Loss of heterozygosity of microsatellite marker D17S1881 was observed in patient 22.** Two traces (A and B) representative of 17p microsatellite marker D17S1881 from patient 22 corresponding to figures 3.12 and 3.13. (A) Representative trace of a control sample where both alleles are present; the values for the area under the control peaks are 167.5 and 153.0 respectively. (B) Representative trace where loss of heterozygosity (LOH) has occurred for marker D17S1881 (210bp); the values for the area under the sample peaks this example are 0 and 87.7 respectively. LOH was calculated by measuring the area under the curve of the samples compared to that of a normalized control (gastritis or muscle epithelium areas from the same patient). LOH was considered when the area under the curve was <0.5 or >2.0.

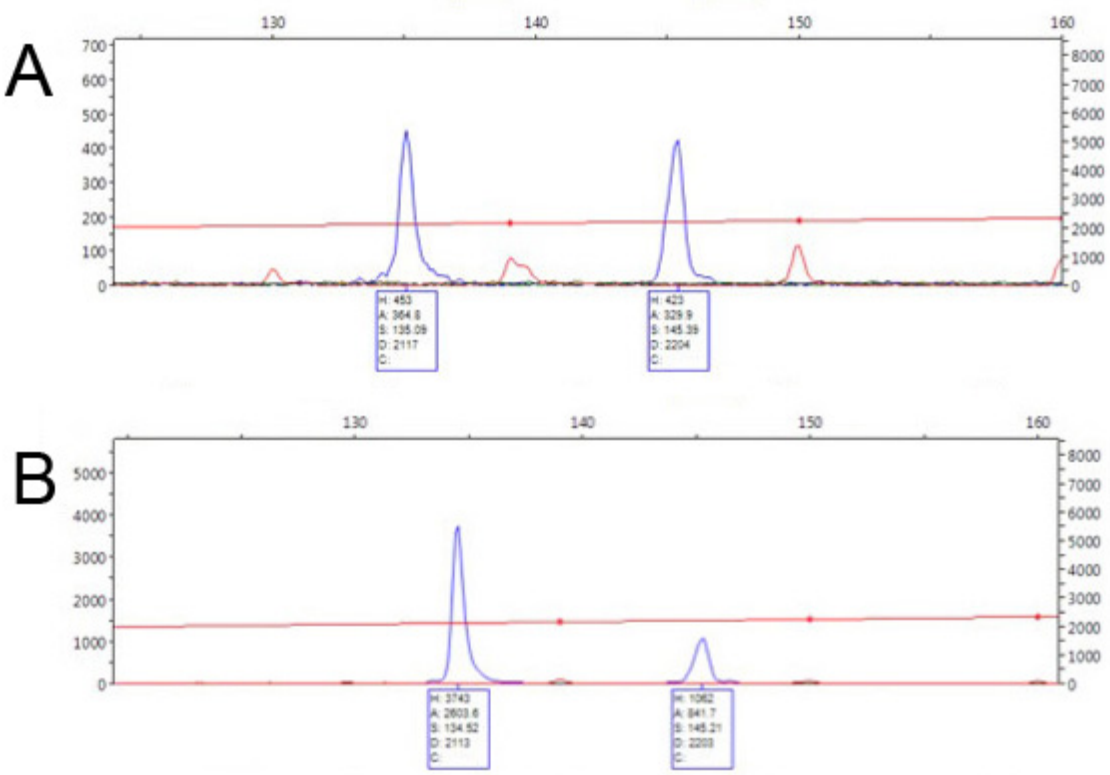

Figure 7.9. **Loss of heterozygosity of microsatellite marker D17S1506E was observed in patient 22.** Two traces (A and B) representative of 17p microsatellite marker D17S1506E from patient 22 corresponding to figures 3.12 and 3.13. (A) Representative trace of a control sample where both alleles are present; the values for the area under the control peaks are 364.8 and 329.9 respectively. (B) Representative trace where loss of heterozygosity (LOH) has occurred for marker D17S1506E (140bp); the values for the area under the sample peaks this example are 2603.6 and 841.7 respectively. LOH was calculated by measuring the area under the curve of the samples compared to that of a normalized control (gastritis or muscle epithelium areas from the same patient). LOH was considered when the area under the curve was <0.5 or >2.0.

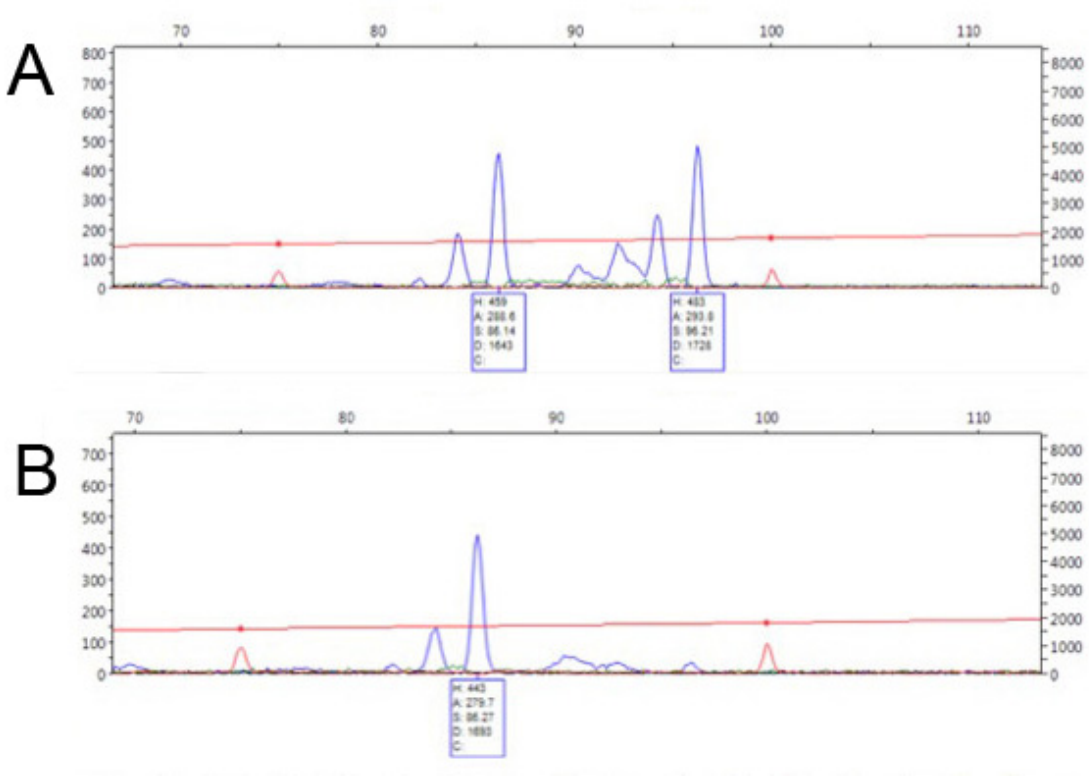

Figure 7.10**. Loss of heterozygosity of microsatellite marker D17S1176 was observed in patient 22.** Two traces (A and B) representative of 17p microsatellite marker D17S1176 from patient 22 corresponding to figures 3.12 and 3.13. (A) Representative trace of a control sample where both alleles are present; the values for the area under the control peaks are 288.6 and 293.8 respectively. (B) Representative trace where loss of heterozygosity (LOH) has occurred for marker D17S1176 (80bp); the values for the area under the sample peaks this example are 279.7 and 0 respectively. LOH was calculated by measuring the area under the curve of the samples compared to that of a normalized control (gastritis or muscle epithelium areas from the same patient). LOH was considered when the area under the curve was <0.5 or >2.0.

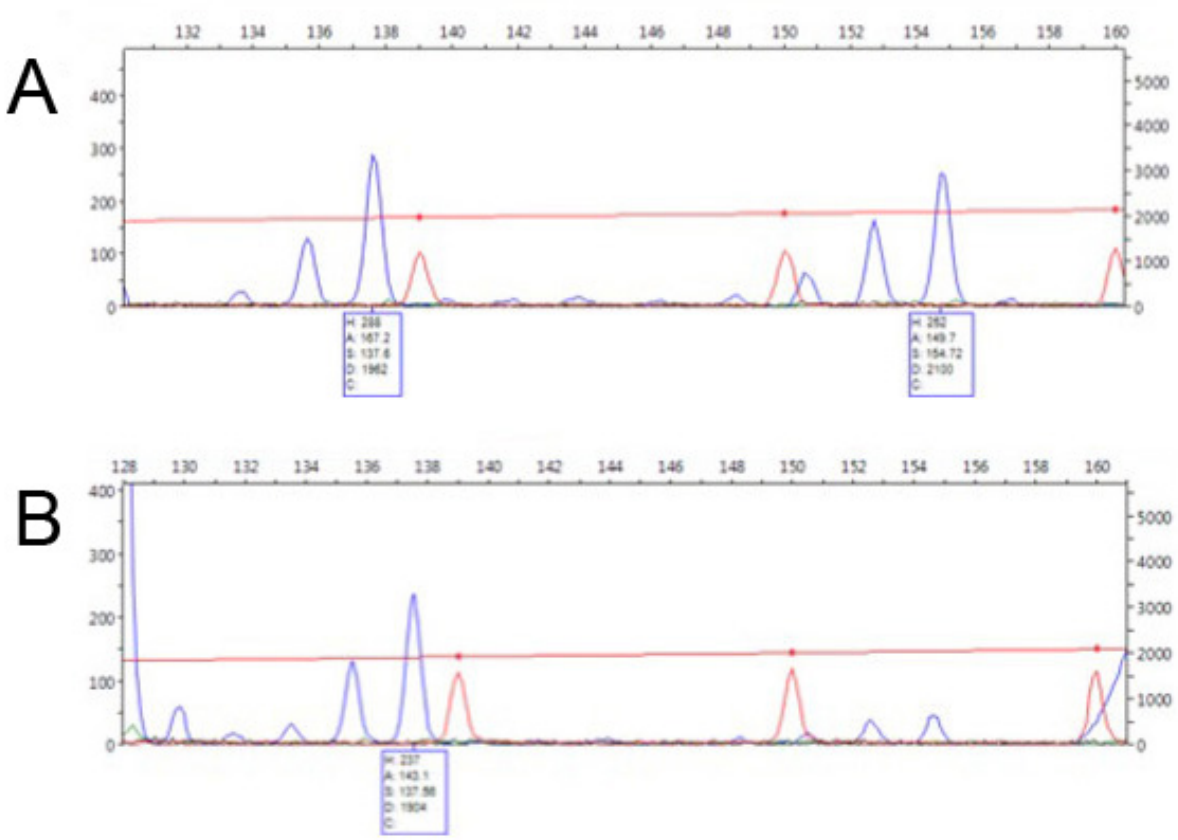

Figure 7.11. **Loss of heterozygosity of microsatellite marker D17S250 was observed in patient 22.** Two traces (A and B) representative of 17q microsatellite marker D17S250 from patient 22 corresponding to figures 3.12 and 3.13. (A) Representative trace of a control sample where both alleles are present; the values for the area under the control peaks are 167.2 and 149.7 respectively. (B) Representative trace where loss of heterozygosity (LOH) has occurred for marker D17S250 (140bp); the values for the area under the sample peaks this example are 143.1 and 0 respectively. LOH was calculated by measuring the area under the curve of the samples compared to that of a normalized control (gastritis or muscle epithelium areas from the same patient). LOH was considered when the area under the curve was <0.5 or >2.0.

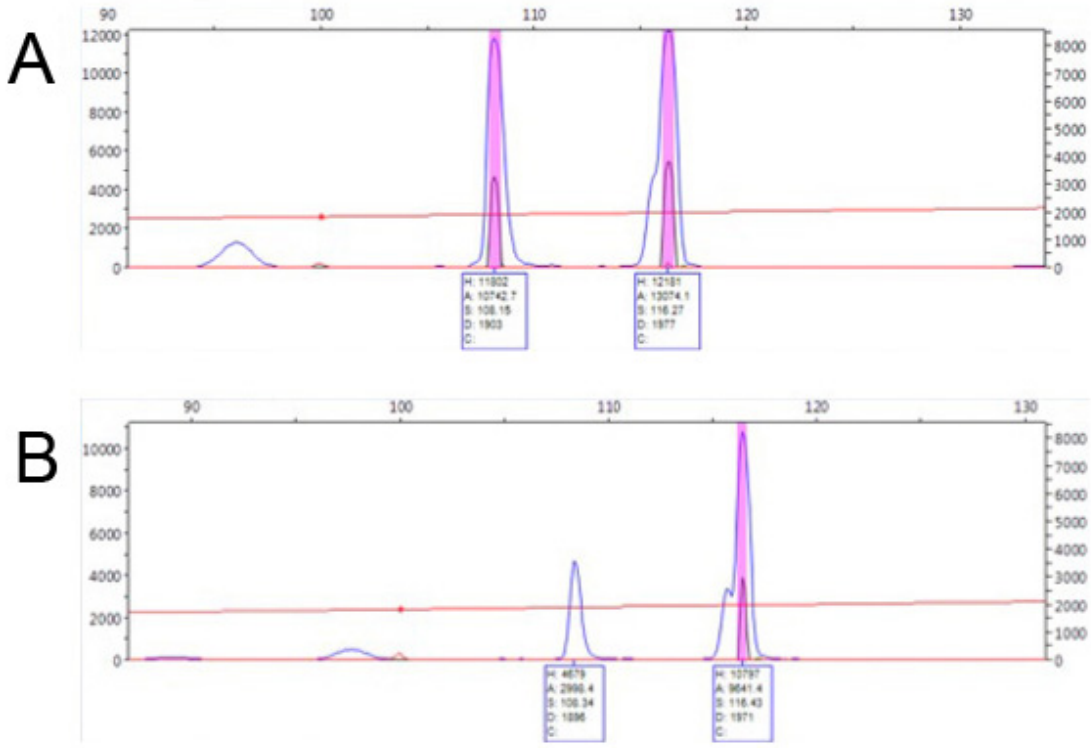

Figure 7.12**. Loss of heterozygosity of microsatellite marker D17S1678 was observed in patient 33.** Two traces (A and B) representative of 17p microsatellite marker D17S1678 from patient 33 corresponding to figures 3.14 to 3.16. (A) Representative trace of a control sample where both alleles are present; the values for the area under the control peaks are 10742.7 and 13074.1 respectively. (B) Representative trace where loss of heterozygosity (LOH) has occurred for marker D17S1678 (120bp); the values for the area under the sample peaks this example are 2998.4 and 9641.4 respectively. The purple vertical line on the traces denotes a high concentration of PCR product. LOH was calculated by measuring the area under the curve of the samples compared to that of a normalized control (gastritis or muscle epithelium areas from the same patient). LOH was considered when the area under the curve was <0.5 or >2.0.

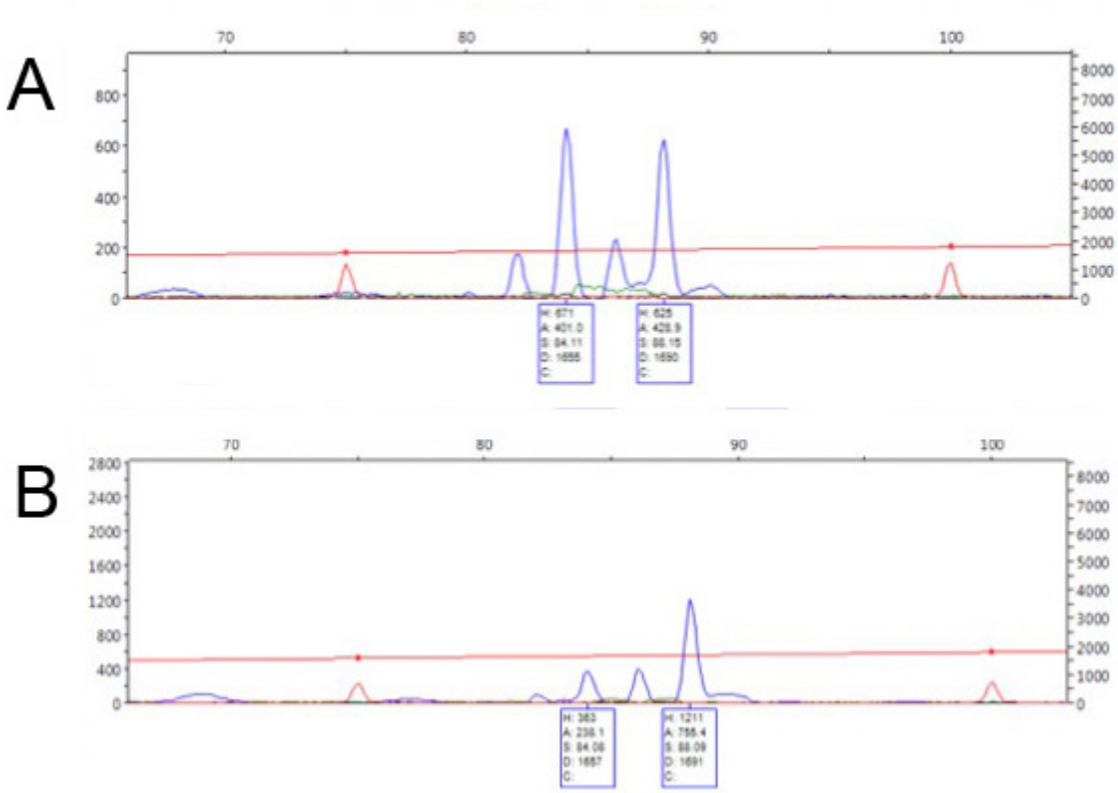

Figure 7.13. **Loss of heterozygosity of microsatellite marker D17S1176 was observed in patient 33.** Two traces (A and B) representative of 17p microsatellite marker D17S1176 from patient 33 corresponding to figures 3.14 to 3.16. (A) Representative trace of a control sample where both alleles are present; the values for the area under the control peaks are 401.0 and 428.9 respectively. (B) Representative trace where loss of heterozygosity (LOH) has occurred for marker D17S1176 (80bp); the values for the area under the sample peaks this example are 238.1 and 755.4 respectively. LOH was calculated by measuring the area under the curve of the samples compared to that of a normalized control (gastritis or muscle epithelium areas from the same patient). LOH was considered when the area under the curve was <0.5 or >2.0.

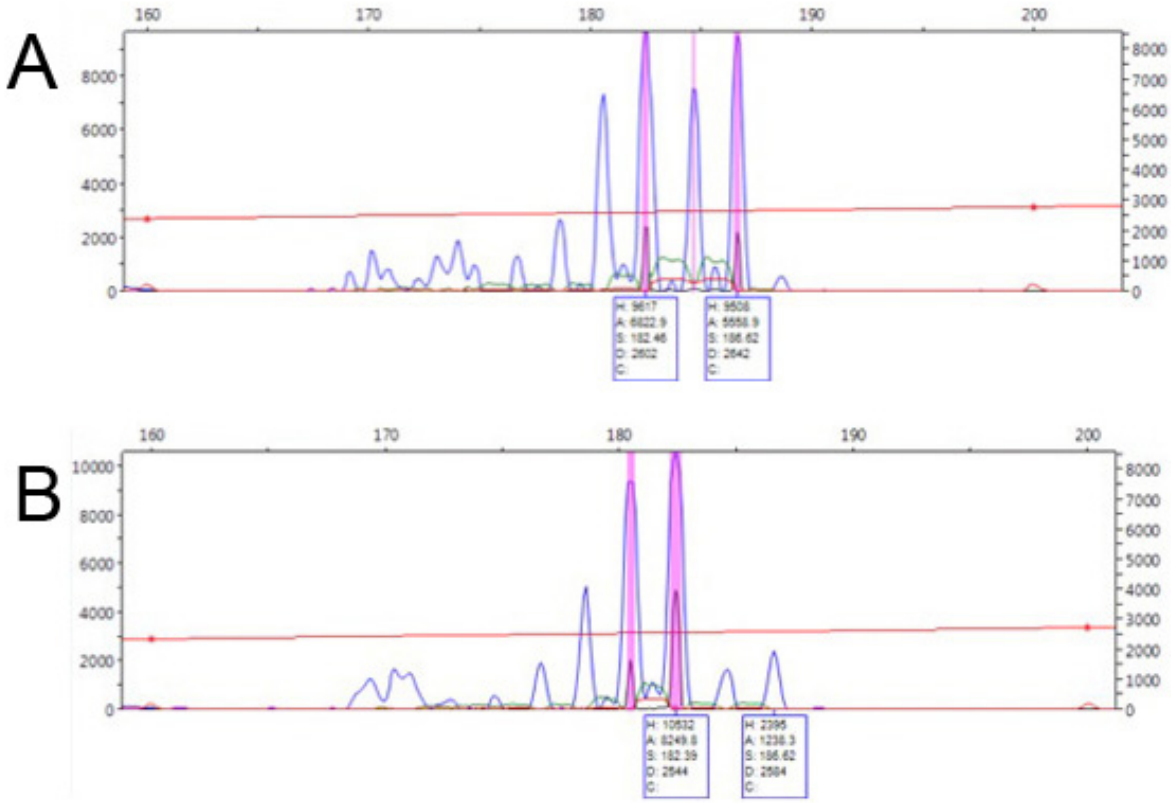

Figure 7.14. **Loss of heterozygosity of microsatellite marker D17S1832 was observed in patient 51.** Two traces (A and B) representative of 17p microsatellite marker D17S1832 from patient 51 corresponding to figures 3.17 and 3.18. (A) Representative trace of a control sample where both alleles are present; the values for the area under the control peaks are 6822.9 and 5558.9 respectively. (B) Representative trace where loss of heterozygosity (LOH) has occurred for marker D17S1832 (180bp); the values for the area under the sample peaks this example are 8249.8 and 1238.3 respectively. The purple vertical line on the traces denotes a high concentration of PCR product. LOH was calculated by measuring the area under the curve of the samples compared to that of a normalized control (gastritis or muscle epithelium areas from the same patient). LOH was considered when the area under the curve was <0.5 or >2.0.

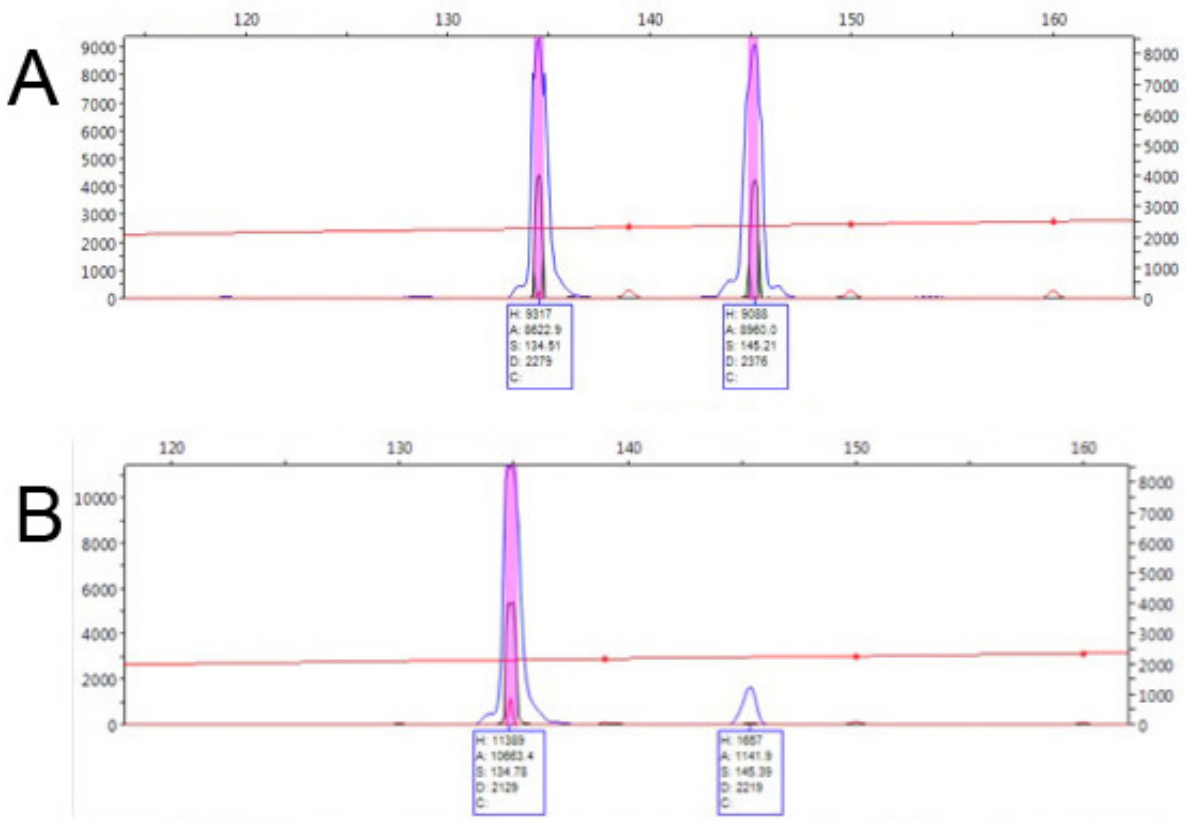

Figure 7.15. **Loss of heterozygosity of microsatellite marker D17S1506E was observed in patient 51.** Two traces (A and B) representative of 17p microsatellite marker D17S1506E from patient 51 corresponding to figures 3.17 and 3.18. (A) Representative trace of a control sample where both alleles are present; the values for the area under the control peaks are 8622.9 and 8960.0 respectively. (B) Representative trace where loss of heterozygosity (LOH) has occurred for marker D17S1506E (150bp); the values for the area under the sample peaks this example are 10663.4 and 1141.9 respectively. The purple vertical line on the traces denotes a high concentration of PCR product. LOH was calculated by measuring the area under the curve of the samples compared to that of a normalized control (gastritis or muscle epithelium areas from the same patient). LOH was considered when the area under the curve was <0.5 or >2.0.

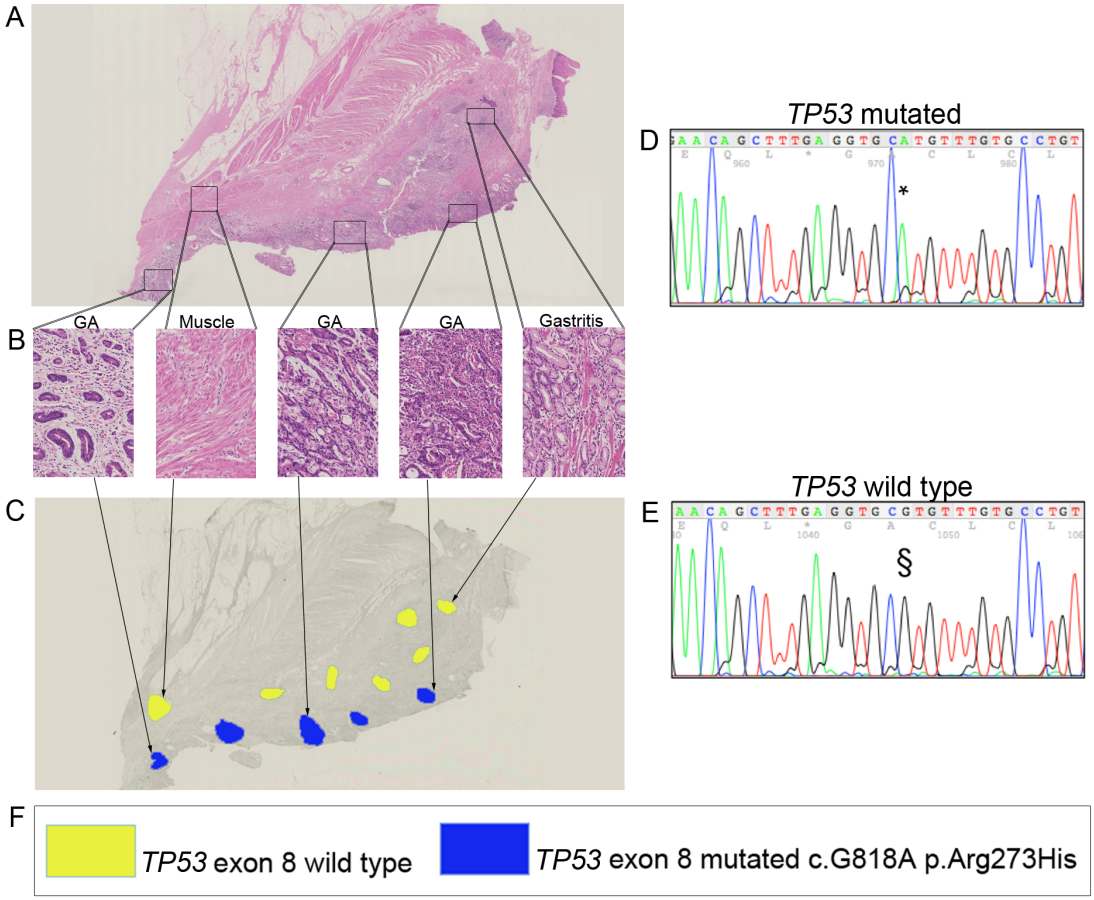

Figure 7.16. ***TP53* mutations found in gastric adenocarcinoma but not in benign areas in patient 27.** (A) A H&E of an entire section of gastric mucosa showing benign areas underneath gastric adenocarcinoma (GA); tissue from patient 27, specimen block 5. (B) Higher power of highlighted areas, showing from left to right an area of GA, a muscle area, two areas of GA area and an area of gastritis. (C) Serial section, showing post laser-capture microdissection (LCM). Yellow areas are *TP53* WT whereas dark blue areas are positive for the *TP53* mutation c.G818A. (D, E) Two representative traces showing the *TP53* mutation c.G818A (D) and a *TP53* WT trace (E). (F) Key for patient 27 on post LCM section.

Table 7.4. **Association of identified mutations and histology shows *TP53* mutations in gastric adenocarcinoma but not in benign areas in patient 27.** This table corresponds to the laser-capture microdissection data presented in Supplementary Figure 7.16; tissue from patient 27, specimen block 5. WT, wild type.

Patient 27:5	Histology	*TP53*
1	GA	MUTATED
2	Muscle	WT
3	GA	MUTATED
4	Gastritis	WT
5	GA	MUTATED
6	Gastritis	WT
7	GA	MUTATED
8	Gastritis	WT
9	GA	MUTATED
10	Gastritis	WT
11	Gastritis	WT
12	Gastritis	WT

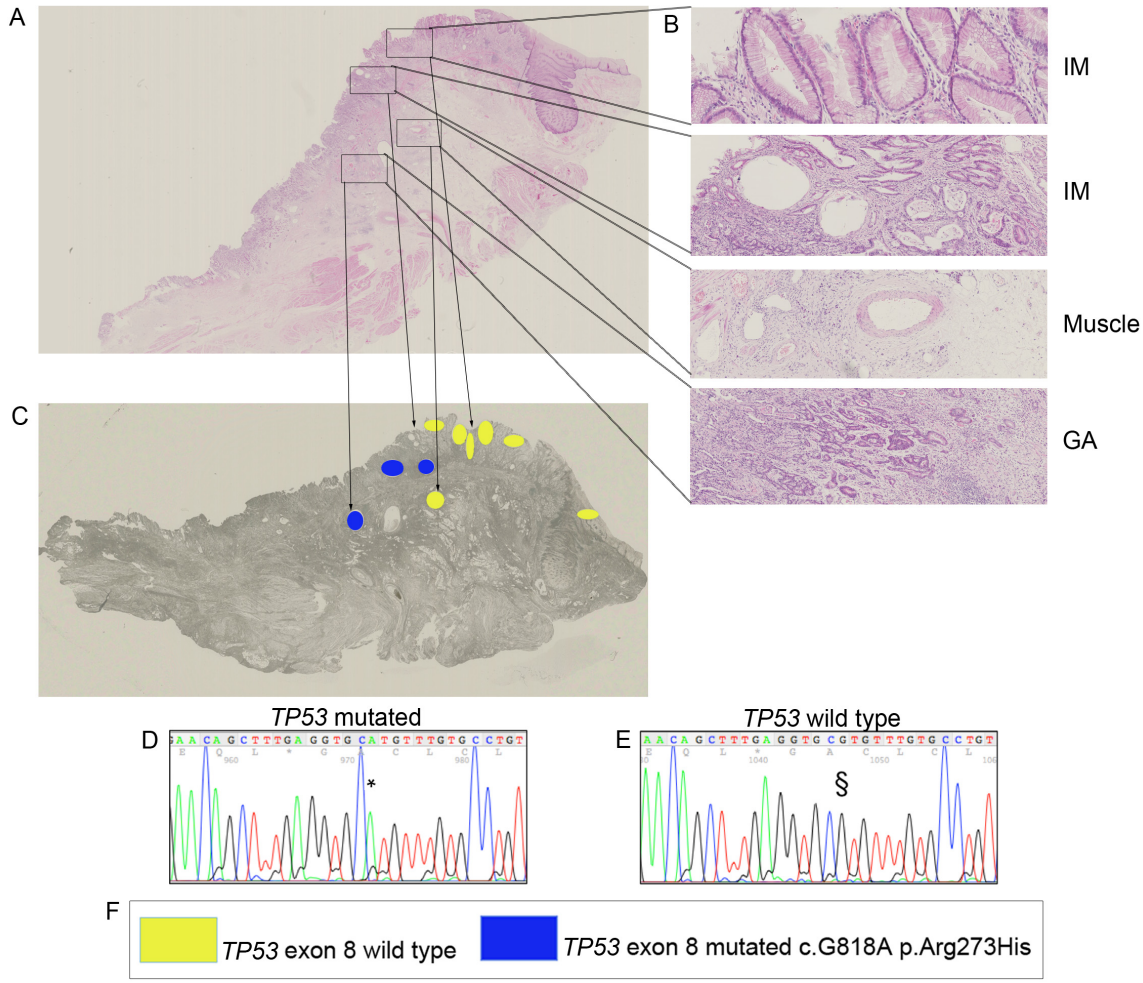

Figure 7.17. ***TP53* mutations found in gastric adenocarcinoma but not in intestinal metaplastic glands in patient 27.** (A) A H&E of an entire section of gastric mucosa showing oesophageal squamous epithelium, gastritis, intestinal metaplasia (IM) and areas of gastric adenocarcinoma (GA) from patient 27, specimen block 3. (B) Higher power of highlighted areas, showing from top to bottom two areas of IM, a muscle area and an area of GA. (C) Serial section showing post laser-capture microdissection (LCM). Yellow areas are *TP53* WT whereas dark blue areas are positive for the *TP53* mutation c.G818A. (D, E) Two representative traces showing the *TP53* mutation c.G818A (D) and a *TP53* WT trace (E). (F) Key for patient 27 on post LCM section.

Table 7.5. **Association of identified mutations and histology shows *TP53* mutations in gastric adenocarcinoma but not in intestinal metaplastic areas in patient 27.** This table corresponds to the laser-capture microdissection data presented in Supplementary Figure 7.17; tissue from patient 27, specimen block 3. WT, wild type.

Patient 27:3	Histology	*TP53*
1	Squamous	WT
2	IM	WT
3	GA	MUTATED
4	IM	WT
5	IM	WT
6	IM	WT
7	IM	WT
8	GA	MUTATED
9	Muscle	WT
10	GA	MUTATED

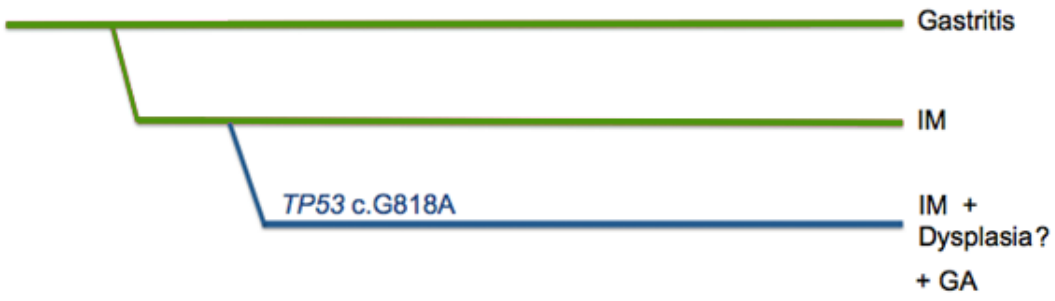

Figure 7.18. **Phylogenetic tree provides evidence for a monoclonal origin for gastric adenocarcinoma in patient 27.** Phylogenetic tree representative of patient 27, the data has been interpreted from the experimental data found in figures 7.1 and 7.2. Tree branches represent either phenotypic or genotypic changes. The wild type genotype is coloured in green and *TP53* mutation c.G818A has been coloured in dark blue. A "?" has been used to highlight likely genotypic and phenotypic events previous to GA development in patient 27.

Table 7.6. **Summary of clinical features in screened samples.** Gender and age information from the screening of 33 oesophageal squamous cell dysplasia and carcinoma (OSCC) specimens for the most commonly reported mutations (see COSMIC database) in OSCC (*256*). (--) stands for patient information not available.

Patients	GENDER	AGE
2	MALE	--
3	FEMALE	34
4	--	--
5	MALE	60
6	MALE	71
7	MALE	69
8	MALE	69
9	FEMALE	72
10	FEMALE	66
12	MALE	57
13	FEMALE	66
14	FEMALE	59
15	FEMALE	78
16	MALE	55
17	MALE	71
18	MALE	71
19	FEMALE	68
20	MALE	53
21	MALE	65
22	--	--
23	--	--
24	--	--
25	MALE	74
26	FEMALE	71
27	MALE	64
28	FEMALE	70
29	MALE	61
30	FEMALE	72
31	FEMALE	58
32	FEMALE	54
33	--	--
34	--	--

8. References

1. May, R., Sureban, S., Hoang, N., Riehl, T., Lightfoot, S., Ramanujam, R., Wyche, J., Anant, S., and Houchen, C. (2009) DCAMKL-1 and LGR5 Mark Quiescent and Cycling Intestinal Stem Cells Respectively, *Stem Cells 10,* 2571-2579.
2. Burkert, J., Wright, N. A., and Alison, M. R. (2006) Stem cells and cancer: an intimate relationship, *J Pathol 209*, 287-297.
3. Cheng, H., and Leblond, C. P. (1974) Origin, differentiation and renewal of the four main epithelial cell types in the mouse small intestine. V. Unitarian Theory of the origin of the four epithelial cell types, *Am J Anat 141*, 537-561.
4. Scadden, D. T. (2006) The stem-cell niche as an entity of action, *Nature 441*, 1075-1079.
5. Lin, H. (2002) The stem-cell niche theory: lessons from flies, *Nat Rev Genet 3*, 931-940.
6. Barker, N., van Es, J. H., Kuipers, J., Kujala, P., van den Born, M., Cozijnsen, M., Haegebarth, A., Korving, J., Begthel, H., Peters, P. J., and Clevers, H. (2007) Identification of stem cells in small intestine and colon by marker gene Lgr5, *Nature 449*, 1003-1007.
7. Rothenberg, M. E., Nusse, Y., Kalisky, T., Lee, J. J., Dalerba, P., Scheeren, F., Lobo, N., Kulkarni, S., Sim, S., Qian, D., Beachy, P. A., Pasricha, P. J., Quake, S. R., and Clarke, M. F. (2012) Identification of a cKit(+) colonic crypt base secretory cell that supports Lgr5(+) stem cells in mice, *Gastroenterology 142*, 1195-1205 e1196.
8. Wilson, A., Laurenti, E., Oser, G., van der Wath, R. C., Blanco-Bose, W., Jaworski, M., Offner, S., Dunant, C. F., Eshkind, L., Bockamp, E., Lió, P., Macdonald, H. R., and Trumpp, A. (2008) Hematopoietic stem cells reversibly switch from dormancy to self-renewal during homeostasis and repair, *Cell 135*, 1118-1129.
9. Blanpain, C., Lowry, W. E., Geoghegan, A., Polak, L., and Fuchs, E. (2004) Self-renewal, multipotency, and the existence of two cell populations within an epithelial stem cell niche, *Cell 118*, 635-648.
10. Potten, C. S., Owen, G., and Booth, D. (2002) Intestinal stem cells protect their genome by selective segregation of template DNA strands, *J Cell Sci 115*, 2381-2388.
11. Potten, C. S., Kovacs, L., and Hamilton, E. (1974) Continuous labelling studies on mouse skin and intestine, *Cell Tissue Kinet 7*, 271-283.
12. Barker, N., and Clevers, H. (2007) Tracking down the stem cells of the intestine: strategies to identify adult stem cells, *Gastroenterology 133*, 1755-1760.
13. Montgomery, R. K., Carlone, D. L., Richmond, C. A., Farilla, L., Kranendonk, M. E., Henderson, D. E., Baffour-Awuah, N. Y., Ambruzs, D. M., Fogli, L. K., Algra, S., and Breault, D. T. (2011) Mouse telomerase reverse transcriptase (mTert) expression marks slowly cycling intestinal stem cells, *Proc Natl Acad Sci U S A 108*, 179-184.
14. Fuchs, E. (2009) The tortoise and the hair: slow-cycling cells in the stem cell race, *Cell 137*, 811-819.

15. Kim, K.-M., and Shibata, D. (2002) Methylation reveals a niche: stem cell succession in human colon crypts, *Oncogene 21*, 5441-5449.
16. Thirlwell, C., Will, O. C. C., Domingo, E., Graham, T. A., McDonald, S. A. C., Oukrif, D., Jeffrey, R., Gorman, M., Rodriguez-Justo, M., Chin-Aleong, J., Clark, S. K., Novelli, M. R., Jankowski, J. A., Wright, N. A., Tomlinson, I. P. M., and Leedham, S. J. (2010) Clonality assessment and clonal ordering of individual neoplastic crypts shows polyclonality of colorectal adenomas, *Gastroenterology 138*, 1441-1454, 1454.e1441-1447.
17. Leedham, S., and Wright, N. (2008) Expansion of a mutated clone-from stem cell to tumour, *J Clin Path, 61:164-171*.
18. Kaur, P., and Potten, C. S. (1986) Cell migration velocities in the crypts of the small intestine after cytotoxic insult are not dependent on mitotic activity, *Cell Tissue Kinet 19*, 601-610.
19. Qiu, J. M., Roberts, S. A., and Potten, C. S. (1994) Cell migration in the small and large bowel shows a strong circadian rhythm, *Epithelial Cell Biol 3*, 137-148.
20. Quante, M., and Wang, T. C. (2009) Stem cells in gastroenterology and hepatology, *Nat Rev Gastroenterol Hepatol 6*, 724-737.
21. Barker, N., van de Wetering, M., and Clevers, H. (2008) The intestinal stem cell, *Genes Dev 22*, 1856-1864.
22. Cairns, J. (2002) Somatic stem cells and the kinetics of mutagenesis and carcinogenesis, *Proc Natl Acad Sci USA 99*, 10567-10570.
23. Sangiorgi, E., and Capecchi, M. R. (2008) Bmi1 is expressed in vivo in intestinal stem cells, *Nat Genet 40*, 915-920.
24. Lessard, J., and Sauvageau, G. (2003) Bmi-1 determines the proliferative capacity of normal and leukaemic stem cells, *Nature 423*, 255-260.
25. Gregorieff, A., Pinto, D., Begthel, H., Destrée, O., Kielman, M., and Clevers, H. (2005) Expression pattern of Wnt signaling components in the adult intestine, *Gastroenterology 129*, 626-638.
26. Bienz, M., and Clevers, H. (2000) Linking colorectal cancer to Wnt signaling, *Cell 103*, 311-320.
27. Leedham, S. J., Brittan, M., McDonald, S. A. C., and Wright, N. A. (2005) Intestinal stem cells, *J Cell Mol Med 9*, 11-24.
28. Jensen, K. B., and Watt, F. M. (2006) Single-cell expression profiling of human epidermal stem and transit-amplifying cells: Lrig1 is a regulator of stem cell quiescence, *Proc Natl Acad Sci U S A 103*, 11958-11963.
29. Jensen, K. B., Collins, C. A., Nascimento, E., Tan, D. W., Frye, M., Itami, S., and Watt, F. M. (2009) Lrig1 expression defines a distinct multipotent stem cell population in mammalian epidermis, *Cell Stem Cell 4*, 427-439.
30. Giannakis, M., Stappenbeck, T. S., Mills, J. C., Leip, D. G., Lovett, M., Clifton, S. W., Ippolito, J. E., Glasscock, J. I., Arumugam, M., Brent, M. R., and Gordon, J. I. (2006) Molecular properties of adult mouse gastric and intestinal epithelial progenitors in their niches, *J Biol Chem 281*, 11292-11300.
31. May, R., Riehl, T. E., Hunt, C., Sureban, S. M., Anant, S., and Houchen, C. W. (2008) Identification of a novel putative gastrointestinal stem cell and adenoma stem cell marker, doublecortin and CaM kinase-like-1, following radiation injury and in adenomatous polyposis coli/multiple intestinal neoplasia mice, *Stem Cells 26*, 630-637.

32. de Lau, W., Barker, N., Low, T. Y., Koo, B. K., Li, V. S., Teunissen, H., Kujala, P., Haegebarth, A., Peters, P. J., van de Wetering, M., Stange, D. E., van Es, J. E., Guardavaccaro, D., Schasfoort, R. B., Mohri, Y., Nishimori, K., Mohammed, S., Heck, A. J., and Clevers, H. (2011) Lgr5 homologues associate with Wnt receptors and mediate R-spondin signalling, *Nature 476*, 293-297.
33. Glinka, A., Dolde, C., Kirsch, N., Huang, Y. L., Kazanskaya, O., Ingelfinger, D., Boutros, M., Cruciat, C. M., and Niehrs, C. (2011) LGR4 and LGR5 are R-spondin receptors mediating Wnt/beta-catenin and Wnt/PCP signalling, *EMBO Rep 12*, 1055-1061.
34. Yin, A. H., Miraglia, S., Zanjani, E. D., Almeida-Porada, G., Ogawa, M., Leary, A. G., Olweus, J., Kearney, J., and Buck, D. W. (1997) AC133, a novel marker for human hematopoietic stem and progenitor cells, *Blood 90*, 5002-5012.
35. Zhu, L., Gibson, P., Currle, D. S., Tong, Y., Richardson, R. J., Bayazitov, I. T., Poppleton, H., Zakharenko, S., Ellison, D. W., and Gilbertson, R. J. (2009) Prominin 1 marks intestinal stem cells that are susceptible to neoplastic transformation, *Nature 457*, 603-607.
36. Van der Flier, L. G., Van Gijn, M. E., Hatzis, P., Kujala, P., Haegebarth, A., Stange, D. E., Begthel, H., van den Born, M., Guryev, V., Oving, I., van Es, J. H., Barker, N., Peters, P. J., van de Wetering, M., and Clevers, H. (2009) Transcription factor achaete scute-like 2 controls intestinal stem cell fate, *Cell 136*, 903-912.
37. Wang, X. Y., Yin, Y., Yuan, H., Sakamaki, T., Okano, H., and Glazer, R. I. (2008) Musashi1 modulates mammary progenitor cell expansion through proliferin-mediated activation of the Wnt and Notch pathways, *Mol Cell Biol 28*, 3589-3599.
38. Glazer, R. I., Wang, X.-Y., Yuan, H., and Yin, Y. (2008) Musashi1: a stem cell marker no longer in search of a function, *Cell Cycle 7*, 2635-2639.
39. Jin, G., Ramanathan, V., Quante, M., Baik, G. H., Yang, X., Wang, S. S. W., Tu, S., Gordon, S. A. K., Pritchard, D. M., Varro, A., Shulkes, A., and Wang, T. C. (2009) Inactivating cholecystokinin-2 receptor inhibits progastrin-dependent colonic crypt fission, proliferation, and colorectal cancer in mice, *J Clin Invest 119*, 2691-2701.
40. Means, A. L., Xu, Y., Zhao, A., Ray, K. C., and Gu, G. (2008) A CK19(CreERT) knockin mouse line allows for conditional DNA recombination in epithelial cells in multiple endodermal organs, *Genesis 46*, 318-323.
41. Humphries, A., and Wright, N. A. (2008) Colonic crypt organization and tumorigenesis, *Nature Reviews Cancer 8*, 415-424.
42. Winton, D. J., and Ponder, B. A. (1990) Stem-cell organization in mouse small intestine, *Proc Biol Sci 241*, 13-18.
43. Bjerknes, M., and Cheng, H. (1999) Clonal analysis of mouse intestinal epithelial progenitors, *Gastroenterology 116*, 7-14.
44. Campbell, F., Fuller, C. E., Williams, G. T., and Williams, E. D. (1994) Human colonic stem cell mutation frequency with and without irradiation, *J Pathol 174*, 175-182.
45. Campbell, F., Appleton, M. A., Fuller, C. E., Greeff, M. P., Hallgrimsson, J., Katoh, R., Ng, O. L., Satir, A., Williams, G. T., and Williams, E. D. (1994)

Racial variation in the O-acetylation phenotype of human colonic mucosa, *J Pathol 174*, 169-174.
46. Campbell, F., Williams, G. T., Appleton, M. A., Dixon, M. F., Harris, M., and Williams, E. D. (1996) Post-irradiation somatic mutation and clonal stabilisation time in the human colon, *Gut 39*, 569-573.
47. Novelli, M. R., Williamson, J. A., Tomlinson, I. P., Elia, G., Hodgson, S. V., Talbot, I. C., Bodmer, W. F., and Wright, N. A. (1996) Polyclonal origin of colonic adenomas in an XO/XY patient with FAP, *Science 272*, 1187-1190.
48. Thomas, G. A., Williams, D., and Williams, E. D. (1988) The demonstration of tissue clonality by X-linked enzyme histochemistry, *J Pathol 155*, 101-108.
49. Novelli, M., Cossu, A., Oukrif, D., Quaglia, A., Lakhani, S., Poulsom, R., Sasieni, P., Carta, P., Contini, M., Pasca, A., Palmieri, G., Bodmer, W., Tanda, F., and Wright, N. (2003) X-inactivation patch size in human female tissue confounds the assessment of tumor clonality, *Proc Natl Acad Sci USA 100*, 3311-3314.
50. Taylor, R. W., Barron, M. J., Borthwick, G. M., Gospel, A., Chinnery, P. F., Samuels, D. C., Taylor, G. A., Plusa, S. M., Needham, S. J., Greaves, L. C., Kirkwood, T. B. L., and Turnbull, D. M. (2003) Mitochondrial DNA mutations in human colonic crypt stem cells, *Journal of Clinical Investigation 112*, 1351-1360.
51. Fellous, T. G., McDonald, S. A. C., Burkert, J., Humphries, A., Islam, S., De-Alwis, N. M. W., Gutierrez-Gonzalez, L., Tadrous, P. J., Elia, G., Kocher, H. M., Bhattacharya, S., Mears, L., El-Bahrawy, M., Turnbull, D. M., Taylor, R. W., Greaves, L. C., Chinnery, P. F., Day, C. P., Wright, N. A., and Alison, M. R. (2009) A methodological approach to tracing cell lineage in human epithelial tissues, *Stem Cells 27*, 1410-1420.
52. Nesti, C., Pasquali, L., Vaglini, F., Siciliano, G., and Murri, L. (2007) The role of mitochondria in stem cell biology, *Biosci Rep 27*, 165-171.
53. Taylor, R. W., and Turnbull, D. M. (2005) Mitochondrial DNA mutations in human disease, *Nat Rev Genet 6*, 389-402.
54. Sciacco, M., Bonilla, E., Schon, E. A., DiMauro, S., and Moraes, C. T. (1994) Distribution of wild-type and common deletion forms of mtDNA in normal and respiration-deficient muscle fibers from patients with mitochondrial myopathy, *Hum Mol Genet 3*, 13-19.
55. Greaves, L. C., Preston, S. L., Tadrous, P. J., Taylor, R. W., Barron, M. J., Oukrif, D., Leedham, S. J., Deheragoda, M., Sasieni, P., Novelli, M. R., Jankowski, J. A. Z., Turnbull, D. M., Wright, N. A., and McDonald, S. A. C. (2006) Mitochondrial DNA mutations are established in human colonic stem cells, and mutated clones expand by crypt fission, *Proc Natl Acad Sci USA 103*, 714-719.
56. Yatabe, Y., Tavaré, S., and Shibata, D. (2001) Investigating stem cells in human colon by using methylation patterns, *Proc Natl Acad Sci USA 98*, 10839-10844.
57. Kim, K.-M., and Shibata, D. (2004) Tracing ancestry with methylation patterns: most crypts appear distantly related in normal adult human colon, *BMC gastroenterology 4*, 8.
58. Clayton, R. N., Pfeifer, M., Atkinson, A. B., Belchetz, P., Wass, J. A., Kyrodimou, E., Vanderpump, M., Simpson, D., Bicknell, J., and Farrell, W. E. (2000) Different patterns of allelic loss (loss of heterozygosity) in recurrent

human pituitary tumors provide evidence for multiclonal origins, *Clin Cancer Res 6*, 3973-3982.
59. Hartmann, A., Rosner, U., Schlake, G., Dietmaier, W., Zaak, D., Hofstaedter, F., and Knuechel, R. (2000) Clonality and genetic divergence in multifocal low-grade superficial urothelial carcinoma as determined by chromosome 9 and p53 deletion analysis, *Lab Invest 80*, 709-718.
60. Salk, J. J., Salipante, S. J., Risques, R. A., Crispin, D. A., Li, L., Bronner, M. P., Brentnall, T. A., Rabinovitch, P. S., Horwitz, M. S., and Loeb, L. A. (2009) Clonal expansions in ulcerative colitis identify patients with neoplasia, *Proc Natl Acad Sci U S A 106*, 20871-20876.
61. Diaz-Cano, S. J., Blanes, A., and Wolfe, H. J. (2001) PCR techniques for clonality assays, *Diagn Mol Pathol 10*, 24-33.
62. Frumkin, D., Wasserstrom, A., Itzkovitz, S., Stern, T., Harmelin, A., Eilam, R., Rechavi, G., and Shapiro, E. (2008) Cell lineage analysis of a mouse tumor, *Cancer Res 68*, 5924-5931.
63. Graham, T. A., and Wright, N. A. (2008) Investigating the fixation and spread of mutations in the gastrointestinal epithelium, *Future oncology (London, England) 4*, 825-839.
64. Galandiuk, S., Rodriguez-Justo, M., Jeffery, R., Nicholson, A. M., Cheng, Y., Oukrif, D., Elia, G., Leedham, S. J., McDonald, S. A., Wright, N. A., and Graham, T. A. (2012) Field cancerization in the intestinal epithelium of patients with Crohn's ileocolitis, *Gastroenterology 142*, 855-864 e858.
65. Hoffmann, W. (2011) Gastric stem cells: of flies and men, *Cell Cycle 10*, 1186-1187.
66. Karam, S. M., Straiton, T., Hassan, W. M., and Leblond, C. P. (2003) Defining epithelial cell progenitors in the human oxyntic mucosa, *Stem Cells 21*, 322-336.
67. Quante, M., Marrache, F., Goldenring, J. R., and Wang, T. C. (2010) TFF2 mRNA transcript expression marks a gland progenitor cell of the gastric oxyntic mucosa, *Gastroenterology 139*, 2018-2027 e2012.
68. Qiao, X. T., Ziel, J. W., McKimpson, W., Madison, B. B., Todisco, A., Merchant, J. L., Samuelson, L. C., and Gumucio, D. L. (2007) Prospective identification of a multilineage progenitor in murine stomach epithelium, *Gastroenterology 133*, 1989-1998.
69. Barker, N., Huch, M., Kujala, P., van de Wetering, M., Snippert, H. J., van Es, J. H., Sato, T., Stange, D. E., Begthel, H., van den Born, M., Danenberg, E., van den Brink, S., Korving, J., Abo, A., Peters, P. J., Wright, N., Poulsom, R., and Clevers, H. (2010) Lgr5(+ve) stem cells drive self-renewal in the stomach and build long-lived gastric units in vitro, *Cell stem cell 6*, 25-36.
70. Nomura, S., Kaminishi, M., Sugiyama, K., Oohara, T., and Esumi, H. (1998) Clonal analysis of isolated intestinal metaplastic glands of stomach using X linked polymorphism, *Gut 42*, 663-668.
71. McDonald, S. A. C., Greaves, L. C., Gutierrez-Gonzalez, L., Rodriguez-Justo, M., Deheragoda, M., Leedham, S. J., Taylor, R. W., Lee, C. Y., Preston, S. L., Lovell, M., Hunt, T., Elia, G., Oukrif, D., Harrison, R., Novelli, M. R., Mitchell, I., Stoker, D. L., Turnbull, D. M., Jankowski, J. A. Z., and Wright, N. A. (2008) Mechanisms of field cancerization in the human stomach: the expansion and spread of mutated gastric stem cells, *Gastroenterology 134*, 500-510.

72. Gutierrez-Gonzalez, L., Graham, T. A., Rodriguez-Justo, M., Leedham, S. J., Novelli, M. R., Gay, L. J., Ventayol-Garcia, T., Green, A., Mitchell, I., Stoker, D. L., Preston, S. L., Bamba, S., Yamada, E., Kishi, Y., Harrison, R., Jankowski, J. A., Wright, N. A., and McDonald, S. A. (2011) The clonal origins of dysplasia from intestinal metaplasia in the human stomach, *Gastroenterology 140*, 1251-1260 e1251-1256.
73. Seery, J. P. (2002) Stem cells of the oesophageal epithelium, *J Cell Sci 115*, 1783-1789.
74. Doupe, D. P., Alcolea, M. P., Roshan, A., Zhang, G., Klein, A. M., Simons, B. D., and Jones, P. H. (2012) A single progenitor population switches behavior to maintain and repair esophageal epithelium, *Science 337*, 1091-1093.
75. Leblond, C. P. (1964) Classification of Cell Populations on the Basis of Their Proliferative Behavior, *Natl Cancer Inst Monogr 14*, 119-150.
76. Seery, J. P., and Watt, F. M. (2000) Asymmetric stem-cell divisions define the architecture of human oesophageal epithelium, *Curr Biol 10*, 1447-1450.
77. Jankowski, J., Hopwood, D., Dovert, R., and Wormsley, K. G. (1993) Development and growth of normal; metaplastic and dysplastic oesophageal mucosa: biological markers of neoplasia, *European journal of gastroenterology & hepatology 5*, 235-246.
78. Jones, P. H., and Watt, F. M. (1993) Separation of human epidermal stem cells from transit amplifying cells on the basis of differences in integrin function and expression, *Cell 73*, 713-724.
79. Goodell, M. A., Brose, K., Paradis, G., Conner, A. S., and Mulligan, R. C. (1996) Isolation and functional properties of murine hematopoietic stem cells that are replicating in vivo, *J Exp Med 183*, 1797-1806.
80. Kalabis, J., Oyama, K., Okawa, T., Nakagawa, H., Michaylira, C. Z., Stairs, D. B., Figueiredo, J.-L., Mahmood, U., Diehl, J. A., Herlyn, M., and Rustgi, A. K. (2008) A subpopulation of mouse esophageal basal cells has properties of stem cells with the capacity for self-renewal and lineage specification, *J Clin Invest 118*, 3860-3869.
81. Croagh, D., Phillips, W. A., Redvers, R., Thomas, R. J., and Kaur, P. (2007) Identification of candidate murine esophageal stem cells using a combination of cell kinetic studies and cell surface markers, *Stem Cells 25*, 313-318.
82. McDonald, S. A. C., Preston, S. L., Lovell, M. J., Wright, N. A., and Jankowski, J. A. Z. (2006) Mechanisms of disease: from stem cells to colorectal cancer, *Nature clinical practice Gastroenterology & hepatology 3*, 267-274.
83. Rosen, J. M., and Jordan, C. T. (2009) The increasing complexity of the cancer stem cell paradigm, *Science 324*, 1670-1673.
84. Reya, T., Morrison, S. J., Clarke, M. F., and Weissman, I. L. (2001) Stem cells, cancer, and cancer stem cells, *Nature 414*, 105-111.
85. Hamburger, A. W., and Salmon, S. E. (1977) Primary bioassay of human tumor stem cells, *Science 197*, 461-463.
86. Lapidot, T., Sirard, C., Vormoor, J., Murdoch, B., Hoang, T., Caceres-Cortes, J., Minden, M., Paterson, B., Caligiuri, M. A., and Dick, J. E. (1994) A cell initiating human acute myeloid leukaemia after transplantation into SCID mice, *Nature 367*, 645-648.
87. Visvader, J. E., and Lindeman, G. J. (2008) Cancer stem cells in solid tumours: accumulating evidence and unresolved questions, *Nature Reviews Cancer 8*, 755-768.

88. Nowell, P. C. (1976) The clonal evolution of tumor cell populations, *Science 194*, 23-28.
89. Barabe, F., Kennedy, J. A., Hope, K. J., and Dick, J. E. (2007) Modeling the initiation and progression of human acute leukemia in mice, *Science 316*, 600-604.
90. Kirkland, S. C. (1988) Clonal origin of columnar, mucous, and endocrine cell lineages in human colorectal epithelium, *Cancer 61*, 1359-1363.
91. Vermeulen, L., Todaro, M., de Sousa Mello, F., Sprick, M. R., Kemper, K., Perez Alea, M., Richel, D. J., Stassi, G., and Medema, J. P. (2008) Single-cell cloning of colon cancer stem cells reveals a multi-lineage differentiation capacity, *Proc Natl Acad Sci U S A 105*, 13427-13432.
92. Garcia, S. B., Novelli, M., and Wright, N. A. (2000) The clonal origin and clonal evolution of epithelial tumours, *International journal of experimental pathology 81*, 89-116.
93. Alison, M. R., Islam, S., and Lim, S. M. (2009) Number crunching in the cancer stem cell market, *Breast Cancer Res 11*, 302.
94. Mani, S. A., Guo, W., Liao, M. J., Eaton, E. N., Ayyanan, A., Zhou, A. Y., Brooks, M., Reinhard, F., Zhang, C. C., Shipitsin, M., Campbell, L. L., Polyak, K., Brisken, C., Yang, J., and Weinberg, R. A. (2008) The epithelial-mesenchymal transition generates cells with properties of stem cells, *Cell 133*, 704-715.
95. Ma, J., Lin, J. Y., Alloo, A., Wilson, B. J., Schatton, T., Zhan, Q., Murphy, G. F., Waaga-Gasser, A. M., Gasser, M., Stephen Hodi, F., Frank, N. Y., and Frank, M. H. (2010) Isolation of tumorigenic circulating melanoma cells, *Biochem Biophys Res Commun 402*, 711-717.
96. Al-Hajj, M., Wicha, M. S., Benito-Hernandez, A., Morrison, S. J., and Clarke, M. F. (2003) Prospective identification of tumorigenic breast cancer cells, *Proc Natl Acad Sci U S A 100*, 3983-3988.
97. Yang, Z. F., Ngai, P., Ho, D. W., Yu, W. C., Ng, M. N., Lau, C. K., Li, M. L., Tam, K. H., Lam, C. T., Poon, R. T., and Fan, S. T. (2008) Identification of local and circulating cancer stem cells in human liver cancer, *Hepatology 47*, 919-928.
98. da Cunha, C. B., Oliveira, C., Wen, X., Gomes, B., Sousa, S., Suriano, G., Grellier, M., Huntsman, D. G., Carneiro, F., Granja, P. L., and Seruca, R. (2010) De novo expression of CD44 variants in sporadic and hereditary gastric cancer, *Lab Invest 90*, 1604-1614.
99. Takaishi, S., Okumura, T., Tu, S., Wang, S. S., Shibata, W., Vigneshwaran, R., Gordon, S. A., Shimada, Y., and Wang, T. C. (2009) Identification of gastric cancer stem cells using the cell surface marker CD44, *Stem Cells 27*, 1006-1020.
100. Schiapparelli, P., Enguita-German, M., Balbuena, J., Rey, J. A., Lazcoz, P., and Castresana, J. S. (2010) Analysis of stemness gene expression and CD133 abnormal methylation in neuroblastoma cell lines, *Oncol Rep 24*, 1355-1362.
101. Nakamura, M., Kyo, S., Zhang, B., Zhang, X., Mizumoto, Y., Takakura, M., Maida, Y., Mori, N., Hashimoto, M., Ohno, S., and Inoue, M. (2010) Prognostic impact of CD133 expression as a tumor-initiating cell marker in endometrial cancer, *Hum Pathol 41*, 1516-1529.
102. Mishra, L., Banker, T., Murray, J., Byers, S., Thenappan, A., He, A. R., Shetty, K., Johnson, L., and Reddy, E. P. (2009) Liver stem cells and hepatocellular carcinoma, *Hepatology 49*, 318-329.

103. Shmelkov, S. V., Butler, J. M., Hooper, A. T., Hormigo, A., Kushner, J., Milde, T., St Clair, R., Baljevic, M., White, I., Jin, D. K., Chadburn, A., Murphy, A. J., Valenzuela, D. M., Gale, N. W., Thurston, G., Yancopoulos, G. D., D'Angelica, M., Kemeny, N., Lyden, D., and Rafii, S. (2008) CD133 expression is not restricted to stem cells, and both CD133+ and CD133- metastatic colon cancer cells initiate tumors, *J Clin Invest 118*, 2111-2120.
104. Lugli, A., Iezzi, G., Hostettler, I., Muraro, M. G., Mele, V., Tornillo, L., Carafa, V., Spagnoli, G., Terracciano, L., and Zlobec, I. (2010) Prognostic impact of the expression of putative cancer stem cell markers CD133, CD166, CD44s, EpCAM, and ALDH1 in colorectal cancer, *Br J Cancer 103*, 382-390.
105. Wu, Y., and Wu, P. Y. (2009) CD133 as a marker for cancer stem cells: progresses and concerns, *Stem Cells Dev 18*, 1127-1134.
106. Schepers, A. G., Snippert, H. J., Stange, D. E., van den Born, M., van Es, J. H., van de Wetering, M., and Clevers, H. (2012) Lineage tracing reveals Lgr5+ stem cell activity in mouse intestinal adenomas, *Science 337*, 730-735.
107. Klonisch, T., Wiechec, E., Hombach-Klonisch, S., Ande, S. R., Wesselborg, S., Schulze-Osthoff, K., and Los, M. (2008) Cancer stem cell markers in common cancers - therapeutic implications, *Trends Mol Med 14*, 450-460.
108. Frank, N. Y., Schatton, T., and Frank, M. H. (2010) The therapeutic promise of the cancer stem cell concept, *J Clin Invest 120*, 41-50.
109. Preston, S. L., Wong, W.-M., Chan, A. O.-O., Poulsom, R., Jeffery, R., Goodlad, R. A., Mandir, N., Elia, G., Novelli, M., Bodmer, W. F., Tomlinson, I. P., and Wright, N. A. (2003) Bottom-up histogenesis of colorectal adenomas: origin in the monocryptal adenoma and initial expansion by crypt fission, *Cancer Res 63*, 3819-3825.
110. Barker, N., Ridgway, R. A., van Es, J. H., van de Wetering, M., Begthel, H., van den Born, M., Danenberg, E., Clarke, A. R., Sansom, O. J., and Clevers, H. (2009) Crypt stem cells as the cells-of-origin of intestinal cancer, *Nature 457*, 608-611.
111. Tian, H., Biehs, B., Warming, S., Leong, K. G., Rangell, L., Klein, O. D., and de Sauvage, F. J. (2011) A reserve stem cell population in small intestine renders Lgr5-positive cells dispensable, *Nature 478*, 255-259.
112. Wong, W.-M., Mandir, N., Goodlad, R. A., Wong, B. C. Y., Garcia, S. B., Lam, S.-K., and Wright, N. A. (2002) Histogenesis of human colorectal adenomas and hyperplastic polyps: the role of cell proliferation and crypt fission, *Gut 50*, 212-217.
113. Wright, N. A. (2000) Epithelial stem cell repertoire in the gut: clues to the origin of cell lineages, proliferative units and cancer, *International journal of experimental pathology 81*, 117-143.
114. Schwitalla, S., Fingerle, A. A., Cammareri, P., Nebelsiek, T., Goktuna, S. I., Ziegler, P. K., Canli, O., Heijmans, J., Huels, D. J., Moreaux, G., Rupec, R. A., Gerhard, M., Schmid, R., Barker, N., Clevers, H., Lang, R., Neumann, J., Kirchner, T., Taketo, M. M., van den Brink, G. R., Sansom, O. J., Arkan, M. C., and Greten, F. R. (2013) Intestinal tumorigenesis initiated by dedifferentiation and acquisition of stem-cell-like properties, *Cell 152*, 25-38.
115. Brittan, M., and Wright, N. A. (2004) The gastrointestinal stem cell, *Cell Prolif 37*, 35-53.
116. Cairns, J. (1975) Mutation selection and the natural history of cancer, *Nature 255*, 197-200.

117. Fitzgerald, R. C. (2008) Dissecting out the genetic origins of Barrett's oesophagus, *Gut 57*, 1033-1034.
118. Morson, B. (1974) President's address. The polyp-cancer sequence in the large bowel, *Proc R Soc Med 67*, 451-457.
119. Potter, J. D. (1999) Colorectal cancer: molecules and populations, *J Natl Cancer Inst 91*, 916-932.
120. Vogelstein, B., Fearon, E. R., Hamilton, S. R., Kern, S. E., Preisinger, A. C., Leppert, M., Nakamura, Y., White, R., Smits, A. M., and Bos, J. L. (1988) Genetic alterations during colorectal-tumor development, *N Engl J Med 319*, 525-532.
121. Fodde, R., Smits, R., and Clevers, H. (2001) APC, signal transduction and genetic instability in colorectal cancer, *Nat Rev Cancer 1*, 55-67.
122. Fearon, E. R., and Vogelstein, B. (1990) A genetic model for colorectal tumorigenesis, *Cell 61*, 759-767.
123. Reid, B. J., Li, X., Galipeau, P. C., and Vaughan, T. L. (2010) Barrett's oesophagus and oesophageal adenocarcinoma: time for a new synthesis, *Nat Rev Cancer 10*, 87-101.
124. Hruban, R. H., Goggins, M., Parsons, J., and Kern, S. E. (2000) Progression model for pancreatic cancer, *Clin Cancer Res 6*, 2969-2972.
125. Polyak, K. (2001) On the birth of breast cancer, *Biochim Biophys Acta 1552*, 1-13.
126. Abnet, C. C., Freedman, N. D., Hu, N., Wang, Z., Yu, K., Shu, X. O., Yuan, J. M., Zheng, W., Dawsey, S. M., Dong, L. M., Lee, M. P., Ding, T., Qiao, Y. L., Gao, Y. T., Koh, W. P., Xiang, Y. B., Tang, Z. Z., Fan, J. H., Wang, C., Wheeler, W., Gail, M. H., Yeager, M., Yuenger, J., Hutchinson, A., Jacobs, K. B., Giffen, C. A., Burdett, L., Fraumeni, J. F., Jr., Tucker, M. A., Chow, W. H., Goldstein, A. M., Chanock, S. J., and Taylor, P. R. (2010) A shared susceptibility locus in PLCE1 at 10q23 for gastric adenocarcinoma and esophageal squamous cell carcinoma, *Nat Genet 42*, 764-767.
127. Chien, A. J., Conrad, W. H., and Moon, R. T. (2009) A Wnt survival guide: from flies to human disease, *J Invest Dermatol 129*, 1614-1627.
128. Klaus, A., and Birchmeier, W. (2008) Wnt signalling and its impact on development and cancer, *Nature Reviews Cancer 8*, 387-398.
129. Giles, R. H., van Es, J. H., and Clevers, H. (2003) Caught up in a Wnt storm: Wnt signaling in cancer, *Biochim Biophys Acta 1653*, 1-24.
130. White, B. D., Chien, A. J., and Dawson, D. W. (2012) Dysregulation of Wnt/beta-catenin signaling in gastrointestinal cancers, *Gastroenterology 142*, 219-232.
131. Kinzler, K. W., Nilbert, M. C., Su, L. K., Vogelstein, B., Bryan, T. M., Levy, D. B., Smith, K. J., Preisinger, A. C., Hedge, P., McKechnie, D., and et al. (1991) Identification of FAP locus genes from chromosome 5q21, *Science 253*, 661-665.
132. Miyoshi, Y., Nagase, H., Ando, H., Horii, A., Ichii, S., Nakatsuru, S., Aoki, T., Miki, Y., Mori, T., and Nakamura, Y. (1992) Somatic mutations of the APC gene in colorectal tumors: mutation cluster region in the APC gene, *Hum Mol Genet 1*, 229-233.
133. Sivak, M. V., Jr., and Jagelman, D. G. (1984) Upper gastrointestinal endoscopy in polyposis syndromes: familial polyposis coli and Gardner's syndrome, *Gastrointest Endosc 30*, 102-104.

134. Nakatsuru, S., Yanagisawa, A., Ichii, S., Tahara, E., Kato, Y., Nakamura, Y., and Horii, A. (1992) Somatic mutation of the APC gene in gastric cancer: frequent mutations in very well differentiated adenocarcinoma and signet-ring cell carcinoma, *Hum Mol Genet 1*, 559-563.
135. Horii, A., Nakatsuru, S., Miyoshi, Y., Ichii, S., Nagase, H., Kato, Y., Yanagisawa, A., and Nakamura, Y. (1992) The APC gene, responsible for familial adenomatous polyposis, is mutated in human gastric cancer, *Cancer Research 52*, 3231-3233.
136. Fang, D.-C., Luo, Y.-H., Yang, S.-M., Li, X.-A., Ling, X.-L., and Fang, L. (2002) Mutation analysis of APC gene in gastric cancer with microsatellite instability, *World J Gastroenterol 8*, 787-791.
137. Gumbiner, B. M. (1995) Signal transduction of beta-catenin, *Curr Opin Cell Biol 7*, 634-640.
138. Polakis, P. (2000) Wnt signaling and cancer, *Genes Dev 14*, 1837-1851.
139. Schlosshauer, P. W., Pirog, E. C., Levine, R. L., and Ellenson, L. H. (2000) Mutational analysis of the CTNNB1 and APC genes in uterine endometrioid carcinoma, *Mod Pathol 13*, 1066-1071.
140. Sparks, A. B., Morin, P. J., Vogelstein, B., and Kinzler, K. W. (1998) Mutational analysis of the APC/beta-catenin/Tcf pathway in colorectal cancer, *Cancer Res 58*, 1130-1134.
141. Ebert, M. P. A., Fei, G., Kahmann, S., Müller, O., Yu, J., Sung, J. J. Y., and Malfertheiner, P. (2002) Increased beta-catenin mRNA levels and mutational alterations of the APC and beta-catenin gene are present in intestinal-type gastric cancer, *Carcinogenesis 23*, 87-91.
142. Park, W. S., Oh, R. R., Park, J. Y., Lee, S. H., Shin, M. S., Kim, Y. S., Kim, S. Y., Lee, H. K., Kim, P. J., Oh, S. T., Yoo, N. J., and Lee, J. Y. (1999) Frequent somatic mutations of the beta-catenin gene in intestinal-type gastric cancer, *Cancer Research 59*, 4257-4260.
143. Clements, W. M., Wang, J., Sarnaik, A., Kim, O. J., MacDonald, J., Fenoglio-Preiser, C., Groden, J., and Lowy, A. M. (2002) beta-Catenin mutation is a frequent cause of Wnt pathway activation in gastric cancer, *Cancer Research 62*, 3503-3506.
144. Tong, J. H., To, K. F., Ng, E. K., Lau, J. Y., Lee, T. L., Lo, K. W., Leung, W. K., Tang, N. L., Chan, F. K., Sung, J. J., and Chung, S. C. (2001) Somatic beta-catenin mutation in gastric carcinoma--an infrequent event that is not specific for microsatellite instability, *Cancer Lett 163*, 125-130.
145. Levine, A. J. (1997) p53, the cellular gatekeeper for growth and division, *Cell 88*, 323-331.
146. Tao, W., and Levine, A. J. (1999) P19(ARF) stabilizes p53 by blocking nucleo-cytoplasmic shuttling of Mdm2, *Proc Natl Acad Sci U S A 96*, 6937-6941.
147. Baker, S. J., Preisinger, A. C., Jessup, J. M., Paraskeva, C., Markowitz, S., Willson, J. K., Hamilton, S., and Vogelstein, B. (1990) p53 gene mutations occur in combination with 17p allelic deletions as late events in colorectal tumorigenesis, *Cancer Res 50*, 7717-7722.
148. Smith, G., Carey, F. A., Beattie, J., Wilkie, M. J. V., Lightfoot, T. J., Coxhead, J., Garner, R. C., Steele, R. J. C., and Wolf, C. R. (2002) Mutations in APC, Kirsten-ras, and p53--alternative genetic pathways to colorectal cancer, *Proc Natl Acad Sci USA 99*, 9433-9438.

149. Potten, C. S. (1998) Stem cells in gastrointestinal epithelium: numbers, characteristics and death, *Philos Trans R Soc Lond B Biol Sci 353*, 821-830.
150. Tamura, G., Kihana, T., Nomura, K., Terada, M., Sugimura, T., and Hirohashi, S. (1991) Detection of frequent p53 gene mutations in primary gastric cancer by cell sorting and polymerase chain reaction single-strand conformation polymorphism analysis, *Cancer Research 51*, 3056-3058.
151. Renault, B., van den Broek, M., Fodde, R., Wijnen, J., Pellegata, N. S., Amadori, D., Khan, P. M., and Ranzani, G. N. (1993) Base transitions are the most frequent genetic changes at P53 in gastric cancer, *Cancer Res 53*, 2614-2617.
152. Shiao, Y. H., Rugge, M., Correa, P., Lehmann, H. P., and Scheer, W. D. (1994) p53 alteration in gastric precancerous lesions, *Am J Pathol 144*, 511-517.
153. Correa, P., and Shiao, Y. H. (1994) Phenotypic and genotypic events in gastric carcinogenesis, *Cancer Research 54*, 1941s-1943s.
154. Flejou, J. F., Gratio, V., Muzeau, F., and Hamelin, R. (1999) p53 abnormalities in adenocarcinoma of the gastric cardia and antrum, *Mol Pathol 52*, 263-268.
155. Hanazono, K., Natsugoe, S., Stein, H. J., Aikou, T., Hoefler, H., and Siewert, J. R. (2006) Distribution of p53 mutations in esophageal and gastric carcinomas and the relationship with p53 expression, *Oncol Rep 15*, 821-824.
156. Anzola, M., Saiz, A., Cuevas, N., Lopez-Martinez, M., Martinez de Pancorbo, M. A., and Burgos, J. J. (2004) High levels of p53 protein expression do not correlate with p53 mutations in hepatocellular carcinoma, *J Viral Hepat 11*, 502-510.
157. Leedham, S. J., Preston, S. L., McDonald, S. A. C., Elia, G., Bhandari, P., Poller, D., Harrison, R., Novelli, M. R., Jankowski, J. A., and Wright, N. A. (2008) Individual crypt genetic heterogeneity and the origin of metaplastic glandular epithelium in human Barrett's oesophagus, *Gut 57*, 1041-1048.
158. Maley, C. C., Galipeau, P. C., Finley, J. C., Wongsurawat, V. J., Li, X., Sanchez, C. A., Paulson, T. G., Blount, P. L., Risques, R.-A., Rabinovitch, P. S., and Reid, B. J. (2006) Genetic clonal diversity predicts progression to esophageal adenocarcinoma, *Nat Genet 38*, 468-473.
159. Chung, S. M., Kao, J., Hyjek, E., and Chen, Y. T. (2007) p53 in esophageal adenocarcinoma: a critical reassessment of mutation frequency and identification of 72Arg as the dominant allele, *Int J Oncol 31*, 1351-1355.
160. Hollstein, M. C., Metcalf, R. A., Welsh, J. A., Montesano, R., and Harris, C. C. (1990) Frequent mutation of the p53 gene in human esophageal cancer, *Proc Natl Acad Sci U S A 87*, 9958-9961.
161. Shiraishi, H., Mikami, T., Yoshida, T., Tanabe, S., Kobayashi, N., Watanabe, M., and Okayasu, I. (2006) Early genetic instability of both epithelial and stromal cells in esophageal squamous cell carcinomas, contrasted with Barrett's adenocarcinomas, *J Gastroenterol 41*, 1186-1196.
162. Mandard, A. M., Hainaut, P., and Hollstein, M. (2000) Genetic steps in the development of squamous cell carcinoma of the esophagus, *Mutat Res 462*, 335-342.
163. Blaydon, D. C., Etheridge, S. L., Risk, J. M., Hennies, H. C., Gay, L. J., Carroll, R., Plagnol, V., McRonald, F. E., Stevens, H. P., Spurr, N. K., Bishop, D. T., Ellis, A., Jankowski, J., Field, J. K., Leigh, I. M., South, A. P., and

Kelsell, D. P. (2012) RHBDF2 mutations are associated with tylosis, a familial esophageal cancer syndrome, *Am J Hum Genet 90*, 340-346.
164. Kim, W. Y., and Sharpless, N. E. (2006) The regulation of INK4/ARF in cancer and aging, *Cell 127*, 265-275.
165. Zhao, G. H., Li, T. C., Shi, L. H., Xia, Y. B., Lu, L. M., Huang, W. B., Sun, H. L., and Zhang, Y. S. (2003) Relationship between inactivation of p16 gene and gastric carcinoma, *World J Gastroenterol 9*, 905-909.
166. Barrett, M. T., Sanchez, C. A., Prevo, L. J., Wong, D. J., Galipeau, P. C., Paulson, T. G., Rabinovitch, P. S., and Reid, B. J. (1999) Evolution of neoplastic cell lineages in Barrett oesophagus, *Nat Genet 22*, 106-109.
167. Xing, E. P., Nie, Y., Wang, L. D., Yang, G. Y., and Yang, C. S. (1999) Aberrant methylation of p16INK4a and deletion of p15INK4b are frequent events in human esophageal cancer in Linxian, China, *Carcinogenesis 20*, 77-84.
168. Ferlay, J., Shin, H. R., Bray, F., Forman, D., Mathers, C., and Parkin, D. M. (2010) Estimates of worldwide burden of cancer in 2008: GLOBOCAN 2008, *Int J Cancer*.
169. Pan, S. Y., and Morrison, H. (2011) Epidemiology of cancer of the small intestine, *World J Gastrointest Oncol 3*, 33-42.
170. Haan, J. C., Buffart, T. E., Eijk, P. P., van de Wiel, M. A., van Wieringen, W. N., Howdle, P. D., Mulder, C. J., van de Velde, C. J., Quirke, P., Nagtegaal, I. D., van Grieken, N. C., Grabsch, H., Meijer, G. A., and Ylstra, B. (2012) Small bowel adenocarcinoma copy number profiles are more closely related to colorectal than to gastric cancers, *Ann Oncol 23*, 367-374.
171. Gore, R. M. (1997) Gastric cancer. Clinical and pathologic features, *Radiol Clin North Am 35*, 295-310.
172. Oliveira, C., Seruca, R., and Carneiro, F. (2006) Genetics, pathology, and clinics of familial gastric cancer, *Int J Surg Pathol 14*, 21-33.
173. Angst, B. D., Marcozzi, C., and Magee, A. I. (2001) The cadherin superfamily: diversity in form and function, *J Cell Sci 114*, 629-641.
174. Haussinger, D., Ahrens, T., Aberle, T., Engel, J., Stetefeld, J., and Grzesiek, S. (2004) Proteolytic E-cadherin activation followed by solution NMR and X-ray crystallography, *EMBO J 23*, 1699-1708.
175. Haussinger, D., Ahrens, T., Sass, H. J., Pertz, O., Engel, J., and Grzesiek, S. (2002) Calcium-dependent homoassociation of E-cadherin by NMR spectroscopy: changes in mobility, conformation and mapping of contact regions, *J Mol Biol 324*, 823-839.
176. Davis, M. A., Ireton, R. C., and Reynolds, A. B. (2003) A core function for p120-catenin in cadherin turnover, *J Cell Biol 163*, 525-534.
177. Aberle, H., Butz, S., Stappert, J., Weissig, H., Kemler, R., and Hoschuetzky, H. (1994) Assembly of the cadherin-catenin complex in vitro with recombinant proteins, *J Cell Sci 107 (Pt 12)*, 3655-3663.
178. D'Souza-Schorey, C. (2005) Disassembling adherens junctions: breaking up is hard to do, *Trends Cell Biol 15*, 19-26.
179. Acloque, H., Adams, M. S., Fishwick, K., Bronner-Fraser, M., and Nieto, M. A. (2009) Epithelial-mesenchymal transitions: the importance of changing cell state in development and disease, *J Clin Invest 119*, 1438-1449.
180. Batlle, E., and Wilkinson, D. G. (2012) Molecular mechanisms of cell segregation and boundary formation in development and tumorigenesis, *Cold Spring Harb Perspect Biol 4*.

181. Seevaratnam, R., Coburn, N., Cardoso, R., Dixon, M., Bocicariu, A., and Helyer, L. (2012) A systematic review of the indications for genetic testing and prophylactic gastrectomy among patients with hereditary diffuse gastric cancer, *Gastric Cancer,* Suppl 1:S153-63.
182. Oliveira, C., Sousa, S., Pinheiro, H., Karam, R., Bordeira-Carrico, R., Senz, J., Kaurah, P., Carvalho, J., Pereira, R., Gusmao, L., Wen, X., Cipriano, M. A., Yokota, J., Carneiro, F., Huntsman, D., and Seruca, R. (2009) Quantification of epigenetic and genetic 2nd hits in CDH1 during hereditary diffuse gastric cancer syndrome progression, *Gastroenterology 136*, 2137-2148.
183. Gaya, D. R., Stuart, R. C., McKee, R. F., Going, J. J., Davidson, R., and Stanley, A. J. (2005) E-cadherin mutation-associated diffuse gastric adenocarcinoma: penetrance and non-penetrance, *Eur J Gastroenterol Hepatol 17*, 1425-1428.
184. More, H., Humar, B., Weber, W., Ward, R., Christian, A., Lintott, C., Graziano, F., Ruzzo, A. M., Acosta, E., Boman, B., Harlan, M., Ferreira, P., Seruca, R., Suriano, G., and Guilford, P. (2007) Identification of seven novel germline mutations in the human E-cadherin (CDH1) gene, *Hum Mutat 28*, 203.
185. Norton, J. A., Ham, C. M., Van Dam, J., Jeffrey, R. B., Longacre, T. A., Huntsman, D. G., Chun, N., Kurian, A. W., and Ford, J. M. (2007) CDH1 truncating mutations in the E-cadherin gene: an indication for total gastrectomy to treat hereditary diffuse gastric cancer, *Ann Surg 245*, 873-879.
186. Pilpilidis, I., Kountouras, J., Zavos, C., and Katsinelos, P. (2011) Upper gastrointestinal carcinogenesis: H. pylori and stem cell cross-talk, *J Surg Res 166*, 255-264.
187. Correa, P., and Piazuelo, M. B. (2012) The gastric precancerous cascade, *J Dig Dis 13*, 2-9.
188. Fox, J. G., and Wang, T. C. (2007) Inflammation, atrophy, and gastric cancer, *J Clin Invest 117*, 60-69.
189. Saikawa, Y., Fukuda, K., Takahashi, T., Nakamura, R., Takeuchi, H., and Kitagawa, Y. (2010) Gastric carcinogenesis and the cancer stem cell hypothesis, *Gastric Cancer 13*, 11-24.
190. Ding, S. Z., Goldberg, J. B., and Hatakeyama, M. (2010) Helicobacter pylori infection, oncogenic pathways and epigenetic mechanisms in gastric carcinogenesis, *Future Oncol 6*, 851-862.
191. Perrin, D., Ruskin, H. J., and Niwa, T. (2010) Cell type-dependent, infection-induced, aberrant DNA methylation in gastric cancer, *J Theor Biol 264*, 570-577.
192. Reis, C. A., David, L., Correa, P., Carneiro, F., de Bolós, C., Garcia, E., Mandel, U., Clausen, H., and Sobrinho-Simões, M. (1999) Intestinal metaplasia of human stomach displays distinct patterns of mucin (MUC1, MUC2, MUC5AC, and MUC6) expression, *Cancer Research 59*, 1003-1007.
193. Gong, C., Mera, R., Bravo, J. C., Ruiz, B., Diaz-Escamilla, R., Fontham, E. T., Correa, P., and Hunt, J. D. (1999) KRAS mutations predict progression of preneoplastic gastric lesions, *Cancer Epidemiol Biomarkers Prev 8*, 167-171.
194. Alpizar-Alpizar, W., Nielsen, B. S., Sierra, R., Illemann, M., Ramirez, J. A., Arias, A., Duran, S., Skarstein, A., Ovrebo, K., Lund, L. R., and Laerum, O. D. (2010) Urokinase plasminogen activator receptor is expressed in invasive cells in gastric carcinomas from high- and low-risk countries, *Int J Cancer 126*, 405-415.

195. Koshikawa, N., Mizushima, H., Minegishi, T., Iwamoto, R., Mekada, E., and Seiki, M. (2010) Membrane type 1-matrix metalloproteinase cleaves off the NH2-terminal portion of heparin-binding epidermal growth factor and converts it into a heparin-independent growth factor, *Cancer Res 70*, 6093-6103.
196. Kubota, E., Kataoka, H., Aoyama, M., Mizoshita, T., Mori, Y., Shimura, T., Tanaka, M., Sasaki, M., Takahashi, S., Asai, K., and Joh, T. (2010) Role of ES cell-expressed Ras (ERas) in tumorigenicity of gastric cancer, *Am J Pathol 177*, 955-963.
197. Mutoh, H., Sashikawa, M., Hayakawa, H., and Sugano, K. (2010) Monocyte chemoattractant protein-1 is generated via TGF-beta by myofibroblasts in gastric intestinal metaplasia and carcinoma without H. pylori infection, *Cancer Sci 101*, 1783-1789.
198. Zhi, K., Shen, X., Zhang, H., and Bi, J. (2010) Cancer-associated fibroblasts are positively correlated with metastatic potential of human gastric cancers, *J Exp Clin Cancer Res 29*, 66.
199. Xu, X., Zhang, X., Wang, S., Qian, H., Zhu, W., Cao, H., Wang, M., Chen, Y., and Xu, W. (2011) Isolation and comparison of mesenchymal stem-like cells from human gastric cancer and adjacent non-cancerous tissues, *J Cancer Res Clin Oncol*. 137(3):495-504.
200. Li, V. S. W., Wong, C. W., Chan, T. L., Chan, A. S. W., Zhao, W., Chu, K.-M., So, S., Chen, X., Yuen, S. T., and Leung, S. Y. (2005) Mutations of PIK3CA in gastric adenocarcinoma, *BMC Cancer 2009 9:157 5*, 29.
201. Tamura, G. (2006) Alterations of tumor suppressor and tumor-related genes in the development and progression of gastric cancer, *World J Gastroenterol 12*, 192-198.
202. Wang, K., Kan, J., Yuen, S. T., Shi, S. T., Chu, K. M., Law, S., Chan, T. L., Kan, Z., Chan, A. S., Tsui, W. Y., Lee, S. P., Ho, S. L., Chan, A. K., Cheng, G. H., Roberts, P. C., Rejto, P. A., Gibson, N. W., Pocalyko, D. J., Mao, M., Xu, J., and Leung, S. Y. (2011) Exome sequencing identifies frequent mutation of ARID1A in molecular subtypes of gastric cancer, *Nat Genet 43*, 1219-1223.
203. Zang, Z. J., Cutcutache, I., Poon, S. L., Zhang, S. L., McPherson, J. R., Tao, J., Rajasegaran, V., Heng, H. L., Deng, N., Gan, A., Lim, K. H., Ong, C. K., Huang, D., Chin, S. Y., Tan, I. B., Ng, C. C., Yu, W., Wu, Y., Lee, M., Wu, J., Poh, D., Wan, W. K., Rha, S. Y., So, J., Salto-Tellez, M., Yeoh, K. G., Wong, W. K., Zhu, Y. J., Futreal, P. A., Pang, B., Ruan, Y., Hillmer, A. M., Bertrand, D., Nagarajan, N., Rozen, S., Teh, B. T., and Tan, P. (2012) Exome sequencing of gastric adenocarcinoma identifies recurrent somatic mutations in cell adhesion and chromatin remodeling genes, *Nat Genet*. 44,570–574.
204. Khayat, A. S., Guimarães, A. C., Calcagno, D. Q., Seabra, A. D., Lima, E. M., Leal, M. F., Faria, M. H. G., Rabenhorst, S. H. B., Assumpção, P. P., Demachki, S., Smith, M. A. C., and Burbano, R. R. (2009) Interrelationship between TP53 gene deletion, protein expression and chromosome 17 aneusomy in gastric adenocarcinoma, *BMC gastroenterology 9*, 55.
205. Ranzani, G. N., Luinetti, O., Padovan, L. S., Calistri, D., Renault, B., Burrel, M., Amadori, D., Fiocca, R., and Solcia, E. (1995) p53 gene mutations and protein nuclear accumulation are early events in intestinal type gastric cancer but late events in diffuse type, *Cancer Epidemiol Biomarkers Prev 4*, 223-231.

206. Nakatsuru, S., Yanagisawa, A., Furukawa, Y., Ichii, S., Kato, Y., Nakamura, Y., and Horii, A. (1993) Somatic mutations of the APC gene in precancerous lesion of the stomach, *Hum Mol Genet 2*, 1463-1465.
207. Tamura, G., Maesawa, C., Suzuki, Y., Tamada, H., Satoh, M., Ogasawara, S., Kashiwaba, M., and Satodate, R. (1994) Mutations of the APC gene occur during early stages of gastric adenoma development, *Cancer Research 54*, 1149-1151.
208. Deng, N., Goh, L. K., Wang, H., Das, K., Tao, J., Tan, I. B., Zhang, S., Lee, M., Wu, J., Lim, K. H., Lei, Z., Goh, G., Lim, Q. Y., Tan, A. L., Sin Poh, D. Y., Riahi, S., Bell, S., Shi, M. M., Linnartz, R., Zhu, F., Yeoh, K. G., Toh, H. C., Yong, W. P., Cheong, H. C., Rha, S. Y., Boussioutas, A., Grabsch, H., Rozen, S., and Tan, P. (2012) A comprehensive survey of genomic alterations in gastric cancer reveals systematic patterns of molecular exclusivity and co-occurrence among distinct therapeutic targets, *Gut 61*, 673-684.
209. Hongyo, T., Buzard, G. S., Palli, D., Weghorst, C. M., Amorosi, A., Galli, M., Caporaso, N. E., Fraumeni, J. F., Jr., and Rice, J. M. (1995) Mutations of the K-ras and p53 genes in gastric adenocarcinomas from a high-incidence region around Florence, Italy, *Cancer Res 55*, 2665-2672.
210. Wu, M. S., Shun, C. T., Sheu, J. C., Wang, H. P., Wang, J. T., Lee, W. J., Chen, C. J., Wang, T. H., and Lin, J. T. (1998) Overexpression of mutant p53 and c-erbB-2 proteins and mutations of the p15 and p16 genes in human gastric carcinoma: with respect to histological subtypes and stages, *J Gastroenterol Hepatol 13*, 305-310.
211. Samuels, Y., Wang, Z., Bardelli, A., Silliman, N., Ptak, J., Szabo, S., Yan, H., Gazdar, A., Powell, S. M., Riggins, G. J., Willson, J. K. V., Markowitz, S., Kinzler, K. W., Vogelstein, B., and Velculescu, V. E. (2004) High frequency of mutations of the PIK3CA gene in human cancers, *Science 304*, 554.
212. Barbi, S., Cataldo, I., De Manzoni, G., Bersani, S., Lamba, S., Mattuzzi, S., Bardelli, A., and Scarpa, A. (2010) The analysis of PIK3CA mutations in gastric carcinoma and metanalysis of literature suggest that exon-selectivity is a signature of cancer type, *Journal of experimental & clinical cancer research : CR 29*, 32.
213. Lee, J., van Hummelen, P., Go, C., Palescandolo, E., Jang, J., Park, H. Y., Kang, S. Y., Park, J. O., Kang, W. K., Macconaill, L., and Kim, K. M. (2012) High-throughput mutation profiling identifies frequent somatic mutations in advanced gastric adenocarcinoma, *PLoS ONE 7*, e38892.
214. Tate, G., Suzuki, T., Nemoto, H., Kishimoto, K., Hibi, K., and Mitsuya, T. (2009) Allelic loss of the PTEN gene and mutation of the TP53 gene in choriocarcinoma arising from gastric adenocarcinoma: analysis of loss of heterozygosity in two male patients with extragonadal choriocarcinoma, *Cancer Genet Cytogenet 193*, 104-108.
215. Guo, C. Y., Xu, X. F., Wu, J. Y., and Liu, S. F. (2008) PCR-SSCP-DNA sequencing method in detecting PTEN gene mutation and its significance in human gastric cancer, *World J Gastroenterol 14*, 3804-3811.
216. Wang, J. Y., Huang, T. J., Chen, F. M., Hsieh, M. C., Lin, S. R., Hou, M. F., and Hsieh, J. S. (2003) Mutation analysis of the putative tumor suppressor gene PTEN/MMAC1 in advanced gastric carcinomas, *Virchows Arch 442*, 437-443.

217. Lagergren, J., Bergstrom, R., Lindgren, A., and Nyren, O. (1999) Symptomatic gastroesophageal reflux as a risk factor for esophageal adenocarcinoma, *N Engl J Med 340*, 825-831.
218. Hvid-Jensen, F., Pedersen, L., Drewes, A. M., Sorensen, H. T., and Funch-Jensen, P. (2011) Incidence of adenocarcinoma among patients with Barrett's esophagus, *N Engl J Med 365*, 1375-1383.
219. Jemal, A., Bray, F., Center, M. M., Ferlay, J., Ward, E., and Forman, D. (2011) Global cancer statistics, *CA Cancer J Clin 61*, 69-90.
220. Reid, B. J., Li, X., Galipeau, P. C., and Vaughan, T. L. (2010) Barrett's oesophagus and oesophageal adenocarcinoma: time for a new synthesis, *Nature Reviews Cancer 10*, 87-101.
221. Maley, C. C., and Reid, B. J. (2005) Natural selection in neoplastic progression of Barrett's esophagus, *Seminars in Cancer Biology 15*, 474-483.
222. Nicholson, A. M., Graham, T. A., Simpson, A., Humphries, A., Burch, N., Rodriguez-Justo, M., Novelli, M., Harrison, R., Wright, N. A., McDonald, S. A., and Jankowski, J. A. (2011) Barrett's metaplasia glands are clonal, contain multiple stem cells and share a common squamous progenitor, *Gut* 61:1380-9.
223. Jankowski, J., Coghill, G., Hopwood, D., and Wormsley, K. G. (1992) Oncogenes and onco-suppressor gene in adenocarcinoma of the oesophagus, *Gut 33*, 1033-1038.
224. Wong, D. J., Paulson, T. G., Prevo, L. J., Galipeau, P. C., Longton, G., Blount, P. L., and Reid, B. J. (2001) p16(INK4a) lesions are common, early abnormalities that undergo clonal expansion in Barrett's metaplastic epithelium, *Cancer Res 61*, 8284-8289.
225. Bailey, T., Biddlestone, L., Shepherd, N., Barr, H., Warner, P., and Jankowski, J. (1998) Altered cadherin and catenin complexes in the Barrett's esophagus-dysplasia-adenocarcinoma sequence: correlation with disease progression and dedifferentiation, *Am J Pathol 152*, 135-144.
226. Crespi, M., Munoz, N., Grassi, A., Qiong, S., Jing, W. K., and Jien, L. J. (1984) Precursor lesions of oesophageal cancer in a low-risk population in China: comparison with high-risk populations, *Int J Cancer 34*, 599-602.
227. Qiu, S. L., and Yang, G. R. (1988) Precursor lesions of esophageal cancer in high-risk populations in Henan Province, China, *Cancer 62*, 551-557.
228. Wang, G. Q., Abnet, C. C., Shen, Q., Lewin, K. J., Sun, X. D., Roth, M. J., Qiao, Y. L., Mark, S. D., Dong, Z. W., Taylor, P. R., and Dawsey, S. M. (2005) Histological precursors of oesophageal squamous cell carcinoma: results from a 13 year prospective follow up study in a high risk population, *Gut 54*, 187-192.
229. Clayton, E., Doupe, D. P., Klein, A. M., Winton, D. J., Simons, B. D., and Jones, P. H. (2007) A single type of progenitor cell maintains normal epidermis, *Nature 446*, 185-189.
230. Hollstein, M. C., Peri, L., Mandard, A. M., Welsh, J. A., Montesano, R., Metcalf, R. A., Bak, M., and Harris, C. C. (1991) Genetic analysis of human esophageal tumors from two high incidence geographic areas: frequent p53 base substitutions and absence of ras mutations, *Cancer Res 51*, 4102-4106.
231. Kwak, E. L., Jankowski, J., Thayer, S. P., Lauwers, G. Y., Brannigan, B. W., Harris, P. L., Okimoto, R. A., Haserlat, S. M., Driscoll, D. R., Ferry, D., Muir, B., Settleman, J., Fuchs, C. S., Kulke, M. H., Ryan, D. P., Clark, J. W., Sgroi, D. C., Haber, D. A., and Bell, D. W. (2006) Epidermal growth factor receptor

kinase domain mutations in esophageal and pancreatic adenocarcinomas, *Clin Cancer Res 12*, 4283-4287.
232. Stoner, G. D., and Gupta, A. (2001) Etiology and chemoprevention of esophageal squamous cell carcinoma, *Carcinogenesis 22*, 1737-1746.
233. Agrawal, N., Jiao, Y., Bettegowda, C., Hutfless, S. M., Wang, Y., David, S., Cheng, Y., Twaddell, W. S., Latt, N. L., Shin, E. J., Wang, L. D., Wang, L., Yang, W., Velculescu, V. E., Vogelstein, B., Papadopoulos, N., Kinzler, K. W., and Meltzer, S. J. (2012) Comparative genomic analysis of esophageal adenocarcinoma and squamous cell carcinoma, *Cancer Discov 2*, 899-905.
234. Shibata, T., Kokubu, A., Saito, S., Narisawa-Saito, M., Sasaki, H., Aoyagi, K., Yoshimatsu, Y., Tachimori, Y., Kushima, R., Kiyono, T., and Yamamoto, M. (2011) NRF2 mutation confers malignant potential and resistance to chemoradiation therapy in advanced esophageal squamous cancer, *Neoplasia 13*, 864-873.
235. Kim, Y. R., Oh, J. E., Kim, M. S., Kang, M. R., Park, S. W., Han, J. Y., Eom, H. S., Yoo, N. J., and Lee, S. H. (2010) Oncogenic NRF2 mutations in squamous cell carcinomas of oesophagus and skin, *J Pathol 220*, 446-451.
236. DeNicola, G. M., Karreth, F. A., Humpton, T. J., Gopinathan, A., Wei, C., Frese, K., Mangal, D., Yu, K. H., Yeo, C. J., Calhoun, E. S., Scrimieri, F., Winter, J. M., Hruban, R. H., Iacobuzio-Donahue, C., Kern, S. E., Blair, I. A., and Tuveson, D. A. (2011) Oncogene-induced Nrf2 transcription promotes ROS detoxification and tumorigenesis, *Nature 475*, 106-109.
237. Hennies, H. C., Hagedorn, M., and Reis, A. (1995) Palmoplantar keratoderma in association with carcinoma of the esophagus maps to chromosome 17q distal to the keratin gene cluster, *Genomics 29*, 537-540.
238. Ellis, A., Field, J. K., Field, E. A., Friedmann, P. S., Fryer, A., Howard, P., Leigh, I. M., Risk, J., Shaw, J. M., and Whittaker, J. (1994) Tylosis associated with carcinoma of the oesophagus and oral leukoplakia in a large Liverpool family--a review of six generations, *Eur J Cancer B Oral Oncol 30B*, 102-112.
239. Stevens, H. P., Kelsell, D. P., Bryant, S. P., Bishop, D. T., Spurr, N. K., Weissenbach, J., Marger, D., Marger, R. S., and Leigh, I. M. (1996) Linkage of an American pedigree with palmoplantar keratoderma and malignancy (palmoplantar ectodermal dysplasia type III) to 17q24. Literature survey and proposed updated classification of the keratodermas, *Arch Dermatol 132*, 640-651.
240. Lemberg, M. K., and Freeman, M. (2007) Cutting proteins within lipid bilayers: rhomboid structure and mechanism, *Mol Cell 28*, 930-940.
241. Lemberg, M. K., and Freeman, M. (2007) Functional and evolutionary implications of enhanced genomic analysis of rhomboid intramembrane proteases, *Genome Res 17*, 1634-1646.
242. Etheridge, S. L., Brooke, M. A., Kelsell, D. P., and Blaydon, D. C. (2013) Rhomboid proteins: a role in keratinocyte proliferation and cancer, *Cell Tissue Res 351*, 301-307.
243. Adrain, C., Zettl, M., Christova, Y., Taylor, N., and Freeman, M. (2012) Tumor necrosis factor signaling requires iRhom2 to promote trafficking and activation of TACE, *Science 335*, 225-228.
244. Freeman, M. (2009) Rhomboids: 7 years of a new protease family, *Semin Cell Dev Biol 20*, 231-239.

245. Zettl, M., Adrain, C., Strisovsky, K., Lastun, V., and Freeman, M. (2011) Rhomboid family pseudoproteases use the ER quality control machinery to regulate intercellular signaling, *Cell 145*, 79-91.
246. McIlwain, D. R., Lang, P. A., Maretzky, T., Hamada, K., Ohishi, K., Maney, S. K., Berger, T., Murthy, A., Duncan, G., Xu, H. C., Lang, K. S., Haussinger, D., Wakeham, A., Itie-Youten, A., Khokha, R., Ohashi, P. S., Blobel, C. P., and Mak, T. W. (2012) iRhom2 regulation of TACE controls TNF-mediated protection against Listeria and responses to LPS, *Science 335*, 229-232.
247. Tokumaru, S., Higashiyama, S., Endo, T., Nakagawa, T., Miyagawa, J. I., Yamamori, K., Hanakawa, Y., Ohmoto, H., Yoshino, K., Shirakata, Y., Matsuzawa, Y., Hashimoto, K., and Taniguchi, N. (2000) Ectodomain shedding of epidermal growth factor receptor ligands is required for keratinocyte migration in cutaneous wound healing, *J Cell Biol 151*, 209-220.
248. McDonald, S. A., Greaves, L. C., Gutierrez-Gonzalez, L., Rodriguez-Justo, M., Deheragoda, M., Leedham, S. J., Taylor, R. W., Lee, C. Y., Preston, S. L., Lovell, M., Hunt, T., Elia, G., Oukrif, D., Harrison, R., Novelli, M. R., Mitchell, I., Stoker, D. L., Turnbull, D. M., Jankowski, J. A., and Wright, N. A. (2008) Mechanisms of field cancerization in the human stomach: the expansion and spread of mutated gastric stem cells, *Gastroenterology 134*, 500-510.
249. Correa, P., Cuello, C., and Duque, E. (1970) Carcinoma and intestinal metaplasia of the stomach in Colombian migrants, *J Natl Cancer Inst 44*, 297-306.
250. Braakhuis, B. J. M., Tabor, M. P., Kummer, J. A., Leemans, C. R., and Brakenhoff, R. H. (2003) A genetic explanation of Slaughter's concept of field cancerization: evidence and clinical implications, *Cancer Res 63*, 1727-1730.
251. Graham, T. A., and McDonald, S. A. C. (2010) Genetic diversity during the development of Barrett's oesophagus-associated adenocarcinoma: how, when and why?, *Biochem Soc Trans 38*, 374-379.
252. Walther, A., Johnstone, E., Swanton, C., Midgley, R., Tomlinson, I., and Kerr, D. (2009) Genetic prognostic and predictive markers in colorectal cancer, *Nat Rev Cancer 9*, 489-499.
253. Bozic, I., Antal, T., Ohtsuki, H., Carter, H., Kim, D., Chen, S., Karchin, R., Kinzler, K. W., Vogelstein, B., and Nowak, M. A. (2010) Accumulation of driver and passenger mutations during tumor progression, *Proc Natl Acad Sci U S A 107*, 18545-18550.
254. Guilford, P., Hopkins, J., Harraway, J., McLeod, M., McLeod, N., Harawira, P., Taite, H., Scoular, R., Miller, A., and Reeve, A. E. (1998) E-cadherin germline mutations in familial gastric cancer, *Nature 392*, 402-405.
255. Shiao, Y. H., Palli, D., Buzard, G. S., Caporaso, N. E., Amorosi, A., Saieva, C., Fraumeni, J. F., Jr., Anderson, L. M., and Rice, J. M. (1998) Implications of p53 mutation spectrum for cancer etiology in gastric cancers of various histologic types from a high-risk area of central Italy, *Carcinogenesis 19*, 2145-2149.
256. www.sanger.ac.uk/genetics/cgp/cosmic. (2012).
257. Machado, J. C., Oliveira, C., Carvalho, R., Soares, P., Berx, G., Caldas, C., Seruca, R., Carneiro, F., and Sobrinho-Simoes, M. (2001) E-cadherin gene (CDH1) promoter methylation as the second hit in sporadic diffuse gastric carcinoma, *Oncogene 20*, 1525-1528.

258. Chan, A. O., Lam, S. K., Wong, B. C., Wong, W. M., Yuen, M. F., Yeung, Y. H., Hui, W. M., Rashid, A., and Kwong, Y. L. (2003) Promoter methylation of E-cadherin gene in gastric mucosa associated with Helicobacter pylori infection and in gastric cancer, *Gut 52*, 502-506.
259. Shima, H., Hiyama, T., Tanaka, S., Yoshihara, M., Arihiro, K., and Chayama, K. (2006) Genetic progression and divergence in superficial esophageal squamous cell carcinoma by loss of heterozygosity analysis, *Oncol Rep 16*, 685-691.
260. Miller, R. (1981) *Simultaneous Statistical Inference*, 2nd ed. Springer Verlag, pages 6-8.
261. Lefort, K., Mandinova, A., Ostano, P., Kolev, V., Calpini, V., Kolfschoten, I., Devgan, V., Lieb, J., Raffoul, W., Hohl, D., Neel, V., Garlick, J., Chiorino, G., and Dotto, G. P. (2007) Notch1 is a p53 target gene involved in human keratinocyte tumor suppression through negative regulation of ROCK1/2 and MRCKalpha kinases, *Genes Dev 21*, 562-577.
262. von Brevern, M., Hollstein, M. C., Risk, J. M., Garde, J., Bennett, W. P., Harris, C. C., Muehlbauer, K. R., and Field, J. K. (1998) Loss of heterozygosity in sporadic oesophageal tumors in the tylosis oesophageal cancer (TOC) gene region of chromosome 17q, *Oncogene 17*, 2101-2105.
263. Saarinen, S., Vahteristo, P., Lehtonen, R., Aittomaki, K., Launonen, V., Kiviluoto, T., and Aaltonen, L. A. (2012) Analysis of a Finnish family confirms RHBDF2 mutations as the underlying factor in tylosis with esophageal cancer, *Fam Cancer 11*, 525-528.
264. Cheng, T. L., Wu, Y. T., Lin, H. Y., Hsu, F. C., Liu, S. K., Chang, B. I., Chen, W. S., Lai, C. H., Shi, G. Y., and Wu, H. L. (2011) Functions of rhomboid family protease RHBDL2 and thrombomodulin in wound healing, *J Invest Dermatol 131*, 2486-2494.
265. Pascall, J. C., and Brown, K. D. (2004) Intramembrane cleavage of ephrinB3 by the human rhomboid family protease, RHBDL2, *Biochem Biophys Res Commun 317*, 244-252.
266. Su, A. I., Wiltshire, T., Batalov, S., Lapp, H., Ching, K. A., Block, D., Zhang, J., Soden, R., Hayakawa, M., Kreiman, G., Cooke, M. P., Walker, J. R., and Hogenesch, J. B. (2004) A gene atlas of the mouse and human protein-encoding transcriptomes, *Proc Natl Acad Sci U S A 101*, 6062-6067.
267. Nakagawa, T., Guichard, A., Castro, C. P., Xiao, Y., Rizen, M., Zhang, H. Z., Hu, D., Bang, A., Helms, J., Bier, E., and Derynck, R. (2005) Characterization of a human rhomboid homolog, p100hRho/RHBDF1, which interacts with TGF-alpha family ligands, *Dev Dyn 233*, 1315-1331.
268. Huovila, A. P., Turner, A. J., Pelto-Huikko, M., Karkkainen, I., and Ortiz, R. M. (2005) Shedding light on ADAM metalloproteinases, *Trends Biochem Sci 30*, 413-422.
269. Sahin, U., and Blobel, C. P. (2007) Ectodomain shedding of the EGF-receptor ligand epigen is mediated by ADAM17, *FEBS Lett 581*, 41-44.
270. Agrawal, N., Frederick, M. J., Pickering, C. R., Bettegowda, C., Chang, K., Li, R. J., Fakhry, C., Xie, T. X., Zhang, J., Wang, J., Zhang, N., El-Naggar, A. K., Jasser, S. A., Weinstein, J. N., Trevino, L., Drummond, J. A., Muzny, D. M., Wu, Y., Wood, L. D., Hruban, R. H., Westra, W. H., Koch, W. M., Califano, J. A., Gibbs, R. A., Sidransky, D., Vogelstein, B., Velculescu, V. E., Papadopoulos, N., Wheeler, D. A., Kinzler, K. W., and Myers, J. N. (2011)

Exome sequencing of head and neck squamous cell carcinoma reveals inactivating mutations in NOTCH1, *Science 333*, 1154-1157.
271. Leedham, S. J., and Wright, N. A. (2008) Human tumour clonality assessment--flawed but necessary, *J Pathol 215*, 351-354.
272. Bignold, L. P., Coghlan, Brian L. D., Jersmann, Hubertus P.A. (2007) *David Paul von Hansemann: Contributions to Oncology*, Springer.
273. van Haaften, G., Dalgliesh, G. L., Davies, H., Chen, L., Bignell, G., Greenman, C., Edkins, S., Hardy, C., O'Meara, S., Teague, J., Butler, A., Hinton, J., Latimer, C., Andrews, J., Barthorpe, S., Beare, D., Buck, G., Campbell, P. J., Cole, J., Forbes, S., Jia, M., Jones, D., Kok, C. Y., Leroy, C., Lin, M. L., McBride, D. J., Maddison, M., Maquire, S., McLay, K., Menzies, A., Mironenko, T., Mulderrig, L., Mudie, L., Pleasance, E., Shepherd, R., Smith, R., Stebbings, L., Stephens, P., Tang, G., Tarpey, P. S., Turner, R., Turrell, K., Varian, J., West, S., Widaa, S., Wray, P., Collins, V. P., Ichimura, K., Law, S., Wong, J., Yuen, S. T., Leung, S. Y., Tonon, G., DePinho, R. A., Tai, Y. T., Anderson, K. C., Kahnoski, R. J., Massie, A., Khoo, S. K., Teh, B. T., Stratton, M. R., and Futreal, P. A. (2009) Somatic mutations of the histone H3K27 demethylase gene UTX in human cancer, *Nat Genet 41*, 521-523.
274. Dalgliesh, G. L., Furge, K., Greenman, C., Chen, L., Bignell, G., Butler, A., Davies, H., Edkins, S., Hardy, C., Latimer, C., Teague, J., Andrews, J., Barthorpe, S., Beare, D., Buck, G., Campbell, P. J., Forbes, S., Jia, M., Jones, D., Knott, H., Kok, C. Y., Lau, K. W., Leroy, C., Lin, M. L., McBride, D. J., Maddison, M., Maguire, S., McLay, K., Menzies, A., Mironenko, T., Mulderrig, L., Mudie, L., O'Meara, S., Pleasance, E., Rajasingham, A., Shepherd, R., Smith, R., Stebbings, L., Stephens, P., Tang, G., Tarpey, P. S., Turrell, K., Dykema, K. J., Khoo, S. K., Petillo, D., Wondergem, B., Anema, J., Kahnoski, R. J., Teh, B. T., Stratton, M. R., and Futreal, P. A. (2010) Systematic sequencing of renal carcinoma reveals inactivation of histone modifying genes, *Nature 463*, 360-363.
275. Varela, I., Tarpey, P., Raine, K., Huang, D., Ong, C. K., Stephens, P., Davies, H., Jones, D., Lin, M. L., Teague, J., Bignell, G., Butler, A., Cho, J., Dalgliesh, G. L., Galappaththige, D., Greenman, C., Hardy, C., Jia, M., Latimer, C., Lau, K. W., Marshall, J., McLaren, S., Menzies, A., Mudie, L., Stebbings, L., Largaespada, D. A., Wessels, L. F., Richard, S., Kahnoski, R. J., Anema, J., Tuveson, D. A., Perez-Mancera, P. A., Mustonen, V., Fischer, A., Adams, D. J., Rust, A., Chan-on, W., Subimerb, C., Dykema, K., Furge, K., Campbell, P. J., Teh, B. T., Stratton, M. R., and Futreal, P. A. (2011) Exome sequencing identifies frequent mutation of the SWI/SNF complex gene PBRM1 in renal carcinoma, *Nature 469*, 539-542.
276. Larkin, J., Goh, X. Y., Vetter, M., Pickering, L., and Swanton, C. (2012) Epigenetic regulation in RCC: opportunities for therapeutic intervention?, *Nat Rev Urol 9*, 147-155.
277. Navin, N., Krasnitz, A., Rodgers, L., Cook, K., Meth, J., Kendall, J., Riggs, M., Eberling, Y., Troge, J., Grubor, V., Levy, D., Lundin, P., Maner, S., Zetterberg, A., Hicks, J., and Wigler, M. (2010) Inferring tumor progression from genomic heterogeneity, *Genome Res 20*, 68-80.
278. Navin, N., Kendall, J., Troge, J., Andrews, P., Rodgers, L., McIndoo, J., Cook, K., Stepansky, A., Levy, D., Esposito, D., Muthuswamy, L., Krasnitz, A., McCombie, W. R., Hicks, J., and Wigler, M. (2011) Tumour evolution inferred by single-cell sequencing, *Nature 472*, 90-94.

279. Swanton, C. Intratumour heterogeneity: evolution through space and time, *Cancer Research 2012 Oct 1;72(19):4875-82*.
280. Merlo, L. M. F., Pepper, J. W., Reid, B. J., and Maley, C. C. (2006) Cancer as an evolutionary and ecological process, *Nature Reviews Cancer 6*, 924-935.